EXPERIMENTAL STUDIES ON MAGNETIC FIELD ASSISTED COMBUSTION OF HYDROCARBON FUELS IN A MULTICYLINDER SPARK IGNITION ENGINE UNDER LIQUID PHASE AND GAS PHASE OPERATION

Thesis

Submitted in the partial fulfillment of the requirements for the Degree of

DOCTOR OF PHILOSOPHY

by

LIBIN P OOMMEN

DEPARTMENT OF MECHANICAL ENGINEERING

NATIONAL INSTITUTE OF TECHNOLOGY KARNATAKA

SURATHKAL, MANGALORE- 575025

March, 2021

EXPERIMENTAL STUDIES ON MAGNETIC FIELD ASSISTED COMBUSTION OF HYDROCARBON FUELS IN A MULTICYLINDER SPARK IGNITION ENGINE UNDER LIQUID PHASE AND GAS PHASE OPERATION

Thesis

Submitted in the partial fulfillment of the requirements for the Degree of

DOCTOR OF PHILOSOPHY

by

LIBIN P OOMMEN

Under the guidance of

Dr. KUMAR G N

Associate Professor

DEPARTMENT OF MECHANICAL ENGINEERING

NATIONAL INSTITUTE OF TECHNOLOGY KARNATAKA

SURATHKAL, MANGALORE- 575025

March, 2021

DECLARATION

I hereby declare that the Research thesis entitled **"EXPERIMENTAL STUDIES ON MAGNETIC FIELD ASSISTED COMBUSTION OF HYDROCARBON FUELS IN A MULTICYLINDER SPARK IGNITION ENGINE UNDER LIQUID PHASE AND GAS PHASE OPERATION"** which is being submitted to the **National Institute of Technology Karnataka, Surathkal** in partial fulfillment of the requirements for the award of the Degree of **Doctor of Philosophy** in **Mechanical Engineering** is a *bonafide report of the research work carried out by me*. The material contained in this Research Thesis has not been submitted to any other Universities or Institutes for the award of any degree.

Register Number: **ME14F20**

Name of the Research Scholar: **LIBIN P OOMMEN**

Signature of the Research Scholar:

Department of Mechanical Engineering

Place: NITK Surathkal

Date: 03/03/2021

CERTIFICATE

This is to certify that the Research Thesis entitled **"EXPERIMENTAL STUDIES ON MAGNETIC FIELD ASSISTED COMBUSTION OF HYDROCARBON FUELS IN A MULTICYLINDER SPARK IGNITION ENGINE UNDER LIQUID PHASE AND GAS PHASE OPERATION"** submitted by **Mr. LIBIN P OOMMEN (Register Number: 148015ME14F20)** as the record of the research work carried out by him, *is accepted as the Research Thesis submission* in partial fulfillment of the requirements for the award of the Degree of **Doctor of Philosophy**.

Dr. Kumar G N

Research Guide

Date: 03/03/2021

Chairman- DRPC

Date: 03/03/2021

ACKNOWLEDGEMENTS

Research and teaching have always been the passion of my life and a doctoral degree was the perfect conduit to a career comprising these elements. As I step on to the first and foremost vestige of scientific exploration, the fulfillment of this dream would remain incomplete without the expression of appreciation and gratitude to the people who made it plausible.

First and foremost, I would like to express my sincere gratitude to my research supervisor **Dr. Kumar G N**, Associate Professor, Department of Mechanical Engineering for his excellent guidance, patience and support throughout the research work. Being my mentor, the support and instigation that he provided proved to be immeasurable. I have observed and learned his way of interaction with students with a lot of grace and enthusiasm. Without his sincere advises and blessings, this work would not have been successful. I also thank **Dr. P. Mohanan**, retired Professor, Department of Mechanical Engineering, who was my initial supervisor and aided in the identification of this research proposal.

I am thankful to **Dr. Shrikantha S Rao**, Professor and Head, Department of Mechanical Engineering for his help and wholehearted support. I would also like to thank **Dr. Prasad Krishna, Dr. K.V. Gangadharan** and **Dr. Narendranath S** who served as the head of the department during this research work.

I would like to acknowledge the inputs given by **Dr. A. U. Ravishankar**, Professor, Department of Civil Engineering and **Dr. Gnanasekharan N**., Assistant Professor, Department of Mechanical Engineering as the members of the Research Progress Assessment Committee. Their queries and corrections have benefitted me in improving the overall quality of this thesis.

The help and support extended by **Mr. Chandrasekhar**, I.C. Engine lab in-charge, **Mr. Vinayraj, Mr. Yashpal** and **Mr. Raviraj** who serve as the technical staff in the lab are invaluable in the procuring, fabrication and service of the experimental rig. The technical

assistance of **Mr. D'Souza** of **Rex associates**, Mangaluru and **Sri. Jaganath** of **Mandovi Motors**, Surathkal in servicing the rig is also acknowledged with gratitude.

With deep gratitude, I would like to acknowledge the help and support of my departmental colleagues **Dr. Shivaprasad K.V., Mr. Nuthan Prasad B.S., Mr. Jayashish Kumar Pandey, Mr. Vipin Allien J, Mr. Jagdeesh S, Mr. Santhosh K, Mr. Tabish Wahidi** and **Mr. Shankar Kodathe** who have helped me with their valuable inputs. The assistance offered by **Mr**. **Shabareesh S Kumar**, former M. Tech student, in conducting the experiments was invaluable and a pleasant memory.

The journey to a doctoral degree is always challenging and exhorting. There were times when I felt down and needed impassioning hands to boost my morale. I would cherish the moral support and friendship offered by **Mr. Sudhish Radhakrishnan, Mr. Niyas S, Mr. Anoop B.N., Mr. Sushanlal Babu, Mr. Fredy James, Mr. Sachin Satheesh** and **Mr. Deepak Narayanan**, Research Scholars from various departments. The moments spent with them were pure bliss that I would like to cherish forever.

The greatest blessing bestowed upon me is my family. My parents, **Mr. P.T. Oommen** and **Mrs. Ammini Oommen** have always encouraged my dreams and remain the pillars of my life. I would like to thank my wife, **Mrs. Meenu Alex** for being the comforting hand and appreciate the patience and moral support she provided me with, during these years. I dedicate this work to my little bundle of joy, my **David**.

Finally, I would like to thank Almighty for guiding me through these years and providing me with the physical, mental and spiritual strength. I thank all who have helped me directly or indirectly in completing this research work.

Place: NITK Surathkal

Date: **LIBIN P OOMMEN**

ABSTRACT

Global energy demand forecasts indicate a growing trend with the ever-rising population and technology that enriches our everyday lives. Ironically, the rise in energy demand is 1.52 per cent per annum relative to the 1.14 per cent growth in population. Fossil oil, being the basic engine of industrial revolution, now meets more than 80 percent of global energy demand. The fossil energy is majorly used in the transport field in Internal Combustion Engines. With the rising trend of individuals using private cars, this share is expected to increase even higher, putting a burden on the energy sources. The over reliance on fossil fuels is so high that in a few decades the fossil reserves are predicted to become exhausted. Studies indicate that the transport industry itself using internal combustion engines contributes to 45 percent of India's overall air pollution. The rapid population growth and increased use of private vehicles has accounted for the countrywide deterioration of air quality. The combustion of fossil fuels in motors leads to the release of harmful contaminants such as CO, HC, CO_2, NO_x and PM of which the percentage content is increasing every year. The transition to e-mobility is challenging and is dependent on path breaking technologies and renewable energy penetration. This is the reason that provokes us to focus our research on the efficient utilization of existing fossil fuel energy and to come up with technologies that improve the fuel economy as well as the emission levels of internal combustion engines.

The present research experimentally investigates the effect of a physical pre-treatment technique of hydrocarbon fuels before combustion in I.C. Engines using high intensity magnetic fields. The performance, combustion and emission characteristics of the engine under varying intensities of uniform magnetic fields created by high grade (N38) NdFeB are studied at four different loads (25%, 50%, 75% and 100%) and four different engine speeds (2000 rpm, 2500 rpm, 3000 rpm and 3500 rpm). The impact of magnetisation pattern on combustion parameters is analyzed by switching between two different patterns (axial and radial) of magnetisation exclusively. The influence of magnetic fields on liquid phase and gaseous phase combustion are analyzed separately by fuelling the

engine with gasoline and LPG exclusively with the aid of suitable engine modifications. The effect of a post combustion treatment technique like part cooled exhaust gas recirculation is studied to come up with an optimal flow rate which benefits the combustion and emission of both liquid and gaseous phase fuels and is integrated with the optimal parameters in magnetic field assisted combustion to investigate the synergetic effect produced on the combustion of gasoline as well as liquefied petroleum gas.

The experiments are conducted on a 10L inline Maruthi Suzuki Zen MPFI spark ignition engine which has modified provisions to operate on neat LPG. A separate gas ECU is provided for the switching between fuel phases. The input given to the gas ECU is the opening signal pulse from the already deployed gasoline ECU which is then modified with a correction factor before being sent to the gas injectors. Four distinct gas injectors are provided in the inlet manifold adjacent to the inlet port of individual cylinders for injecting LPG. These gas injectors are maneuvered by solenoid valves driven by 12V DC supply. The specifications of the gas injectors like nozzle diameter are designed corresponding to power generated per cylinder. Correspondingly injectors of nozzle diameter 1.75 mm is chosen for the given test engine. The NdFeB magnets of a particular magnetisation pattern are mounted on the fuel line with a non magnetic stainless steel covering adjacent to the fuel injector. A system for recirculating partially cooled exhaust gases into the combustion zone is designed for our experimentation. Prior to the data acquisition, the engine is operated for some time to reach steady state operation. Experimental error is minimized by taking average value of three readings at each test points.

Initially experiments are conducted to study the performance, combustion and emission characteristics of the engine with axial magnetic fields applied on liquid phase hydrocarbons at various load and speed conditions. In the subsequent stages, the engine is fueled by gas phase hydrocarbons and then the axial fields are replaced using radial fields on both fuel phases. In the next part of investigation, the effect of locus of magnetisation is studied with respect to a single fuel phase. The optimal flow rate of part cooled EGR is

experimentally estimated for both fuel phases which is then integrated with the initially optimized parameters of magnetic fields and experimented in the final phase.

Experimental results show that the effect of magnetic field assisted combustion is much more pronounced in the case of liquid phase hydrocarbons, owing to the continuous arrangement of hydrocarbon molecules in the liquid phase. Radial magnetisation pattern is observed to be more effective in molecular restructuring in both the fuel phases because of its ability to ionize the molecules in all directions. Magnetic field assisted combustion proves to be beneficial in improving the fuel economy and thermal efficiency of the engine under both fuel phases. Experimental results also indicate that recirculation of partially cooled exhaust gases are beneficial in enhancing the combustion and emission characteristics of the engine up to an optimum limit and are particularly useful in the reduction of oxides of nitrogen which in the normal case is enormous in LPG combustion. The synergetic effect of both these techniques is especially beneficial in terms of fuel economy, thermal efficiency and NO_x emissions of the engine under both phases of hydrocarbons.

Keywords: Liquefied Petroleum Gas, Gasoline, Magnetic field assisted combustion, NdFeB rare earth magnets, Exhaust Gas recirculation, Combustion, Emission, Coefficient of Variation, Combustion stability.

CONTENTS

LIST OF FIGURES

LIST OF TABLES

LIST OF PLATES

NOMENCLATURE

MFAC	Magnetic Field Assisted Combustion
AM	Axial Magnetic Fields
RM	Radial Magnetic Fields
EGR	Exhaust Gas Recirculation
LPG	Liquefied Petroleum Gas
BP	Brake Power
BSFC	Brake Specific Fuel Consumption
BTE	Brake Thermal Efficiency
CP	Cylinder Pressure
NHRR	Net Heat Release Rate
IMEP	Indicated Mean Effective Pressure
COV	Coefficient of Variation
HC	Hydrocarbon
CO_2	Carbon dioxide
NO_x	Oxides of Nitrogen
ppm	Parts Per Million
RPM	Revolutions Per Minute
P_{max}	Maximum Pressure
deg	degree
CA	Crank Angle
G	Gauss

Chapter-1

Introduction

1.1 Overview

Fossil fuels are intricately woven into the fabric of our everyday lives in both obvious and subtle ways. The widespread usage of fossil resources immensely improved the living conditions across the globe and the productive and meaningful lives that we are accustomed to today would be impossible without them. There is an enduring economic and social need for fossil fuels and often misguided criticisms ignore the central role that hydrocarbons play in our lives.

The projections of global energy demand is showing an increasing trend with the ever increasing population and technologies that enrich our day to day lives. Interestingly, the increase in demand of energy is 1.52% per year compared to the increase in population of 1.14%. Being the fundamental driver of industrial revolution, fossil energy still meets more than 80% of global energy demands. The trend of global energy utilization over the decades is given in fig 1.

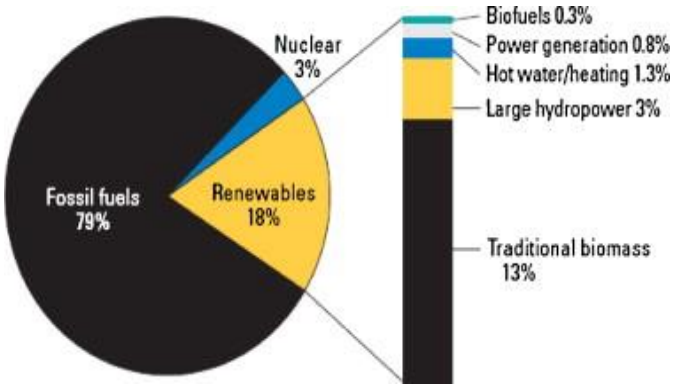

Fig 1.1: Share of global energy utilization (Source: Statistical Review of World Energy 2015)

India is currently ranked third in the consumption of oil with 212 million tons after USA and China. India has very limited reserves of oil and gas and the net import of crude oil and petroleum products is around 147 million tons worth of 5612 billion INR. Although we are developing and promoting the usage of renewable energy sources, more than 79% of India's energy needs are still met by fossil fuels. The energy intensity of transportation sector has been identified as 7.66% whereas in industrial sector it is 5.47% (trading economics report 2014). In other words, the fossil energy is utilized mostly in the transportation sector. With the increasing trend of usage of private vehicles by individuals, this share is expected to rise even more, creating a pressure on the energy sources. The over dependence on fossil fuels is so high that the fossil reserves are expected to get depleted in a few decades.

Another global transboundary problem associated with the fossil fuels is the ever-increasing rate of environmental pollution associated with it. Air quality is one of the gravest anxieties in India recently. A number of natural and anthropogenic sources are responsible for the poisoning of ambient air. According to the Air Quality Life Index (AQLI) statistics, the life expectancy of 660 million population in India would increase by one year if India could achieve its own air quality standards (Greenstone et al. 2017). The economic losses arising from higher health care expenditures and less productive work force in this country pile up to more than 0.5 trillion dollars per year (OECD report, 2014). The extent of pollution is so massive that out of 15 most polluted cities around the world, 14 lie in India currently. Criteria pollutants like PM, SO_2, NO_x, CO and O_3 exceed the air quality standards in urban and industrial areas throughout the year, posing serious health hazards to the residents. Table 1.1 compares the current magnitude of pollutants in Delhi NCR region with global and Indian ambient air quality standards, as published by Central Pollution Control Board.

Depending upon the physio chemical characteristics of pollutants and their concentrations, these pollutants result in numerous physical ailments and mortality (Oommen et al. 2020). The increased mortality rate from cardio pulmonary causes and

respiratory morbidity has been associated with the inhalation of polluted air (Olmo, 2011). Cross sectional and time series studies have proved that exposure to motor exhaust can result in myocardial infarctions, premature birth, low birth weight and excessive plasma viscosity (Kunzli et al. 2005, Jerret et al. 2010, Folinsbee et al. 1992). Air Pollution is increasingly linked to the rising levels of male infertility (Kampa et al. 2008). The Presence of CO in the inhaled air can cause hematological ailments and even cancer (Azem et al. 2016).

Table 1.1: Comparison of magnitude of pollutants with global and Indian AAQS (Oommen & Kumar 2021)

Criteria Pollutant	**Global AAQS ($\mu g/m^3$)**	**Indian AAQS ($\mu g/m^3$)**	**Original Value (Dec 2019) ($\mu g/m^3$)**
PM 2.5	25	60	260
PM 10	50	100	142
NO_x	40	80	180
SO_2	20	80	68
CO	02-03	04	15
Ozone	100	100	119

Statistics shows that transport sector utilizing internal combustion engines itself contribute to 45% of total air pollution in India. The rapid growth of population and increased trend of private vehicles have accounted for the degradation of air quality throughout the country. The combustion of fossil fuels in automotive engines result in the emission of toxic pollutants like CO, HC, CO_2, NO_x and PM with the percentage of these constituents increasing every year. The technology leap to BS VI is expected to cut down the emission levels of PM and NO_x by 80% and 25% respectively (BS VI Policy report 2018).

The anticipated depletion of fossil fuels in the near future and the adverse effects of pollution from fossil fuel combustion have made the researchers around the world to focus on hybrid or electric vehicles. But according to the current scenario, the

electrification process need to tackle a number of challenges to make it a viable replacement to the existing IC Engines. The most challenging factor is the cost associated with battery technology. The higher cost of batteries is due to the expensive materials needed for holding massive amounts of charge. The finite supply of elements that are used in battery production makes this technology difficult to be adopted. The supply chain of electric vehicles has a concernful background. Lithium ion batteries make use of Cobalt that is linked to news and reports of child labour. The mining of Lithium poses concerns about environmental degradation and land use conflicts in Tibet and Bolivia. It is impossible to recycle the batteries in an environmentally safe manner which makes the adoption of this technology even more challenging.

The transition to electrification is even more challenging to developing economies like India. The available options are either to get Cobalt and Lithium at very high prices and develop the technology or to import batteries as such. The easier path is the import route which will hike the import dependence on China to 70% or more. The adoption of battery technology will also kill the manufacturing industries of automotive parts like transmission systems, clutches, exhaust pipes etc. The motor mechanics need to be reskilled to enable them to repair EV's with sophisticated electronics. So it is quite clear that the transition towards battery powered vehicles is challenging and requires major break throughs to make it cost effective and receptive to the common end users. This realization provokes us to focus on the effective utilization of existing fossil fuel energy and to come up with technologies that improve the fuel economy as well as the emission levels of Internal Combustion Engines.

1.2 Spark Ignition Engines

From the day of inception by Nicolas Otto, spark ignition engines remained the sole driver of automobile transport until late 70's and still contributes to the major share of light duty vehicles. Although these engines can be fueled using Natural gas, LPG, methanol and derivatives, ethanol and derivatives and Hydrogen, gasoline is the commonly used fuel for SI engines. The developments in petroleum refining technologies

like thermal cracking and catalytic cracking have made gasoline production inexpensive and available as the best suited fuel for light duty automotive engines. The fuel system in any spark ignition engine essentially consist of a fuel tank, fuel pipes, fuel and air filters, carburetor or fuel injectors and intake manifold (Mingzhang et al. 2014). In spark ignition engines, spark timing has a significant effect on both performance and emission characteristics. The peak of cylinder pressure curve is attained adjacent to TDC position only at the optimum spark timing which will vary with the nature of fuels. In a basic gasoline engine, a mixture of liquid fuel and air is generated in the carburetor and it is then admitted into the combustion chamber. This process is known as carburetion which has many drawbacks as listed below.

- The quality and quantity of mixture supplied to various cylinders vary due to difference in lengths of induction passages in multi cylinder engines. Fuel condensation also affects the mixture quality.
- The mechanical components of carburetors like throttle valves, pipes, bends, jets and choke tubes offer restriction to the passage of mixture resulting in a loss of volumetric efficiency.
- The wear and tear occurring to mechanical parts of the carburetor results in less operating efficiency.
- At low operating temperatures, there is chance of freezing to occur unless some counter measure is employed beforehand.
- The absence of flame traps can result in the fuel getting ignited outside the carburetor and also backfires.

1.3 Multipoint Port Fuel Injection (MPFI) System

In order to avert the drawbacks of carburetor system, multipoint injection system was developed in 1980. While the carburetor system depends on suction created by intake air accelerated by a venture tube to draw the fuel into the airstream, the MPFI system atomizes the fuel through small nozzles at very high pressures and injects a fine spray of fuel ahead of intake valve. The composition of Air-fuel mixture in each working cycle is

extremely important for the smooth operation of the engine. In modern multipoint injection systems, each cylinder is provided with a dedicated injector which is activated individually to precisely meter the timing and quantity of the injected fuel. The Electronic Control Unit calculates and supplies precise quantity and quality of mixture at the right moment which will avoid the wetting of manifold walls with fuel and improve the overall combustion efficiency of the engine. MPFI system include a throttle position sensor to detect the degree of throttle opening, IAC valve to supply bypass air, fuel pressure regulator to maintain the pressure at about 2.55 bar, fuel injectors, Electronic control module, map sensor to convert the pressure change in intake manifold to voltage change, Indicated Air Temperature sensor that measures the air temperature and a heated oxygen sensor which detects the concentration of oxygen in the exhaust gas to regulate the mixture ratio.

1.4 LPG as an alternative fuel in engines

Liquefied Petroleum Gas is the planetary name for mixtures of hydrocarbons constituted mainly of propane and butane stored in the liquid state. In the ordinary state, LPG is colorless, odorless and denser than air. A distinctive and unpleasant smell is added to detect the smallest of leakages by the inclusion of a stanching agent named ethyl mercaptan. It is non toxic, non corrosive and free of lead and is widely used for domestic cooking purpose.

LPG is mainly produced from the processing of natural gas and refining of crude oil. The residual organic material formed over millions of years from buried living organisms of early geological eras get converted to propane rich petroleum through the processes of diagenesis and catagenesis (Walters 2007). Diagenesis occurs through microbial action below 50º C through dehydration, condensation, cyclization and polymerization. On the other hand, Catagenesis happens at high temperatures of 50º C to 200º C through thermo catalytic cracking, decarboxylation and hydrogen disproportionation (Akramkhodzhayev et al. 1986). About 3% of LPG is obtained from a barrel of crude oil during the refining process.

The isolation of propane from a mixture of petrochemicals including methane, ethane, propene, isobutene, isobutene, butadiene, pentane and pentene is a complex process which needs to be carefully carried out because the presence of any such impurity can affect the liquefaction process. Liquefaction of these component gases is done at appropriate temperatures and pressures specified by ASTM which makes it acceptable as a fuel gas. The impervious quality standard makes LPG an environmentally alluring fuel and is often referred to as a clean burning fuel because it contains less number of carbon molecules with higher ratio of carbon to hydrogen (Changming et al. 2010).

LPG is widely utilized in internal combustion engines now a days due to its higher octane number, higher combustion efficiency, lower emissions and easier availability (Gumus 2011). When the mixture is in slightly leaner region (equivalence ratio of 0.9 to 1.0) flame propagation speed of LPG is comparatively higher than gasoline and hence LPG has better combustion characteristics in lean burn operations. The research octane number (RON) of LPG is higher in the case of LPG enabling operation at higher compression ratios and hence yielding better thermal efficiencies (Ceviz 2005). The acceleration and idling performances are improved since the distribution of gaseous phase fuel between cylinders is enhanced. As there is a reduction in the wear of cylinder bore and deposits in the combustion chamber and spark plugs, the life of the engine is considerably increased under LPG operation.

Although LPG has a number of properties that make it compatible as an auto gas, there are some cons associated with it as well. The spatial requirement and storage of LPG cylinders is one among them. The power output of the engine is reduced under LPG operation. When the engine is fuelled by LPG comparatively higher ignition energy is required which results in higher starting load on the batteries. Owing to the higher combustion temperatures and flame velocity, the emission of oxides of Nitrogen increases exponentially when compared to the combustion of liquid fuels. Another major disadvantage of LPG is the safety concerns associated with it. As it is heavier than

ambient air, LPG tends to accumulate adjacent to the ground surface in case of any leakage leading to serious fire hazards.

1.5 Physical Properties and Characteristics of LPG

In India, commercial LPG is a mixture of butane (55%) and propane (45%) containing both saturated and unsaturated hydrocarbons. The marketing of LPG is governed by Indian Standard Code IS-4576 and test methods are governed by IS-1448. In the following subsections, we are going to discuss about the physical properties and combustion characteristics of LPG which make it suitable for use as a fuel.

1.5.1 Density

At atmospheric pressure and temperature, LPG exists as a gas which is 1.5 to 2.0 times heavier than atmospheric air. The vapor pressure of LPG varies with its composition and temperature and is usually in the range of 220 kilopascals at 20ºC. After liquefaction, the density is approximately half of that of water (0.525 to 0.580 at 15ºC). Owing to the fact that LPG is heavier than air, it would accumulate at the ground level causing accidents.

1.5.2 Vapor Pressure

The pressure in which LPG is stored inside the cylinders will be equal to the vapor pressure corresponding to the temperature of LPG in the storage vessel. Vapor pressure depends up on temperature and the composition of the mixture of hydrocarbons. When stored as a liquid, for each degree centigrade of temperature rise, the vapor pressure rises by almost 15 kg/sq.cm. Hence it is not advisable to overfill the storage cylinders.

1.5.3 Flammability

LPG has an explosive range of 1.8% to 9.5% volume of gas in air which is narrower than other gaseous fuels. Hence the usage of LPG is associated with safety issues in the eventuality of a leakage. The self ignition temperature of LPG is around 410 to 580ºC. The unloading of LPG cargoes using air pressure is not advisable as the entrapped air is hazardous in unpurged vessels.

1.5.4 Combustion

The volume of products is increased during the combustion of LPG as it requires up to 50 times its own volume of air. Hence it is advisable to provide sufficient ventilation when LPG is burnt so that any chance of asphyxiation due to the depletion of oxygen can be averted. The combustion temperatures will be higher in the case of LPG operation with the peak cylinder pressures occurring nearer to dead centre position.

1.5.5 Odor

LPG in its natural state is colorless and odorless and hence any leakage is difficult to be identified. Due to this reason, a stanching agent named ethyl mercaptan is added to it which imparts a foul smell to the gas making it easier to identify the escaping gas. The addition of fouling agent is done as per IS-4576 standards.

1.5.6 Color

In both liquid as well as gaseous phase, LPG is colorless. In the event of a leakage, a whitish fog is formed on the container due to the condensation of water vapor. This is an alternative method to identify the leakage of LPG.

1.5.7 Toxicity

LPG vapor pocess mild anesthetic properties and is slightly toxic. In larger concentrations, it can cause suffocation and asphyxiation because it tends to displace oxygen and tries to accumulate in the ground level.

1.5.8 Storage

The storage of LPG is done mostly in the liquid phase in pressure vessels. The liquefied LPG gas storage can also be under ground in custom built storage caverns. The storage cylinder must always be upright with valves closed whenever not in use. The LPG cylinders should be prevented from falling and protected from impact and damages.

Table 1.2 Comparison of Physical Properties of LPG with Gasoline (Masum et al. 2013, Tiyan et al. 2010, Nayak et al. 2017)

Sl. No.	Physical Properties	LPG	Gasoline
1	Composition	55% C_4H_{10}+ 45% C_3H_8	C_8H_{18}
2	Vapor Pressure at 65ºC	16.8	0.29
3	Gross Calorific Value (kJ/kg)	49700	42900
4	Specific gravity at 15 ºC	0.54	0.75-0.76
5	Stoichiometric air fuel ratio	15.5	14.7
6	Ignition temperature (ºC)	488-502	257
7	Research Octane Number	112	95
8	Max. flame temperature (ºC)	1985	2002
9	Latent Heat of Vaporization	426	180-350
10	Boiling Point (ºC)	-22	25

1.6 Cycle by Cycle Variations

The fundamental problem associated with internal combustion engines since the time of its invention is the cycle by cycle variations in combustion. Combustion process in spark ignition engine is not repetitive in all the cycles. If the pressure trace inside the combustion chamber is observed for some duration, the variation can be observed quite clearly. In a normal functioning engine, the peak cylinder pressures in subsequent engine cycles can vary up to 30% (Johanson 2003). This cyclic variation in combustion is the major limiting factor for parameters that can enhance the performance of the engine and also increases the level of emissions. The study of cyclic variations is significant because the optimum spark timing is set for average cycle and the spark time will be over advanced or retarded for other cycles resulting in a loss of power and efficiency.

The pressure inside the combustion chamber varies with the crank angle as a result of cylinder volume change, combustion, heat transfer to the chamber walls, flow into and out of crevice regions and leakage (Heywood 1988). From early days, fluctuations in combustion have been studied in terms of cylinder pressure. Hence pressure related parameters are often used to quantify the intensity of fluctuation. The magnitude and location of peak pressures is the frequently used parameter. Another commonly used parameter is the variation in Indicated Mean Effective Pressure (IMEP) developed in each cycle. A statistical tool for analyzing the fluctuations in combustion is the Coefficient of Variation (COV) of peak pressures and IMEP. COV is calculated as the ratio of standard deviation to the mean value of the data population. COV of IMEP is a good indicator of engine behavior and is an effective tool in designing the transmission system since it is a measure of torque fluctuations.

The major liability of analyzing the fluctuations in terms of pressure related parameters is the lack of awareness of the processes happening inside the combustion chamber. The only rational way of pressure variation from cycle to cycle is the variation occurring in the combustion process. Thus pressure data can be used in a heat release model and heat release function can be analyzed to study the cyclic fluctuations instead of pressure trace. The heat release data is a good indicator of cyclic variations in early stages of flame development and during the entire combustion process. The heat release calculation may be replaced by flame location detection in the quest of detailed information.

The analysis of flame photographs at different engine cycles suggest dispersion in burning rate and these fluctuations arise due to the following factors.

- The cycle to cycle variation in gas motion inside the combustion chamber
- The variations in mixture quality supplied to cylinders during each cycle
- The variations in supply of air and fuel to a cylinder during each cycle

The variations in gas motion adjacent to the spark plug convect the flame at different velocities and in different directions (Heywood 1988). This influences the interaction of flame with the cylinder walls. Alterations in turbulent velocity fluctuations adjacent to the spark plug effects variations in flame kernel development. The variation in the shape of the flame front is caused by the changes in mean flow throughout the combustion chamber. Any modifications to the operating parameters of the engine should be monitored on the basis of cyclic variations to ensure stable combustion. If the engine is operated beyond the stable combustion limit, it will not be able to achieve its complete potential of efficient and clean combustion.

1.7 Magnetic Field Assisted Combustion

The hydrocarbon fuels employed in IC Engines can be pretreated in a number of physical or chemical methods to enhance the burning efficiency of the engines. Magnetic field assisted combustion is one such technique of physically altering the molecular alignment of hydrocarbons inorder to improve its combustion characteristics. Magnetic conditioning of fuels has been under the focus of research for the past three decades by researchers around the globe. Both permanent magnets and electro magnets have been experimented for this application and the results reported are encouraging.

Any hydrocarbon fuel is a compound of molecules. These molecules consist of a number of atoms that are in turn made up of nucleus and electrons. Thus, it is quite clear that both positive and negative electrical charges exist in the molecules. These molecules in their natural state form a cluster within themselves and will not actively interlock with the oxygen molecules during combustion. Hydrocarbons can be polarised by the exposure to external magnetic fields (Ueno 1985). The effect of such magnetism is the creation of a moment caused by the movement of outer electrons of a hydrocarbon chain, moving the electrons into states of higher principal quantum number.

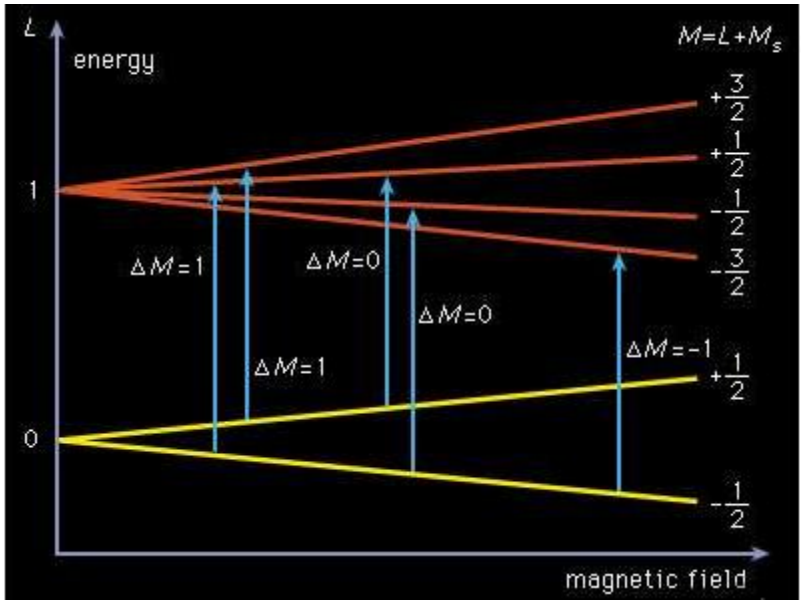

Fig 1.2: Excitation of electrons into higher energy level through magnetisation (Britannica)

This state effectively breaks down the fixed valence electrons that part take in the bonding process of fuel compounds. The hydrocarbons become directionalised and align the conduced magnetic moment into a dipole relationship within itself (Faris et al. 2010). On the application of a magnetic field, the hydrocarbon molecules of a fuel get ionized and realigned, resulting in the weakening of Vander Vaal's bonds followed by the declustering of existing hydrocarbon clusters. Subsequently, this will result in the active interlocking between fuel and oxygen molecules, ensuring better completion of combustion process.

In the process of combustion of a hydrocarbon fuel, it is the outer shell of hydrogen that gets combusted first. Hydrogen exists in two distinctive forms- ortho hydrogen and para hydrogen. The ortho and the para variants of hydrogen differ in the relative orientation of nuclear spin of the two protons. In the para state, spin of the protons is anti-parallel where as in the ortho molecule, the spin is parallel. This spin orientation has a pronounced effect on the behaviour of the molecule. Ortho hydrogen is found to be unstable and more reactive than para state. The fuel molecules will normally be in the

para state with opposite spins, getting attracted to each other, forming clusters. When the fuel is mixed with air at that particular condition, all the molecules of the fuel may not combine with the oxygen molecules in the air for combustion and hence some of the fuel molecules escape into the atmosphere as unburnt gas. When magnetic treatment is carried out, the molecules that normally occur in the para state gets oriented into the active ortho state, thus weakening the bonds between fuel molecules (Fatih et al. 2010)

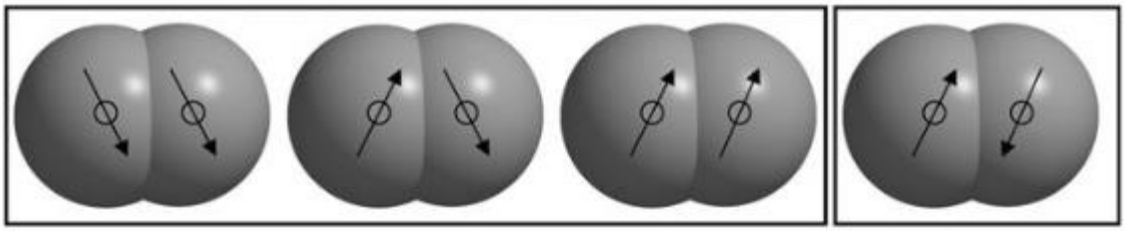

Fig 1.3: Schematic representation of ortho and para configurations of hydrogen (Olsson 2003)

Faraday's law states that when a field is introduced perpendicular to that circuit, electro-motive force acts upon the electron, by which the nature of motion of atomic orbits gets altered. Hence, a diamagnetic ion subjected to magnetism exhibits positive ionization which in turn helps the hydrocarbons to attract and bond with negatively charged oxygen.

From the thermodynamic point of view, the consumption of fuel is completely dependent on its combustion enthalpy. The enthalpy of a reaction can be calculated by using the bonding energy of reactants and products. If the magnetic treatment is able to alter the bonding energy of hydrocarbon molecules, the consumption rate of fuel will get altered as well. Thus, the reduction in the bonding energy directly affects the enthalpy and subsequently affects the rate of consumption of fuel. The weakening of bonds between fuel molecules also aid in the formation of more bonds with oxygen molecules, ensuring an increase in combustion efficiency. Hence the performance and emission characteristics of an engine are expected to improve when the hydrocarbons are pre-treated under strong magnetic fields.

1.8 Exhaust Gas Recirculation

Exhaust Gas Recirculation is a technique employed in internal combustion engines for the control of NO_x emissions. In this technique, a part of the exhaust gases is taken from the exhaust manifold and reintroduced into the intake manifold allowing it to mix with the fresh charge. The substitution of burnt gases which do not take part in combustion for oxygen rich ambient air reduces the proportion of cylinder contents available for combustion. This results in a correspondingly lower heat release and peak cylinder temperatures and thus restricts the formation of NO_x.

The total burned gas inside the combustion chamber acts as a diluent to the unburned mixture. The total burned gas fraction is the combination of residual gas from the previous cycle and the recirculated exhaust introduced into the cylinder (Heywood 1988). The residual gas fraction from the previous cycle is dependent on various factors such as load on the engine, valve overlap timing, air-fuel ratio and compression ratio. Due to the dilution of unburned charge, the absolute temperature achieved after combustion varies inversely with the mass fraction of burned gas. Thus the reduction in NOx by EGR is effected by the combined effect of displacement of oxygen by inert exhaust gases and the reduced combustion temperature due to the higher heat capacity of carbon dioxide and water vapour in the exhaust.

The amount of EGR tolerated by an engine depends upon operating parameters like speed, load and the equivalence ratio along with its combustion characteristics. The addition of optimum percentage of EGR is significant because EGR substantially reduces the rate of combustion making stable combustion difficult to achieve. The maximum amount of EGR tolerance in a spark ignited engine varies between 15 to 30%. EGR tolerance will be higher in faster burning engines than in slower burning engines. The reduction in combustion rates and increase in cyclic fluctuations with increasing EGR rates can result in higher emission of hydrocarbons. EGR is found to have very little effect on CO emissions within the tolerance limits.

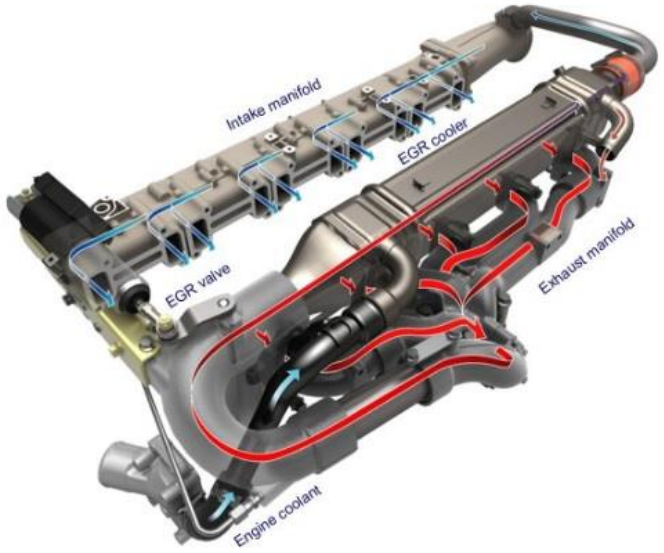

Fig 1.4: EGR with single stage cooling in a Euro IV engine (source: Scania)

Depending upon the configuration, EGR systems are classified into Long Route systems and Short Route systems. In the long route system EGR is driven by the pressure drop between intake and exhaust gas streams. In the short route systems, turbo chargers are included in which the engine operates at higher intake pressure than the mean exhaust pressure. A more common classification of EGR systems is on the basis of temperature. In hot EGR systems, the exhaust gases are recirculated as such by insulating the exhaust pipes so that the charge temperature is increased. In cooled EGR systems, an intercooler is used to partially or fully cool the exhaust gases before recirculating into the intake manifold (Agrawal et al. 2014). Based on pressure, EGR systems are classified into low pressure route systems and high pressure route systems. In the low pressure route system, EGR is passed from downstream of turbine to the upstream of compressor and vice versa in the case of high pressure systems.

Along with the advantages that EGR offers to engines, there are certain disadvantages also. EGR causes the reduction of oxygen inside the combustion chamber thereby increasing the generation of particulates. Hence EGR is often a trade off between NOx and particulates and need to be carefully designed specific to the engine operation. The

power output of the engine is affected when EGR is employed and many a time the EGR valve needs to be closed when full power is in demand. The calibration of transient EGR is complex because EGR valve is unable to respond to changes in demand instantly. Poor distribution of EGR between the cylinders of a multicylinder engine leads to increased emissions.

1.9 Components of EGR

1.9.1 EGR Valve

EGR valve is the most significant component of any EGR system. It is usually mounted on a channel in between the intake and exhaust manifolds and helps in regulating the amount of exhaust gases to be recirculated to the engine inlet. The pneumatic EGR valves have the advantage of better thermal resistance but have a problem of low actuation force for opening of the valves. The earlier versions of pneumatic valves are currently replaced by electric valves because of their faster operation and precise control. The electric EGR valves consist of the valve body, actuator and a position sensor which will together aid in its efficient operation.

Fig 1.5: Pneumatic and electrically operated EGR valves (source: Hella)

1.9.2 EGR Intercooler

This component is specifically applicable for systems that utilise partially or fully cooled EGR. The function of intercooler is to cool the exhaust gases before recirculating into the engine cylinder. During cold start operations, the intercooler is most often bypassed. The intercooler will be essentially a heat exchanger in which the heat of the exhaust gases is taken away by a working fluid or ambient air convectively. The EGR cooler increases the EGR efficiency and brings down the NOx emissions drastically.

1.10 Present Work

The present study deals with the experimental investigation on the effect of magnetic field assisted combustion on combustion, performance and emission characteristics of a multi cylinder MPFI SI engine fuelled by a liquid phase (gasoline) and a gaseous phase (LPG) fuel. The experimental study is carried out on a Maruthi Zen made engine of 44.5 kW capacity provided with necessary instrumentation for the measurement of combustion, performance and emission characteristics. Varying intensities of magnetic field created by strong rare earth based NdFeB magnets are applied on the fuel line to investigate the effects produced on the engine combustion. An eddy current dynamometer is provided to load the engine and a sequence of experiments are carried out with variation in operating parameters such as load and speed, magnetic field intensities, magnetisation pattern and polarity. The same test engine is modified to run on neat LPG incorporating a commercial LPG kit and a gas ECU and the experiments are repeated for the gaseous fuel. An Exhaust gas recirculation set up is fabricated to supply the engine with a part cooled EGR and experiments are conducted to study the optimum EGR percentage which will boost the performance and emissions of the engine. The parameters like magnetic field intensity, magnetisation pattern and EGR flow rate are optimised at four different loads and speeds. The synergetic effect of optimum EGR percentage and optimum magnetic field intensity is also studied for both fuel phases. The emissions exhausted from the engine are analysed using a five gas analyser unit which shows the content of Carbon monoxide, Carbon dioxide, hydrocarbons, oxides of

nitrogen and oxygen. The cycle to cycle fluctuations in combustion are studied using statistical tools. The optimised results are compared with the baseline readings of both the fuels.

1.11 Organisation of Thesis

The thesis has been structured into five chapters beginning with this introduction. In the introduction chapter the background of the problem is discussed and the technologies utilised are introduced. In the second chapter in depth literature review is carried out on the various techniques employed in this work. It includes the study of LPG as an engine fuel, magnetic field assisted combustion, exhaust gas recirculation and cycle by cycle variations in combustion and how the previous research on these topics turned out. With reference to this literature review, the research gap is identified and specific research objectives are designed. The third chapter explains the experimental set up, equipments and instrumentation utilised in the present work. The modifications made on the engine, procedure followed for the selection of magnetic material and grades are all discussed in detail. In chapter four the experimental methodology is discussed along with the error and uncertainty analysis of various measurements. The results obtained from the experimental work along with the discussions are presented in chapter five. The conclusions drawn from this research is presented along with the recommendations for future research on this topic in the final chapter.

CHAPTER 2

LITERATURE REVIEW

The serious threat of depletion of fossil resources and the exponential growth in their demand has hovered the global energy security. This necessitates the exploration of competent energy policies for transportation and power production to balance the supply and demand of fossil energy. Special care need to be taken on the impact that is caused on the environment due to the stringent emission norms adopted globally to resist environmental degradation. In this chapter a comprehensive review of literature is carried out on the application of LPG as an alternative fuel, the impact of magnetic field on structure and properties of hydrocarbon fuels, the effect of magnetic field assisted combustion on the performance and emission characteristics of combustion engines, cycle by cycle variations in combustion and the influence of exhaust gas recirculation in modifying the combustion properties of the fuel employed. This survey of literature has been carried out from various international journals, white papers, conference proceedings, dissertations, transactions and energy reports in which similar research is reported.

2.1 APPLICATION OF LPG AS AN ALTERNATIVE FUEL

The standard fuels that can be employed in spark ignited internal combustion engines as alternative fuels are CNG, LPG, ethanol, methanol and hydrogen (Schoenung 2001, Durgun 1988). Liquefied Petroleum Gas is a promising alternative fuel to combustion engines because of their reduced cost, higher calorific value, high octane number and cleaner emissions. As it can be produced from natural gas, LPG can be considered a renewable fuel with advantage over gasoline in case of economy and emissions. Many researchers have studied the performance and emission characteristics of engines operating under neat LPG as well as LPG blends which will be discussed below.

Price et al. (2003) analyzed the thermodynamic performance of evaporator in Ford Focus over the entire power range. The switch over characteristics from gasoline to LPG was studied by conducting tests at two extreme operating temperatures. They observed minimal effect of LPG composition on performance parameters due to the similar calorific values of the constituents. The evaporator performed acceptably under LPG fuelling for periods of lower than usual engine efficiencies.

The flame propagation and combustion attributes of LPG fuel was experimentally studied by Lee and Ryu (2005) by employing Laser deflection method and Schlieren photography. They observed that the flame propagation velocity of LPG got to maximum value at stoichiometric equivalence ratio in the constant volume combustion chamber. The flame propagation speed of LPG was found to be higher when the ambient pressure was reduced. The flame speed of LPG was found to be higher than that of gasoline in the leaner range and stoichiometric equivalence ratios.

Bayraktar and Durgun (2005) studied the effect of LPG fuelled operation on the combustion characteristics of a single cylinder engine. Their experimental results reported significant refinement in emissions under LPG operation. But the effects produced on certain performance parameters and structural elements of the engine were not encouraging. They recommended the operation of LPG at higher compression ratios because of higher research octane number which can improve the fuel efficiency and engine efficiency subsequently.

A specially designed electronic circuit to accurately control the air fuel ratio was employed to inject gasoline and LPG into the manifold of a two stroke engine and the effects were studied by Loganathan and Ramesh (2007). They observed that the brake thermal efficiency of the test engine was higher during LPG operation when compared to gasoline fuelled operation. The injection pulse width that effectuated maximum brake thermal efficiency begot the minimum emission levels of hydrocarbons. A slightly higher level of exhaust temperature and HC emissions were reported for LPG when compared to gasoline which could be tackled by the usage of suitable after treatment devices and

optimised spark timings. The fluctuations in combustion and the peak cycle pressure were lower in the case of LPG operation.

The performance and emission characteristics of a variable compression ratio engine powered by LPG were investigated by Ozcan and Yamin (2008). They reported that the performance and emission characteristics of LPG fuelled engines can be enhanced by the variable stroke technique. Diminutive stroke lengths increased the cylinder temperature and pressures thereby inducing mechanical as well as thermal stresses on the structural components of the engine.

Jothi et al. (2008) studied the effect of exhaust gas recirculation on a homogenous charge compression ignition engine under LPG operation. They added diethyl ether in liquid state immediately before the intake manifold which melds with LPG air mixture. Considerable reduction in the oxides of nitrogen was observed in the case of recirculation when compared to normal operation of the engine under LPG fuelling.

The emission characteristics of newly introduced bifuel automotive engine employing gasoline and LPG were studied by Saraf et al. (2009) in accordance with Bharat stage III norms. They reported that the hydrocarbon emission levels varied between 18 ppm to 63 ppm and oxides of nitrogen varied between 800 ppm and 3900 ppm. The power per unit displacement, torque output and brake mean effective pressure is observed to be more for gasoline operation than in LPG mode.

Lee et al. (2009) studied the effect of blending of dimethyl ether in LPG in a spark ignition engine. Their experiment showed that the engine operated with stability up to 20% blending of DME. The blended fuel resulted in slightly increased emission levels of hydrocarbons and NO_x at lower engine speeds. The lower energy content of DME in the blended fuel also resulted in the deterioration of output power and brake specific fuel consumption of the test engine. The high cetane number of DME also triggered intense knocking which further deteriorated the performance of the fuel blend.

Shankar and Mohanan (2010) investigated LPG injection into a multi cylinder multi port fuel injection gasoline engine and the effect produced on combustion, performance and emission characteristics of the engine. The authors observed an adverse effect on NOx emissions as they advanced the static ignition timing. Their results also proved that improved fuel economy and hence a higher thermal efficiency can be achieved from SI engines when LPG is used as the fuel instead of gasoline.

Different alternative fuels including hydrogen and LPG were comparatively studied on the basis of the performance and combustion characteristics generated by them by Pourkhesalian et al. (2010). They observed that the volumetric efficiency of the test engine decreased up to 28% when hydrogen was used as the fuel as opposed to gasoline. The output power of the engine under gasoline exceeded all the tested alternative fuels and they concluded that liquid fuels are able to generate more power with lesser oxides of nitrogen emissions than the gaseous fuels.

Massi (2012) attempted to analyze the combustion characteristics of LPG in a spark ignited engine in dual fuel mode employing a standard conversion kit. He reported the debilitation of performance characteristics in port injection system caused by the decline of volumetric efficiency and inadequate fuel delivery. The air requirement for the combustion of LPG was found to be 46% lesser than gasoline. He also reported that the venturi area of the mixer in the conversion kit influences the power output.

The effects produced on the emission characteristics of the engine by the alterations in volumetric efficiency at different blending percentages of LPG were studied by Gumus (2011). The engine was operated in a sequential multi point injection system with the LPG content varying from 25% to 100%. His results showed that the volumetric efficiency of the engine reduced significantly with increasing LPG content. Air-fuel ratio was found to decrease with increasing percentage of LPG. The increasing levels of LPG had a positive impact on exhaust emissions. The carbon monoxide and hydrocarbon emissions reduced up to 53.3% and 72.6% respectively when the engine was operated under neat LPG.

Wu et al. (2012) investigated the reduction of pollutant emissions and improvement of engine performance utilizing semi direct injection of LPG in an SI engine. The conventional engine was retrofitted by introducing a new intake port with enhanced swirl of intake flow. The semi direct injection consisting of higher swirl resulted in reduction of brake specific energy consumption up to 19.2%. The emission levels of CO and NO_x reduced by 94% and 47% respectively but the HC levels increased by 4.5%.

Elnajjar et al. (2013) experimentally analyzed the effect of varying compositions of LPG on a single cylinder spark ignition engine. They observed that the variation in LPG composition had negligible effect on engine efficiency. However the variations in composition strongly influenced levels of combustion noise generated.

Erkus et al. (2013) studied and compared the carburetion and injection techniques for LPG fuel in a single cylinder SI engine. Their experimental results indicated that higher output power, lower fuel consumption and minimal exhaust emissions are observed in the LPG gas injection system compared to the carburettor system.

The research octane number (RON) and the motor octane number (MON) for LPG fuel were experimentally calculated by Morganti et al. (2013). They reported that both the research octane number and the motor octane number for LPG are higher than that of gasoline and hence suggested that LPG could be used at higher compression ratios to improve the performance and emission characteristics of the engine.

Sulaiman et al. (2013) experimentally analyzed the performance of a single cylinder spark ignition engine under LPG operation. Their results showed that the output power of the engine reduced up to 4% under LPG fuelling when compared to gasoline operation. Interestingly, the fuel economy of the test engine improved up to 28.38% in the case of LPG operation which led to an increase in the thermal efficiency of the engine.

Pipitone and Genchi (2014) investigated the simultaneous combustion of gasoline and LPG on a standard CFR engine equipped with double injection system. They observed a quadratic dependence of octane number as function of concentration of LPG. They concluded that higher compression ratios could be adopted in bifuel engines owing to the improved knock resistance which may lead to higher efficiencies and improved fuel economy of the engine.

Morganti et al. (2015) studied the parameters that influenced auto ignition of LPG in a CFR engine. They observed that both fuel oxidation and auto ignition was strongly promoted by nitric oxide (NO). They also concluded that cognitive concentrations of hydrocarbons and carbon monoxide had a negligible effect on the auto ignition characteristics of LPG.

The influence of LPG injection temperature on the performance and emission characteristics of a single cylinder spark ignited engine was investigated by Ceviz et al. (2015). By accurately controlling the LPG temperature before injection, the performance of the engine along with the emission of NO could be enhanced. Compared to the normal injection of LPG, the injection with controlled temperature resulted in the decrease of oxides of nitrogen up to 2%.

Cinar et al. (2016) reported the impact of various valve lift positions on a single cylinder SI engine when LPG is utilized as the fuel. The application of LPG led to the reduction in torque, power and efficiency of the engine. However positive results were obtained in the case of engine emissions.

A mixture of LPG and hydrogen was experimented by Kacem et al. (2016) in an SI engine. Their test results suggested that the exhaust emissions of the engine vastly reduced under LPG operation. The effect of hydrogen enrichment on in-cylinder flow characteristics were analyzed numerically and experimentally. A reduction of 3.25% was observed in NOx under LPG-hydrogen operation as compared to gasoline operation.

Nayak et al. (2017) studied the effect of varying blend percentages of LPG in a multi cylinder MPFI SI engine for different load and speed ranges. They observed that CO and HC emissions reduced significantly with increasing percentage of LPG. The emission of oxides of nitrogen increased to almost four times under neat LPG operation. Peak cylinder pressures and mean effective pressures increased in proportion to the LPG ratio with the combustion becoming more inconsistent at higher speeds. Their study also showed that water-methanol induction could be used for reducing NO_x under LPG operation.

Nutu et al. (2017) experimented the utility of LPG as a fuel in diesel engines. Experiments were carried out on a turbocharged diesel engine under 40% load and an engine speed of 1750 rpm. At a substitution ratio of 25%, the brake specific energy consumption of the engine reduced up to 20%. The emission of NOx was also found to decrease to almost 25% at the same substitution ratio. As the combustion of diffusive mixture reduced in the presence of LPG in the combustion chamber the smoke levels were found to diminish. Also the maximum rate of pressure rise in the case of LPG was higher when compared to baseline operation.

Ravi et al. (2017) studied the effect of exhaust gas recirculation on a spark ignition engine to arrive at the optimum flow rate of recirculation which provided the best performance characteristics. The incylinder temperature got reduced by the inclusion of cooled EGR and subsequently the generation of thermal NOx reduced substantially. When the flow rate of EGR was increased further beyond the optimum values, the charge got over diluted leading to deterioration in combustion which was evident from partial and complete misfires.

2.2 EFFECT OF MAGNETIC FIELDS ON PROPERTIES OF HYDROCARBONS AND FLAME BEHAVIOR

Shoogo Ueno (1985) studied the effect of magnetic fields on the structure of flames and gas flows under external combustion using methane, propane and hydrogen as test gases.

He observed that the shapes of the flames were drastically changed by the magnetic field, independent of the gases used. The combustion velocity was also found to increase in proportion to the gradient of the field. In another study (1987) they observed that combustion velocities and temperatures are influenced by magnetic fields. Gradient magnetic fields of the range 20-200 T/m were able to bring down the combustion temperature of alcohol up to 200ºC. It was also observed that the concentration of paramagnetic oxygen otherwise disturbed by other gases could be restored by the applied magnetic field.

Guo et al. (1988) proposed the effects of magnetic field on the physio-chemical properties of individual hydrocarbons. They observed a fractional change in viscosity of hydrocarbon fuel on the application of a magnetic field. The magnitude of viscosity change was found to be increasing with increasing strength of the magnetic field. The more the carbon numbers of the normal paraffinic hydrocarbons, the more rate of decrease of viscosity was observed. Their study showed that surface tension of hydrocarbons also decreased marginally upon magnetisation.

Wakayama (1992) observed that a combustion reaction was initiated when a fuel gas is made to flow in a downward gradient magnetic field. His investigation on methane diffusion flames proved that a negative gradient field increased the combustion rates for diffusion flames whereas the field had little effect on premixed flames. He also suggested that a gradient magnetic field can control a chemical reaction in which the magnetic susceptibilities of individual species are involved.

The potential of a constant magnetic field in altering the propagation conditions of a combustion wave was studied by Morozov et al. (1999). They observed an increase of combustion velocity by 30% in a 0.27T magnetic field. This increase in combustion velocity is attributed to the degree of agglomeration of the system in a magnetic field. A combustion electromotive force is developed owing to the ionisation of the reagents and intermediate products in the combustion front.

Baker and Varagani (2000) examined laminar diffusion slot flames under non-uniform magnetic fields. Slot flames were chosen for the study because of the simplicity of obtaining a symmetric magnetic field around them during mathematical modeling. They observed a decrease in maximum flame temperature with the application of an upward decreasing magnetic field.

The numerical simulation of airflow at intake under the influence of magnetic field was studied by Iwata et al. (2000). They reported that after achieving a steady state the flow of air doubled in the case with magnetic field at the same pressure difference. The reason for the increased air flow was due to the removal of congestions at the intake by the applied field.

Tung et al. (2001) studied the changes in fluidity of crude oil in the presence of magnetic forces. Paraffin crystallization induced by the magnetic fields was analyzed under scanning electron microscope. They deduced the dependence of viscosity change of crude oil on magnetic field strength, temperature and the duration of applied fields. The effect produced on the viscosity is owed to the changes brought about in electron rotation and translation patterns by the applied magnetic field.

The effect of a magnetic field on the structural and rheological properties of crude oils with various concentrations of resins, asphaltenes, and paraffin hydrocarbons was examined by Loskutova et al. (2003). It was found that in high viscosity oils, the characteristics such as viscosity, antioxidant and paramagnetic properties are affected when subjected to magnetisation. The time of complete recovery of paramagnetic and antioxidant properties coincides with the recovery time of the rheological characteristics of petroleum.

A strong pulse magnetic field with suitable duration was applied in the investigation of Tao (2004) which was found to reduce the viscosity of gasoline and diesel. The viscosity reduction was only for some hours and the original property values were regained after some time. In another study Tao &Xu (2006) investigated the

relationship between applied magnetic field and viscosity of an MR fluid and crude oil, the optimum duration of magnetic field application and the average size of particle clusters when duration of applied magnetic field is increased. It became evident that the Paraffin particles have different magnetic permeability from the solvent which resulted in the viscosity reduction.

The time required for heating a fixed quantity of kerosene was taken as a parameter for the calculation of thermal efficiency by Saksono (2005). Magnetic intensity, pole orientation, fuel flow rate and distance of magnet from burner were varied for examining the effects. From his research, it is evident that magnetisation can increase the efficiency of kerosene stove, the maximum improvement being 17.5%.

Chang and Weng (2006) observed an increase in the number of hydrogen bonds in liquid water when the strength of applied magnetic field was increased. They deduced that the size of any molecular cluster can be controlled under the influence of an external magnetic field. The molecular dynamics simulations revealed that the molecular structure became more stable with enhanced bonding capability under magnetic fields with reduction in self diffusion coefficients.

Gillion et al. (2008) conducted experiments on a burner to which propane is issued vertically through an open cylindrical cavity, which is placed inside the air gap of an axisymmetric superconducting magnet. The interaction of magnetic field on combustion was explained based on three mechanisms-Lorentz force, direct effect on chemical reactions and indirect effect on oxygen.

Evdokimov & Kornishin (2009) carried out a critical study to disprove the earlier published physics of viscosity reduction due to magnetic fuel conditioning. They concluded that that viscosity reduction due to MFC occurs due to disaggregation of colloids in the oil.

The effect of a high downward decreasing magnetic density on a laminar methane diffusion flame was studied by Legros et al. (2011). A flickering of flame was observed

in their study with downward gradient magnetic flux ranging from 0.4 to 1.4 T^2/m. They also suggested that buoyancy and shear stress may be strengthened by the magnetic force, thus hastening the instability onset.

The effect of magnetisation on n-hexane and benzene in molecular and electronic scale was investigated by Jalali et al. (2013). Their tests using UV-visible and FT-IR techniques suggested that Frank-Condon factor (FC), which is a measure of vibrational states of molecules, is affected by magnetisation. On exposure to strong magnetic fields, the hydrocarbon molecules got modified by activating new vibrational modes. This resulted in increased kinetic energy and free energy of fuel, thereby increasing the combustion enthalpy.

The effect of magnetic field on fuel properties was studied by Ugare et al. (2014) whose findings include a reduction in density up to 1.25% and an increase in calorific value by 1.19% when gasoline was used as the test fuel. This effect is accounted on the change in orientation of hydrocarbons from para to ortho state under the influence of strong magnetic fields.

Kumar & Shakher (2015) conducted experiments on premixed, partially premixed and diffusion flames generated by butane torch burner in the absence of magnetic field and in the presence of uniform and non-uniform magnetic fields. They studied dimensionless parameters like magnetic Grashoff number, magnetic Froude number and Reynolds number to find out how butane fames are affected in the presence of a magnetic field. It is evident from their results that oxygen concentration is reduced because of dominance of momentum force on butane gas.

Agarwal et al. (2015) made use of a Tablot interferometer to study the impact caused by magnetisation on the temperature profile of a diffusion flame. They observed that an upward increasing magnetic field resulted in the decrease in flame temperature and vice versa. Their study also proved that very little or no effect is produced on the temperature of a flame by a uniform magnetic field.

The Effect of magnetic field on physical properties and Cetane number of diesel fuel was investigated by Elamin et al. (2015). Density and viscosity reduced on magnetisation because some of the branched and ring compounds are converted to linear hydrocarbon chains. In addition, they observed an increase in Cetane number of diesel from 56.6 to 60.3, which indicates that the quality of fuel was improved.

The interaction of magnetic fields with combustion was studied through various dimensionless numbers by Singh (2015). He studied Froude number, Grashoff number and Reynolds number and assessed that flame behavior is affected by magnetic fields.

An experimental investigation of properties of methane laminar combustion under strong magnetic fields was conducted by Wein-Fei Wu et al. (2016). In this natural gas fuelled test, they observed that an increasing gradient field intensity in the vertical direction resulted in an increase of flame temperature by 52 K on an average.

An experimental study of combustion of wood biomass using the propane co-fire and swirl-induced stabilization of the flame reaction zone was carried out by Barmina et al. (2016). They concluded that the field-enhanced mixing of the flame compounds and combustion of the volatiles promotes a radial expansion of the flame reaction zone, decreasing CO and H_2 mass concentration and increasing the CO_2 and NO_x volume concentration and total amount of produced heat. Their results have shown that the magnetic force, acting on the flame flow enhances the mass transfer of paramagnetic oxygen in a field direction to the surface of burning wood fuel by enhancing recirculation with the reverse axial flow formation and more intensive mixing of the flame compounds.

The variations induced on flame velocity, composition, temperature and combustion efficiency profiles by a magnetic field were experimentally studied by Barmina and Zake (2018). Their results show that the enhanced mass transfer due to magnetism significantly disturbs the axial and tangential velocity and composition profiles. Thus, combustion reactions get enhanced along the outside part of the reaction zone.

2.3 STUDIES ON MAGNETIC FIELD ASSISTED COMBUSTION IN ENGINES

NdFeB magnets of varying intensities were placed with their north poles facing the radiator core on a single cylinder two stroke spark ignition engine by Govindasamy et.al (2007). Brake Thermal Efficiency and peak pressure of the engine increased by 3.2% and 6.1% respectively together with a reduction of unburnt hydrocarbons and Carbon monoxide. In another work (2007) they applied mono pole technology and deduced that peak pressure increases for each cycle as the magnetic strength was increased. Govindasamy & Dhandapani (2008) tested the magnetic conditioning of Jatropha Biodiesel on a single cylinder four stroke diesel engine. Thermal Efficiency increased up to 5% and emission of NO_x became near zero.

A reduction of SFC by 15% together with a decrease in emission concentration of CO, HC and NO_x was obtained by Fatih et al. (2010) when permanent magnets were used on a four cylinder four stroke petrol engine. They also observed that magnetic ionization of the fuel helped in dissolving the carbon build up in fuel injector, carburetor and in combustion chamber thus improving the overall life of the engine. The concentration of methane reduced up to 40% as the magnetic field aided in more complete burning of the fuel.

Faris et al. (2010) investigated the effect of magnetic field on microstructure of fuel using ultraviolet and infrared absorption spectrums. They reported that the strength of ultraviolet absorption increased significantly when the aromatic hydrocarbons were magnetized. The increased absorption strength corresponds to higher probability of transition of electrons to higher energy levels from the Π-bond conjugated system. As more and more electrons transit from ground state to higher energy states the C=C bonds in the aromatic rings get split in the course of combustion resulting in the breaking of molecular clusters thereby improving combustion efficiency. The tests were extended on to a two stroke spark ignition engine in which specific fuel consumption showed a reduction up to 14%. Emission of UBHC and CO decreased up to 30% and 40% respectively, but an increase in 10% was noted in carbon dioxide emission.

The performance and emissions of a single cylinder four stroke VCR petrol engine was investigated with ignition timing varying between 5 degree and 30 degree bTDC in steps of 5 degrees each by Habbo et al. (2011) using magnetic coils of 1000G and 2000G. Considerable decrease in specific fuel consumption and a significant decrease in exhaust were noted. There was also a fall in exhaust gas temperature up to 8%.

Both the fuel and air lines of a single cylinder, vertical diesel engine were magnetised using permanent magnets by Jain et al. (2012). They observed that maximum reduction in fuel consumption was at highest loads when the load is varied from 0 to 10 kg. The authors suggested the usage of neoprene insulation to prevent thermal damage to the magnets. The mileage of the vehicle increased in the range of 10-40% in their tests.

Two electromagnetic fuel savers with cores made up of plain carbon steel and copper were developed by Siregar and Nainggolan (2012) and tested both in laboratory and on road conditions. Copper core was found more effective in inducing magnetic force than steel, though theory proposed the opposite case.

Attar et al. (2013) conducted tests on a stationary diesel engine as well as on board a motor bike with applied magnetic intensities varying from 2000G to 8000G. The mileage of the bike was found to increase about 7kmpl in the on board tests. The authors suggested that field intensity values above the optimum case can deteriorate the engine performance because higher magnetic intensities cause the viscous heating of the fuel.

A set of on board experiments were carried on engines of various automobile brands fuelled with magnetically conditioned gasoline by Garg et al. (2014). All brands showed an improvement in performance and emission characteristics, though the percentage of improvement varied depending on the make of the engine. On an average mileage increased by 15 to 25%.

Vijayakumar et al. (2014) applied NdFeB magnets of 6000G coated with Ni-Cu-Ni on a single cylinder four stroke diesel engine. AFR was found to change from 31.38 to

33.8 with a noticeable improvement in performance and emission characteristics. They suggested that magnetic fields are able to enhance the internal energy of the fuel through molecular radicalization which resulted in easier and better combustion.

Abdel-Rehim et al. (2014) conducted a series of experiments to explore the effect of magnetic fuel treatment on the performance of combustion engines. Gasoline, diesel and natural gas were tested in two different engines with different configurations under the exposure of magnetic field. Their study concluded that the highest impact of magnetisation was on gasoline fuel compared to the other two fuels. They suggested that magnetic fields would have higher influence on liquid phase fuels because of their ability to transform into simpler structures. The magnetic effect on hydrocarbons would be lost faster in the gaseous phase because of random organization of molecules. The fuel economy of the engine improved up to 15.5% with the applied magnetic field under gasoline operation.

Patel et al. (2015) made investigations on a diesel engine with the application of magnetic conditioning alongside catalytic convertor. Maximum improvement in performance and emission characteristics was obtained by the combination of both technologies. The amount of CO_2 and O_2 in the exhaust increased with these modifications.

Sala & Notti (2015) installed an electromagnetic device on board a fishing vessel. An overall reduction of 4.6% was observed in fuel consumption after the installation of magnetic device. CO reduced by 14.1%, but CO_2 increased by 11.4%. An inspection proved that the injectors of the vessel that used the magnetic device were in a cleaner and better condition.

Khedawan & Gaikwad (2015) studied the effect of magnetic fields on hydrocarbon-based refrigerant R600 and non-hydrocarbon based R134A for a vapour compression system. Fuel consumption and exhaust concentration reduced for

hydrocarbon based R600 upon magnetic conditioning. There was no effect for the magnetic field on non-hydrocarbon based refrigerants.

A Mercedes Benz engine fuelled by Iraqi gasoline was magnetised and put under study by Mohammed Al-Rawaf (2015). A reduction of fuel consumption by 5.5% and an increase in brake thermal efficiency up to 13.5% was obtained in this work.

Gabina et al. (2016) studied the utility of magnetic devices in increasing the energy efficiency of fishing vessels. They tested three independent magnetic devices on three different compression ignition engines under different operating conditions. Fuel consumption was found to decrease at larger loads in laboratory conditions. A notable reduction in CO emissions at lower engine speeds was also observed.

Gad (2016) conducted experiments on a single cylinder, four-stroke kirloskar diesel engine only at full load and no load conditions. SFC reduced by 3% to 8.5% from no load to full load. CO emission reduced by 10% and 4.5% whereas NO_x reduced by 13% and 24% respectively.

The impact on the performance and emissions of a diesel generator when a magnetic tube is included in the fuel intake was investigated by Chen et al. (2017). A decrease in specific fuel consumption of 3.5% and an increase of brake thermal efficiency by the same magnitude was observed in their experiments.

Tipole et al. (2017) investigated the performance of a diesel engine with magnetic flux integrated on the fuel line. Experiments were conducted on a single cylinder four stroke diesel engine at a constant speed of 1500 rpm with the load varying from 0 to 8 kg. The highest improvement in fuel economy was observed with an intensity of 9000 G after which the fuel consumption began to increase again. A drop in fuel saving pattern was observed as the load on the engine was increased.

Kurji and Imran (2018) conducted tests on a single cylinder four stroke CI engine with permanent magnets installed before the injection pump. Fuel consumption reduced

up to 15.71% owing to reduced surface tension due to magnetisation. The emissions like CO, HC and NO_x also reduced significantly.

Sahoo and Jain (2019) investigated the effect of magnetic fuel conditioning in a diesel engine with nano fuel additives. NdFeB magnets of magnetic intensity 3000 G were chosen for experimentation along with CuO nano fuel. Magnetic field effected better atomisation and dispersion of fuel particles resulting in higher thermal efficiencies. The ideal position of placing the magnets was experimentally concluded to be adjacent to the fuel injector. An average 4% improvement was observed in the case of fuel economy and thermal efficiency. Carbon monoxide and NO_x showed a reduction of 17% and 19% respectively under magnetic conditioning.

The effect of a magnetic intensity of 9000 G on a multi cylinder gasoline engine was studied by Niaki et al. (2019). Magnetic fuel conditioning was observed to improve the fuel economy in the range of 4 to 12%. The emissions of HC and NO_x reduced up to 18% and 10% respectively under the influence of the magnetic field.

2.4 STUDIES RELATED TO CYCLIC VARIATIONS IN COMBUSTION

The performance and emission characteristics of any automotive engine can be improved by achieving lean burning. The major challenge associated with lean burn operation is the increase in cyclic variations of combustion induced by it. The cyclic variations in combustion can affect the engine performance and can even affect the drivability of the vehicle. Hence the operating conditions with lean mixtures are limited by the cyclic variations. Both physical and chemical phenomena can result in these variations. Research has alluded that a 10% increment in output power could be achieved with the same amount of fuel if the cycle by cycle variations in combustion could be eliminated (Heywood 1988).

The dependence of non-homogeneity on cyclic variations in combustion was investigated by Pundir et al. (1981). They reported that at a given mixture strength the charge non homogeneity increased the cyclic variations.

Yammamoto and Misumi (1987) employed multiple regression analysis to diagnose the source of cyclic variations in a lean burn SI engine. They identified that the heat quantity variation was the major source of IMEP variations. The dependence of emission of unburned hydrocarbons on cyclic variability was drawn by Chen et al. (1993). They reported that cyclic variations in combustion could be lessened by reducing the hydrocarbon emissions which will in turn increase the engine's performance.

Ozdor et al. (1994) reviewed the available literature with specific discussions on various parameters and their contributions to combustion variability in spark ignition engines. They observed that the quantitative effect of various variables on cyclic variation could be identified from pressure related parameters like IMEP and P_{max}. The influence of swirl on cyclic variations in a lean burn spark ignition engine was investigated by Whitelaw and Xu (1995). They observed that combustion rate was retarded by the extent of residual burned gas which increased the cyclic combustion variability.

Ishli et al. (1997) studied the variability in mean effective pressures under lean burn. They distinguished the factors responsible for variations in IMEP as burning velocity during initial phase of combustion, mass of fuel burned and variations during the dilatory phase of expansion stroke. The impact of spark gap and combustion chamber geometry on lean burn limit was analysed by Einewall and Johansson (2000). They reported that the geometry of combustion chamber is significant in lean burn operation. The combustion chambers that promoted slow burning with very low turbulence were found to induce more variations in combustion.

Lee and Kim (2001) observed that the stability of combustion is dependent on the cyclic variations in combustion and suggested that the analysis of cycle to cycle variation is the optimum tool for improving the fuel economy and exhaust emissions of the engine. The influence of cyclic combustion variations on the emissions of oxides of nitrogen was numerically analysed by Villarroel (2004). He suggested that the study of combustion variations should be considered in the overall evaluation of NO_x emissions.

Zervas (2004) developed correlations between cyclic variations and combustion parameters in a natural gas fuelled spark ignition engine. The coefficient of variation of cylinder pressure values corresponding to each crank angle was calculated and plotted against the crank locations. The cyclic dispersion was quantified using the peak integral of the COV curve. Maximum fluctuations in combustion were observed during the second period of combustion where the burned mass fraction lies between 0.5 and 1.

Ceviz and Yuksel (2005) studied the combustion variations occurring on a multi cylinder FIAT SI engine. They observed that the coefficient of variation in IMEP reduced with the usage of ethanol-gasoline blends. Consequently it led to the reduction in the emission of hydrocarbons and carbon monoxide and an increase in the percentage content of carbon dioxide. In another work (2006) they studied the lean operation of an SI engine with LPG as the fuel. The coefficient of variation of IMEP of the engine reduced under LPG operation indicating stable combustion. They suggested that the reduction in cyclic variations is owed to the increased flame speed and mixing characteristics of LPG which eventually reduces the emissions as well.

A spark ignited engine fuelled by CNG and hydrogen was analyzed experimentally for cyclic variations by Ma et al. (2008). Their results showed that hydrogen addition enabled the reduction of coefficient of variation of peak pressures and mean effective pressures as well. The limit of lean operation could hence be extended with the addition of hydrogen as a fuel. The time series of peak pressures for various spark advances were experimentally analyzed by Litak et al. (2009) in a multi cylinder SI engine. In this work the dependence of combustion variability on spark advance was statistically proven through histograms and return maps. The cyclic variations in a lean burn SI engine were studied by Ceviz et al. (2011). The authors investigated the effect of excess air on cycle to cycle variations, performance and emissions of the test engine. They deduced that the thermal efficiency of the engine could be increased by increasing the air excess coefficient under low loads.

Nayak et al. (2015) studied the cycle by cycle variations in combustion of a multi cylinder MPFI engine fuelled by liquefied petroleum gas. The peak pressures were found to increase with increasing percentage of LPG. Their results showed that LPG exhibited better combustion properties than gasoline but at the cost of increased variations in combustion. A statistical study on the correlation between combustion variability and knock was performed by Chen et al. (2017) on a PFI engine. The authors arrived at a linear correlation between burn rate and cycle to cycle variation. The tendency of knocking increased with a hype in combustion variation.

2.5 STUDIES RELATED TO EXHAUST GAS RECIRCULATION

Park et al. (2001) conducted an experiment on gasoline engine to assess the effects of EGR on combustion efficiency and emission criteria. They studied difference in IMEP to check combustion rate and stability. Introduction of EGR reduced NO_x level at a range of 25-89% with reduced power and BSFC. Therefore, it was necessary to advance spark to maintain firm combustion rate which lessens IMEP correspondingly. Also, advancing of spark timing developed increased brake power.

Abd-Alla (2002) investigated the outcomes of EGR in combustion engines and showed that EGR in C.I engine only lowered ejection of NO_x level chiefly, whereas in S.I engines predominant fall in NOx rate was obtained by applying EGR up to 25%. It also improvised fuel economy as a result of high heat release in cylinder but had a drawback of diminishing the combustion process. Hot EGR in dual fuelled engine raised engine performance and lowered NO_x, smoke release rate almost to zero. Cooled EGR though reduced NO_x ejection level was found to bring down the engine efficiency.

Olsson et al. (2003) surveyed on outcomes of EGR in a turbocharged multicylinder HCCI engine. As a result of minimal CO and HC release, there was an uplift in combustion efficiency. For attaining higher EGR value temperature of intake was maximized. In, turbocharged phase, because of drop in pressure and mass flow loss taking place, a constructive upshot of exhaust temperature with EGR was seen.

Avinash Kumar Agarwal et al. (2004) experimented the effects of EGR on dissipated temperature and smoke in a two-cylinder, air-cooled, direct injection C.I engine. Implementation of EGR minimized NO_x emission, but a drastic increase in PM level was noticed which can be controlled by the use of particulate trap technology. Temperature of dissipated gas diminished along with rise in smoke level due to higher value of EGR applied. Mainly, all these outcomes did not have any adverse effects on thermal efficiency and fuel consumption rate of the engine.

Vianna et al. (2005) experimented on S.I engine by amalgamation of EGR with turbocharger and by maximization of compression ratio to improvise engine working and lessen pollutants emitted. Firstly step-up of compression ratio from 8.2:1 to 8.9:1 diminished NO_x by its half value and boosted output by 10%. Secondly turbocharging configuration gave out better performance with an output power increment of 33% along with greater reduction of emissions which was attained by appropriate evaluation of spark timing, air-fuel ratio and amount of recirculation required.

Exhaust gas recirculation for better part and full load fuel economy in a turbocharged four cylinder spark ignition engine was studied by Carins et al. (2006) .They perceived that the fusion of both external and internal EGR supplicated ignition resulting in combustion and improved fuel efficiency at low loads. The concoction of surplus fuel, air and cooled external type EGR at higher loads imposed better resistance to knock and gave out superior combustion rate. In addition, it reduced the release of pollutants, in specific, unburnt HC by 70%, CO by 80% and CO_2 by 17%.

Introduction of graded EGR in LPG fuelled S.I engine operating with lower fuel proportioned A/F was studied by Youngwin Woo et al. (2006). They reported that the inlet operation schedule in cylinder was suitable for grading EGR. This graded EGR helped in attaining burning at high speeds, thus lessening burning time and raised heat loss level by 10% with 30% EGR rate. In addition, application of 20% EGR helped in diminishing NO_x discharge rate, specifically to an extent of 70%. They also outlined a positive influence of graded EGR on fuel economy.

Maiboon et al. (2007) conducted tests on out-turn of EGR upon combustion and discharge rates in a DICI engine. They reported fall in NO_x release with developing temperature at the inlet. Also, by expanding EGR value at small loads, there was shrivel in PM and NO_x ejection with a negative outcome of growth in BSFC, HC and CO release. Hence, they outlined that the possible way of lowering NO_x release without disturbing engine efficiency was giving constant A/F ratio value during introduction of EGR.

Influence of EGR upon efficiency and working of diesel engine was studied by Walker et al. (2008) which reported that the rise in EGR caused slight fall in engine efficiency with tiniest escalation in BSFC value. Emissions of NO_x dropped upon hiking EGR rates which also pushed up the smoke intensity.

Wang et al. (2010) analyzed EGT in direct injection spark ignition (DISI) engine for performance characteristics at part load. They studied that the use of exhaust gas trap lowered BSFC by 5 to 16% which is more desirable in lower load condition and ejection of CO, HC and NO_x reduced. NO_x depleted by 70% due to steps followed in mixing and evaporation in DISI engine. Pressure at inlet upswinged and the use of NOV caused problem in spark ignition which shortened the combustion rate. Still the step of using compression ratio with EGT at its higher value developed combustion timing. Increase in thermal efficiency was noted as a result of second-injection mass-ratio. They pointed that the role of second-injection mass-ratio is vital in the process of combustion and ejection.

The consequences of exhaust gas recycle delineated on spark ignition engine at full load criteria was audited by Galloni et al. (2010). They noticed spark advance and refinement in knock resistance showed up better engine performance, leading to lower fuel consumption, as a result of EGR installation at higher loads. Also EGR at wide open throttle increased spark advance which in turn expanded torque and minimized volumetric efficiency. They also showed that it was possible to attain low exhaust gas temperature with EGR by the use of three-way catalysts.

Wasiu et al. (2011) experimented on outcomes of actual EGR on SI direct injection engine working on CNG fuel. Increase in level of EGR brought down fuel consumed by engine along with lowered torque. There was noticeable deduction in discharge rates of NO and CO with EGR. Also, increased EGR put down O_2 in cylinder which had a consequence of push in unburnt hydrocarbons emissions.

Tutak et al. (2011) reported implementation of EGR in S.I test engine to check the emission criteria. It was noticed that the temperature of EGR diminished engine performance and mean effective pressure in addition to a rise in nitrogen oxides level. But cooled EGR had a chief role in minimizing NO release rate.

Shu et al. (2012) reported a study of exhaust recirculation on a petrol engine. EGR method enhanced fuel economy mainly. Hot EGR enhanced the rate of combustion and engine efficiency whereas cooled EGR raised volumetric efficiency level. Comparatively, release rate of NO_x came down with tiniest hike in HC and CO emission levels in cooled EGR. The cooled EGR also promoted the stepping down of knocking effect in engine.

Ponnusamy et al. (2012) experimented EGR on a single cylinder four stroke SI engine coated with several catalysts to test engine efficiency and discharge rates. They deduced that the catalytic coatings with 10% EGR lessened NO_x discharge level among which copper coating reduced the most, by value 48%. This was followed by other coatings like nickel and chromium which lowered NO_x release by 4% and 7% respectively. Further increasing EGR pushed brake thermal efficiency down with surge in HC and CO release rates.

Shojaeefard et al. (2013) tested cooled EGR on a four stroke turbocharged S.I engine to analyze the level of knock resistance and lessen the pollutants released. It was clarified that the usage of cooled EGR was a reason for reduction in BSFC by 14% and fall of CO and NO_x emission rates. The cut down in CO release was a result of EGR replacing high grade charges at full load.

Vincenzo et al. (2014) assessed the impact of injection of low pressure, cooled EGR on downsized turbocharged gasoline engine. At full load operation, greater knock resistance ability was attained with ameliorated fuel efficiency. The brake specific fuel consumption lowered by 5.9%. But there was a snag due to the extension in combustion timings.

Cooled EGR was tested in a turbocharged PFI petrol engine by Song et al. (2014) under lower pressure rates. For this purpose they increased compression ratio from 9 to 11 and came out with the results that the consumption of fuel diminished at a rate of 4.5% for 2000rpm. Installing EGR with it gave an additional improvement of 3.8%.

Nair et al. (2015) analyzed single cylinder air cooled four stroke Enfield SI engine with EGR to inspect the performance and emissions. They observed a cut in fuel usage by 10% for gas recirculated from exhaust having a value of 4.8% and slight enhancement in engine power. When gasoline was replaced with ethanol, emission came down predominantly by 40-50%.

Niranjan et al. (2015) aimed at experimenting hot and cooled EGR on CI engines to examine their outcomes on exhaust temperature, NO_x emission and engine performance using fuels such as diesel, bio-diesel and blends of bio diesel. It was analyzed that when diesel or bio-diesel were used as charges, there was a minimal release of NO_x. Eventually, this led to a drop down in engine performance. The use of cooled EGR led to poor combustion, which lessened the release of NO_x. Discharge of pollutants also decreased by blending of fuel which was proven by using 10% cooled EGR.

Chaichan et al. (2016) scrutinized the performance of a direct injection multicylinder CI engine using diesel methanol blended fuel upon application of hot and cool EGR. The action of hot EGR though reduced NO_x release levels, reduced engine thermal efficiency and brake power. But blending of methanol with diesel overcame the harmful outcomes of EGR on efficiency. The volumetric efficiency enhanced by 2.9% on addition of 10%

methanol. Cool EGR improved all the engine combustion parameters like power, thermal efficiency etc. Also, there was uplift in ignition delay on proper cooling of EGR.

The outcomes of cotton seed B20 biodiesel fuel and EGR on a single cylinder diesel engine was examined to test the efficiency, exhaust and combustion by Lahane et al. (2016) which concluded high NO_x emission levels with drop in CO and HC levels due to neat combustion of B20 biodiesel fuel. It also lowered the ignition delay period. But application of EGR at 4-6% lessened NO_x levels with slight rise in CO and HC discharge rate. However the rate of fuel consumption hiked with use of both EGR and B-20 biodiesel fuel.

Xu et al. (2016) observed that the spark timing could be advanced by 8 degrees giving 4.1% fuel reduction on adding 12% EGR. This happened as a result of less knock as EGR stepped down the temperature of in cylinder. Also, there was an appreciable reduction in fuel consumed and increased thermal efficiency was obtained. It was noticeable that the combustion particle accumulation increased and nucleation of combustion particles lowered by introducing EGR onto engine.

Bozic et al. (2017) demonstrated the technique to check the impacts on combustion parameters when stoichiometric fuel air ratio was introduced along with EGR in a petrol engine. It was tested for fixed and optimized spark timing which revealed that dilution of EGR improved IMEP of combustion process and dropped NO_x release. Also the application of EGR promoted better performance of engine avoiding almost all the abnormal conditions.

Ravi et al. (2017) investigated the effect of EGR rates in declining NO_x without influencing the performance characteristics of an LPG fuelled SI engine. They recognized that higher EGR rate widen HC and cooled EGR leads to misfire in engines at lower loads. For NO_x reduction, 5-10% EGR was found to be feasible with lean mixtures. They also noted that the percentage of EGR requirement were 25, 16 and 9 for 0.99, 1.07 and 1.21 kg/h of flow rate of fuel.

Jung et al. (2018) discussed the methodology on dedicated EGR capacity in enhancing engine efficiency under air-fuel ratio having lower fuel rate and in stoichiometric mixture condition. They observed increased burning effect on applying stoichiometric fuel with increase in CO and H_2 and lowered ignition on mixing water and CO_2 with it. They obtained higher thermal efficiency on amalgamation of dedicated EGR with A/F of lower fuel content by 42.9%. For stoichiometric charges, exhaust gas temperature increased with implementing dedicated EGR but a modest decrease in temperature with maximizing A/F ratio of lower fuel rate with D-EGR was observed.

Based on first and second law of thermodynamics, an investigation was undertaken for boosted gasoline engine by Li et al. (2018) to test the influence of cooled EGR on fuel economy and its efficiency in the conversion process. They noticed the hike in brake thermal efficiency by 1.1-4.1% on installing 12-17% of EGR. However, the increase in EGR alleviated the knocking tendency. They illustrated that the enhancement in fuel efficiency in conversion were on two aspects, one by diminish in heat losses influenced by EGR and the other by substituting EGR instead of rich fuel.

Lulic et al. (2018) studied the impact of EGR on S.I engine knocking rate which was mainly based on consequences of chemical thermal and propagation of flame conditions. Analysis made use of cooled EGR and hot air at intake port. It was evident that chemical conditions had zero effect on knocking. But the prime reason in pushing up the knock rate was found to be temperature of the end gases.

Rakopoulos et al. (2018) examined the impacts of EGR and temperature on a diesel engine for combustion and emission rates by changing injection durations. It seemed to lower incylinder temperature and pressure due to delay in ignition time. Cooled EGR installation minimized cylinder pressure and temperature, raised soot level and ignition duration, whereas hot EGR on installing gave higher cylinder temperature, minimal pressure and suppressed retard in ignition duration and lessened NO_x rate. Further fall off in engine efficiency was seen by a value of 6.2% on implementing 30% hot EGR and cooled EGR degraded efficiency by 3.7%.

Wasiu et al. (2018) examined impacts of EGR on efficiency and emissions of a stratified charge direct injection engine fuelled with compressed natural gas. On increasing rate of EGR, a drastic drop in NO_x level was noted which worsened the engine efficiency. But the method of boosting EGR had economically positive impact on fuel consumption rate.

2.6 Summary of Literature

A thorough survey of literature has shown that LPG can be employed as an effective alternative fuel in combustion engines. Previous research asserts positive impact of LPG on the performance and emission characteristics of the engines. The higher flame speed and higher octane number of LPG extends the limit of engine operation which can further improve the thermal efficiency of the engine. Many researches proved that combustion process is enhanced in the presence of strong magnetic fields. The polarization of hydrocarbon molecules leads to the disintegration of clusters which in turn improves the mixing of fuel with the oxidizer enhancing combustion. Exhaust Gas Recirculation is a proven technology in reducing emissions of the engine, especially oxides of nitrogen which will be substantially higher in the case of LPG combustion. Several modes of EGR have been explored by the previous researchers and the pros and cons of each have been documented.

2.7 Research Gap

A profound review of literature has exposed that very limited research has been done on the magnetic field assisted combustion of gaseous fuels. LPG, an extensively used automotive fuel has never been experimented under magnetic fields. Also extensive studies on combustion characteristics like in cylinder pressures and net heat release during each cycle in magnetic field assisted combustion has been rarely examined. The statistical analysis of combustion stability under strong magnetic fields is also not found in the existing literature. Experimental studies on exhaust gas recirculation in LPG fueled engines are very limited. Previous researches on magnetic field assisted combustion have

not examined the synergetic effect of beneficial techniques like exhaust gas recirculation which can provide added boons in combustion. These research gaps in technical literature motivate us in defining our research objectives which are enlisted in the coming section.

2.8 Objectives of the Research

Based on the reappraisal of literature we concluded that no works have been done on the magnetic field assisted combustion of liquefied petroleum gas combined with recirculation of exhaust gas. Therefore, the present study is aimed at investigating the effects of magnetic field assisted combustion of hydrocarbon fuels in liquid phase (gasoline) and gas phase (LPG) operation on the performance, combustion and emissions of a multi cylinder spark ignition engine along with the synergetic effect of part cooled exhaust gas recirculation. The operating parameters like load and speed of the engine, flow rate of recirculated gas, distance of magnetisation, intensity and field pattern of the applied magnetic field are varied for this investigation. The main goal of this experimental work is to optimize the magnetic field intensity, field pattern, distance of magnetisation and EGR flow rate which in combination will provide the best performance and emission characteristics of the test engine.

2.8.1 Specific Objectives of the Research

1. To study the performance combustion and emission characteristics of the multicylinder MPFI Spark ignition engine under gasoline and neat LPG with suitable modifications to the engine at various speed and load conditions.
2. To study the effect of axial magnetisation on the performance combustion and emission characteristics of the test engine under liquid phase (gasoline) and gaseous phase (LPG) operation and to arrive at optimum field intensity in axial pattern.
3. To study the effect of radial magnetisation on the performance combustion and emission characteristics of the test engine under liquid phase (gasoline) and

gaseous phase (LPG) operation and to arrive at optimized field intensity and magnetisation pattern.

4. To study the effect of distance of magnetisation in optimized magnetic field assisted combustion of hydrocarbons.
5. To study the performance combustion and emission characteristics of the engine with different flow rates of part cooled EGR under gasoline and neat LPG operation to arrive at the optimized flow rate of recirculated gases in each case.
6. To study the synergetic effect of optimum flow rate of part cooled EGR on optimized magnetic field assisted combustion of liquid phase hydrocarbons (gasoline).
7. To study the synergetic effect of optimum flow rate of part cooled EGR on optimized magnetic field assisted combustion of gaseous phase hydrocarbons (LPG).

2.9 Scope of the Research

The experimental investigation of magnetic field assisted combustion was performed on a multicylinder MPFI spark ignition engine in combination with part cooled exhaust gas recirculation. The test engine was modified to run on neat liquefied petroleum gas and loaded by an eddy current type dynamometer. The hydrocarbon fuels in liquid phase and gaseous phase are subjected to strong magnetic fields of varying intensities and two different magnetisation patterns and the impact produced on combustion is studied. A separate set up is fabricated for recirculating part cooled EGR into the intake manifold. The optimized flow rate of part cooled EGR is experimented along with optimized magnetic field and the synergetic effect is studied and compared for gasoline and LPG. This research is particularly useful as this technique can be implemented on already existing and newly developed hydrocarbon based fuels to power internal combustion engines with advantages in fuel economy and exhaust emissions.

CHAPTER 3

EXPERIMENTAL TEST RIG AND INSTRUMENTATION

In this chapter we discuss the development of experimental test rig including modifications made on the test engine and fabrications, materials utilized and their selection criteria and the instrumentation employed to monitor and measure the experimental data. Modifications and fabrications are so made as to satisfy the research objectives presented in the previous chapter. Discussion on instrumentation includes the description of all equipments that are utilized during the experiment to monitor the data. The criteria and procedure of selection of materials for the experiment are discussed in detail. The photograph of the materials and instrumentation are entailed wherever necessary in the different sections of this chapter.

3.1 Engine Test Rig

A 1.0L Maruthi Suzuki Zen made inline four cylinder engine with multipoint port fuel injection system (MPFI) was wielded to acquire the experimental data for this research work. The maximum power of the test engine is 44.5 kW at 6000 rpm. The engine has a lone camshaft overhead layout with two inlet and two exhaust valves per cylinder. A single fuel injector present in the intake runner injects the fuel into the intake port. The load on the test engine is applied and maintained using an eddy current type dynamometer. Necessary instrumentation is made to measure the experimental data including crank angle measurements, cylinder pressure, air flow, fuel flow, temperature and load measurements. An 8 channel interface is used to interface the signals from these instruments to a digital computer. The engine has a standalone panel box which accommodates air box, fuel tank, fuel measuring unit, manometer, differential pressure transmitters for fuel and air flow measurements, engine indicator and process indicator. The provision of cooling water is arranged using a Rotameter and the flow of water is regulated using calorimeter. The schematic of the experimental rig is shown in figure 3.1 and the photographic view is given in plate 3.1.

The developed experimental test rig permits the investigation of engine performance through brake power, indicated power, frictional power, brake thermal efficiency, indicated thermal efficiency and brake specific fuel consumption. National Instruments based USB-6210 data acquisition system assimilates the signals from various sensors and interface into the PC. The online performance and combustion monitoring and analysis is performed using a software package named IC Engine Soft provided by Apex Innovations Pvt. Ltd. This software estimates the combustion parameters in terms of heat release rate and incylinder pressure in terms of crank angle. The comprehensive specifications of the test engine and included instrumentation are furnished as Appendix I.

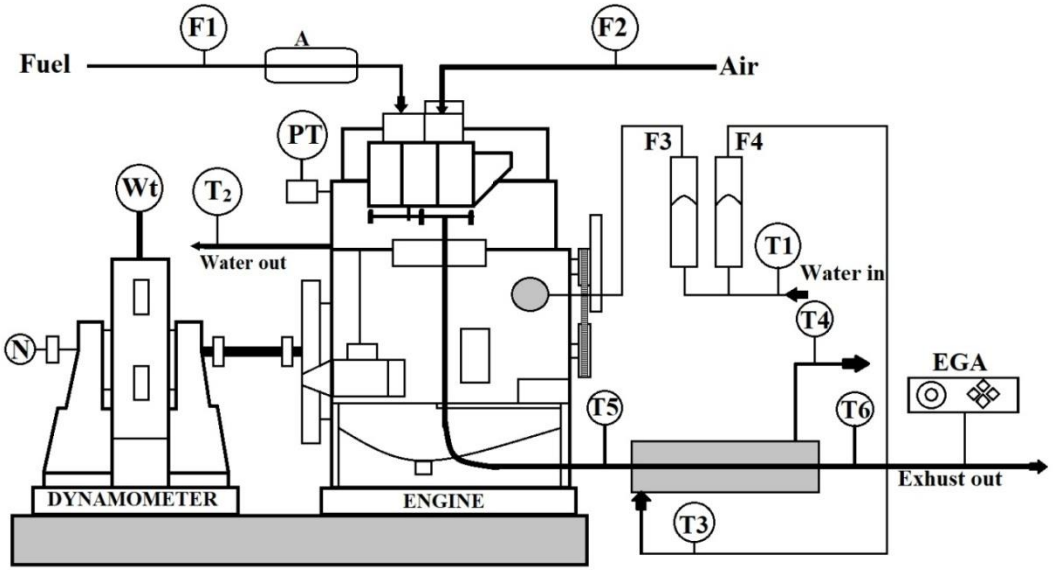

F1- Differential pressure unit for fuel flow; F2- DP unit for air flow; F3- Engine Rotameter; T1- coolant temperature at inlet; T2- coolant temperature at outlet;
T3- thermocouple for initial temperature of calorimeter water;
T4- thermocouple for exit temperature of calorimeter water; T5- thermocouple for initial temperature of exhaust gas; T6- thermocouple for exit temperature of exhaust gas; N- Engine speed decoder; PT- piezoelectric transducer; Wt- dynamometer load; A- NdFeB assembly

Fig 3.1: Schematic representation of experimental test rig

Plate 3.1 Experimental setup with engine and control panel

3.2 Modifications on the test engine for LPG operation

A phase of this experimental work requires the engine to be operated with liquefied petroleum gas. The modifications made on the set up for operating the engine under neat LPG are discussed in this section. Four distinct gas injectors are provided in the inlet manifold adjacent to the inlet port of individual cylinders for injecting LPG. These gas injectors are maneuvered by solenoid valves driven by 12V DC supply. The specifications of the gas injectors like nozzle diameter are designed corresponding to power generated per cylinder. Correspondingly injectors of nozzle diameter 1.75 mm is chosen for the given test engine. A discrete gas ECU (AEB 2001 Injection Control Unit) is provided to operate the solenoid valves and to control the actuation period of the injectors. Figure 3.2 shows the onscreen image of AEB ICU with switch over modes.

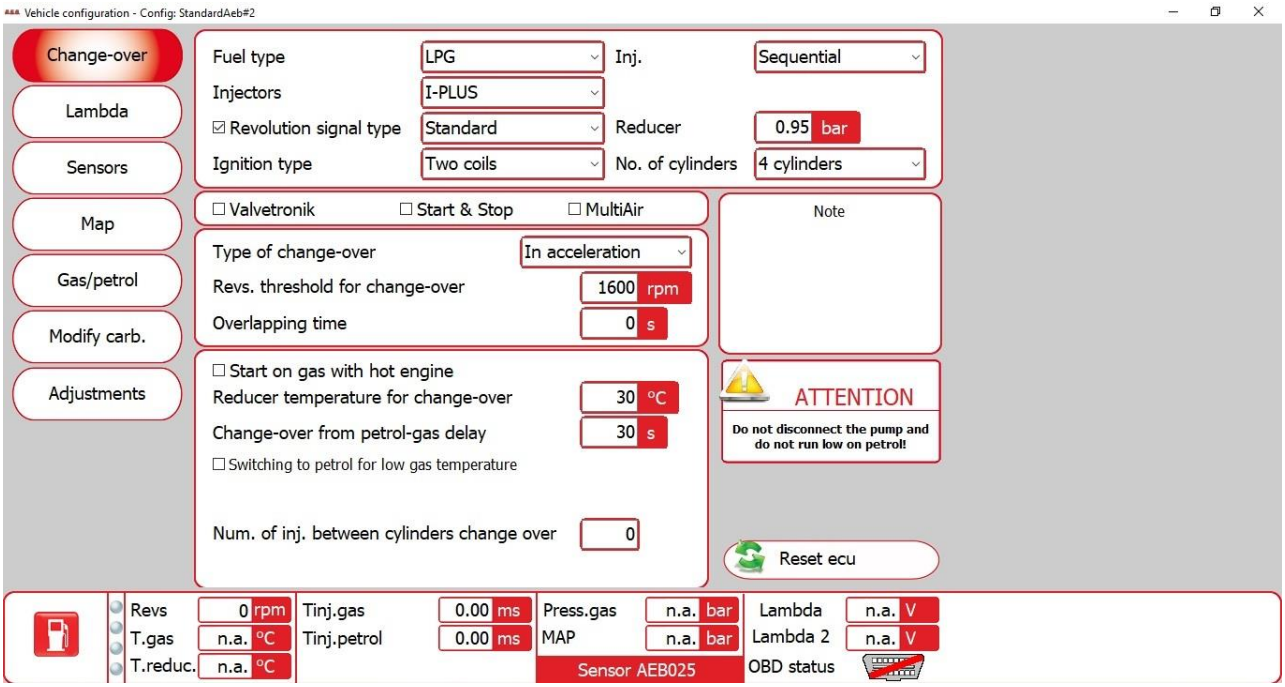

Fig 3.2: Onscreen image of AEB gas injection control unit with switch over modes

Commercial LPG cylinders weighing 19.2 kg stored in a pressure of 4 to 8 bar are utilized for the experiments. The maximum vapor pressure of LPG stored in the cylinder at 40ºC is 1050 kPa. From the LPG cylinder, the gas flows at high pressure through an unreduced pressure regulator though a copper pipe to the vaporizer. The iron particles from the storage cylinder that may travel along with the gas is absorbed using an electromagnetic strainer which is powered by the battery. The vaporizer provided in the supply line helps in the vaporization of the fuel which is then supplied at desired pressures. In the vaporizer unit, thermal energy is transferred into the fuel inorder to reduce the tank pressure so that LPG gets evaporated to the superheated phase (Price et al. 2004). The required thermal energy for this process is provided by the engine cooling water carrying heat after engine jacket circulation. To meet the requirement of amount of gas and supply pressure the evaporator is equipped with a reference pressure from inlet manifold. The block diagram of LPG injection system is shown in figure 3.3.

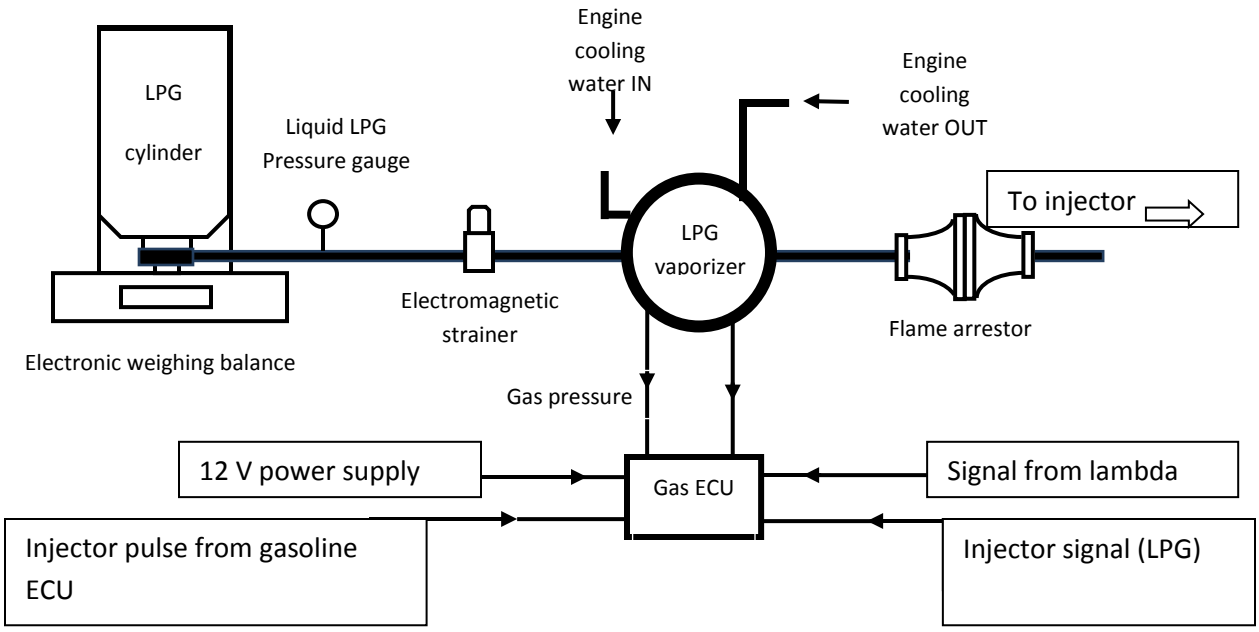

Fig 3.3: Schematic representation of LPG injection system

3.2.1 LPG Gas ECU

The mission of the gas ECU in the injection system is to actuate the opening and closing of injectors through solenoid valve operation and to regulate the duration of injection in accordance with the operating conditions of the engine. Khatri et al. (2009) proposed the concept of operation of a gas ECU based on master slave theory for bifuel application. To serve its purpose the gas ECU utilizes a sequential injection controller of fourth generation OSCAR-N OBD CAN. The input given to the gas ECU is the opening signal pulse from the already deployed gasoline ECU which is then modified with a correction factor before being sent to the gas injectors. The numerical value of correction factor depends upon the density of liquid gasoline and LPG vapor and also considers the signals from MAP sensor which indicates the applied load and lambda sensor which indicates the content of oxygen in the exhaust.

The emulator system provided in the gas ECU surcease the gasoline injection signals and gives a modified signal to gasoline ECU to prevent the occurrence of a fault signal when the engine is operated on LPG. The switching from gasoline fuelled

operation to LPG operation can be effected through the control panel in the software or through a manually operated switch. The technical specifications of injection control unit are provided in Appendix II. The gas ECU in the LPG kit used is shown in plate 3.2.

Plate 3.2 Gas ECU in the LPG conversion kit

3.2.2 Safety Provisions in LPG operation

The storage, handling and operation of gaseous fuels is difficult than liquid fuels because of their hazardous nature. Special care and safety considerations needs to be addressed while using gaseous fuels for experimentation. Propane and butane, the constituent gases of LPG pocess alarmingly low ignition temperature which is around 40ºC. Hence the eventuality of explosion through auto ignition of the gas comes into the picture. Explosion can also happen as a result of flames propagating back into the fuel line during engine operation. To prevent such flash back accidents the working circuit is given the provision of a flame arrestor which is connected in series. The function of flame arrestor is to quench the flames that travel back from combustion chamber to the storage cylinder by deploying wound crimped metal ribbon type flame cell element known as honeycomb.

Plate 3.3 Flame arrestor unit

Plate 3.4 LPG gas injectors

The honeycomb construction has an inbuilt matrix of openings that absorbs the flame thereby quenching it in the process. During normal working of the engine, free flow of gas or vapor is permitted through the flame arrestor from the piping into the injector unit. On the occurrence of a flash back the arrestor absorbs the flame and prevents the flame from travelling back into the LPG cylinder triggering an explosion. Plates 3.3 and 3.4 shows the flame arrestor unit and the gas injectors utilized in the LPG circuit.

Another safety consideration in LPG operated engines is the leakage of gas in the pipelines. Leakage can also happen in the injectors due to the wear and tear as they get old. These leakages, even though of small quantity can trigger auto ignition during combustion process. The higher density of LPG causes the leaked gas molecules to settle down inside the cylinder creating hot spots of auto ignition. The usage of ordinary pipelines is discouraged in the case of LPG because of increased chances of leakage. The occurrence of gas leakage from pipelines can result in hazardous explosions as leaked gas doesn't get away easily owing to higher density of molecules. To avert the chances of leakage, seam-less copper pipes are used to transport the gas into the combustion site. Also, periodic inspection needs to be carried out for leakages in the circuit and in the injectors.

3.3 Experimental Setup for Magnetic Field Assisted Combustion

The pre-treatment of combustible hydrocarbons is possible only under the presence of strong magnetic fields that can polarize the molecules and effect a realignment of the hydrocarbon structure. Such magnetic fields can be generated either by electromagnets of suitable power or by permanent rare earth magnets. If electromagnets are used for the purpose, the cost of powering the magnets will result in economic disadvantage. Hence permanent rare earth type magnetic materials like NdFeB or SmCo can be utilised for polarizing the fuel whose magnetic properties are compared in table 3.1.

Neo-delta magnets are chosen for our experimentation as it is the most powerful magnetic material available till date owing to its high energy density, coercivity values ranging up to 2600 kA/m and very high persistence. The high strength of this magnetic material is mostly because the tetragonal crystal structure pocess very high uniaxial magneto crystalline anisotropy (Haavisto et al. 2014).

Table 3.1: Comparison of Magnetic properties of SmCo and NdFeB materials

Magnetic material	**Energy Product (kJ/m3)**	**Remanence (G)**	**Coercivity (kA/m)**	**Curie Temp (^{o}C)**
SmCo	159-175	9000	636	750
NdFeB	262-278	11700-12100	860-915	310

The energy product of NdFeB is 40% higher and density is 12% lower as compared to delta magnets (SmCo). The magnetic dipole moment of neodymium atom is large due to the four unpaired electrons which gives the $Nd_2Fe_{14}B$ material high saturation magnetisation thereby enabling it to store large amounts of magnetic energy, almost 18 times that of SmCo magnets (Muljadi et al. 2019). Now that we have chosen

the magnetic material, the concern remaining is the choice of a suitable grade of NdFeB that has commensurable magnetic properties and an ability to resist thermal fatigue, demagnetisation and corrosion. For this purpose we consider the concerned properties of various grades of NdFeB magnetic material in table 3.2.

Table 3.2: Comparison of Magnetic properties of various grades of NdFeB

NdFeB grades	**Br (G)**	**H_c (kA/m)**	**H_{cj} (kA/m)**	**BH_{max} (kJ/m^3)**
N33	11300	836	955	247
N35	11700	867	955	263
N38	12100	899	955	287
N40	12400	923	955	302
N42	12800	923	955	318
N45	13200	875	955	318
N48	13800	836	875	366
N50	14000	796	875	382

It can be observed that the normal and intrinsic coercivity of NdFeB material decreases steadily from grades higher than N45. Based on the magnetic properties, commercial availability and cost, grade N38 is chosen for experimentation. As NdFeB material exhibit the property of magnetic anisotropy two different shapes of magnets are chosen to vary the magnetisation pattern. Rectangular blocks are used to create axial fields and special ring shaped magnets are applied to generate radial fields. The rectangular and ring structured NdFeB magnets are depicted in plates 3.5 and 3.6 respectively.

Neo-delta magnets can only be used at air humidity up to 50% without the application of special coatings (Kurniawan 2017). Due to this reason, a standard Ni-Cu-Ni coating is provided to NdFeB magnets during the manufacturing process. Bonded NdFeB permanent magnets are observed to exhibit better corrosion resistance than

sintered NdFeB (Kristiantoro et al. 2016). But the higher energy product, higher density and relatively simple geometries make sintered NdFeB preferable than its polymer bonded counterpart (Brown and Chen 2002). Therefore, sintered N38 NdFeB magnets of required intensities with standard Ni-Cu-Ni coatings are fastened to the fuel line of the test engine adjacent to the injector to effectuate magnetic field assisted combustion for our investigation. The schematic representation of provision of magnetic field in the experimental circuit is shown in figure 3.4.

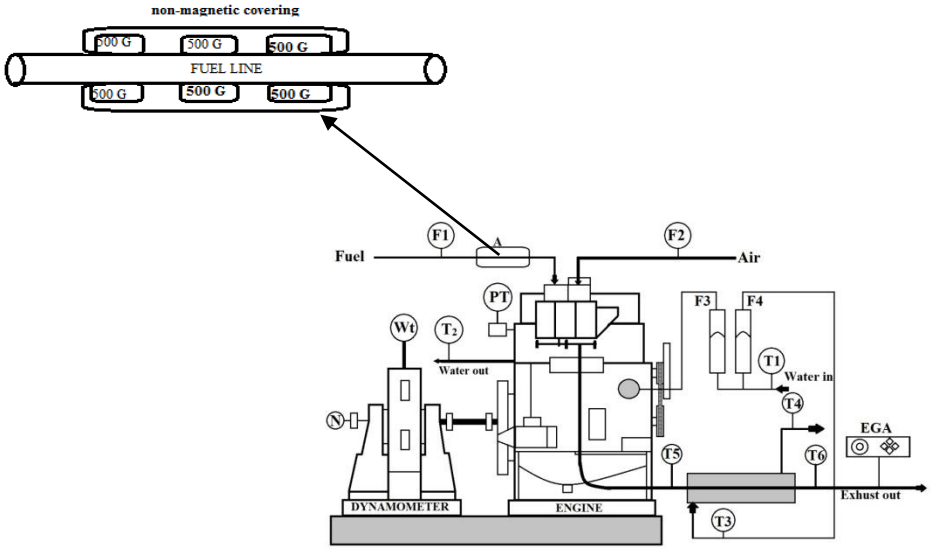

Fig 3.4: provision of magnetic field in the experimental circuit

Plate 3.5 Rectangular type axial NdFeB

Plate 3.6 Ring type radial NdFeB magnets

3.4 Experimental Setup for Exhaust Gas Recirculation

Exhaust Gas Recirculation is a technique employed in internal combustion engines for the control of NOx emissions. In this technique, a part of the exhaust gases is taken from the exhaust manifold and reintroduced into the intake manifold allowing it to mix with the fresh charge. The substitution of burnt gases which do not take part in combustion for oxygen rich ambient air reduces the proportion of cylinder contents available for combustion. This results in a correspondingly lower heat release and peak cylinder temperatures and thus restricts the formation of NO_x.

A system for recirculating partially cooled exhaust gases into the combustion zone is designed for our experimentation. A ball valve arrangement is provided in the tail pipe section of the exhaust manifold to take samples of exhaust gas for analysis using the five gas analyzer. From the valve the piping is divided into two parts- one for discharging the exhaust gases into the atmosphere and another one to carry a part of exhaust for recirculation process.

Plate 3.7 Fabrication for part cooled exhaust gas recirculation

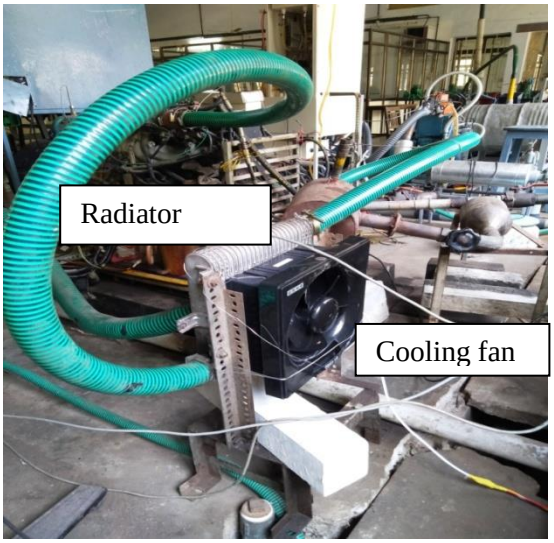

Plate 3.8 Radiator assembly for EGR

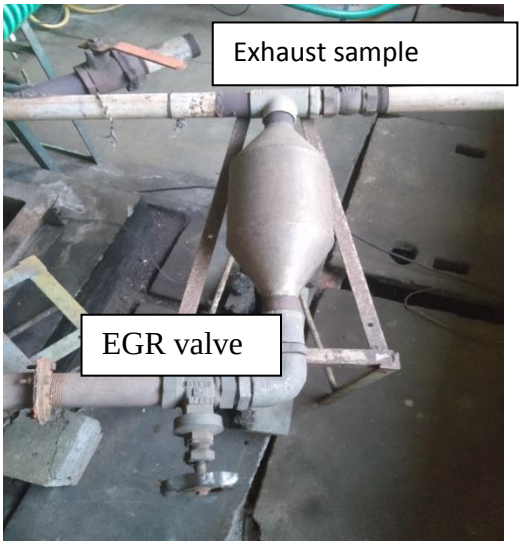

Plate 3.9 EGR valve and piping

The latter piping opens into an expander where the high pressure exhaust gases are expanded and partially cooled. An EGR valve is provided to manually control the amount of recirculation. After the EGR valve, a radiator assembly is provided in which the required amount of exhaust gases are again cooled by convective heat transfer using a cooling fan arrangement. The cooled exhaust gases are then carried to intake manifold through hose pipes.

3.5 Measurement System

Necessary instrumentation is provided on the experimental test rig to measure and monitor different parameters during experimental work. A brief description of the major instruments and measuring systems are provided in this section.

3.5.1 Air and Fuel flow Measurements

The flow of air during the engine operation is fluctuating to cope up with the operation requirements. Inorder to measure this pulsating air flow, an air box with orifice is utilized. The orifice in the air box aids in damping the fluctuations and the differential pressure across the orifice is measured by a manometer. The flow of air through the orifice is connected in parallel to a U-tube manometer and a differential pressure unit.

The pressure difference across the orifice is sensed by the differential pressure unit and the information is sent to the transducer. The transducer generates a DC voltage corresponding to this signal which is first converted into a digital signal and processed by the software program to indicate the flow rate of air in mm of water column and kg/h.

Similarly, the consumption of fuel is calculated by measuring the volume of fuel flowing in a given duration and multiplying it with the fuel density value. A glass burette is provided on the control panel which is calibrated in ml to measure the volume flow rate of fuel. Time taken by the engine to consume that particular volume of fuel is monitored on a digital stop watch. At the same time, the fuel consumption rate is measured by the combustion analysis software as well. This is made possible by a differential pressure unit connected to the fuel burette. When the fuel cock is turned to the measuring position the differential pressure unit senses the pressure head and generates an analog signal which is processed by IC Engine Soft which then displays the flow rate of fuel in kg/h. This automatic measurement of fuel flow rate requires the value of density of the fuel used which should be entered in the software prior to the tests.

These two measurement techniques are applicable only to liquid fuels and when LPG is used for experimentation, the calculation of flow rate of gas should be made separately on mass basis. In this technique the LPG cylinder is placed on an electronic weighing scale of 100 kg capacity. The weighing scale has a least count of 10 grams and displays the weight digitally. The consumption of LPG gas for particular time duration is made on mass basis and the flow rate is manually calculated.

3.5.2 Engine Speed Measurement

An inductive pick up sensor is provided on the test rig along with the eddy current dynamometer control unit which senses the engine speed during the operation. As the dynamometer shaft rotates adjacent to the inductive pick up sensor the rotary encoder unit communicates a voltage pulse whose frequency can be decoded to engine speed in rpm and is displayed digitally on an indicator provided in the control panel.

3.5.3 Engine Load Measurement

The load on the engine is measured using an eddy current type dynamometer. The construction of the eddy current dynamometer includes a stator with number of electromagnets and a rotor attached to the output shaft of the engine. As the rotor rotates a magnetic flux is set up by the electromagnets and thus eddy currents are generated in the stator. The developed eddy current opposes the movement of rotor loading the engine in the process. The generated eddy currents are dissipated in the form of heat and hence the dynamometer should be provided with a cooling arrangement. A strain gauge type load cell is mounted under the arm of dynamometer which measures the torque and sends a signal to the computer to provide the load.

3.5.4 Cylinder Pressure measurement

Analysis of cylinder pressure is essential for studying the combustion process and cyclic variability. For this purpose a piezo electric pressure transducer is provided in the cylinder head directly above the first cylinder. This transducer records the cylinder pressure date for a specified number of cycles which helps us in analyzing the cycle to cycle variations. The PCB Piezotronics Inc made transducer is flush mounted and enables the measurement of pressure data with one degree crank angle resolution. The pressure-crank angle data acquired through this sensor is accessed on a digital computer working on windows 10 platform through NI based data logger NI USB-6210. A combustion analysis software package named IC Engine Soft which is installed in the computer decodes the signals and writes the pressure data into excel files which can be accessed by the users. A continuous supply of cooling water is provided to cool off the sensor body and maintains it at a normal temperature. The crank angle data is measured by a rotary encoder which together with the transducer aids us in acquiring the simultaneous data which is then displayed on the computer as pressure-crank angle or pressure-volume plots.

3.5.5 Magnetic Intensity Measurement

The magnetic intensity of permanent magnets is measured using a gauss meter which is named after the great scientist Carl Friederich Gauss. The modern Gauss meter is an advanced version of Gauss' magnometer. It consists of a gauss probe, the meter and a cable for connection and works on the principle of Hall effect. To measure the magnetic intensity, the instrument is switched on and the probe which is available on the end is placed on the magnet to be measured. When the magnet is slid over the sensor, the highest rating picked up on the meter is noted which corresponds to the Gauss value of that particular magnet. Both the intensity and direction of magnetic fields can be measured using this instrument.

3.5.6 Exhaust Emission Measurement

The quality of exhaust gases emitted from the test engine is analyzed using an AVL digas 444 analyzer unit which is shown in fig 3.1. The analyzer measures the concentration of constituent gases like CO, CO_2, HC, O_2 and NO_x in the exhaust in percentage volume or parts per million basis. The test rig is not provided with any after treatment devices and raw emissions which correspond to automobile exhausts are taken for the analysis. The specification of the five gas emission analyzer is given in table 3.3 and the measurement panel of the analyzer unit is shown in plate 3.9.

Plate 3.10 Measurement Panel of AVL exhaust gas analyzer

Table 3.3: Technical specifications of the exhaust gas analyzer unit

Measured Pollutants	Measurement Range	Instrument Resolution
CO	0-10 (% Vol)	0.01 % Vol
HC	0-20000 (ppm)	10 ppm
CO_2	0-20 (% Vol)	0.1 % Vol
O_2	0-22 (% Vol)	0.01 % Vol
NO_x	0-5000 (ppm)	1 ppm
λ	0-9.999 (calculated)	0.001

3.5.7 Calibration of Instruments and Experimental Precautions

The instruments are calibrated before they are used in the experimental data collection. The dynamometer, load cell, exhaust gas analyzer and the pressure transducer are calibrated by their respective suppliers. The repeatability of data is ensured when the experiment are conducted. Prior to the data acquisition, the engine is operated for some time to reach steady state operation. Experimental error is minimized by taking average value of three readings at each test points. Periodic leak checks are done for LPG fuel line and injectors to ensure safety. Fire extinguishers are provided near to the rig incase of any occurrence of fire. Storage devices like HDD are kept away at a safe distance from the strong magnetic field. A warning board is also hung to keep away people with pacemakers from the impact of magnetic fields.

CHAPTER 4

METHODOLOGY AND EXPERIMENTAL PROCEDURE

The scheme and lay out of experimental work to fulfill the research objectives are discussed in this chapter. The methodology of research is carefully designed and fractionated into four stages. To begin with experiments are done on the test engine to access the baseline operating characteristics which forms the base for comparison of our experimental results. In the first phase the effect of magnetic field assisted combustion of gasoline and LPG are studied separately under axial and radial magnetisation patterns for different speeds and loads of the engine. The optimized magnetisation pattern with optimized magnetic field intensity corresponding to each fuel is arrived at the end of first phase. In the second stage, the effect of part cooled EGR on gasoline and LPG combustion is investigated for multiple EGR flow rates, engine loads and speeds to arrive at an optimum flow rate for each fuel. In the third phase the distance of optimized magnetisation from injectors is varied in three stages to study the effect produced on combustion and emissions of the engine and to arrive at an optimized distance of magnetisation. In the final phase the synergetic effect of optimized part cooled EGR and optimized magnetic intensity with optimized magnetisation pattern and magnetisation distance on combustion of gasoline and LPG is studied at the same set of speeds and loads.

4.1 Scheme of Experimentation

The experimental study involves four different phases. Before the onset of first phase, the baseline operation of the engine is studied under gasoline fuelled operation and LPG fuelled operation for four different speeds and loads of the engine. The ignition timing is kept at 5 degree bTDC. The results of this experiment forms the base for comparison for the results yielded during further experiments. In the first phase of experimentation, the performance, combustion and emissions of the engine under magnetic field assisted combustion is studied. During this phase two types of

magnetisation pattern- axial and radial are experimented for both gasoline and LPG. The magnetic intensity is varied for both patterns in three stages- 3200 Gauss, 4800 Gauss and 6400 Gauss. The engine load is varied between 25%, 50%, 75% and 100% of the full load for four different engine speeds (2000 rpm, 2500 rpm, 3000 rpm and 3500 rpm) and the results are compared with the combustion of non magnetised fuels. After the first phase of experimentation we are able to arrive at an optimized magnetisation pattern with an optimized magnetic intensity that provides the best performance and emission characteristics of the engine under both gasoline and LPG operation.

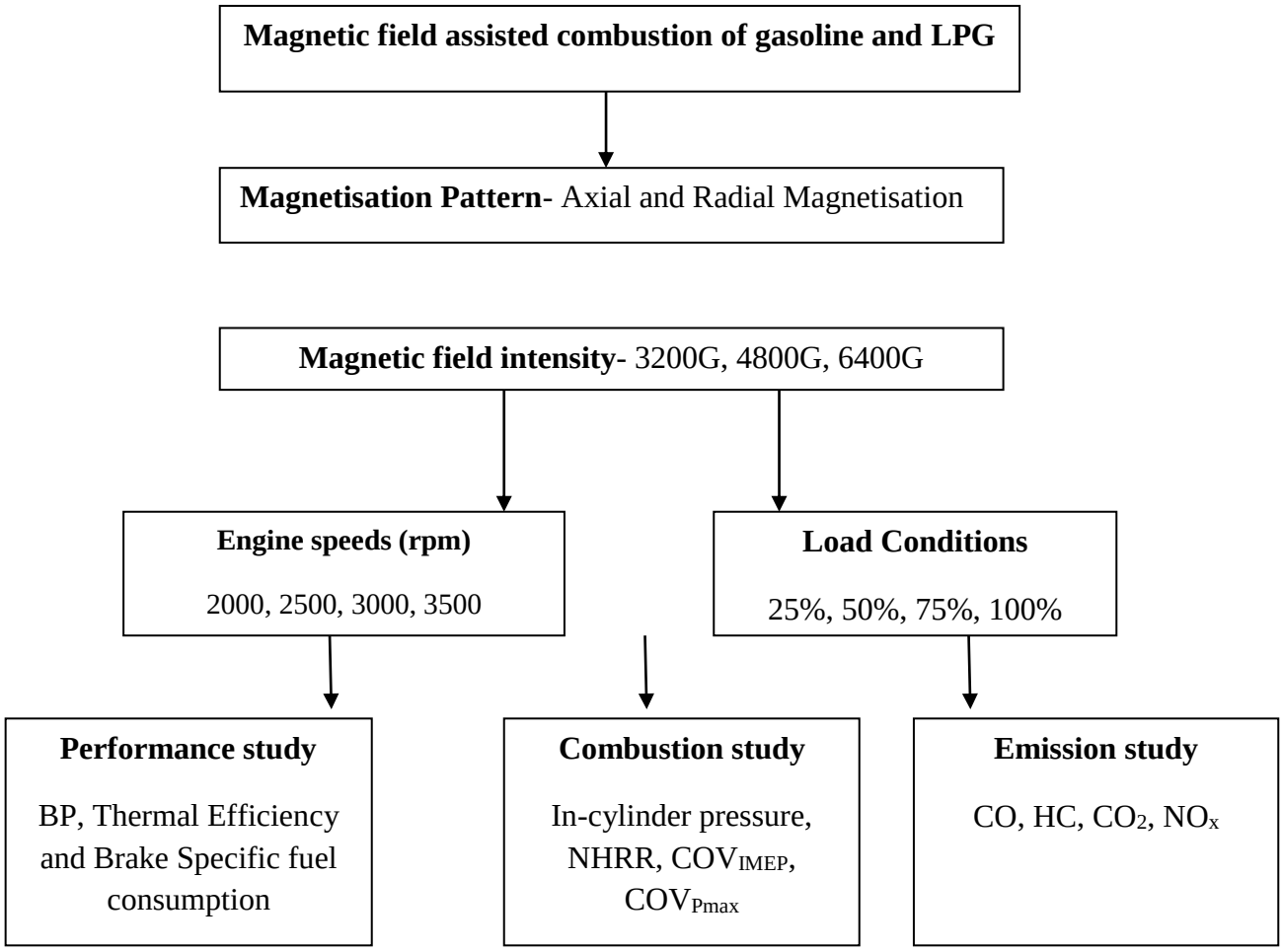

Fig 4.1: Scheme of experiments with Magnetic Field Assisted Combustion of gasoline and LPG

In the second phase of experimentation a provision of part cooled exhaust gas recirculation is provided to the engine under neat gasoline and neat LPG operation. The flow rate of recirculation is varied in three stages- 12%, 18% and 24% and the performance, combustion and emission characteristics are studied for engine loads of 25%, 50%, 75% and 100% of full load and engine speeds of 2000, 2500, 3000 and 3500 rpm. The stability of combustion is analyzed statistically to have an insight of EGR tolerance limit. After this phase of experimentation, we are able to arrive at the optimum flow rate of part cooled EGR which will provide the best operating characteristics for the engine for operation under both the fuels.

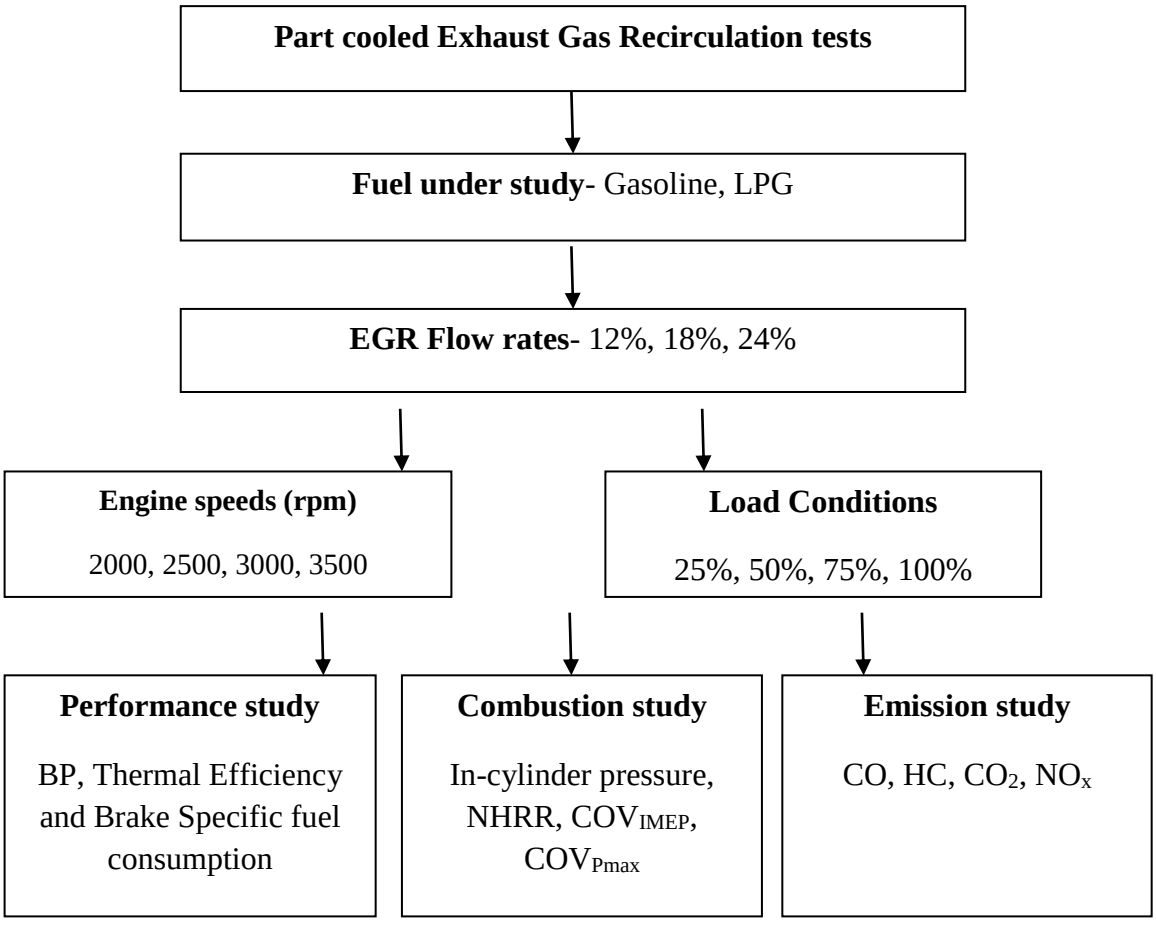

Fig 4.2: Scheme of experiments with part cooled exhaust gas recirculation

In the third phase of experimentation, the optimized magnetic intensity of optimized magnetisation pattern is implemented on the test engine at various positions of magnetisation when running under the fuel which showed the best results for magnetised combustion during phase 1. Three different positions are experimented to analyze the effect of distance of magnetisation on magnetic field assisted combustion- 0 cm (reference point/adjacent to injector), 10 cm and 20 cm from injector. At the end of this phase we will be able to arrive at the optimum distance of magnetisation from the injector side which will give the best results with magnetic field assisted combustion.

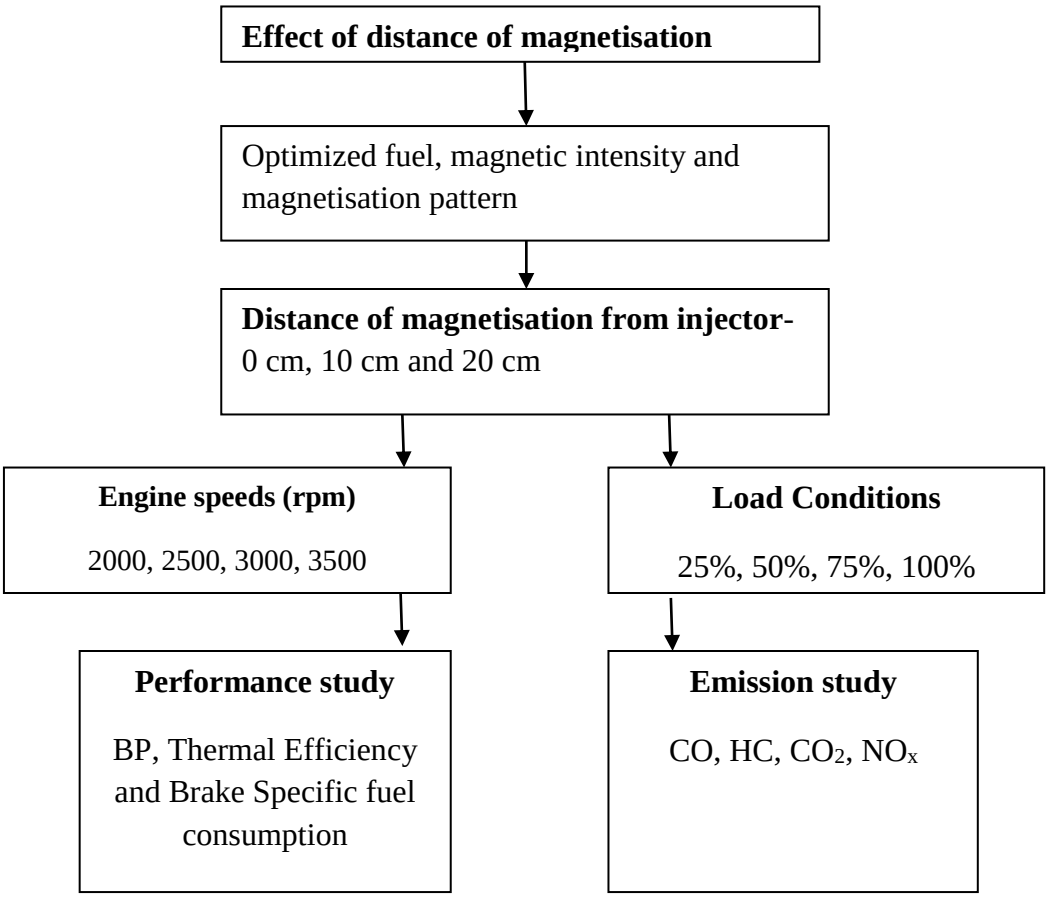

Fig 4.3: Scheme of experimentation for optimized distance of magnetisation

In the final phase, the optimized magnetic intensity with optimized magnetisation pattern and optimized distance of magnetisation is applied along with the optimized flow rate of part cooled EGR to study the synergetic effect produced on performance, combustion and emissions of the engine. This study is conducted on both liquid phase and gaseous phase fuel to make a comparative inference on the effect produced by magnetic field assisted combustion on fuel phase.

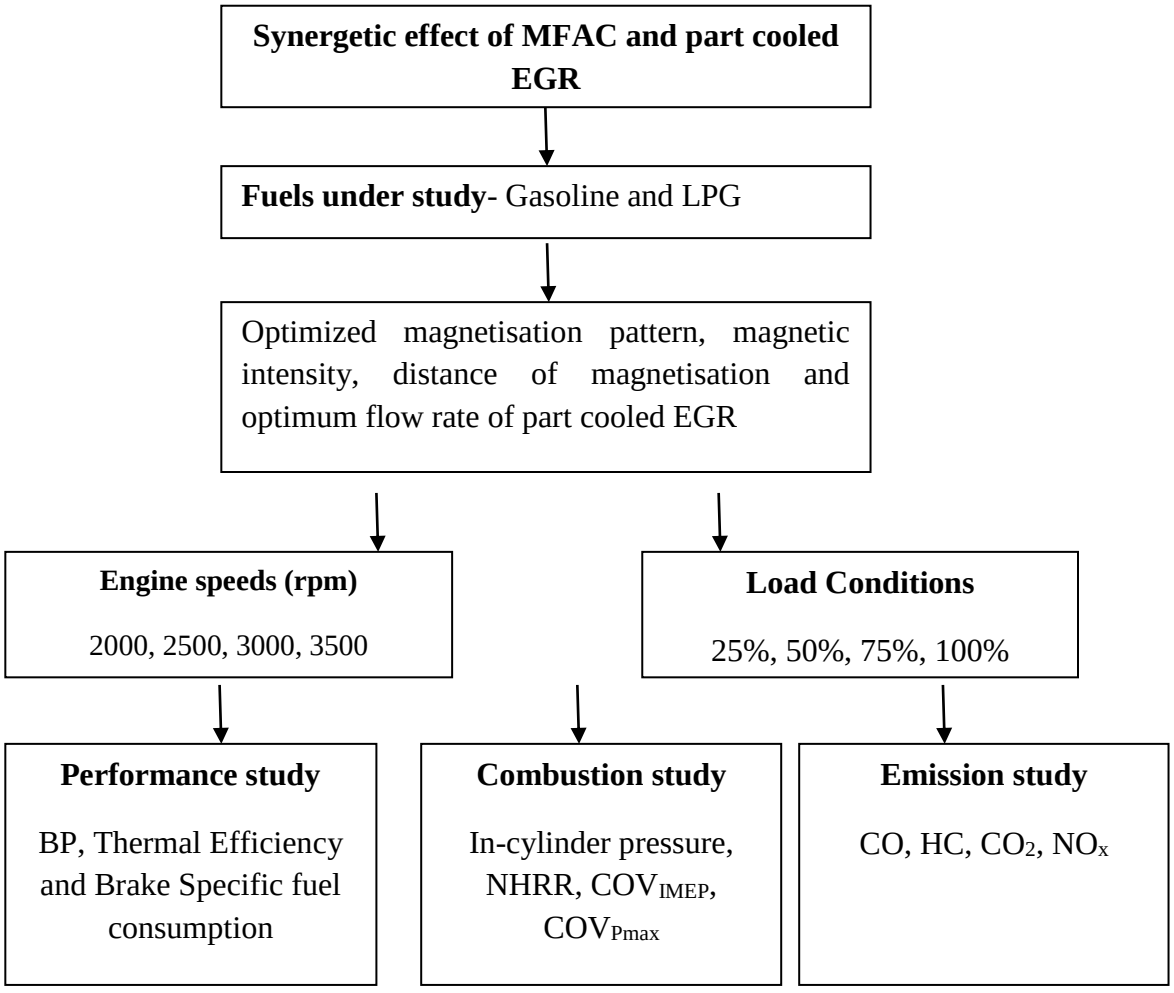

Fig 4.4: Scheme of experimentation for synergetic effect of MFAC and part cooled EGR

4.2 Determination of Combustion Stability

The stability of combustion is one of the most important parameters to be analyzed whenever a modification in fuel or operating parameters is experimented on an

engine. The extend of lean burning and tolerance of EGR are all subjected to the stability of combustion. Although the stability of combustion could be deduced from the engine performance and emission data, a substantial and conclusive evidence of it can be made through a statistical analysis of coefficient of variation (COV) of indicated mean effective pressures and peak pressures during the working cycle.

IMEP is a parameter which is independent of geometry and number of cylinders in the test engine which is by definition the indicated work output per unit swept volume. Mathematically,

$$IMEP = \frac{w_i}{v_s} \tag{4.1}$$

Where W_i is the indicated work in N-m

V_s is the swept volume per cylinder in cubic meters

Brown (2001) proposed an equation to compute IMEP from experimental pressure and volume data which is given by

$$IMEP = \frac{\Delta\theta}{V_s} \sum_{i=n1}^{i=n2} P(i) \frac{dV_i}{d\theta} \tag{4.2}$$

In which P_i corresponds to cylinder pressure at crank position I (Pa), V_i corresponds to cylinder volume at crank angle I (cubic meters), V_s is the swept volume of cylinder (cubic meters), n_1 is the BDC induction crank angle and n_2 corresponds to BDC exhaust crank angle. The combustion analysis software deduces IMEP from pressure-crank angle history. Coefficient of Variation is calculated as

$$COV_{IMEP} = \frac{\sigma_{IMEP}}{\mu_{IMEP}} \tag{4.3}$$

Where σ is the standard deviation and μ is the average value of data.

Standard deviation of the IMEP data set is calculated as

$$\sigma = \sqrt{\frac{\sum_1^n \{IMEPi - \mu(IMEP)\}^2}{n-1}} \quad (4.4)$$

Where n is the number of cycles under study.

Using the above mentioned expressions, COV is computed statistically. If the COV_{IMEP} value exceeds 5, combustion is deduced to be unstable as the value of COV of stable combustion lies within 5. Hence this tool can be effectively utilized to analyze the extend of stability of combustion for a given modification in fuel or engine operating parameters.

4.3 Heat Release Rate

The heat release pattern decides the rate of pressure rise which subsequently influence the vibrations and noise of the engine (Mathur and Sharma, 1976). The combustion behavior of fuels can be quantified by the combustion pressure data. For the design and optimization of engines, it is essential to monitor peak pressures, rate of change in pressure, mass fraction burned, rate of heat release and the chamber temperature. The estimation of heat release rate aids us in having a quantified assessment of combustion rate and combustion diagnostics.

The analysis of heat release characteristics estimate the amount of heat addition required to produce the observed pressure variations. In this research work, we aim to analyze the heat release rate and pattern for the magnetised fuel combustion as well as for recirculation of exhaust gases. The analysis of heat release is made from the data obtained from 100 consecutive combustion cycles.

The heat release analysis is effectuated on the basis of first law of thermodynamics with the intake and exhaust valves closed making the engine a closed system. The cylinder contents are considered to be a single zone of which the thermodynamic properties are uniform and constituted by mean values. The first law of thermodynamics as applicable to this case can be expressed as

$$\frac{dQ}{dt} - p\frac{dV}{dt} + \sum_i m_i h_i = \frac{dU}{dt} \quad (4.5)$$

Where Q is the heat transferred (J), p is the pressure (Pa), V is the volume (cubic meter), m_i is the mass of injected fuel, h_i is the enthalpy (J/kg) and U is the internal energy (J). The only mass which is crossing the system boundary is the injected fuel and hence the mass-enthalpy term in the expression can be reframed to mass of fuel enthalpy. Using a simplified assumption that the net heat release is the difference in energy released from combustion and the energy lost to the walls through heat transfer, the above equation can be reframed to

$$\frac{dQ}{dt} = p\frac{dV}{dt} + \frac{dU}{dt} \tag{4.6}$$

If a further assumption can be made that the contents of the cylinder can be modeled as ideal gas

$$\frac{dQ}{dt} = p\frac{dV}{dt} + mc_v\frac{dT}{dt} \tag{4.7}$$

In which c_v corresponds to the specific heat at constant volume. The temperature term in this expression can be eliminated by differentiating the ideal gas law because temperature term is mostly unavailable in pressure analysis.

$$\frac{dQ_{net}}{dt} = \frac{\gamma}{\gamma-1}p\frac{dV}{dt} + \frac{1}{\gamma-1}V\frac{dp}{d\theta} \tag{4.8}$$

In this equation, γ corresponds to the ratio of specific heats and Q_{net} is the net heat release rate in J/deg. In a spark ignition engine the value of γ is obtained by matching single zone model analysis to a two zone model analysis for various fuels.

Heat transfer in the combustion chamber occurs by both convection and radiation in between the burning gases, cylinder walls, cylinder head, intake and exhaust valves and piston during the working cycle. Amongst the two modes, convection comprises the major part. Considering the impact of heat transfer to the walls of combustion chamber, the gross heat release is expressed as

$$\frac{dQ_{Gross}}{d\theta} = \frac{dQ_{Net}}{d\theta} + \frac{dQ_{ht}}{d\theta} \qquad (4.9)$$

4.4 Analysis of Errors and Uncertainties in parameters

Uncertainties and errors in measurements arise from instruments, measurement techniques and environmental factors. Uncertainty in measured parameters is analyzed based on Gaussian distribution method in which confidence limit is set as ±2σ. Twenty sets of readings are taken at the same operating conditions and uncertainty is estimated using the expression

$$w_t = \frac{2\sigma_i}{\bar{x}} \times 100 \qquad (4.10)$$

Where $\bar{x}$ is the mean of a number of readings and σ_i is the standard deviation of the parameter to be measured. The mean and the standard deviation of a number of measured data is obtained from experiments. The measured parameters include engine load, engine speed, time for fuel and air flow etc. To conduct the error analysis, 20 sets of readings are measured at a particular operating condition and the uncertainty values are calculated using the above mentioned equation. Kline and McClintock (1953) proposed a method of estimating the uncertainty in experimental data. If the uncertainties of various experimental data are expressed in the same odds, these data can be applied to analyse some selected results of experiments. The uncertainty in the calculated result is analysed based on uncertainties in initial measurements.

If a measured quantity R depends on n number of independent parameters x_1, x_2, x_3...x_n, then R is given as

$$R=R\ (x_1, x_2, x_3...x_n)$$

If w_1, w_2,...w_n are the uncertainties of measured parameters and if w_R is the uncertainty obtained in the result, R is computed as the function of measured parameters x_1, x_2, x_3...x_n as per the relation $x_1 \pm w_1$, $x_2 \pm w_2$, ... $x_n \pm w_n$. If the uncertainties of various experimental data are expressed in the same odds, the uncertainty in calculated result is computed as

$$w_R = \left(\left[\frac{\partial R}{\partial x_1} w_1\right]^2 + \left[\frac{\partial R}{\partial x_2} w_2\right]^2 + \cdots + \left[\frac{\partial R}{\partial x_n} w_n\right]^2\right)^{1/2} \quad (4.11)$$

At a particular operating condition, this expression can be utilised to calculate the uncertainties in parameters such as brake power, thermal efficiency and mass flow of air and fuel. The estimated uncertainty values of the measured parameters are represented in table 4.1.

Table 4.1: Uncertainty values of experimental parameters

Parameter	**Uncertainty**
Speed	±0.25
Torque	±0.32
Fuel flow rate	±0.81
NOx emission	±4.13
HC emission	±4.92
CO emission	±0.05
Brake Thermal Efficiency	±0.1
Brake Power	±0.3
Dynamometer load	±0.1
Time taken	±0.3

CHAPTER 5

RESULTS AND DISCUSSION

A Maruthi Zen made multicylinder MPFI engine is modified to operate on liquefied petroleum gas with suitable gas ECU and injection system and Magnetic field assisted combustion has been experimented under gasoline and LPG to study the impact on liquid phase and gaseous phase fuels under varying operating conditions. These operating conditions include magnetisation pattern, magnetic field intensity, distance of magnetisation relative to the injectors, flow rate of part cooled EGR, four loads and four engine speeds. The performance, combustion and emission characteristics of the test engine is studied under these conditions and optimized in each step. The results of these experiments are presented along with their discussion in this chapter. The results and discussion chapter has been divided into 9 sections in a specific order which aids the optimization of desired parameters. In the end, all the optimized conditions are experimented together for both the fuels to investigate the synergetic effect produced by recirculation and MFAC. In the discussion part, similar results obtained by other researchers are quoted or cited wherever needed for justification.

5.1 Effect of Axial Magnetisation (AM) pattern on Magnetic field assisted combustion of liquid phase hydrocarbons (gasoline)

In this section the effect of axial magnetisation pattern has been studied for varying intensities of magnetic fields for the engine fueled by gasoline under four loading conditions and four engine speeds and compared with the normal performance, combustion and emission characteristics of the engine with non magnetised fuel. The performance characteristics of the engine are assessed based on the power output, brake specific fuel consumption and brake thermal efficiency.

5.1.1 Brake power

The power output developed by an engine is a good indicator of the potency of any modification under study. The aim of every engine research is to increase the power output for the same or reduced amount of fuel consumed by increasing the energy utilization thereby improving the efficiency and economy. The brake power output characteristics of the test engine under different intensities of axial magnetisation pattern for four different loading conditions and four engine speeds are shown in figures 5.1-5.4.

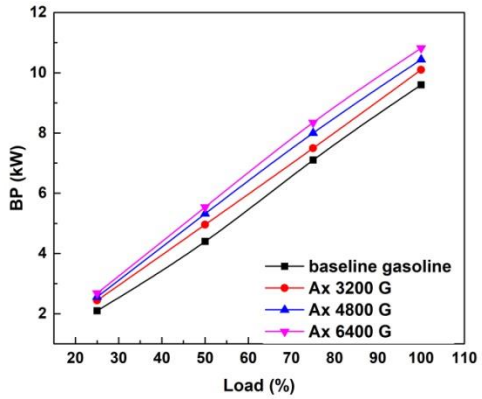

Fig 5.1 Variation in BP with AM at 2000 rpm

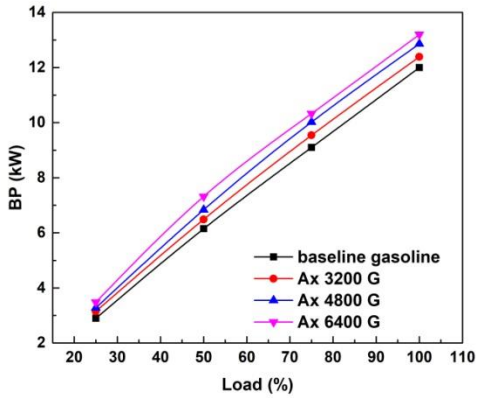

Fig 5.2 Variation in BP with AM at 2500 rpm

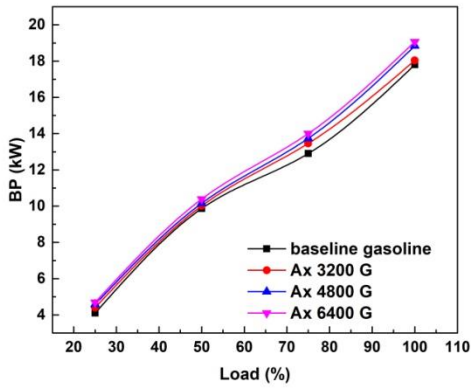

Fig 5.3 Variation in BP with AM at 3000 rpm

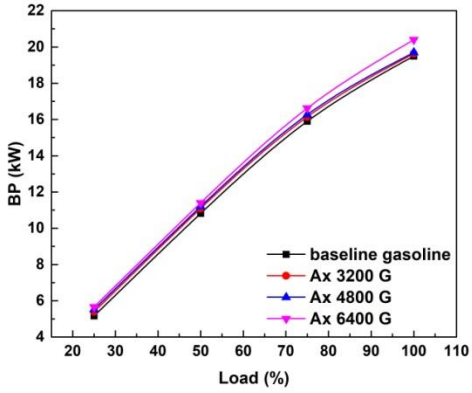

Fig 5.4 Variation in BP with AM at 3500 rpm

It can be observed that the power output of the engine increases with each stage of magnetisation at all loads and speeds under study. The applied magnetic field polarizes the hydrocarbon molecules causing the pseudo clusters to break away and results in more efficient burning thus resulting in an increased power output (Vijayakumar 2014). The maximum increase in power output is experienced at 6400 Gauss magnetisation which shows an improvement up to 5.12% compared to the output obtained from normal gasoline operation without magnetisation.

5.1.2 Brake Specific Fuel Consumption

The fuel consumption characteristics of the test engine under different stages of axial magnetisation are depicted in figures 5.5-5.8. The brake specific fuel consumption of the engine is observed to decrease under each stage of magnetisation at all loads and speeds experimented. The reduction in fuel consumption is due to the ability of magnetic field to divide the molecular clusters into smaller particles with more specific surface area for binding with oxygen molecules ensuring better utilization of the fuel (Govindasamy 2007). The fuel economy of the engine shows an improvement up to 13.9% under axial magnetisation of 6400 Gauss.

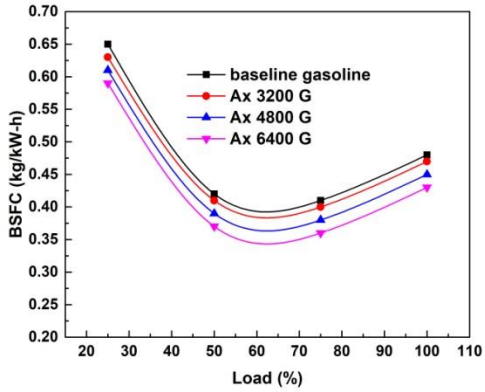

Fig 5.5 Variation in BSFC with AM at 2000 rpm

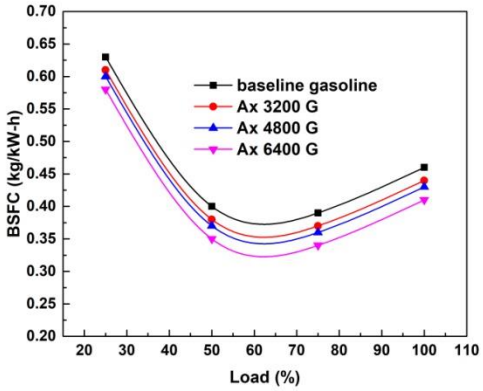

Fig 5.6 Variation in BSFC with AM at 2500 rpm

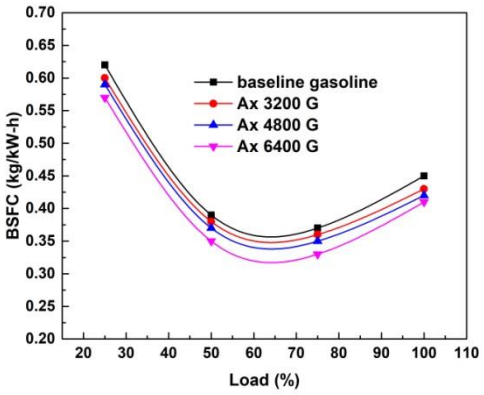

Fig 5.7 Variation in BSFC with AM at 3000 rpm

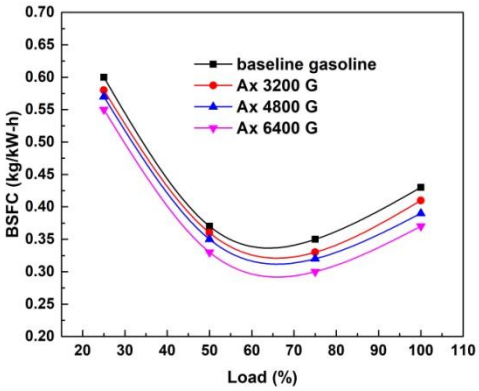

Fig 5.8 Variation in BSFC with AM at 3500 rpm

5.1.3 Brake Thermal Efficiency

The brake thermal efficiency of the engine under various intensities of axial magnetisation at four engine speeds is shown in figures 5.9-5.12. It can be seen that the thermal efficiency of the engine increases with load up to 75% loading and then decreases. The maximum efficiency of the engine is observed at 75% load where the fuel economy is maximum. The increase in intensity of the magnetic field results in increase of the thermal efficiency through improved fuel economy and a raise in power output. In this case, the maximum thermal efficiency is observed at 6400 Gauss magnetisation where an improvement up to 3.32% is noted.

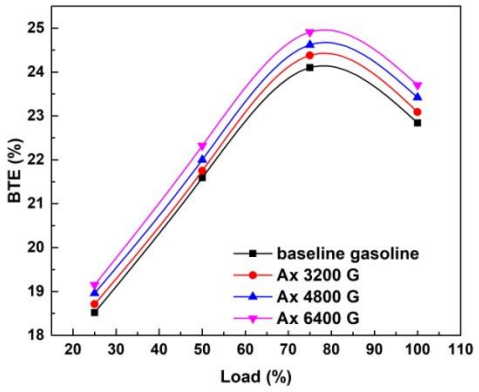

Fig 5.9 Variation in BTE with AM at 2000 rpm

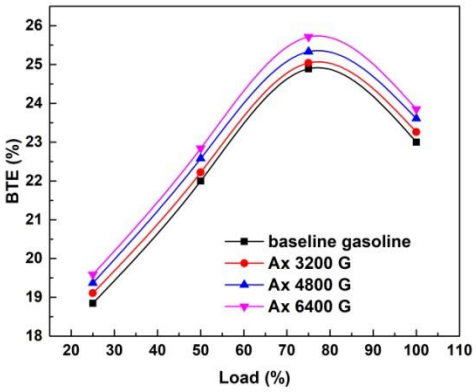

Fig 5.10 Variation in BTE with AM at 2500 rpm

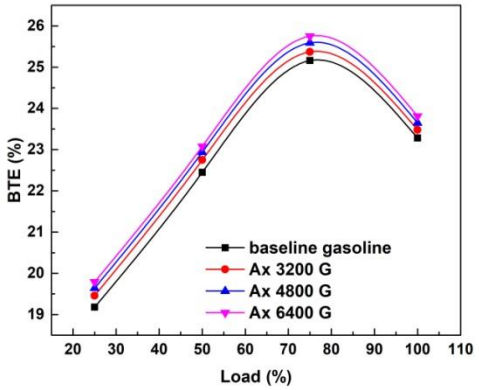

Fig 5.11 Variation in BTE with AM at 3000 rpm

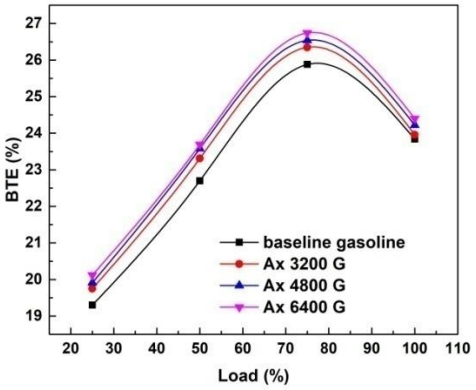

Fig 5.12 Variation in BTE with AM at 3500 rpm

5.1.4 In-cylinder Pressure

The analysis of in-cylinder pressure is an effective tool for diagnosing combustion characteristics. For this purpose, the pressure data for 100 consecutive cycles are acquired using the software and the average value of these data is computed and plotted against the crank angle positions at which they are generated. It can be observed that there is a considerable variation in pressure from cycle to cycle. For an effective comparison, the

average pressure generated during the magnetic field assisted combustion under three different magnetic intensities are plotted and compared with the baseline pressure data. The comparison of in-cylinder pressures for an engine speed of 2500 rpm is shown in figure 5.13. A slight increase in cylinder pressure is noted as the intensity of magnetisation is increased in stages which are owed to the enhanced combustion under stronger magnetic fields (Govindasamy 2007).

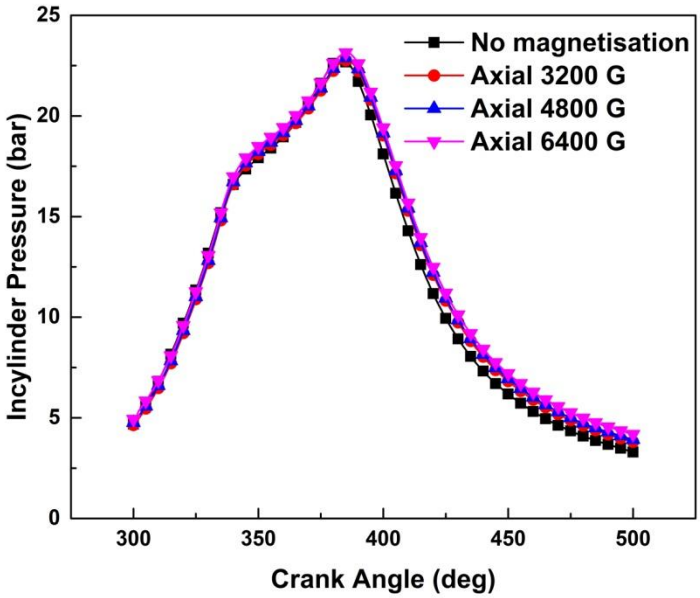

Fig 5.13 Variation in cylinder pressure with AM at 2500 rpm

5.1.5 Net Heat Release Rate

The analysis of heat release rate decodes information about the quality of combustion happening inside the combustion chamber. The net heat release rate data of 100 consecutive cycles are recorded and averaged for each intensity of magnetic fields under axial magnetisation pattern and plotted with comparison to the baseline heat release data of gasoline. The comparison of NHRR characteristics of combustion under various intensity magnetic fields for an engine speed of 2500 rpm is shown in figure 5.14.

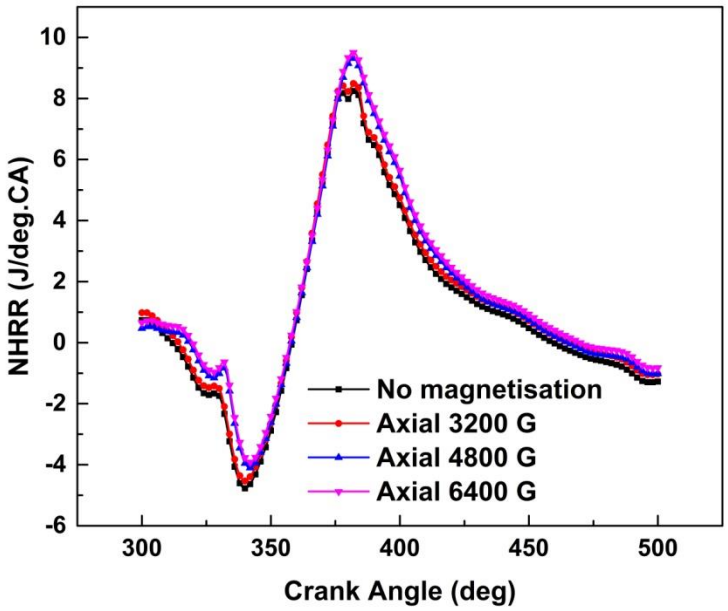

Fig 5.14 Variation in NHRR with AM at 2500 rpm

It can be observed that the heat release rate initially decreases until the start of combustion from which it increases till the point where maximum combustion is achieved and then further decreases. As the intensity of magnetisation of the hydrocarbons is increased in stages, the heat release also increases slightly. The maximum magnitude of heat release is observed under 6400 Gauss field where the fuel is maximum polarized.

5.1.6 Analysis of Stability of Combustion

The cyclic variation in combustion is the major limiting factor for parameters that can enhance the performance of the engine and also for the level of emissions exhausted. The study of cyclic variations is significant because the optimum spark timing is set for average cycle and the spark time will be over advanced or retarded for other cycles resulting in a loss of power and efficiency. The analysis of stability of combustion can be

made by the statistical study of coefficient of variation of maximum pressures and Indicated Mean Effective Pressures.

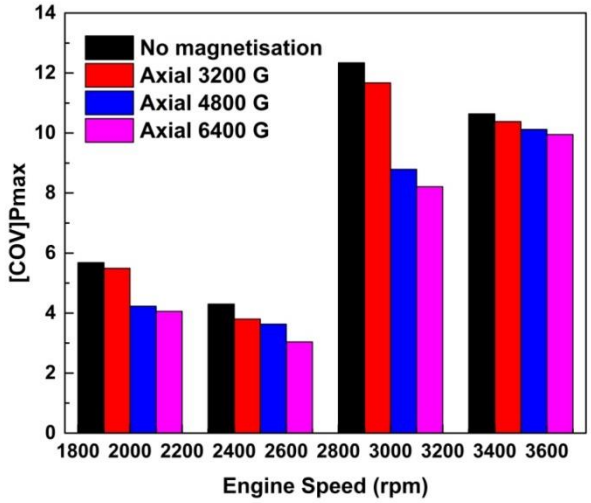

Fig 5.15 COV of P_{max} in axial magnetisation of gasoline at various engine speeds

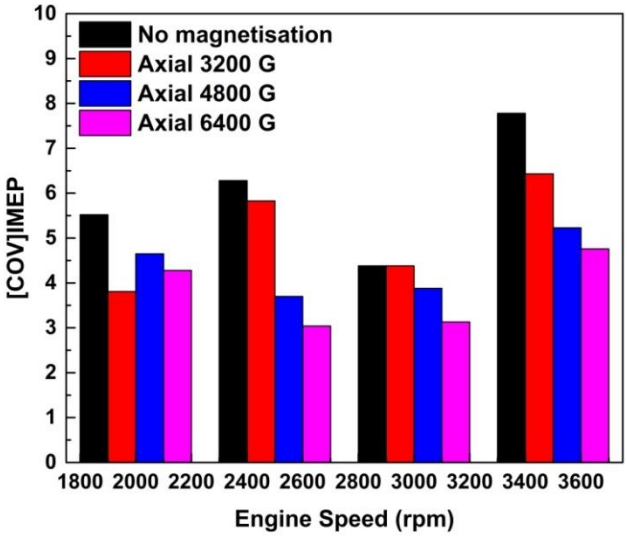

Fig 5.16 COV of IMEP in axial magnetisation of gasoline at various engine speeds

The COV of P_{max} and COV of IMEP of magnetic field assisted combustion of gasoline for various engine speeds are represented in figures 5.15-5.16. If the COV_{IMEP} value exceeds 5, combustion is deduced to be unstable as the value of COV of stable combustion lies within 5. Hence this tool can be effectively utilized to analyze the extend of stability of combustion for a given modification in fuel or engine operating parameters. It can be observed from the analysis that COV of peak pressures and IMEP are both reducing as the intensity of magnetisation is increased in stages. The COV of IMEP values lie well within 5 when the intensity of magnetic field is raised to 6400 Gauss which indicates stable combustion.

5.1.7 Emission of Carbon monoxide

Carbon monoxide is a colorless and odorless gas which is a direct indicator of the extent of combustion. If inhaled, this gas combines with hemoglobin of our blood with an affinity of more than three times to that of oxygen and reduces the oxygen carrying capacity of blood drastically thus resulting in serious health ailments and even death. If the combustion occurring inside the engine cylinder becomes incomplete by any means, the percentage content of carbon monoxide in the exhaust increases.

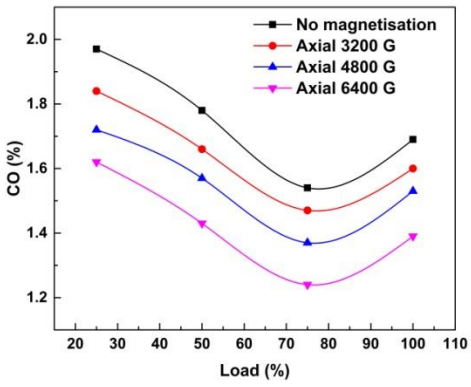

5.17 Variation in emission of CO with AM at 2000 rpm

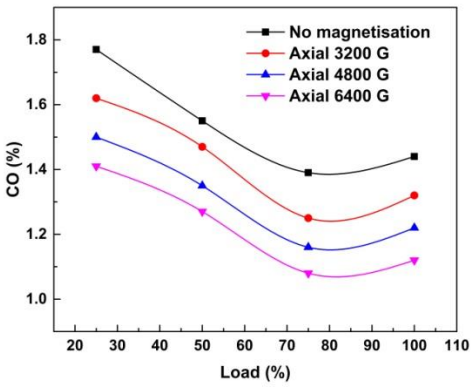

5.18 Variation in emission of CO with AM at 2500 rpm

Under axial magnetisation pattern, it can be observed that the emission of carbon monoxide reduces with each stage of applied magnetic field. The percentage content of CO in the exhaust is reduced up to 19.63% under 6400 Gauss field when compared to the non-magnetised combustion of gasoline as observed from figures 5.17- 5.20.

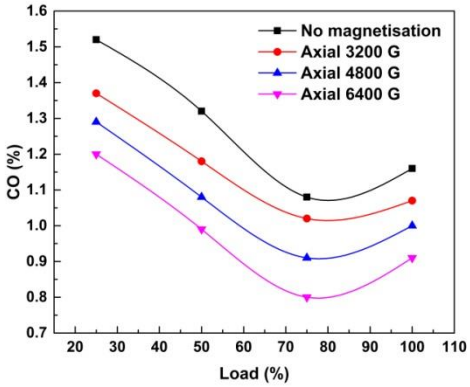

Fig 5.19 Variation in emission of CO with AM at 3000 rpm

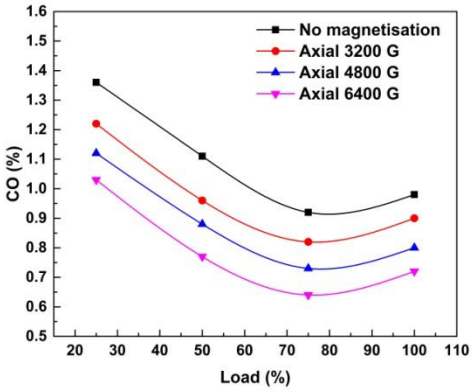

Fig 5.20 Variation in emission of CO with AM at 3500 rpm

5.1.8 Emission of Carbon dioxide

Carbon dioxide is a green house gas which is an essential by product of combustion of hydrocarbon fuels. Although it contributes to the green house effect and global warming, it is considered as a necessary evil. When the combustion is all the more complete, the levels of carbon dioxide emission are bound to increase. In other words, the emission of carbon dioxide follows the opposite trend of that of carbon monoxide. The emission characteristics of Carbon dioxide at four engine speeds and loads under magnetic field assisted combustion of gasoline are depicted in figures 5.21- 5.24.

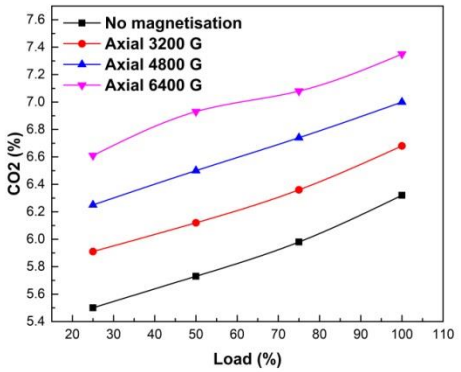

Fig 5.21 Variation in emission of CO_2 with AM at 2000 rpm

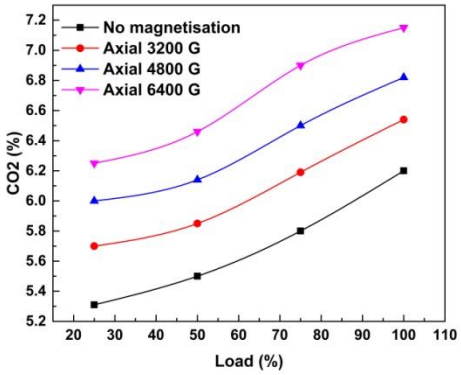

Fig 5.22 Variation in emission of CO_2 with AM at 2500 rpm

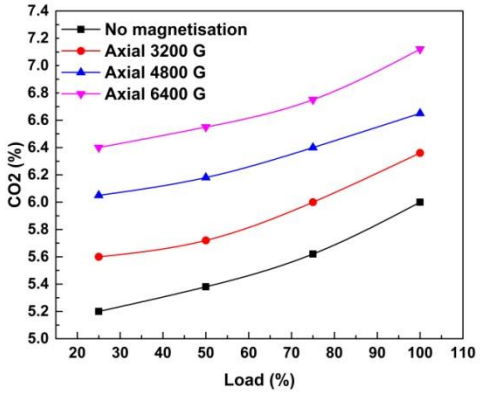

Fig 5.23 Variation in emission of CO_2 with AM at 3000 rpm

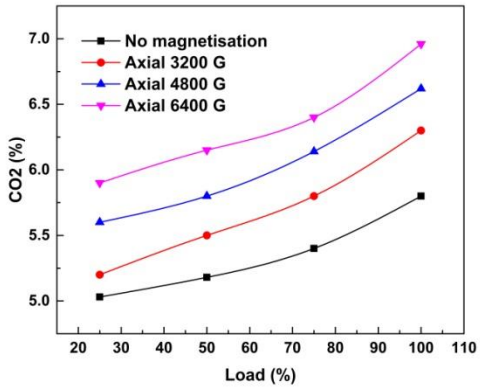

Fig 5.24 Variation in emission of CO_2 with AM at 3500 rpm

The emission of CO_2 is found to increase with the applied load at all tested speeds. The molecular alignments of hydrocarbons get reformed under strong magnetic fields which eventually results in enhanced combustion (Govindasamy et al. 2007). As the extend of completion of combustion is improved in magnetic field assisted combustion the percentage of carbon dioxide in the exhaust increases simultaneously, as observed from the plots. The maximum increase in carbon dioxide emissions under axial magnetisation pattern is observed for 6400 Gauss field.

5.1.9 Emission of Hydrocarbons

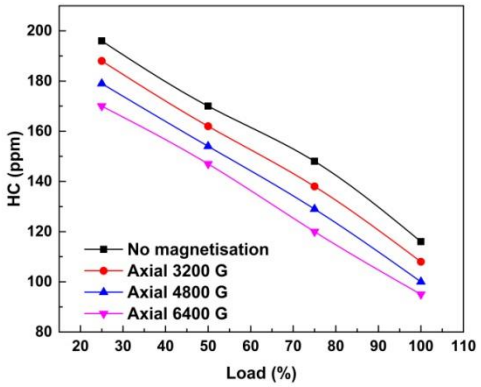

Fig 5.25 Variation in emission of HC with AM at 2000 rpm

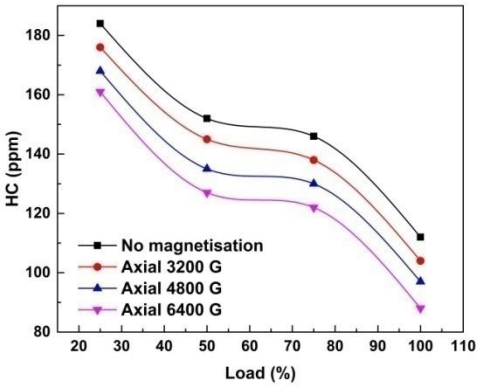

Fig 5.26 Variation in emission of HC with AM at 2500 rpm

The emission of hydrocarbons is mainly influenced by the quality of combustion and availability of oxygen. When sufficient oxygen is not available for combustion, the emission of hydrocarbons increase. Under the influence of strong polarizing fields, the fuel becomes more receptive to oxygen (Fatih et al. 2010) through the breakdown of cage like clusters, thus admitting more oxygen molecules into the interior carbon atoms enhancing the combustion process.

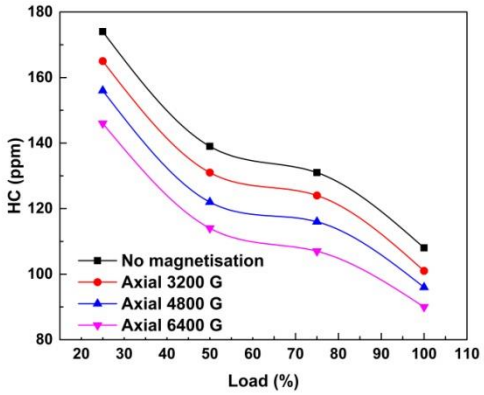

Fig 5.27 Variation in emission of HC with AM at 3000 rpm

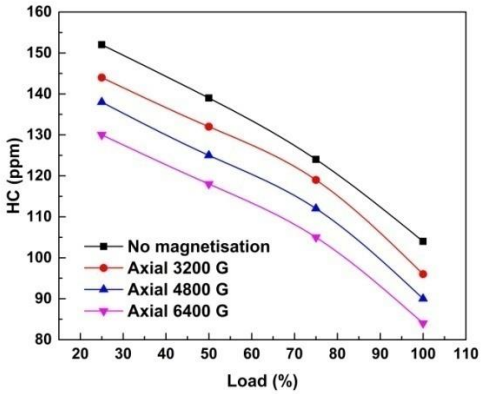

Fig 5.28 Variation in emission of HC with AM at 3500 rpm

This effect is reflected in the emission of hydrocarbons from the test engine at different speeds and loads which is shown in figures 5.25- 5.28. It can also be observed that as the engine speed increases, the extent of combustion increases resulting in reduced hydrocarbon emissions.

5.1.10 Emission of Oxides of Nitrogen

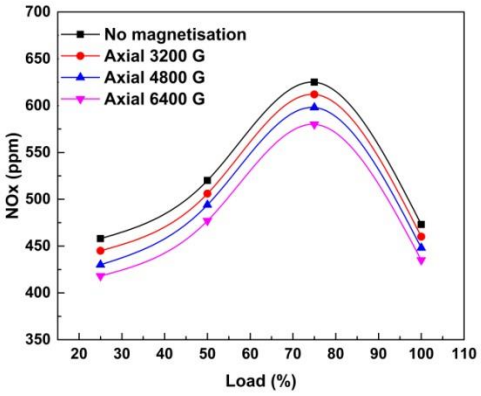

Fig 5.29 Variation in emission of NO_x with AM at 2000 rpm

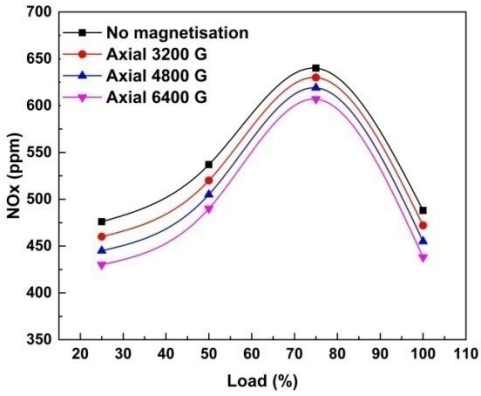

Fig 5.30 Variation in emission of NO_x with AM at 2500 rpm

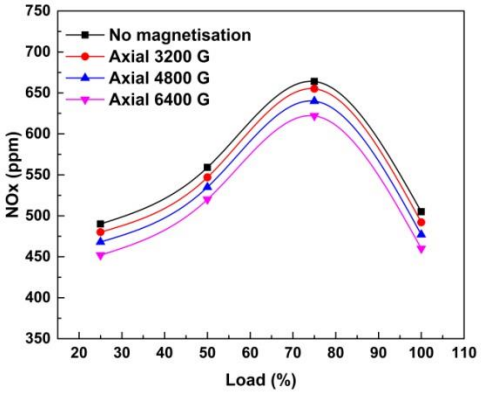

Fig 5.31 Variation in emission of NO_x with AM at 3000 rpm

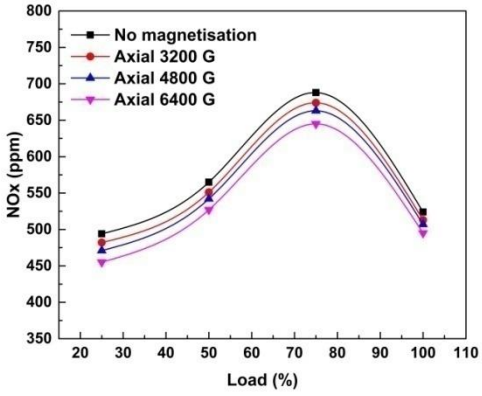

Fig 5.32 Variation in emission of NO_x with AM at 3500 rpm

The air that is furnished for combustion has a nitrogen content of over 77%. Although this nitrogen is inert at lower temperatures, the temperatures prevailing inside the

combustion chamber which is around 1100ºC makes nitrogen to react with oxygen forming various oxides which are toxic and are classified as NO_x in general. The emission trends of NO_x under axial magnetisation of gasoline are shown in figures 5.29-5.32. It can be observed that there is a minute reduction in the emission of NO_x as the intensity of applied magnetic field is increased. When compared to the reduction obtained in the case of other emissions, the reduction in NO_x is negligible because of the temperature dependence of NO_x generation (Fatih et al. 2010).

5.2 Effect of Radial Magnetisation (RM) pattern on Magnetic field assisted combustion of liquid phase hydrocarbons (gasoline)

In the second stage of experimentation, the axial magnetic field is replaced by radial field of the same magnetic intensity to investigate the effect of magnetisation pattern on magnetic field assisted combustion of hydrocarbons. For this radially magnetised NdFeB rings are mounted on the fuel line. Sintered N38 grade rings are provided a coating of Ni-Cu-Ni as in the case of axially magnetised blocks to resist thermal corrosion. The magnets are given a stainless steel covering for preventing any loss in intensity during the operation. The reference conditions of measurement and the operating conditions are maintained the same and the performance, combustion and emission characteristics of the test engine are evaluated under radial magnetic fields.

5.2.1 Brake Power

The power output characteristics of the test engine under varying intensities of radial magnetic fields, four engine speeds and loads are depicted in figures 5.33- 5.36. The trend of power output is observed to be the same as in the case of axial magnetic fields. A slight increase is observed in the magnitude of output power with the radial field when the same intensity fields of axial and radial patterns are compared. Radial magnetic fields generate higher magnetic moment and output torque when compared to the axial field of same intensity (Morcos 2002). An increase of 10.07% is obtained in this case in output when compared to the normal baseline combustion of gasoline.

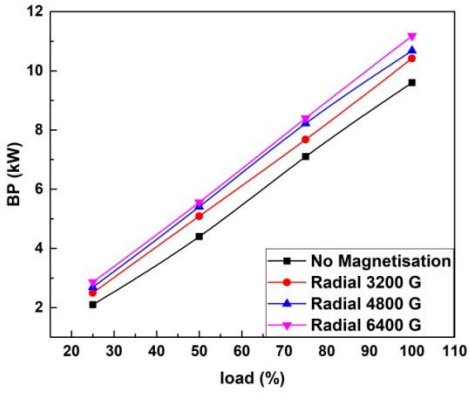

Fig 5.33 Variation in BP with RM at 2000 rpm

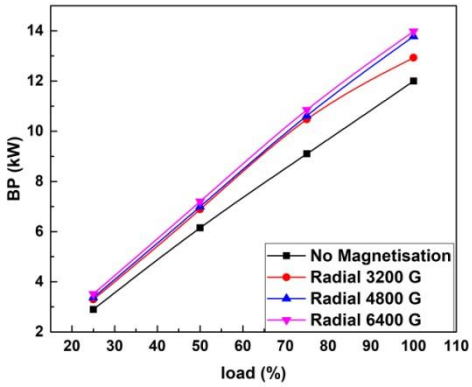

Fig 5.34 Variation in BP with RM at 2500 rpm

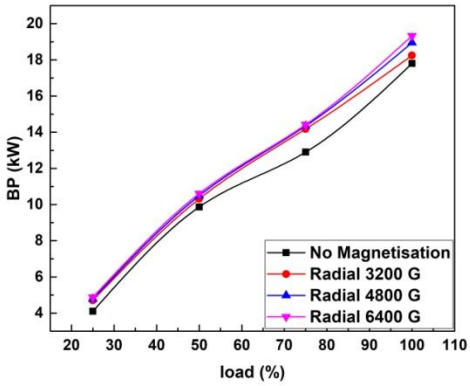

Fig 5.35 Variation in BP with RM at 3000 rpm

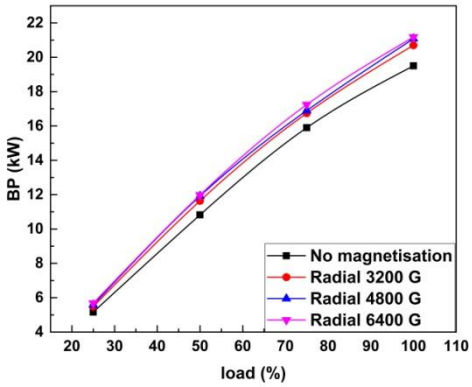

Fig 5.36 Variation in BP with RM at 3500 rpm

5.2.2 Brake Specific Fuel Consumption

As in the case of axial magnetisation of gasoline, the consumption of fuel reduces up to 75% loading and then increases with 75% load being the fuel economic point. This pattern holds true for all the speeds experimented. The consumption of fuel is found to reduce further for radial magnetic field than in the case of axial fields of same intensity. This improvement in fuel economy is due to the improved ability of radial magnetic field to influence the hydrocarbons in all directions with higher magnetic moment which can influence the motion of charged particles (Chryssomalakos 2003). The BSFC

characteristics of the test engine under radial magnetic fields are represented in figures 5.37- 5.40. An improvement of up to 14.82% is observed in fuel economy when compared to the non-magnetised operation of gasoline.

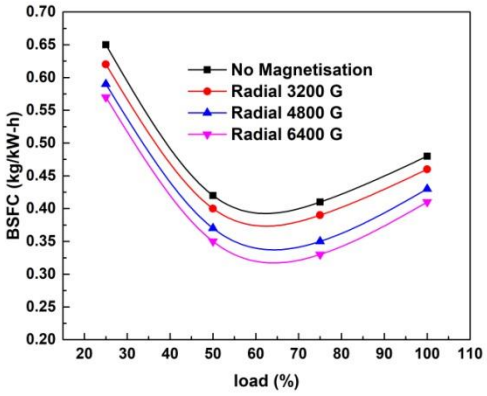

Fig 5.37 Variation in BSFC with RM at 2000 rpm

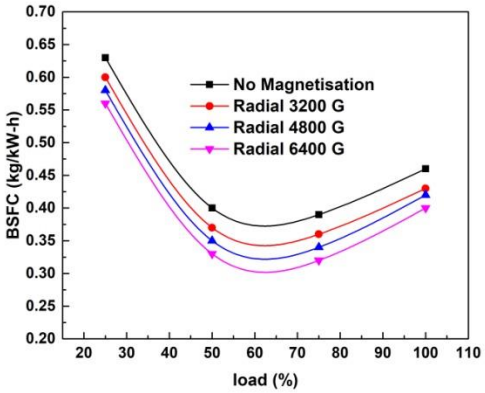

Fig 5.38 Variation in BSFC with RM at 2500 rpm

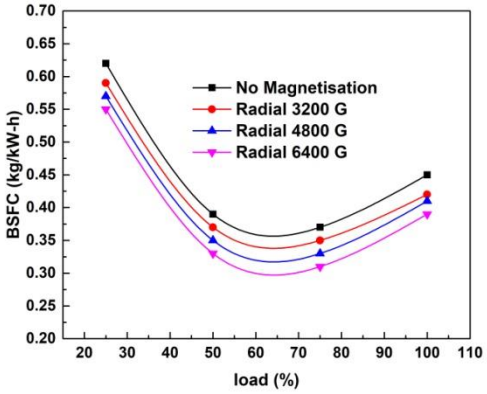

Fig 5.39 Variation in BSFC with RM at 3000 rpm

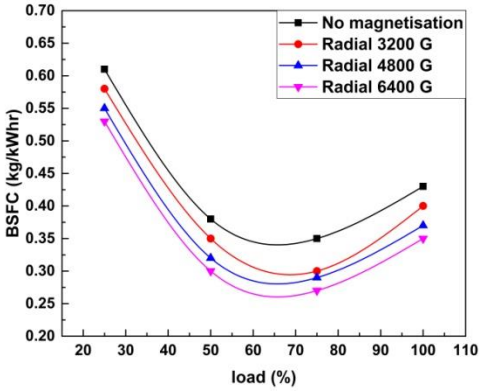

Fig 5.40 Variation in BSFC with RM at 3500 rpm

5.2.3 Brake Thermal Efficiency

The thermal efficiency characteristics of the test engine fuelled by radially magnetised gasoline under different loads and speeds are shown in figures 5.41- 5.44.

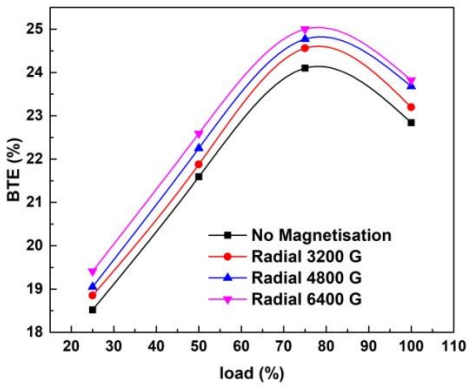

Fig 5.41 Variation in BTE with RM at 2000 rpm

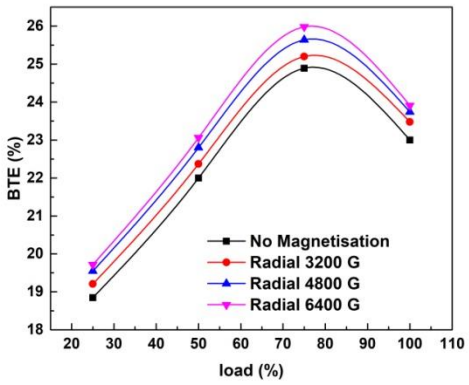

Fig 5.42 Variation in BTE with RM at 2500 rpm

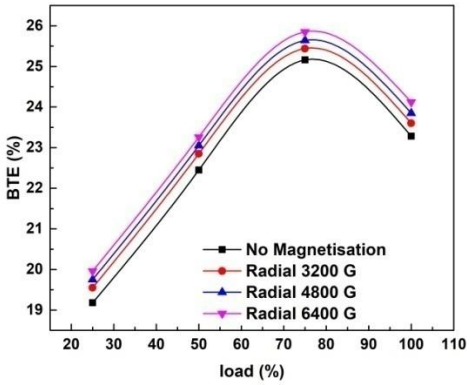

Fig 5.43 Variation in BTE with RM at 3000 rpm

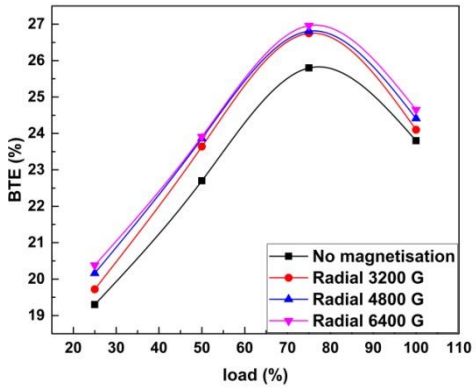

Fig 5.44 Variation in BTE with RM at 3500 rpm

Similar to the axial fields, the trend of BTE curves remain the same with the maximum efficiency point obtained at 75% loading for all the speeds. It can be observed that the efficiency of the engine increases when fuelled by polarized gasoline in stages of increasing intensities. The improvement in BTE under radial fields is slightly higher than that in the case of axial fields owing to the improvements yielded in the case of output power and fuel economy. Thermal efficiency of the test engine is found to increase up to 4.17% under radially magnetised gasoline which is 0.85% higher than that in the case of axially magnetised gasoline.

5.2.4 In-cylinder Pressure

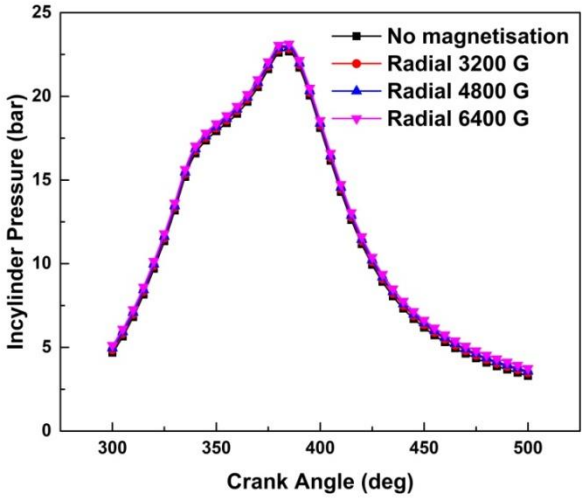

Fig 5.45 Variation in cylinder pressure with RM at 2500 rpm

The in-cylinder pressure analysis is made using data samples of 100 combustion cycles of which the average value is plotted against the respective crank angle position for each stage of magnetic intensities. Even though considerable variations are observed between the pressure values in each cycle, the variation in cylinder pressure is ever so little with the magnetised hydrocarbon. A minute increase can be noted in pressure when the fuel is polarized. This improvement is explained on the basis of higher diffusion of fuel molecules from the free stream to the sub layers under the influence of strong magnetic fields which tends to negate the thickening of boundary layer near TDC due to the effect of high Reynolds number (Govindasamy et al. 2007). As a result, reaction rate is enhanced which in turn enhances the combustion and leads to higher pressures in the combustion chamber. The variation in cylinder pressure with different intensities of radially magnetised gasoline at 2500 rpm is shown in figure 5.45.

5.2.5 Net Heat Release Rate

The Net Heat Release Characteristics of gasoline under radial magnetisation for an engine speed of 2500 rpm is shown in figure 5.46. As in the case of axial magnetisation, the trend of heat release pattern remains the same with a slight increase in the magnitude of heat transfer. The crank positions corresponding to the peak heat release points are observed to remain intact for all the intensities. The higher availability of oxygen to the hydrocarbon molecules during the magnetic field assisted combustion aids in the higher release of heat in the combustion cycles. As observable from the plot, the peak heat release points lie immediately adjacent to the TDC position.

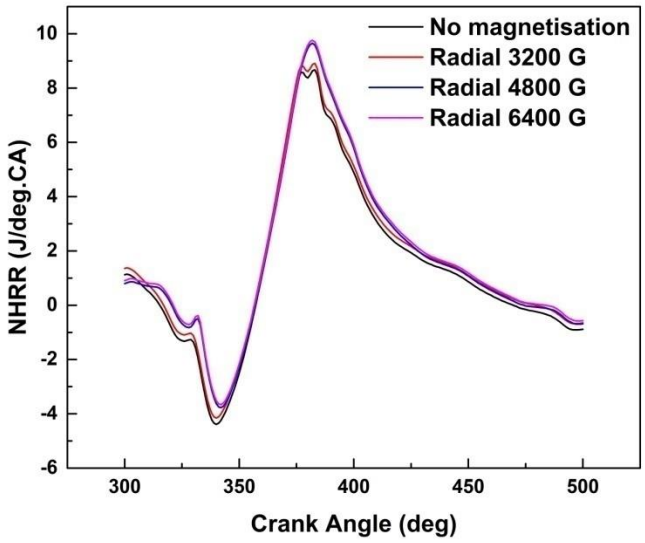

Fig 5.46 Variation in Net Heat Release Rates with RM at 2500 rpm

5.2.6 Analysis of Stability of Combustion

The stability of combustion is analyzed statistically from the coefficient of variation of P_{max} and IMEP which is computed from the mean and standard deviation of pressure data. Figures 5.47 and 5.48 shows the variation in COV of P_{max} and COV of IMEP with radially magnetised gasoline. Similar to the case in axial magnetisation, the Coefficient of

Variation of maximum pressures and indicated mean effective pressures is found to reduce indicating the diminishment of cyclic variations in combustion. There is not much difference in the magnitude of reduction of combustion variations between the two experimented patterns of magnetisation.

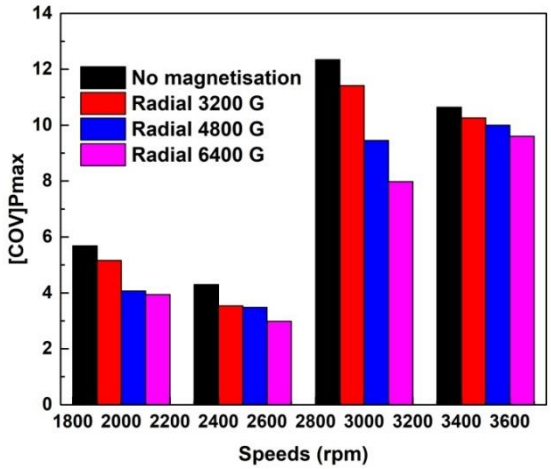

Fig 5.47 COV of P_{max} in radial magnetisation of gasoline at various engine speeds

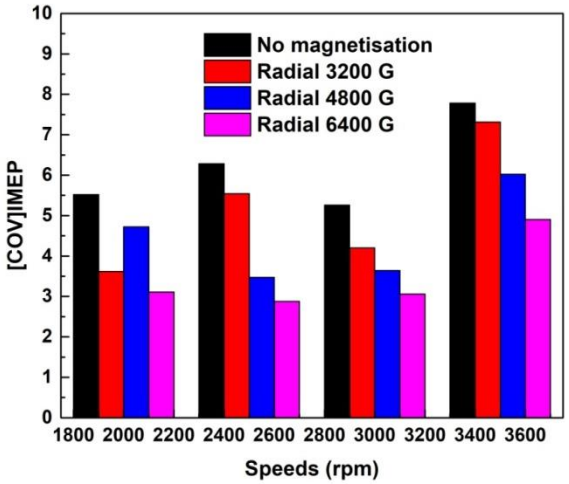

Fig 5.48 COV of IMEP in radial magnetisation of gasoline at various engine speeds

From the analysis, it can be observed that the COV of IMEP values lie well within 5 in the case of radial magnetisation as well when the intensity of magnetic field is raised to 6400 Gauss which indicates stable combustion.

5.2.7 Emission of Carbon monoxide

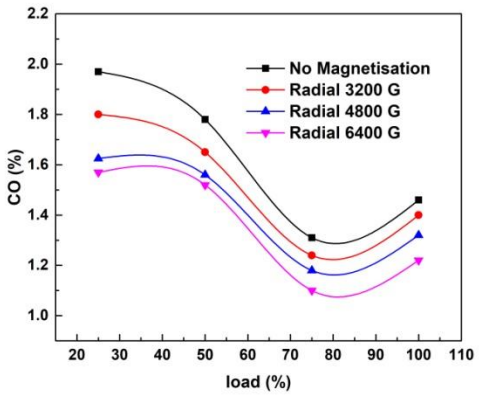

Fig 5.49 Variation in CO emission with RM at 2000 rpm

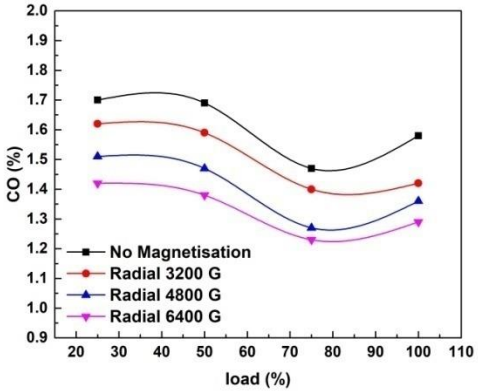

Fig 5.50 Variation in CO emission with RM at 2500 rpm

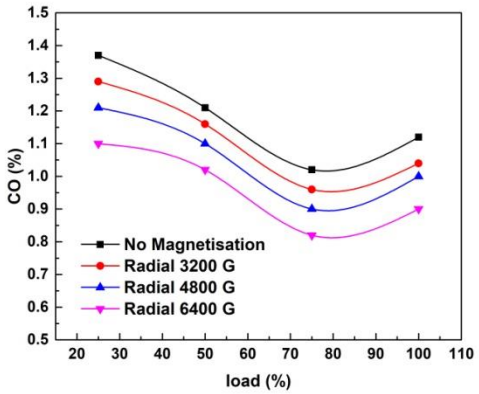

Fig 5.51 Variation in CO emission with RM at 3000 rpm

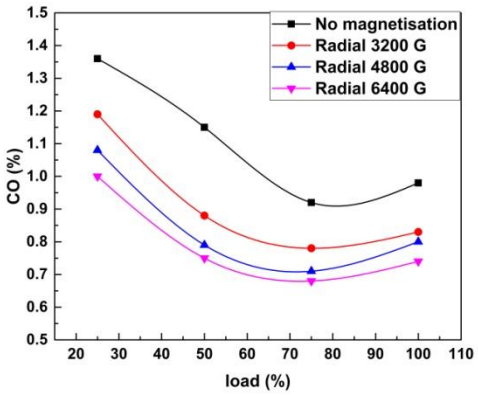

Fig 5.52 Variation in CO emission with RM at 3500 rpm

Carbon monoxide is a toxic pollutant occurring only in the exhaust which is formed as a result of incomplete combustion. The incomplete combustion can occur due to insufficient supply of air and insufficient time for burning (Mathur 1994). Even though

the complete elimination of CO may not be practically possible, the reduction of percentage content of this pollutant can be considered ideal.

The emission characteristics of CO under various intensities of radial magnetic fields are shown in figures 5.49- 5.52. It can be observed that the percentage content of CO decreases in stages of increasing intensity of the applied field. This is because of the enhanced availability of oxygen molecules for the combustion of hydrocarbon due to the dissociation of pseudo clusters enabled by the magnetic fields (Faris et al. 2010). When the throttle is closed during the deceleration, oxygen supply to the engine is hindered which results in the increased content of CO at lower speeds of the engine (Mathur et al. 1994). The magnitude of reduction of CO in the case of radially magnetised gasoline ranges up to 12.29% which is higher than that in the case of axial fields owing to the enhanced combustion features of radial fields.

5.2.8 Emission of Carbon dioxide

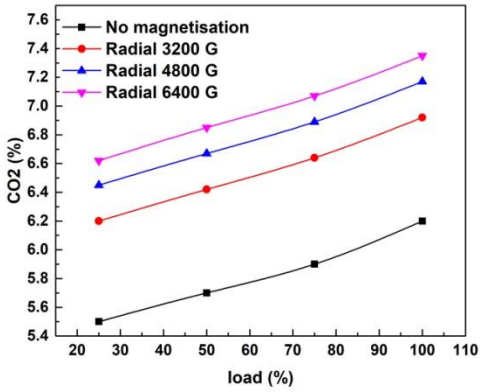

Fig 5.53 Variation in CO_2 emission with RM at 2000 rpm

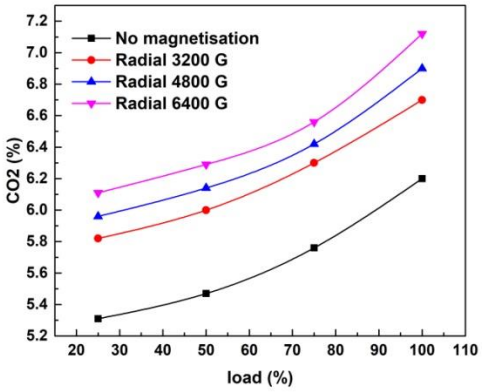

Fig 5.54 Variation in CO_2 emission with RM at 2500 rpm

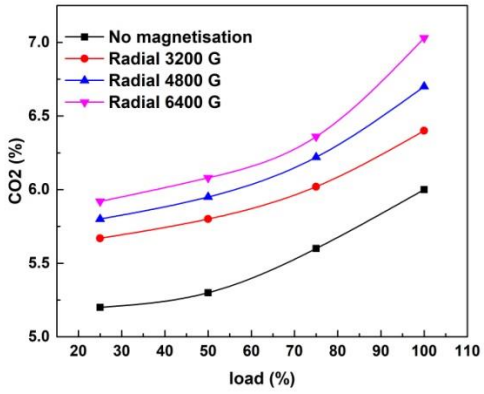

Fig 5.55 Variation in CO_2 emission with RM at 3000 rpm

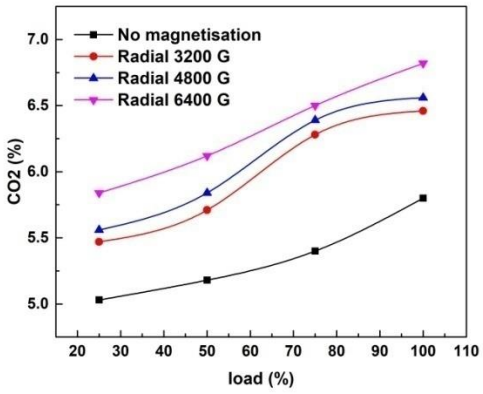

Fig 5.56 Variation in CO_2 emission with RM at 3500 rpm

The emission characteristics of carbon dioxide with radially magnetised gasoline as fuel are depicted in figures 5.53- 5.56. As discussed in the previous case, the emission of carbon dioxide is showing an increasing trend in magnetic field assisted combustion. The polarized hydrocarbons aid in enhanced combustion which promotes the generation and emission of carbon dioxide. Compared to the axial fields, the generation of CO_2 shows an increase of 2.45% in radial magnetic fields.

5.2.9 Emission of Hydrocarbons

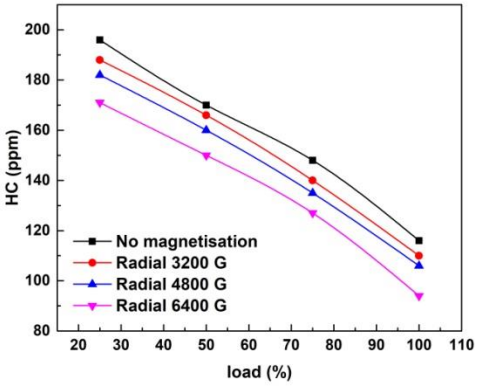

Fig 5.57 Variation in HC emission with RM at 2000 rpm

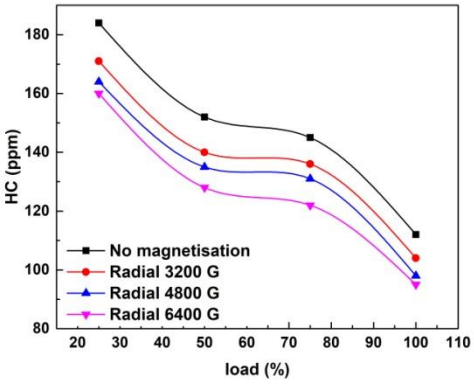

Fig 5.58 Variation in HC emission with RM at 2500 rpm

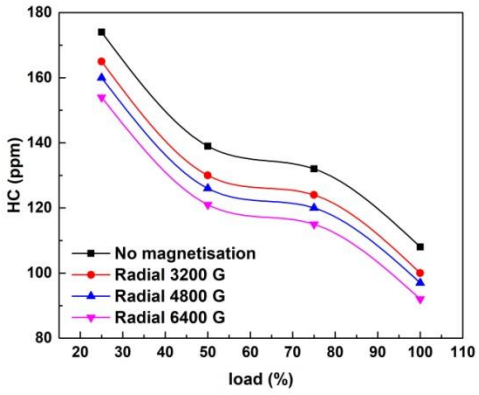

Fig 5.59 Variation in HC emission with RM at 3000 rpm

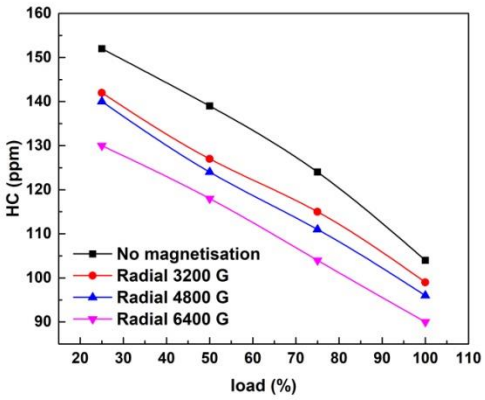

Fig 5.60 Variation in HC emission with RM at 3500 rpm

The emission of hydrocarbons is closely associated with the quality of combustion occurring inside the combustion chamber. As in the case of carbon monoxide emissions, incomplete combustion can lead to higher concentrations of HC in the exhaust. Sudden deceleration of the engine and low speed operations are usually associated with increased emissions of HC (Heywood 1998). As the combustion is enhanced through better availability of oxygen to the interior carbon atoms of the fuel molecules, the concentration of HC in the exhaust is observed to reduce in stages. The maximum reduction in HC is observed with radial 6400 Gauss field where the content of HC is reduced by 9.72%. In comparison with axially magnetised gasoline, HC emissions are further reduced by 1.8% under radial magnetic fields.

5.2.10 Emission of Oxides of Nitrogen

The NO_x emission is found to increase with load till 75% loading where it is the highest and then decreases at all tested speeds. The emission characteristics of NO_x under various intensities of radially magnetised gasoline are provided in figures 5.61- 5.64. It is clear from the plots that unlike other regulated emissions from a spark ignited engine, the emission of NO_x is the least affected under magnetic field assisted combustion.

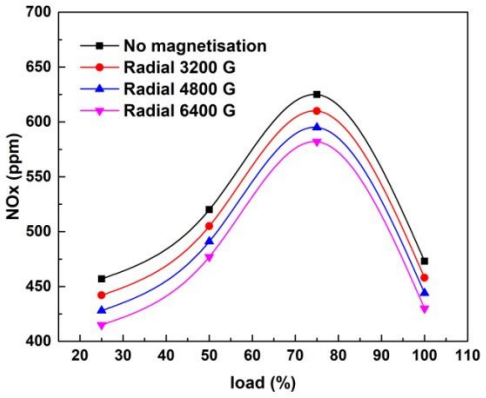

Fig 5.61 Variation in NO_x emission with RM at 2000 rpm

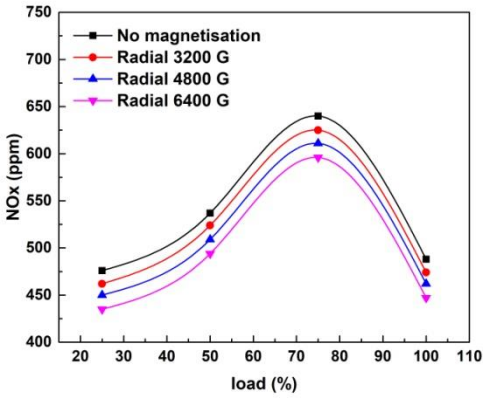

Fig 5.62 Variation in NO_x emission with RM at 2500 rpm

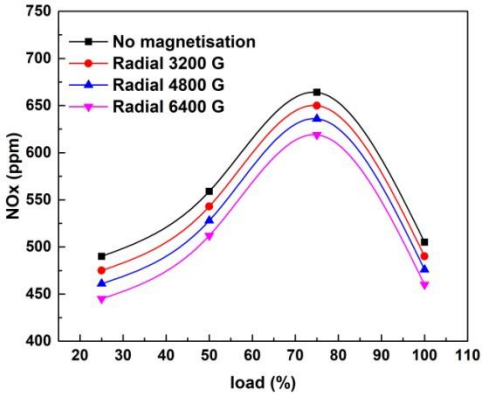

Fig 5.63 Variation in NO_x emission with RM at 3000 rpm

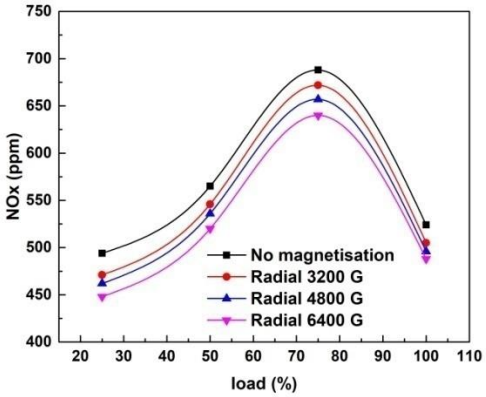

Fig 5.64 Variation in NO_x emission with RM at 3500 rpm

Similar to the results obtained in the case of axial magnetisation, emission of NO_x is observed to decrease very slightly with increasing intensities of magnetic fields. The variation between the curves is evident in the lower loads but strenuous to differentiate at the full load operation because of the temperature dependence of NO_x generation. With comparison to the axially magnetised fuel, the emission of NO_x reduces further by 1.6% in some conditions where as the reduction is negligible in the others.

5.3 Effect of Axial Magnetisation (AM) pattern on Magnetic field assisted combustion of gaseous phase hydrocarbons (LPG)

In the first two stages of experimentation, the effects of axial and radial magnetic fields on the combustion of liquid phase hydrocarbons were studied. In this case, the influence of varying intensities of axial magnetic field on the magnetic field assisted combustion of a gas phase hydrocarbon is investigated. For this, the test engine is fuelled by neat liquefied petroleum gas with suitable modifications as discussed in chapter 3. The magnetic mounting is provided on the LPG fuel line adjacent to the injectors. The engine is operated in conditions similar to which gasoline was experimented.

5.3.1 Brake Power

The power output characteristics of the test engine under LPG fuelling are represented in figures 5.65- 5.68. When the engine is fuelled by neat LPG, the power output obtained is comparatively higher than gasoline fuelled operation. This is especially noticeable at higher engine speeds where the flame propagation velocity of LPG is higher compared to gasoline (Nayak et al. 2016). Hence the brake power of the engine under neat LPG operation is found to be improved by 23.8% when compared to the normal gasoline operation.

The magnetic field has an influence over the gas phase hydrocarbons because of the same underlying physical phenomenon as discussed in the previous case and is evident from the increase in power output. Similar to the observations in the case of gasoline, the brake power of the engine is found to increase slightly with increasing intensities of applied magnetic field and is found to be highest with the field intensity of 6400 Gauss.

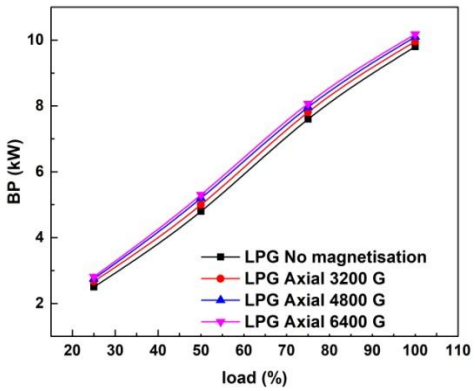

Fig 5.65 Variation in BP with AM of LPG at 2000 rpm

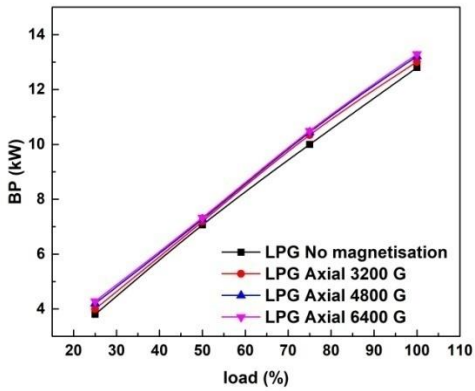

Fig 5.66 Variation in BP with AM of LPG at 2500 rpm

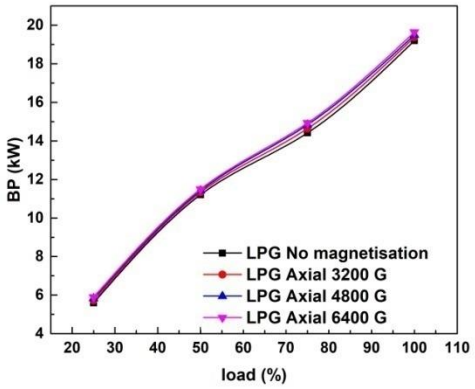

Fig 5.67 Variation in BP with AM of LPG at 3000 rpm

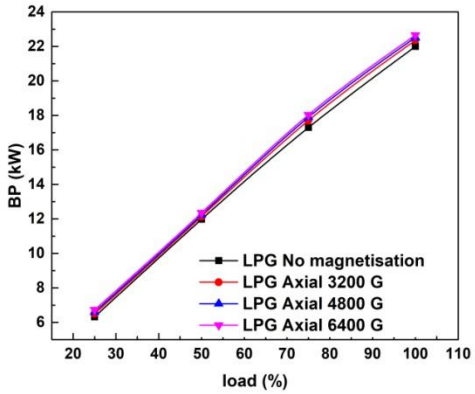

Fig 5.68 Variation in BP with AM of LPG at 3500 rpm

The increase in brake power in the case of magnetised LPG is observed to be less in comparison with the liquid phase fuel. The liquid phase fuels pocess a comparatively contiguous arrangement of molecules which enables superior realignment when subjected to strong enough magnetic fields. This effect will be inferior in the case of gas phase hydrocarbons with the molecules distanced apart and hence the influence on combustion is lower. Under axial magnetisation pattern, the brake power of the test engine under LPG operation shows an improvement up to 2.66%.

5.3.2 Brake Specific Fuel Consumption

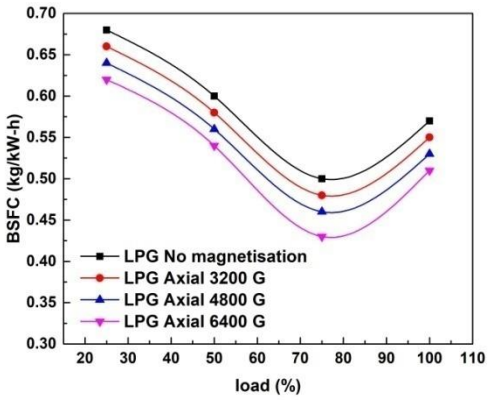

Fig 5.69 Variation in BSFC with AM of LPG at 2000 rpm

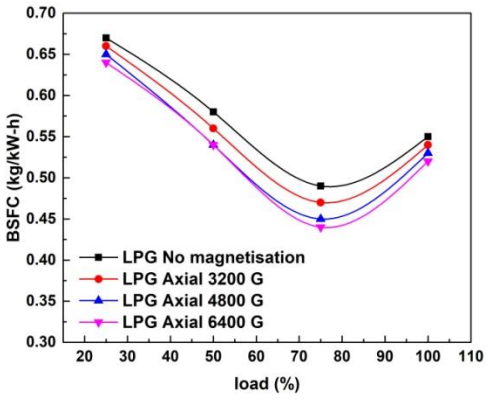

Fig 5.70 Variation in BSFC with AM of LPG at 2500 rpm

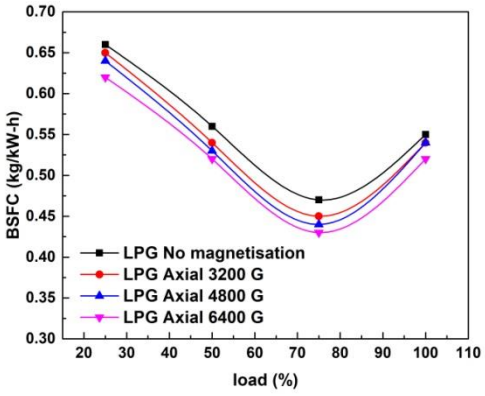

Fig 5.71 Variation in BSFC with AM of LPG at 3000 rpm

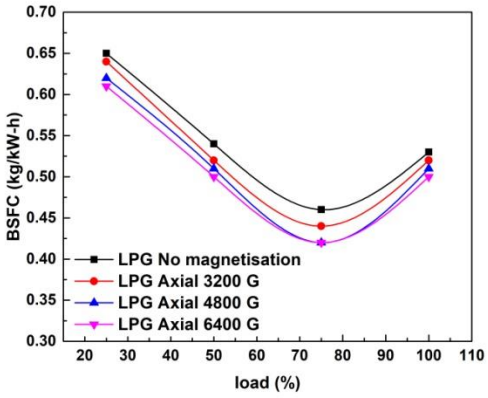

Fig 5.72 Variation in BSFC with AM of LPG at 3500 rpm

Figures 5.69- 5.72 represent the fuel consumption characteristics of the test engine under the magnetic field assisted combustion of LPG. At quarter loads the brake power generated is low at all tested speeds and thus making highest fuel consumption points in all the plots. The higher self ignition temperature of LPG when compared to gasoline causes higher combustion duration and thus the magnitude of specific fuel consumption is observed to be higher in the case of LPG (Nayak et al. 2016).

Under increasing intensities of axial magnetic field, the brake specific consumption of LPG is found to decrease in steps with the maximum improvement of fuel economy noted for 6400 Gauss field where a reduction of 6.15% is observed. The access of sufficient quantities of oxygen which is otherwise hindered through the pseudo association of hydrocarbon structures is made functional by the polarizing magnetic fields which enable the better utilization of fuel in the combustion process (Sahoo et al. 2019). This results in the reduction in consumption of fuel, resulting in superior fuel economy.

5.3.3 Brake Thermal Efficiency

The thermal efficiency of the engine operated under neat LPG is lower when compared to the normal gasoline operation. The higher ignition temperature of LPG results in a longer ignition delay and hence higher combustion duration. The resultant reduction in average burning rate causes an increased consumption of fuel which leads to reduction in efficiency (Ceviz et al. 2005).

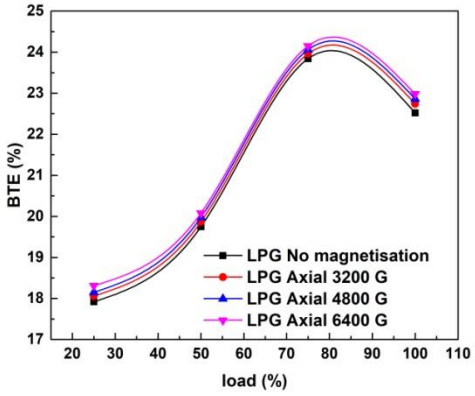

Fig 5.73 Variation in BTE with AM of LPG at 2000 rpm

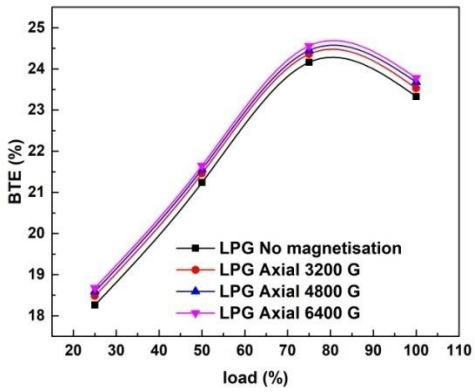

Fig 5.74 Variation in BTE with AM of LPG at 2500 rpm

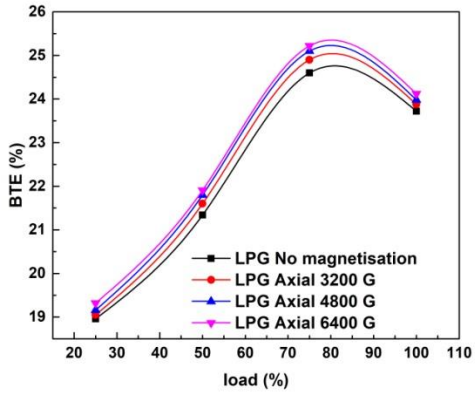

Fig 5.75 Variation in BTE with AM of LPG at 3000 rpm

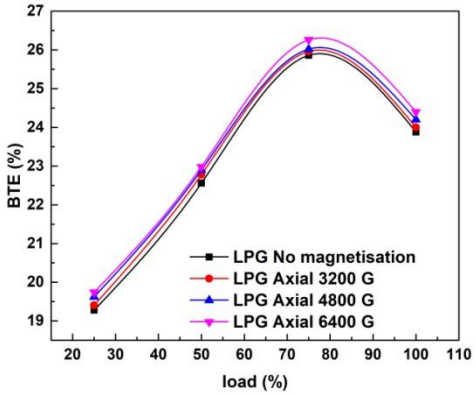

Fig 5.76 Variation in BTE with AM of LPG at 3500 rpm

When LPG is magnetised, thermal efficiency of the engine is observed to be increasing marginally at all load and speed conditions as observed in figures 5.73- 5.76 owing to the improvement obtained in fuel economy as well as power output. The improvement gained in efficiency is lesser compared to that in the liquid phase hydrocarbon. An improvement up to 2.23% is observed in the case of axially magnetised LPG.

5.3.4 In-cylinder Pressure

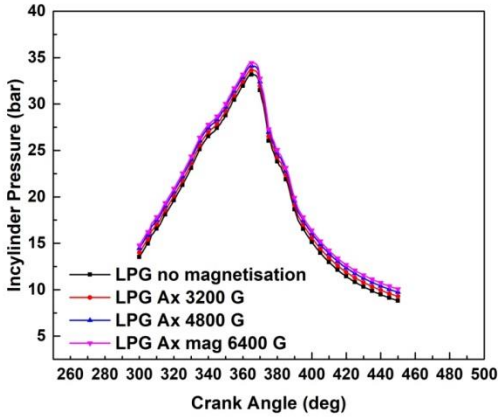

Fig 5.77 Variation in cylinder pressure of LPG with AM at 2500 rpm

The variation of cylinder pressures for 100 consecutive cycles with axially magnetised LPG as the fuel at 2500 rpm is represented in figure 5.77. The combustion of LPG results in an increase of peak pressures inside the combustion chamber due to its higher flame speed (Nayak et al. 2016). The increment in peak pressures is more pronounced at higher engine speeds and indicates that LPG provides better combustion properties when compared to gasoline. Compared to normal gasoline operation, the peak pressure points occur much closer to the top dead centre in LPG combustion. When magnetised LPG is used as the fuel, a slight increase is observed in the magnitude of peak pressures at the original crank angle position. This is a good indication that the magnetic fields have a positive influence on gas phase combustion as well.

5.3.5 Net Heat Release Rate

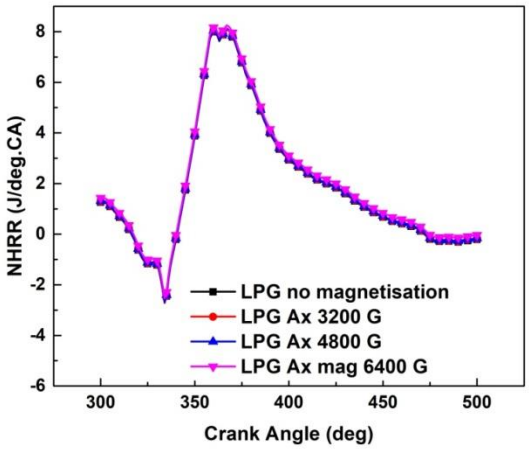

Fig 5.78 Variation in Net Heat Release Rates of LPG with AM at 2500 rpm

The physical and chemical properties of the hydrocarbons are the foremost parameters which influence the heat release rate after combustion. It is clear from the plot that the peak locations of heat release have increased in the case of LPG combustion when compared with normal gasoline operation. LPG being a gaseous phase fuel mixes well with air and hence burns more rapidly with better heat release characteristics.

The net heat release rate of axially magnetised LPG at 2500 rpm is shown in figure 5.78. Axial magnetisation in varying intensities resulted in a slight improvement in peak heat release rates further. The effect produced by magnetisation on the NHRR characteristics is very limited compared to the effect in gasoline combustion. The location of peak heat release points is adjacent to the top dead centre position.

5.3.6 Analysis of Combustion Stability

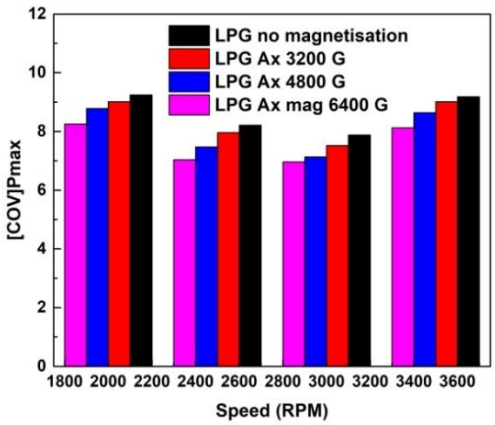

Fig 5.79 COV of P_{max} in axial magnetisation of LPG at various engine speeds

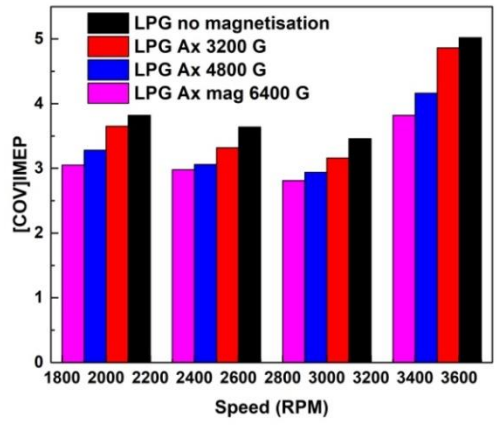

Fig 5.80 COV of IMEP in axial magnetisation of LPG at various engine speeds

The cyclic variations in combustion pressures eventually affect the performance and emissions of the engine. The stability of combustion is analyzed though the COV of P_{max} and COV of IMEP to understand the variations in combustion pressures. The COV of Pmax and COV of IMEP plots of axially magnetised LPG are shown in figures 5.79-5.80.

It can be observed that the variations in combustion are reduced when the fuel is subjected to strong magnetic fields. With a magnetic intensity of 6400 Gauss, the COV of IMEP values lay well within 5 at all the tested speeds which indicate stable combustion. The reduction in fluctuations in combustion is reflected in the improved performance as well as the emissions of the engine.

5.3.7 Emission of Carbon Monoxide

The concentration of Carbon monoxide in the exhaust gas is usually lower than that in the combustion chamber but is significantly more than equilibrium concentration for exhaust conditions (Heywood 1998).

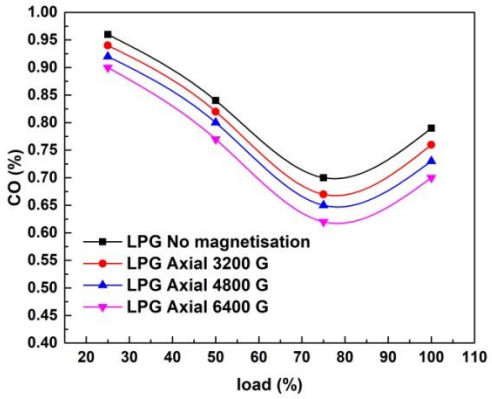

Fig 5.81 Variation in emission of CO with AM for LPG at 2000 rpm

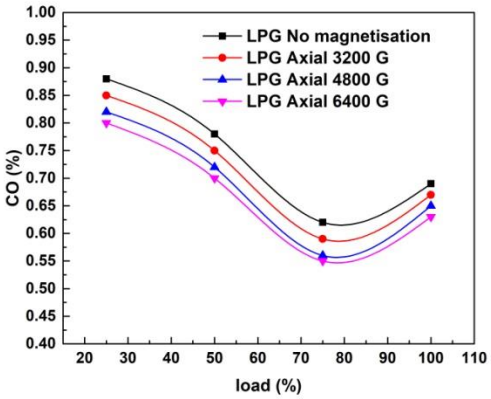

Fig 5.82 Variation in emission of CO with AM for LPG at 2500 rpm

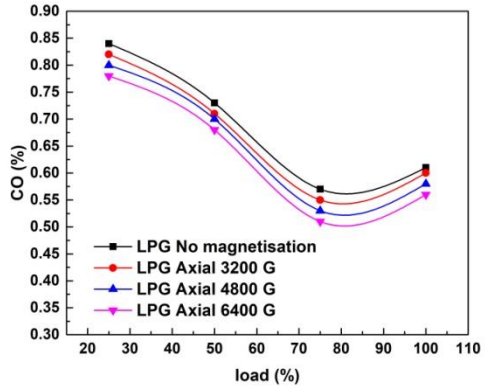

Fig 5.83 Variation in emission of CO with AM for LPG at 3000 rpm

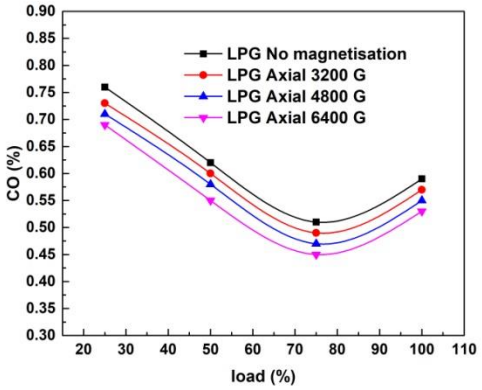

Fig 5.84 Variation in emission of CO with AM for LPG at 3500 rpm

When the engine is operated under neat LPG, because of better mixing of fuel and air, the levels of CO formation is observed to be lesser than in gasoline fuelled condition. However the trend of CO formation remains the same for all tested loads and engine speeds. The emission characteristics of CO for axially magnetised LPG are depicted in figures 5.81- 5.84.

The declustering of molecular associations by the strong magnetic fields resulted in reduced emissions of CO at all engine speeds. The maximum reduction in CO is obtained for a field intensity of 6400 Gauss where CO levels fall by 13.15% than the baseline operation of LPG. This is in accordance with the results obtained for magnetised Natural gas in a single cylinder SI engine (Abdel-Rehim et al. 2014).

5.3.8 Emission of Carbon dioxide

The trend of emission of carbon dioxide with LPG under axial magnetisation is shown in figures 5.85- 5.88. Because of the enhanced combustion properties of LPG over gasoline, the percentage content of CO_2 in the exhaust is more in the case of LPG combustion. As discussed in the case of liquid hydrocarbons, magnetic field assisted combustion further leads to the generation of more amount of carbon dioxide. This trend remains the same for all the load and speed conditions of the engine.

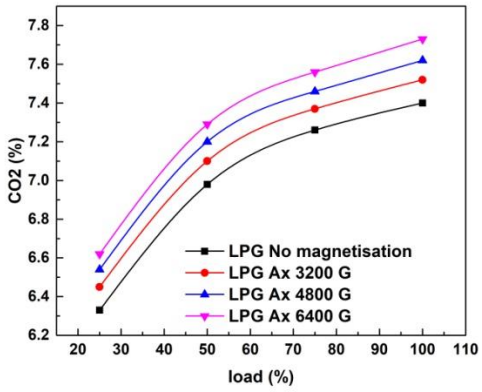

Fig 5.85 Variation in emission of CO_2 with AM for LPG at 2000 rpm

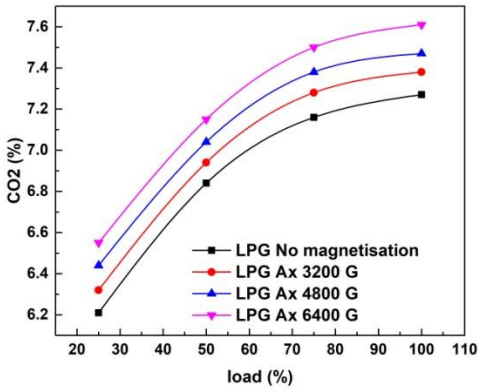

Fig 5.86 Variation in emission of CO_2 with AM for LPG at 2500 rpm

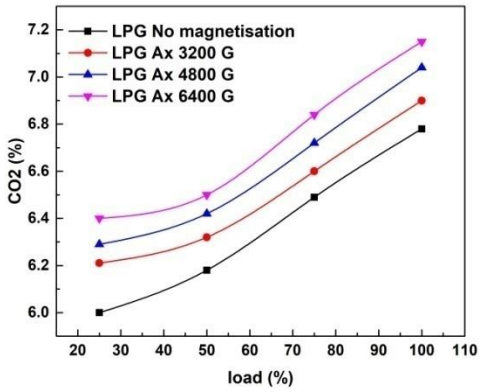

Fig 5.87 Variation in emission of CO_2 with AM for LPG at 3000 rpm

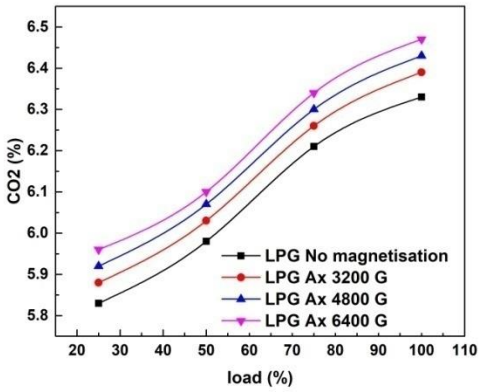

Fig 5.88 Variation in emission of CO_2 with AM for LPG at 3500 rpm

Compared to the baseline emission of CO_2, axial magnetic field intensity of 6400 Gauss resulted in 2.5% higher emission levels.

5.3.9 Emission of Hydrocarbons

Organic emissions are most often the consequence of incomplete combustion and is expressed in terms of total hydrocarbon concentration in the exhaust in parts per million. HC emissions can be considered as an evocative index of combustion inefficiency (Heywood 1998).

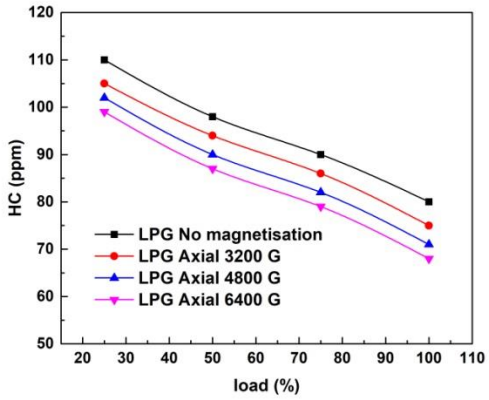

Fig 5.89 Variation in emission of HC with AM for LPG at 2000 rpm

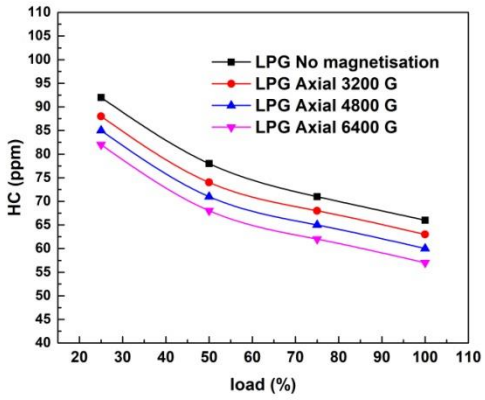

Fig 5.90 Variation in emission of HC with AM for LPG at 2500 rpm

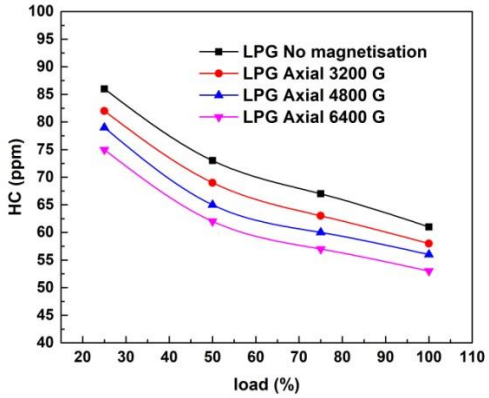

Fig 5.91 Variation in emission of HC with AM for LPG at 3000 rpm

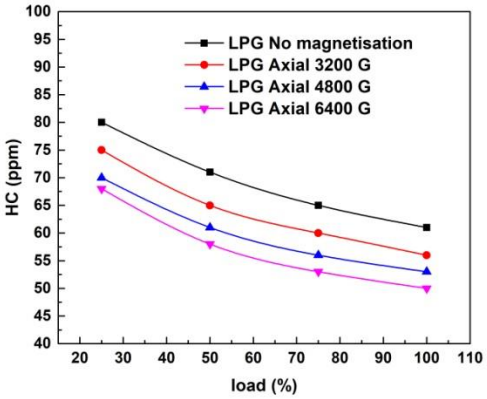

Fig 5.92 Variation in emission of HC with AM for LPG at 3500 rpm

With comparison to gasoline combustion, the concentration of hydrocarbons in the engine exhaust is vastly reduced in the case of LPG fuelled operation. The lower aromatic content in LPG is the major reason for the reduced emission of hydrocarbons (Lee et al. 1986). When magnetised, combustion becomes more efficient thus further reducing the content of HC in the exhaust. The HC emission patterns at various engine speeds under axial magnetic fields are shown in figures 5.89- 5.92.

5.3.10 Emission of Oxides of Nitrogen

While LPG has advantages over gasoline in most of the combustion and emission related parameters, the major drawback associated with it is the significant increase in NO_x emissions. The content of NO_x in the exhaust is expressed in parts per million and is found to be more than three times to that observed in gasoline combustion. The higher flame propagation speed of LPG results in increased burning rate and enhanced combustion which eventually results in the generation of high amount of NO_x (Nayak et al. 2016).

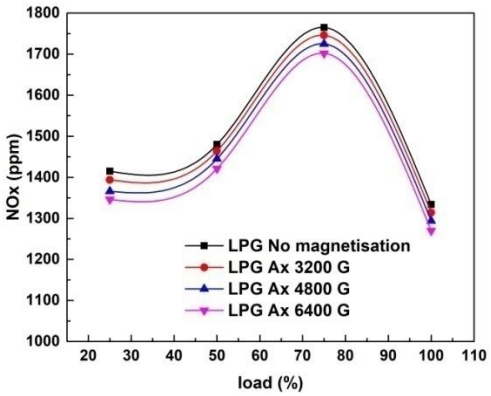

Fig 5.93 Variation in NO_x emission with AM of LPG at 2000 rpm

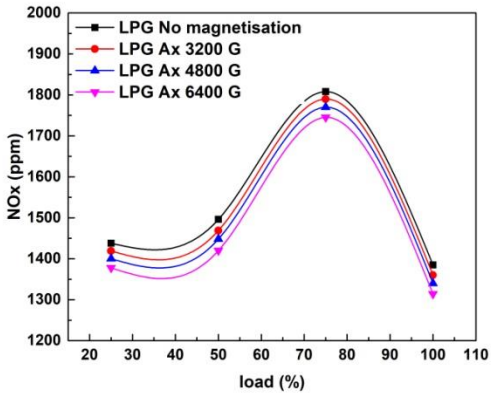

Fig 5.94 Variation in NO_x emission with AM of LPG at 2500 rpm

It can be observed that for LPG combustion, the concentration of NO_x steadily increases with load till 75% loading and then decreases. This trend holds true for all the experimented speeds. Figures 5.93- 5.96 show the emission characteristics of NO_x under various intensities of axially magnetised LPG. There is no demarkable reduction in NO_x content for full load operation at all speeds of the engine. However, a slight reduction is observed at lower load which in effect is insignificant compared to that in the combustion of liquid fuels.

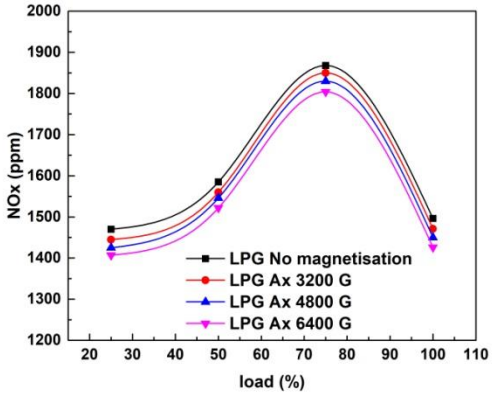

Fig 5.95 Variation in NO_x emission with AM of LPG at 3000 rpm

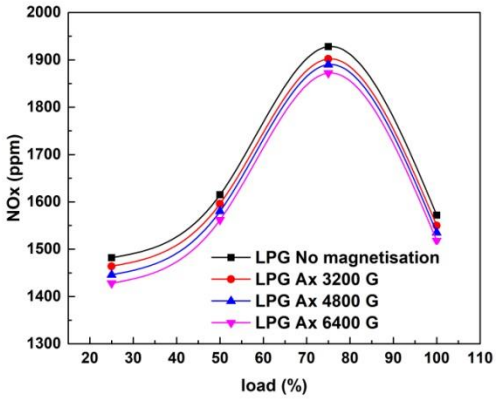

Fig 5.96 Variation in NO_x emission with AM of LPG at 3500 rpm

5.4 Effect of Radial Magnetisation (RM) pattern on Magnetic field assisted combustion of gaseous phase hydrocarbons (LPG)

To investigate the effect of radial magnetic fields on the combustion of gas phase hydrocarbons, radially magnetised NdFeB rings are mounted on the fuel line. Sintered N38 grade rings are provided a coating of Ni-Cu-Ni similar to the case of axially magnetised blocks to resist thermal corrosion. Experiments are conducted on the test engine with neat LPG as the fuel maintaining the same operating conditions as in the case of axial fields.

5.4.1 Brake Power

The power output characteristics of the test engine for various speed and load conditions at different intensity radial magnetic fields are represented in figures 5.97- 5.100. It can be observed that as the strength of magnetic fields is increased, the power output of the engine increases proportionally. The molecular pseudo clusters formed due to the physical attractive forces between positively and negatively charged particles in the hydrocarbon molecules are dissociated by the polarizing magnetic fields which improve the combustion properties of the fuel which in turn results in enhanced power (Sahoo et

al. 2019). Similar to the case of liquid hydrocarbons, the effect is higher in the case of radial fields with improvement in brake power ranging up to 3.44%.

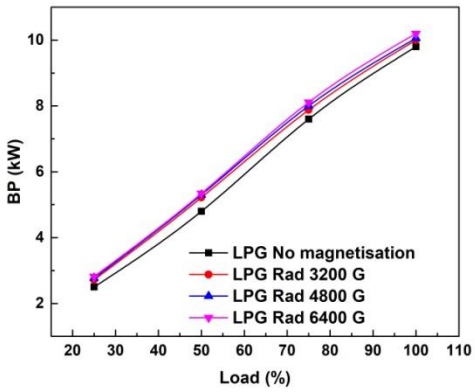

Fig 5.97 Variation in BP with RM of LPG at 2000 rpm

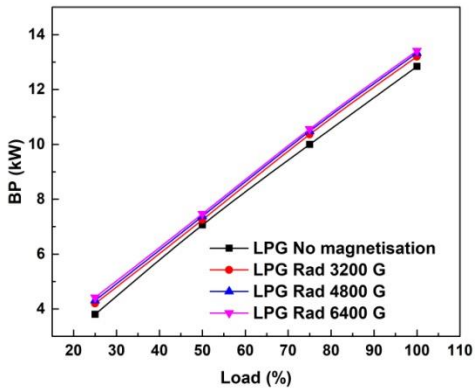

Fig 5.98 Variation in BP with RM of LPG at 2500 rpm

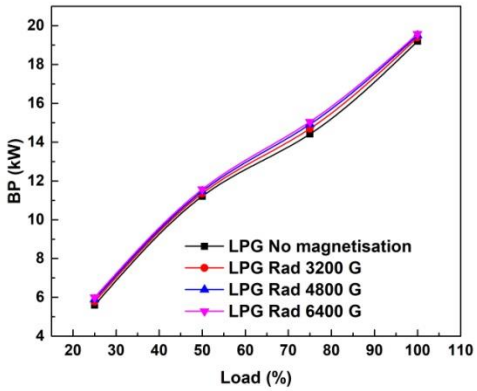

Fig 5.99 Variation in BP with RM of LPG at 3000 rpm

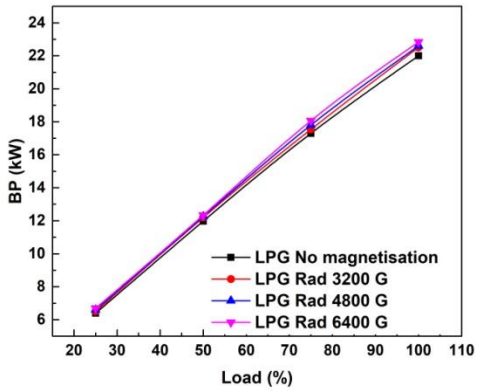

Fig 5.100 Variation in BP with RM of LPG at 3500 rpm

5.4.2 Brake Specific Fuel Consumption

The reduction in average burning rate caused by the prolonged duration of combustion of LPG effectuates greater consumption of fuel resulting in the degradation of fuel economy than during the normal gasoline operation.

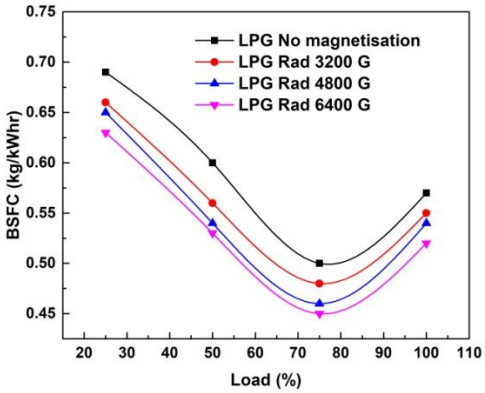

Fig 5.101 Variation in BSFC with RM of LPG at 2000 rpm

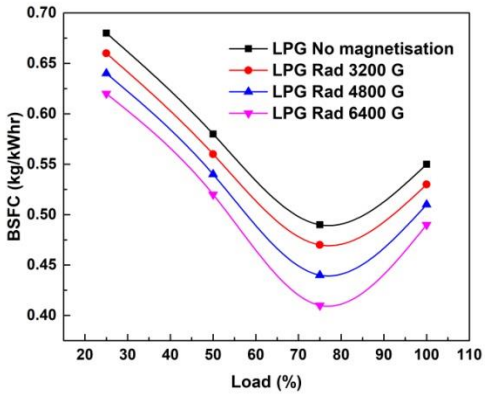

Fig 5.102 Variation in BSFC with RM of LPG at 2500 rpm

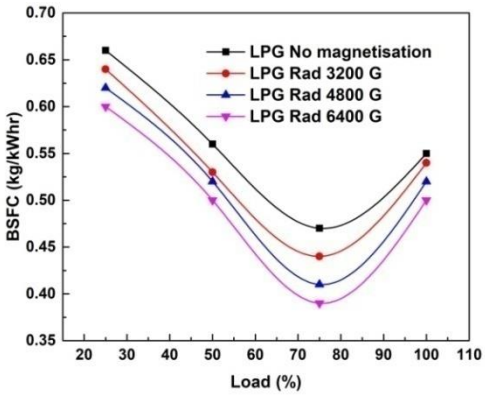

Fig 5.103 Variation in BSFC with RM of LPG at 3000 rpm

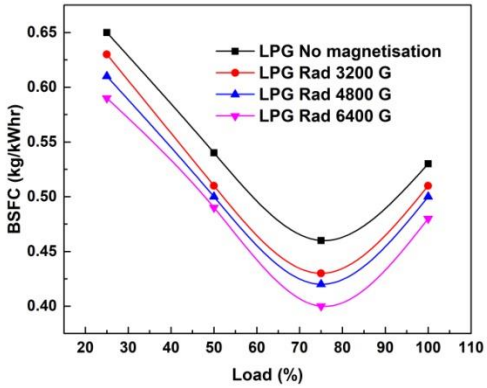

Fig 5.104 Variation in BSFC with RM of LPG at 3500 rpm

The trends of consumption of LPG at various speeds remain similar to that in the case of axial magnetic fields. A reduction in consumption of fuel is observed for all intensities of magnetic field till 75% load point where the fuel economy is the maximum. The movements of outer electrons into higher principal energy states driven by the applied magnetic fields weaken the Vander Waals bonds in the hydrocarbons which ultimately results in better association of fuel molecules with oxygen (Faris et al. 2010). Through this process the better utilization of fuel is accomplished thus resulting in improved fuel economy. This effect is less pronounced in gas phase hydrocarbons like LPG where the

molecules are spaced apart discontinuously and hence the improvement in fuel economy is limited up to 9.23% which is inferior to the improvement obtained in the case of gasoline. The BSFC trend of radially magnetised LPG is shown in figures 5.101- 5.104.

5.4.3 Brake Thermal Efficiency

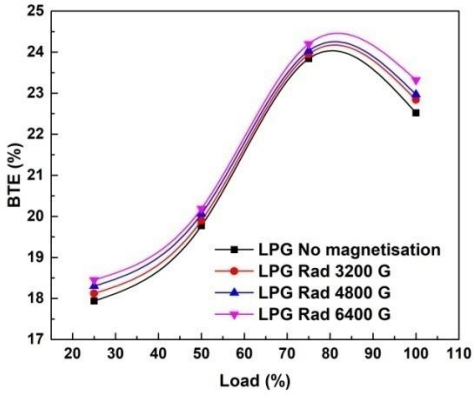

Fig 5.105 Variation in BTE with RM of LPG at 2000 rpm

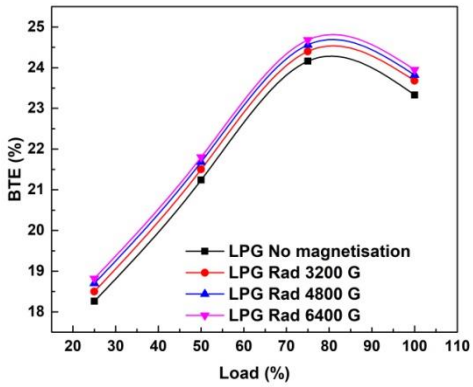

Fig 5.106 Variation in BTE with RM of LPG at 2500 rpm

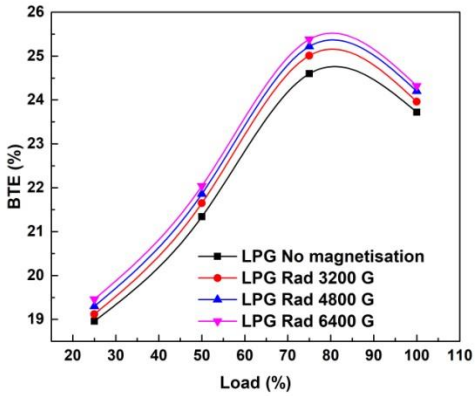

Fig 5.107 Variation in BTE with RM of LPG at 3000 rpm

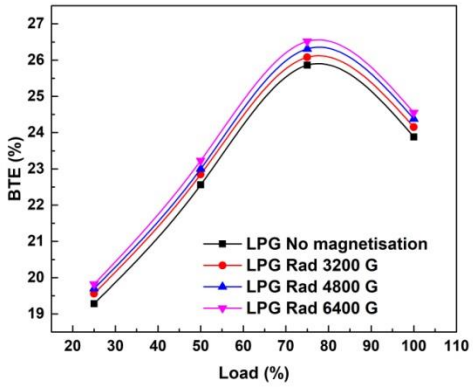

Fig 5.108 Variation in BTE with RM of LPG at 3500 rpm

The thermal efficiency characteristics of the test engine operated with radially magnetised LPG are represented in figures 5.105- 5.108. The improvement yielded in

power output and fuel economy through radial magnetic fields is reflected in the thermal efficiency values as well at all tested conditions. Though a slight increment is observed in the efficiency values in comparison with the axial fields, the impact of magnetisation is inferior to that in liquid phase hydrocarbons. The maximum improvement in thermal efficiency under the radial fields is limited to 2.24% than the baseline operation of LPG.

5.4.4 In-cylinder Pressure

The variation in incylinder pressure with different intensity radial magnetic fields for gas phase hydrocarbons at an engine speed of 2500 rpm is depicted in figure 5.109. The plot is generated for average pressure values calculated from 100 consecutive cycles of combustion.

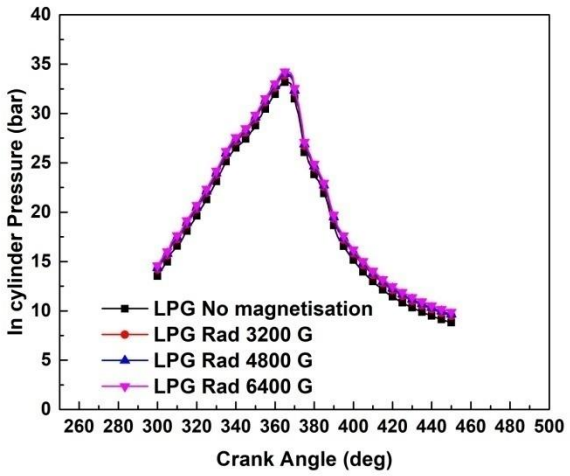

Fig 5.109 Variation in cylinder pressure of LPG with RM at 2500 rpm

Similar to the case of axial fields, the magnitude of peak pressures is observed to increase slightly as the intensity of magnetisation is raised. However the crank positions corresponding to the peak cylinder pressures remain the same. The location of peak pressures is observed to be adjacent to TDC unlike in the case of gasoline where the peak pressure occurs 15-20 degrees after TDC. Radial magnetic field with its ability to create

more torque ripple (Morcos 2002) is observed to enhance the cylinder pressure values than its axial counterpart.

5.4.5 Net Heat Release Rate

The Net Heat Release Characteristics of LPG under radial magnetisation for an engine speed of 2500 rpm is shown in figure 5.110. As in the case of axial magnetisation, the trend of heat release pattern remains the same with a minute increase in the magnitude of heat transfer. The crank positions corresponding to the peak heat release points are observed to remain intact for all the intensities. The higher availability of oxygen to the hydrocarbon molecules during the magnetic field assisted combustion aids in the higher release of heat in the combustion cycles. As observable from the plot, the peak heat release points lie immediately adjacent to the TDC position.

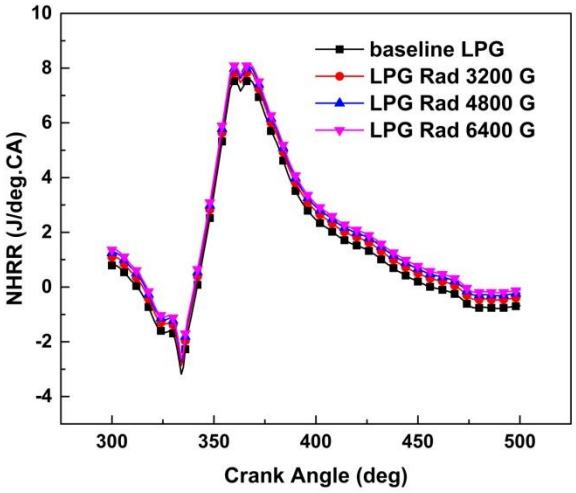

Fig 5.110 Variation in NHRR of LPG with RM at 2500 rpm

5.4.6 Analysis of Stability of Combustion

The stability of combustion is analyzed statistically from the coefficient of variation of P_{max} and IMEP which is computed from the mean and standard deviation of pressure

data. Figures 5.111 and 5.112 shows the variation in COV of P_{max} and COV of IMEP with radially magnetised LPG.

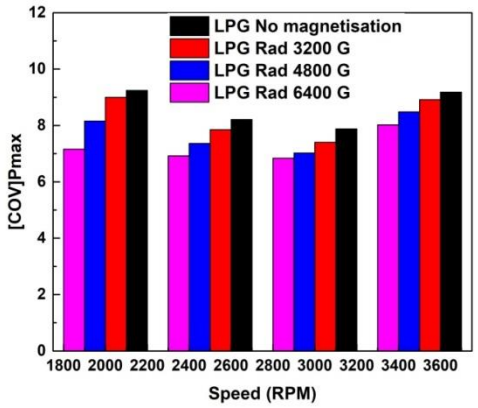

Fig 5.111 COV of P_{max} in radial magnetisation of LPG at various engine speeds

Similar to the case in axial magnetisation, the Coefficient of Variation of maximum pressures and indicated mean effective pressures is found to reduce indicating the diminishment of cyclic variations in combustion. There is not much difference in the magnitude of reduction of combustion variations between the two experimented patterns of magnetisation.

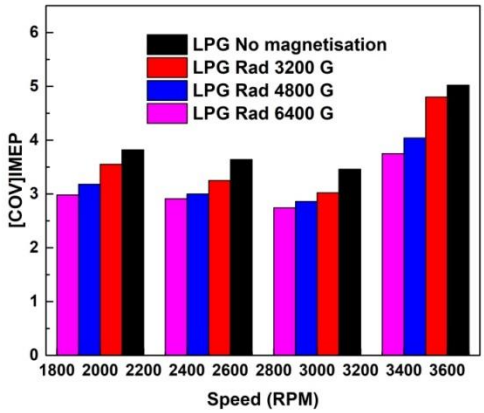

Fig 5.112 COV of IMEP in radial magnetisation of LPG at various engine speeds

5.4.7 Emission of Carbon monoxide

The emission characteristics of CO under various intensities of radial magnetic fields with LPG as fuel are shown in figures 5.113- 5.116. As discussed in the case of axial fields, the emission of CO is brought down when neat LPG is used to fuel the engine. It can also be observed that the percentage content of CO decreases in stages of increasing intensity of the applied field.

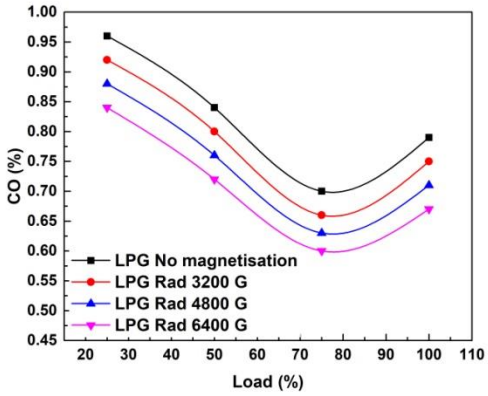

Fig 5.113 Variation in emission of CO with RM for LPG at 2000 rpm

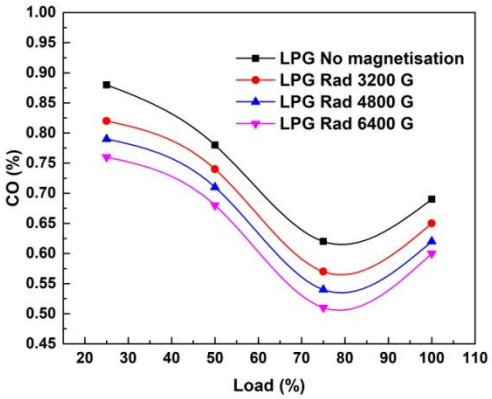

Fig 5.114 Variation in emission of CO with RM for LPG at 2500 rpm

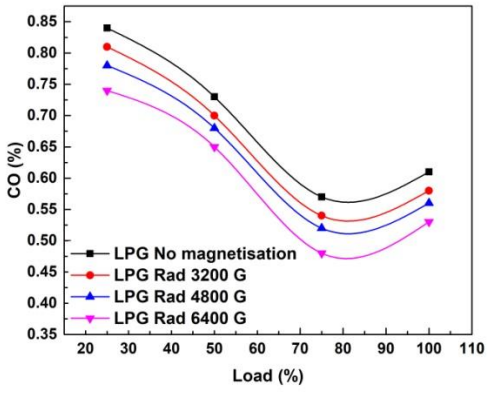

Fig 5.115 Variation in emission of CO with RM for LPG at 3000 rpm

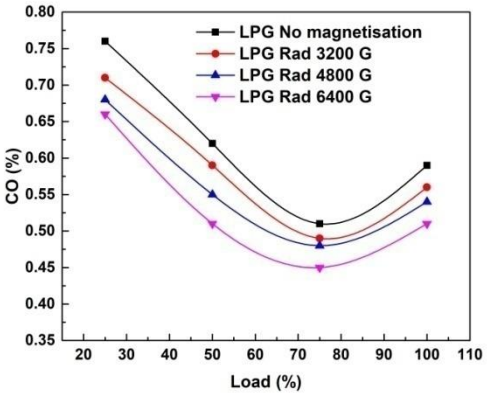

Fig 5.116 Variation in emission of CO with RM for LPG at 3500 rpm

This is because of the enhanced availability of oxygen molecules for the combustion of hydrocarbon due to the dissociation of pseudo clusters enabled by the magnetic fields (Faris et al. 2010). The magnitude of reduction of CO in the case of radially magnetised LPG ranges up to 9.78% which is higher than that in the case of axial fields owing to the enhanced combustion features of radial fields. The reduction obtained in the emission of CO is an indication of enhancement of combustion efficiency under the influence of magnetic fields.

5.4.8 Emission of Carbon dioxide

The emission of CO_2 is found to increase with the applied load at all tested speeds. The molecular alignments of hydrocarbons get reformed under strong magnetic fields which eventually results in enhanced combustion (Govindasamy et al. 2007). As the extend of completion of combustion is improved in magnetic field assisted combustion the percentage of carbon dioxide in the exhaust increases simultaneously, as observed from the plots. The maximum increase in carbon dioxide emissions under axial magnetisation pattern is observed for 6400 Gauss field.

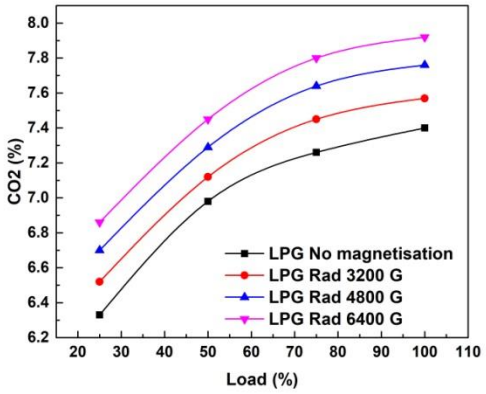

Fig 5.117 Variation in emission of CO_2 with RM for LPG at 2000 rpm

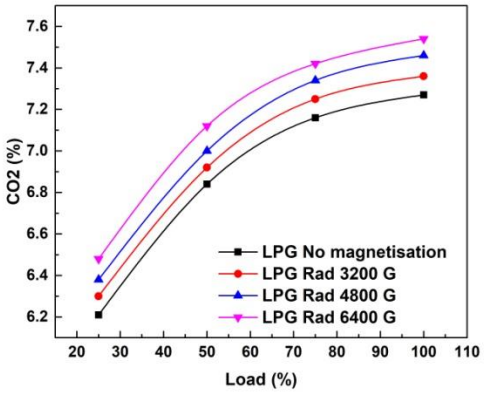

Fig 5.118 Variation in emission of CO_2 with RM for LPG at 2500 rpm

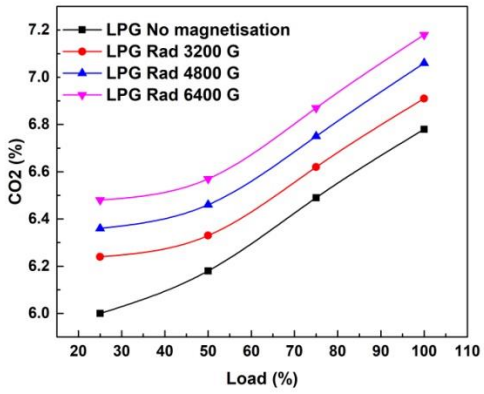

Fig 5.119 Variation in emission of CO_2 with RM for LPG at 3000 rpm

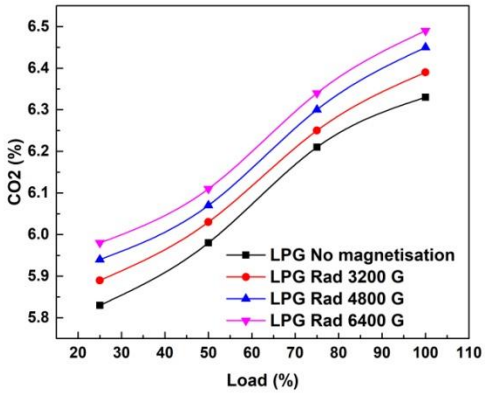

Fig 5.120 Variation in emission of CO_2 with RM for LPG at 3500 rpm

The percentage content of carbon dioxide in the exhaust for radial magnetic fields is observed to be higher because of attainment of superior combustion efficiency under them. The emission trends of CO_2 for LPG under radial fields are depicted in figures 5.117- 5.120.

5.4.9 Emission of Hydrocarbons

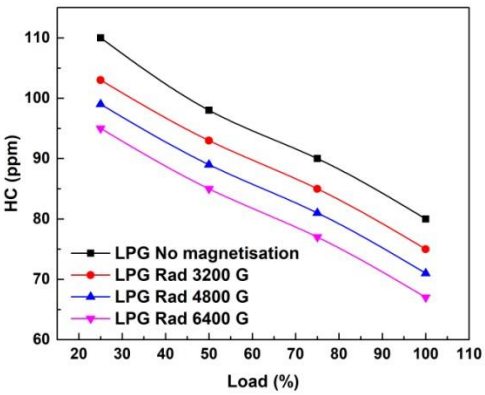

Fig 5.121 Variation in emission of HC with RM for LPG at 2000 rpm

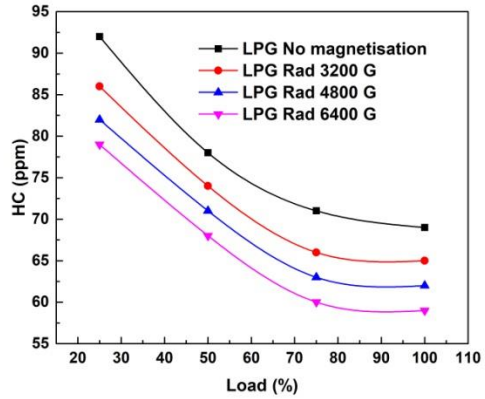

Fig 5.122 Variation in emission of HC with RM for LPG at 2500 rpm

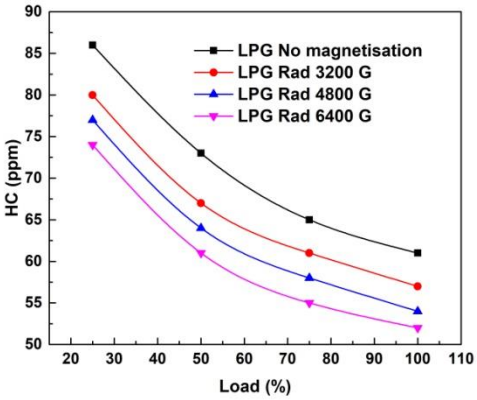

Fig 5.123 Variation in emission of HC with RM for LPG at 3000 rpm

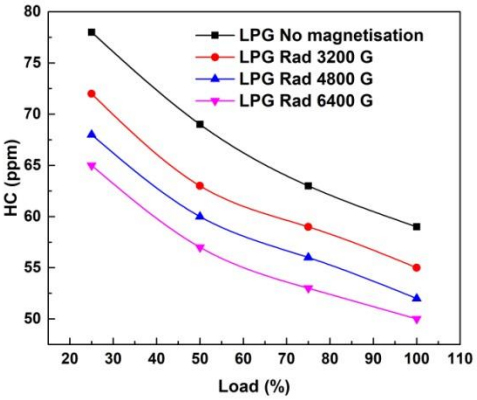

Fig 5.124 Variation in emission of HC with RM for LPG at 3500 rpm

The gaseous hydrocarbons treated by strong magnetic fields tend to decluster enabling the better penetration of oxygen into the interior carbon atoms thus increasing the combustion efficiency. As a result of increased combustion efficiency the emission of hydrocarbons through the exhaust is reduced. Under radial fields the concentration of HC in the exhaust is reduced up to 16.66% with the maximum reduction under radial 6400 Gauss field which is substantially higher (5.13%) than the reduction obtained for the same intensity field of axial magnetisation. The variation in HC emissions for varying intensities of radially magnetised LPG are shown in figures 5.121- 5.124.

5.4.10 Emission of Oxides of Nitrogen

The elevated temperatures prevailing inside the combustion chamber makes the otherwise inert nitrogen to react with oxygen forming various oxides which are toxic and are classified as NO_x in general. The emission trends of NO_x under radial magnetisation of LPG are shown in figures 5.125- 5.128. It can be observed that there is a minute reduction in the emission of NO_x as the intensity of applied magnetic field is increased which is more or less similar to the magnitude of reduction obtained with axial magnetic fields.

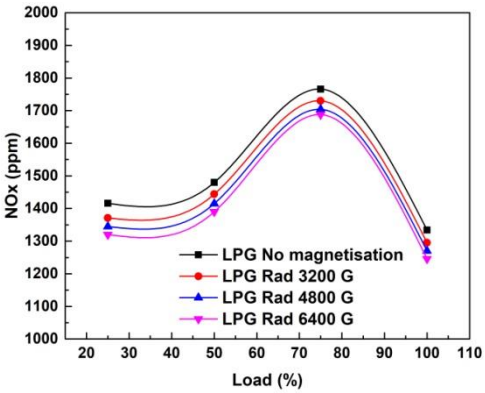

Fig 5.125 Variation in emission of NO_x with RM for LPG at 2000 rpm

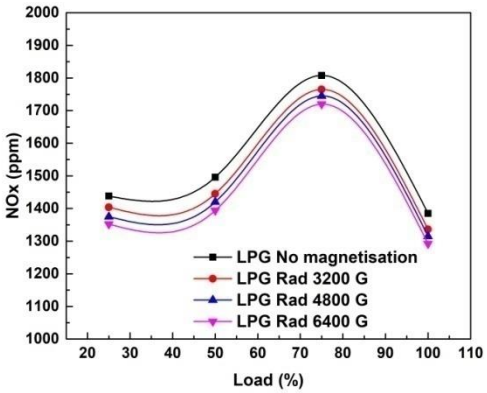

Fig 5.126 Variation in emission of NO_x with RM for LPG at 2500 rpm

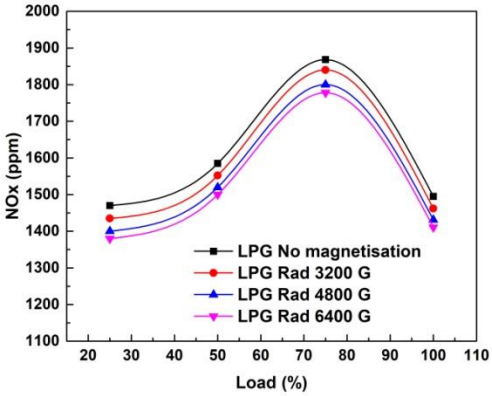

Fig 5.127 Variation in emission of NO_x with RM for LPG at 3000 rpm

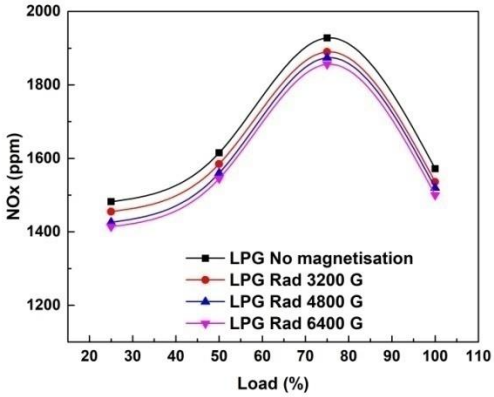

Fig 5.128 Variation in emission of NO_x with RM for LPG at 3500 rpm

Summary

- The performance parameters of the engine like brake power, BSFC and thermal efficiency are found to improve under all stages of axial and radial magnetic fields for both liquid phase and gaseous phase hydrocarbons.
- The combustion parameters like in-cylinder pressure and net heat release rate are positively influenced by magnetic field assisted combustion. Moreover, the stability of combustion which is analyzed statistically through the coefficient of

variation shows that Magnetic field assisted combustion is effective in reducing the cyclic fluctuations in combustion.

- Under both patterns of magnetic fields experimented on both phases of hydrocarbons, the emission of carbon monoxide and hydrocarbons reduce comprehensively. NO_x emissions reduce very slightly with increase in magnetic intensities and the emission of CO_2 is found to increase with all stages of magnetisation.
- Of all the tested magnetic intensities, maximum improvement in combustion and emission attributes are obtained for 6400 gauss field for both the magnetisation patterns in both phases of hydrocarbons, making it the preferred magnetic intensity for further stages of experimentation.
- The radial magnetic fields generated by sintered NdFeB rings are observed to influence the combustion parameters to an extend higher than axial fields of same intensity, making it the preferred magnetisation pattern for further stages of experimentation.
- Magnetic Field Assisted Combustion is observed to be more effective with the combustion of liquid phase hydrocarbons owing to the contiguous arrangement of molecules.

5.5 Effect of Part cooled Exhaust Gas Recirculation on combustion of liquid phase hydrocarbons (Gasoline)

In this phase of experimentation, various flow rates of part cooled exhaust gases are recirculated into the engine intake fuelled by gasoline to study the impact produced on performance, combustion and emission of the test engine. The aim of current phase of experimentation is to arrive at an optimum flow rate of part cooled EGR that gives the best possible performance of the engine with minimum compromise on emissions when the engine is operated by non-magnetised gasoline. The excess heat from the exhaust gases is removed by passing it through a radiator assembly in which heat is taken away convectively. The EGR flow rates is varied between 0%, 12%, 18% and 24% using an

EGR valve and the performance, combustion and emission characteristics of the engine under each flow rate is studied. The deterioration in combustion is also studied by analyzing the combustion stability through the statistical analysis of coefficient of variation of Indicated Mean Effective Pressures.

5.5.1 Brake Power

A drop in the developed brake power is noted for all four speed and load conditions of the engine for all the flow rates of EGR experimented. The drop in power is found to be minimum at lower loads and increases with increment in loading and EGR flow rates. This is due to the decrease of oxygen concentration inside the cylinder with the inert gases that absorb some part of the heat of combustion, thus reducing the power output delivered by the engine (Yangchang et al. 2018). The variation in brake power with EGR flow rates is depicted in figures 5.129- 5.132. It can be observed that the maximum reduction in output power is at 24% EGR.

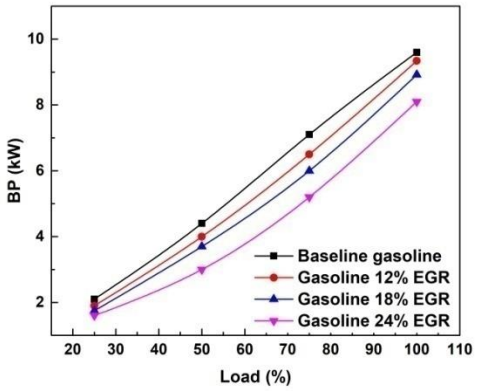

Fig 5.129 Variation in BP for gasoline with part cooled EGR at 2000 rpm

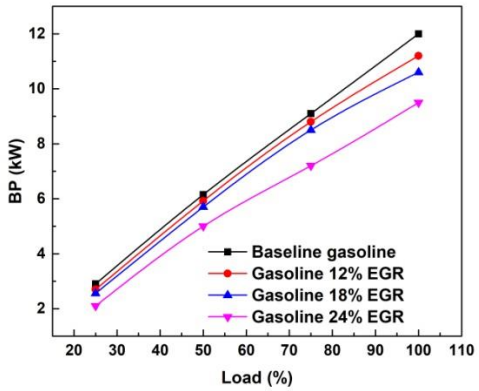

Fig 5.130 Variation in BP for gasoline with part cooled EGR at 2500 rpm

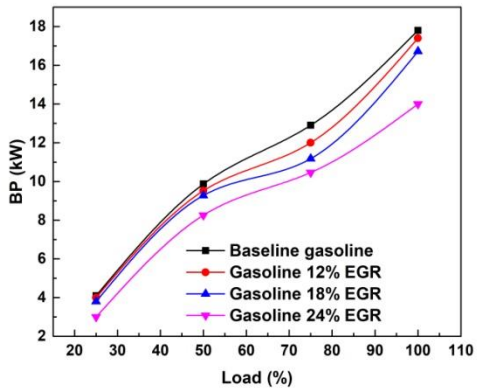

Fig 5.131 Variation in BP for gasoline with part cooled EGR at 3000 rpm

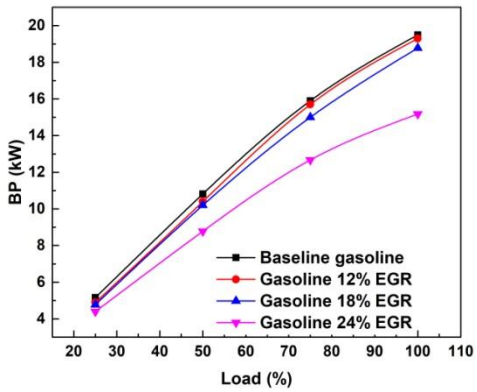

Fig 5.132 Variation in BP for gasoline with part cooled EGR at 3500 rpm

5.5.2 Brake Specific Fuel Consumption

The variation in brake specific fuel consumption with increasing flow rates of EGR is depicted in figures 5.133- 5.136. It can be observed from the trend that the bsfc of the engine reduces in each stage up to 18% of EGR addition and there after it increases rapidly. This is because, the recirculated inert gases effectively displace a portion of combustible charge inside the combustion chamber there by reducing the quantity of charge available for combustion.

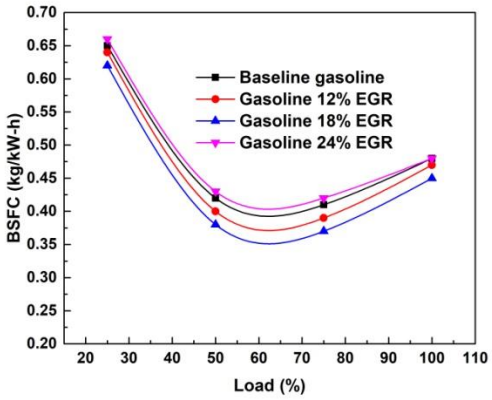

Fig 5.133 Variation in BSFC for gasoline with part cooled EGR at 2000 rpm

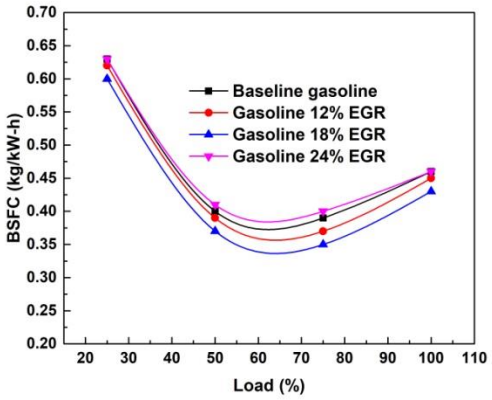

Fig 5.134 Variation in BSFC for gasoline with part cooled EGR at 2500 rpm

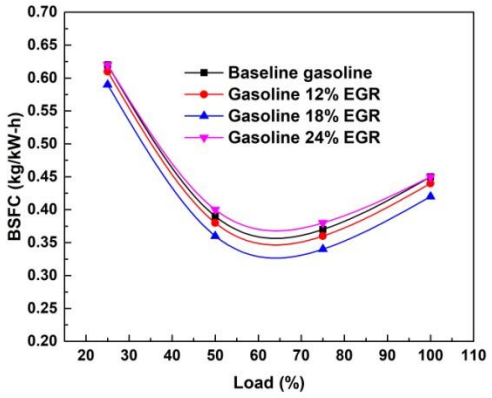

Fig 5.135 Variation in BSFC for gasoline with part cooled EGR at 3000 rpm

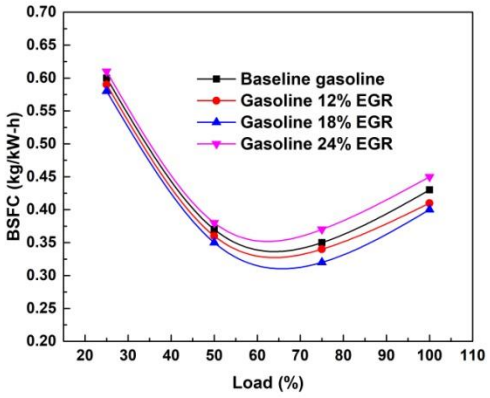

Fig 5.136 Variation in BSFC for gasoline with part cooled EGR at 3500 rpm

The improvement obtained in fuel economy is mainly due to the increase of ratio of specific heats of working gases and reduction of heat transfer through the combustion chamber walls (Alger et al. 2008). But after an optimum flow rate, if the EGR rate is further increased, the performance of the engine is deeply affected due to partial misfires as represented in the plot below. The maximum fuel efficiency is observed for 18% EGR flow rate .

5.5.3 Brake Thermal Efficiency

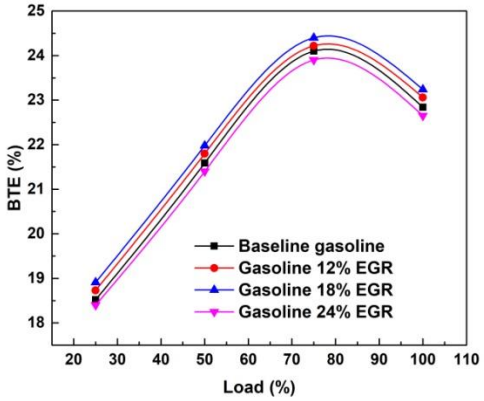

Fig 5.137 Variation in BTE for gasoline with part cooled EGR at 2000 rpm

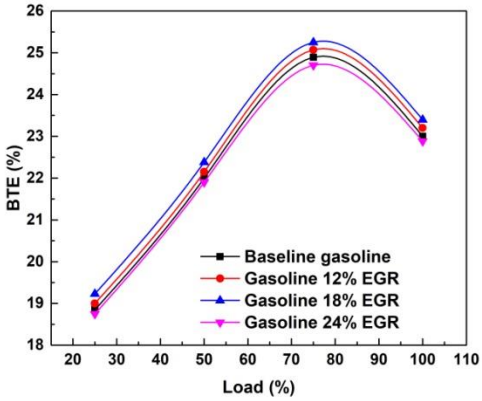

Fig 5.138Variation in BTE for gasoline with part cooled EGR at 2500 rpm

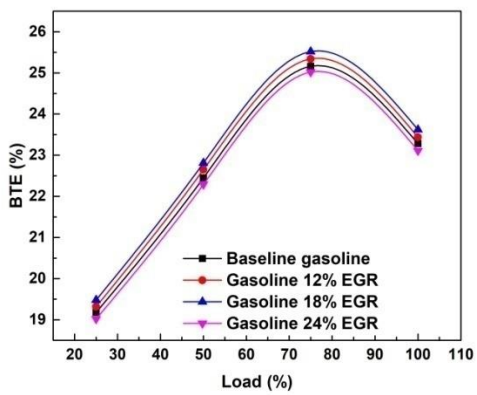

Fig 5.139 Variation in BTE for gasoline with part cooled EGR at 3000 rpm

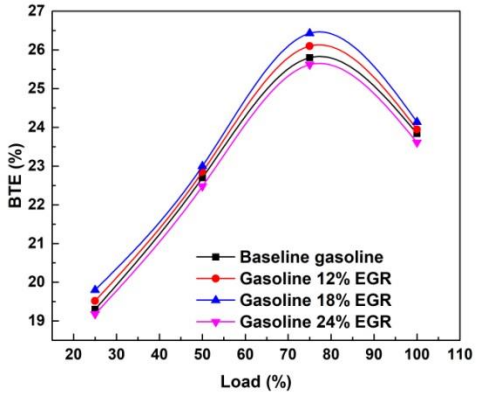

Fig 5.140 Variation in BTE for gasoline with part cooled EGR at 3500 rpm

Brake Thermal Efficiency is the function of thermal input from the fuel used. It represents the effectiveness with which the engine converts thermal energy from the fuel into mechanical energy. It can be seen that the addition of EGR increases the thermal efficiency up to an optimum EGR flow rate and then reduces sharply with any more addition of EGR. The improvement obtained in BTE is due to the reduction in pumping losses, reduced heat transfer and increase of ratio of specific heats (Caton et al. 2013).

A significant thermodynamic property required for the effective conversion of thermal energy into work in engines is the ratio of specific heats 'ϒ'. As the dilution due to EGR increases, gas temperature decreases, 'ϒ' increases and hence thermal efficiency increases. Mathematically,

$$\eta_e = \eta_{th}\eta_b\eta_{glh}(1-\Phi_w)\eta_m$$

Where η_b is the combustion efficiency, η_{glh} is the degree of constant volume heat release, Φ_w is the fraction of in cylinder heat transfer loss and η_m is the mechanical efficiency. In this equation, the increase in η_m through reduced pumping losses, decrease in Φ_w through the reduction in heat transfer losses and increase in η_{th} due to increased gamma value contribute to increase in effective efficiency of the engine (Li et al. 2013). The

variation in thermal efficiencies with different flow rates of part cooled EGR is depicted in figures 5.137- 5.140. It can be observed that maximum increase in efficiency is at 18% EGR flow rate at all engine speeds.

5.5.4 In-cylinder Pressure

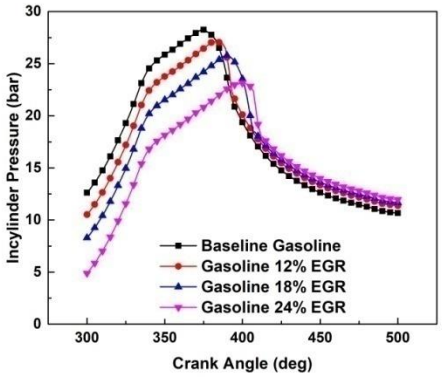

Fig 5.141 Variation in CP with various flow rates of part cooled EGR at 2500 rpm

The combustion characteristic of an engine is best represented by the analysis of in-cylinder pressures and net heat release rates. Fig 5.141 shows the variation in in-cylinder pressures with various flow rates of EGR at 2500 rpm. It can be observed that the addition of cooled exhaust gases reduces the in-cylinder peak pressures in all stages. The addition of EGR increases the specific heat capacity of gases and decreases the availability of oxygen, thereby reducing the peak values of pressures. (Caton et al. 2013). Moreover, the combustion duration is increased with each stage of EGR, shifting the peak pressure points further away from TDC.

5.5.5 Net Heat Release Rate

As a result of reduced combustion temperatures, the peak values of heat release rate are also reduced. (Cairns et al. 2006). A shift in the peak HRR is noticed towards BTDC due to a reduction in the combustion rate. The NHRR characteristic of the engine is shown in figure 5.142.

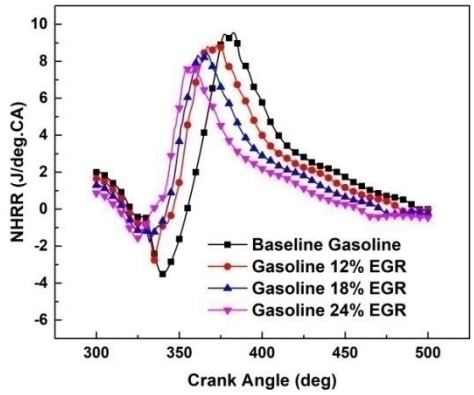

Fig 5.142 Variation in NHRR with various flow rates of part cooled EGR at 2500 rpm

5.5.6 Analysis of Stability of Combustion

The recirculation of burned gases from the exhaust is expected to deteriorate the quality of combustion. Too much dilution of the combustible mixture may lead to partial and sometimes complete misfires. This makes the analysis of stability of combustion significant for the various flow rates of EGR under experimentation.

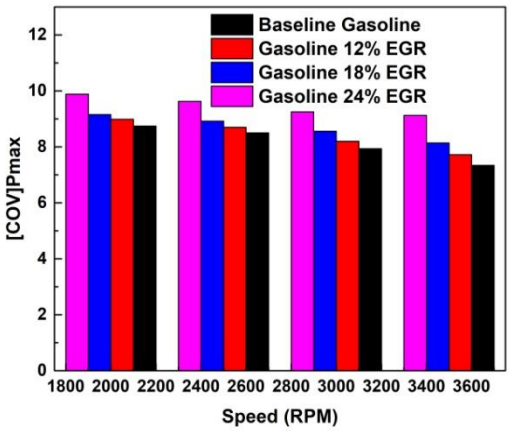

Fig 5.143 Variation of COV of P_{max} for different flow rates of part cooled EGR

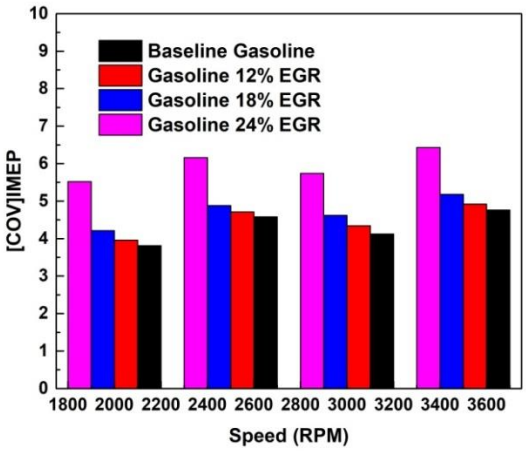

Fig 5.144 Variation of COV of IMEP for different flow rates of part cooled EGR

Combustion stability is determined based on the values of coefficient of variation of pressures (P_{max} and IMEP) which is analytically computed from the mean and standard deviation of pressure data at various engine speeds. The COV of P_{max} and COV of IMEP under different dilution rates of part cooled EGR for various engine speeds are shown in figure 5.143 and 5.144.

It is clear from these plots that as the dilution rate of combustible charge is increased in stages, the cyclic variations in combustion also increase proportionally. When an optimum flow rate of recirculation is crossed, the levels of fluctuations shoot up causing partial and complete misfires. It can be observed that for 24% recirculation, the COV of IMEP values lie well above 5 which denote that the combustion is highly unstable. At 18% recirculation the values lie around 5 which shows that the tolerance limit of dilution is approximately around 18% and any further addition of EGR affects the stability of combustion.

5.5.7 Emission of Carbon monoxide

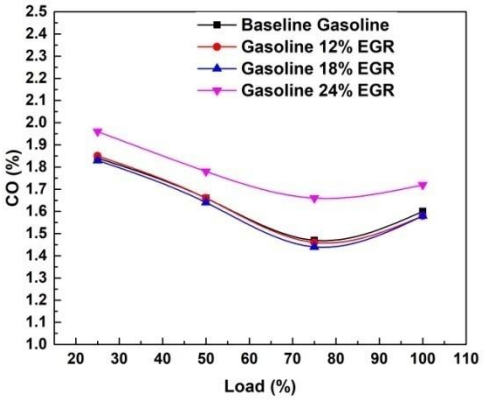

Fig 5.145 Variation in CO emission with different flow rates of EGR at 2000 rpm

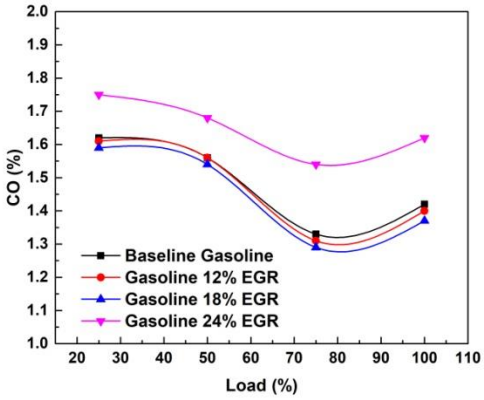

Fig 5.146 Variation in CO emission with different flow rates of EGR at 2500 rpm

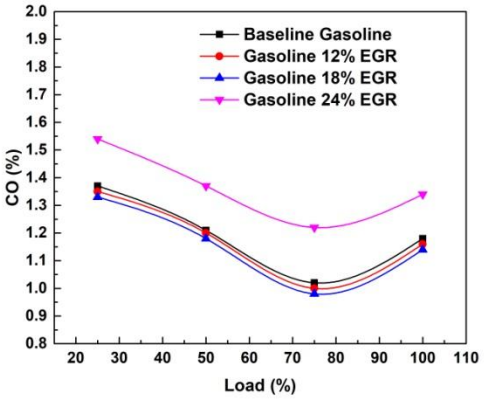

Fig 5.147 Variation in CO emission with different flow rates of EGR at 3000 rpm

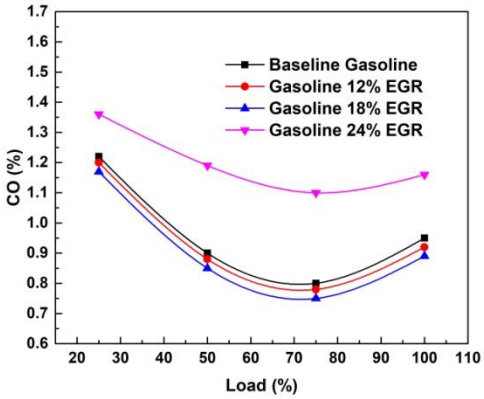

Fig 5.148 Variation in CO emission with different flow rates of EGR at 3500 rpm

Carbon monoxide is a toxic byproduct of combustion which is lighter than air. Carbon monoxide is an index of combustion quality and an increase in CO reflects the deterioration of combustion. If hot EGR is applied, there is a chance of dissociation of CO_2 which may lead to increase in CO percentage at all rates of dilution (Hacohen et al. 1995). The inclusion of part cooled EGR initially has very little effect on the percentage

content of CO in the exhaust. However, after an optimum flow rate of EGR, the levels of CO in the exhaust shoots up to high levels due to misfires as seen from figures 5.145-5.148.

5.5.8 Emission of Carbon dioxide

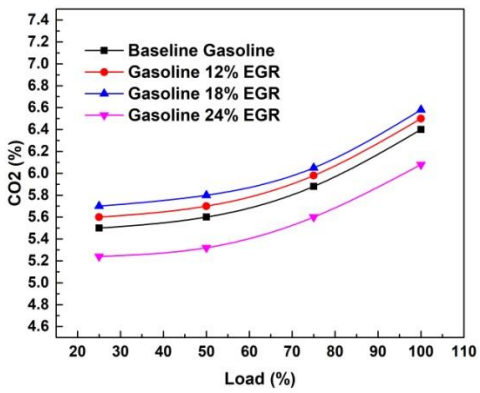

Fig 5.149 Variation in CO_2 emission with different flow rates of EGR at 2000 rpm

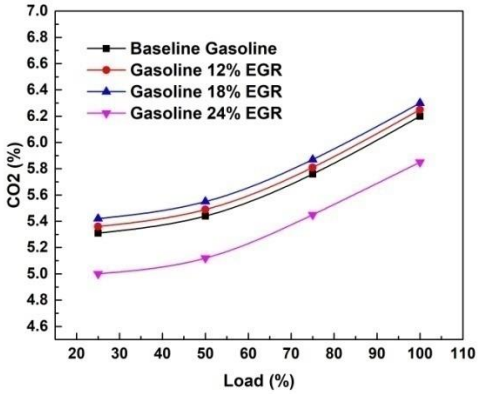

Fig 5.150 Variation in CO_2 emission with different flow rates of EGR at 2500 rpm

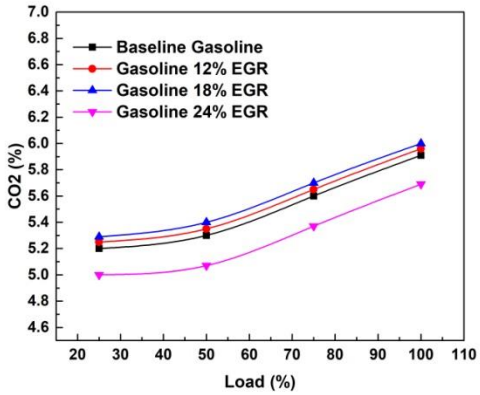

Fig 5.151 Variation in CO_2 emission with different flow rates of EGR at 3000 rpm

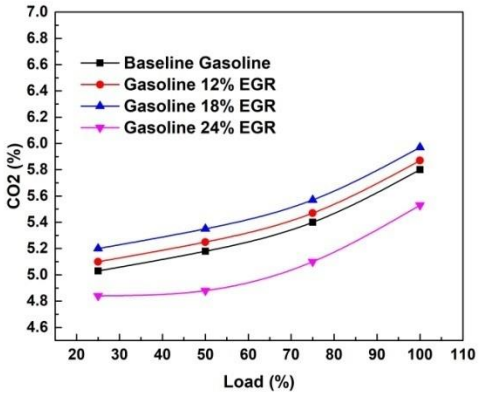

Fig 5.152 Variation in CO_2 emission with different flow rates of EGR at 3500 rpm

Carbon dioxide is a green house gas that promotes global warming. It is also considered as a measure of complete combustion in engines. With the addition of part cooled EGR,

the percentage content of carbon dioxide in the exhaust slightly increases for 12% and 18% recirculation. However, as the EGR percentage is increased beyond 18%, the levels of carbon dioxide reduce sharply at all speeds, indicating the occurrence of incomplete combustion. The emission trend of carbon dioxide at various engine speeds is shown in figures 5.149- 5.152.

5.5.9 Emission of Hydrocarbons

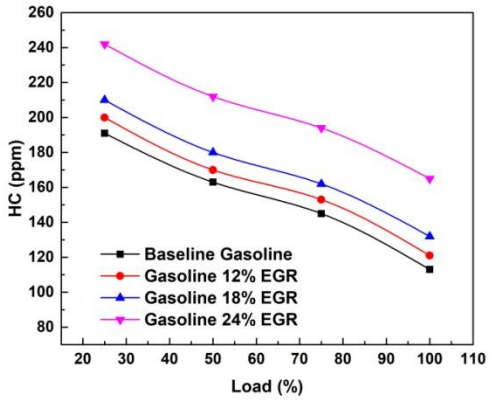

Fig 5.153 Variation in HC emission with different flow rates of EGR at 2000 rpm

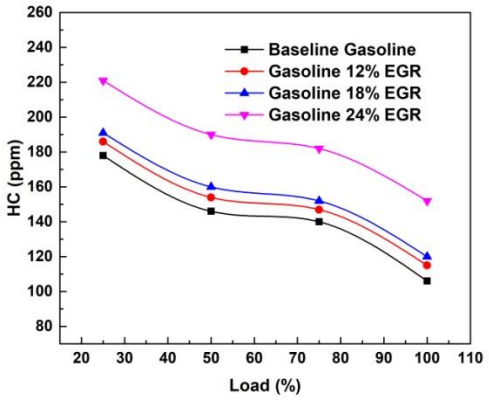

Fig 5.154 Variation in HC emission with different flow rates of EGR at 2500 rpm

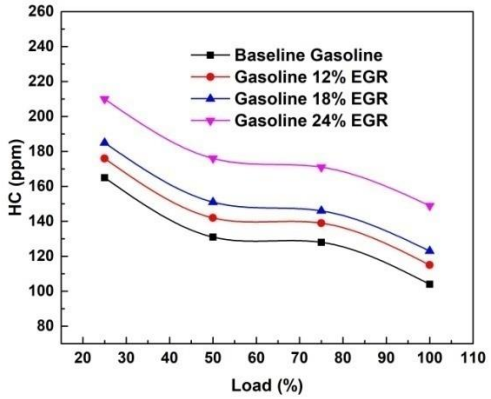

Fig 5.155 Variation in HC emission with different flow rates of EGR at 3000 rpm

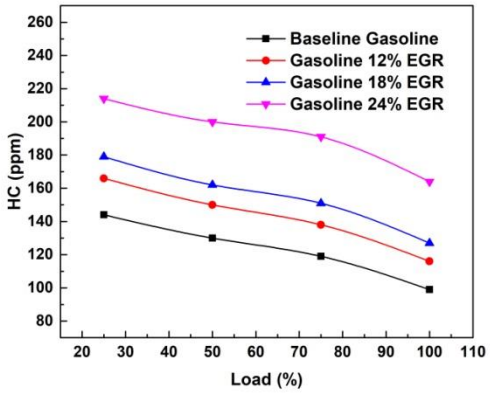

Fig 5.156 Variation in HC emission with different flow rates of EGR at 3500 rpm

The emission of unburnt hydrocarbons increases with each stage of EGR addition. As the cooled fraction in EGR content is increased, the stability of combustion is reduced and the amount of UBHC in the exhaust increases (Hacohen et al. 1995). Figures 5.153-5.156 show the variation in UBHC emission with various flow rates of cooled EGR at various speeds of the engine. It is clearly observable that the maximum emission of UBHC occurs with 24% recirculation of exhaust gases where an increase of 46.15% is noted.

5.5.10 Emission of Oxides of Nitrogen

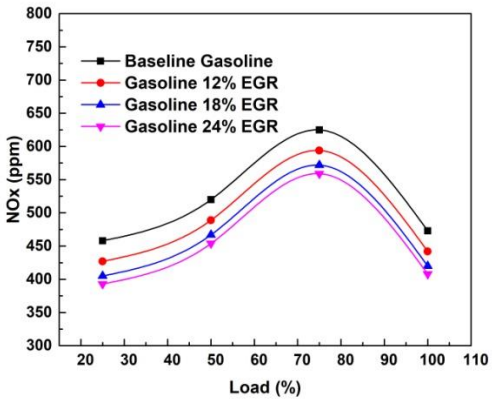

Fig 5.157 Variation in NO_x emission with different flow rates of EGR at 2000 rpm

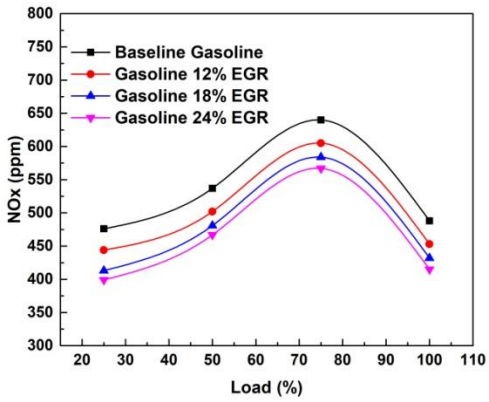

Fig 5.158 Variation in NO_x emission with different flow rates of EGR at 2500 rpm

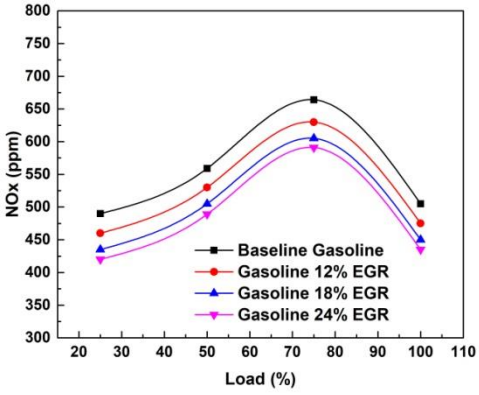

Fig 5.159 Variation in NO_x at 3000 rpm

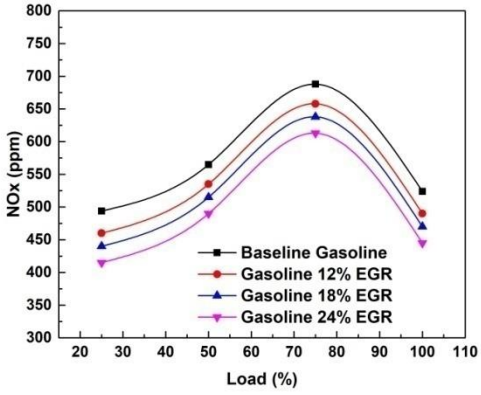

Fig 5.160 Variation in NO_x at 3500 rpm

The recirculation of cooled exhaust gases reduces the availability of oxygen inside the cylinder by displacing some part of oxygen with inert exhaust gases. This effectively reduces the local flame temperatures by spatial broadening of the flame. Also, the increase in specific heat capacity of gases inside the combustion zone which results in endothermic reactions that ends up in lower combustion temperatures (Shojaeefard et al. 2013). As the peak combustion temperatures are lowered, the formation of thermal NO_x reduces significantly. The dilution of combustible mixture without additional oxygen restricts NO_x generation (Caton et al. 2013). The variation in NO_x with various EGR rates is represented in figures 5.157- 5.160. It can be observed that NO_x levels reduce significantly with each stage of EGR addition.

5.6 Effect of Part cooled Exhaust Gas Recirculation on combustion of gaseous phase hydrocarbons (LPG)

The aim of this phase of experimentation is to arrive at an optimum flow rate of part cooled EGR that gives the best possible performance of the engine with minimum compromise on emissions when the engine is operated by non-magnetised neat liquefied petroleum gas. The excess heat from the exhaust gases after combustion is removed by passing it through a radiator assembly in which heat is taken away convectively. The EGR flow rates is varied between 0%, 12%, 18% and 24% using an EGR valve and the performance, combustion and emission characteristics of the engine under each flow rate is studied at different speed and loading conditions.

5.6.1 Brake Power

The variation in brake power with different flow rates of part cooled EGR for the combustion of LPG is shown in figures 5.161- 5.164. When compared to the normal gasoline operation, the output power of the engine improves under LPG fuelling because of the faster propagation of flames.

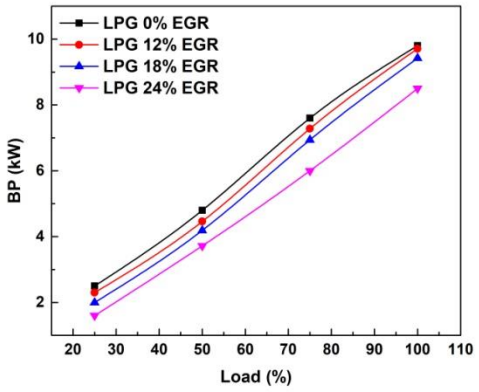

Fig 5.161 Variation in BP for LPG with part cooled EGR at 2000 rpm

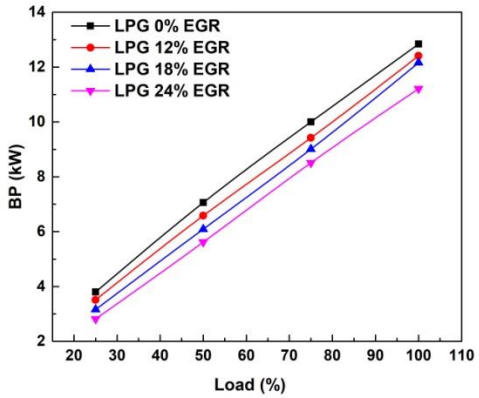

Fig 5.162 Variation in BP for LPG with part cooled EGR at 2500 rpm

It can be observed from the trend that the power output of the engine is affected by the recirculation. The recirculated gases absorb some part of the heat of combustion and reduce the concentration of oxygen inside the combustion chamber (Yangchang et al. 2018) which results in the reduction of power output. The minimum power is noted for 24% EGR where a reduction up to 20.5% is observed. The trend remains the same at all engine speeds experimented.

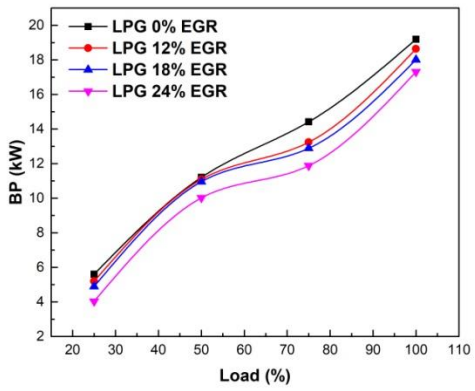

Fig 5.163 Variation in BP for LPG with part cooled EGR at 3000 rpm

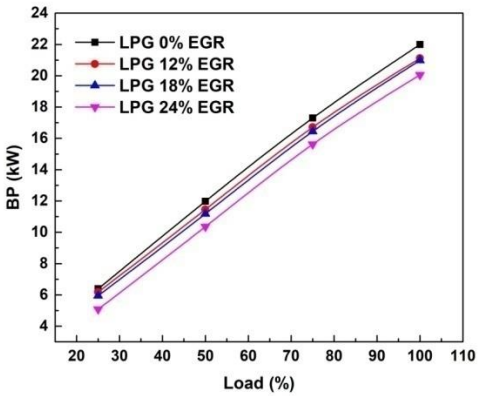

Fig 5.164 Variation in BP for LPG with part cooled EGR at 3500 rpm

5.6.2 Brake Specific Fuel Consumption

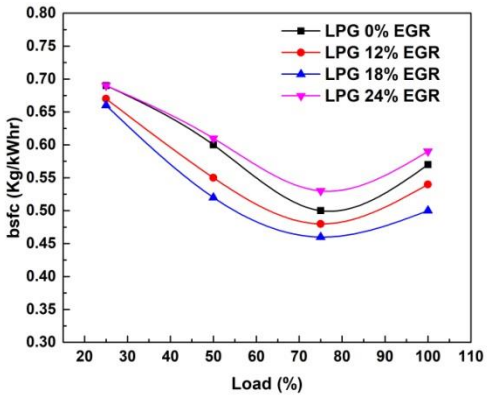

Fig 5.165 Variation in BSFC for LPG with part cooled EGR at 2000 rpm

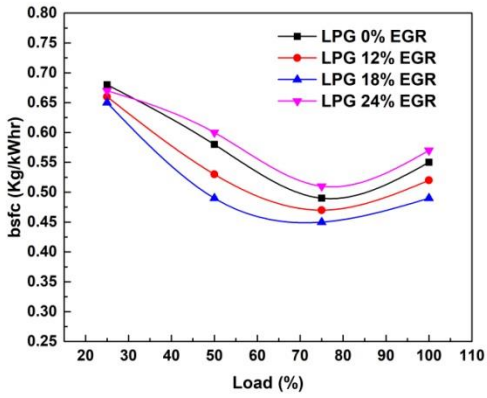

Fig 5.166 Variation in BSFC for LPG with part cooled EGR at 2500 rpm

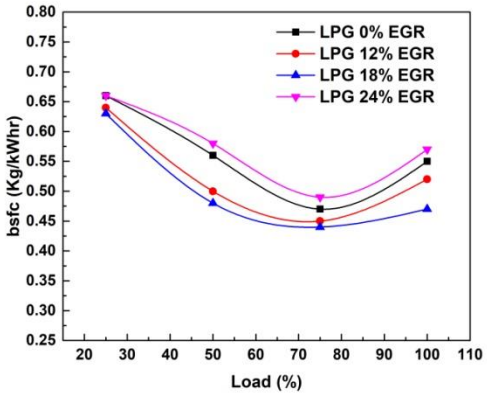

Fig 5.167 Variation in BSFC for LPG with part cooled EGR at 3000 rpm

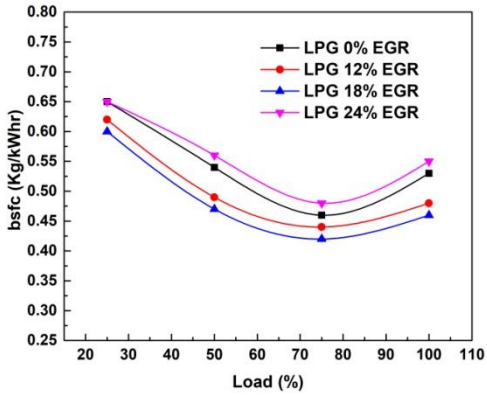

Fig 5.168 Variation in BSFC for LPG with part cooled EGR at 3500 rpm

The fuel consumption characteristics of the engine fuelled by LPG with different flow rates of part cooled EGR for different load and speed conditions of the engine are shown in figures 5.165- 5.168. In comparison with gasoline fuelled operation, the consumption of fuel is higher in LPG combustion (Nayak et al. 2016). The recirculation of part cooled inert gases up to an optimum flow rate improves the fuel economy of the engine by effectively displacing some portion of the combustible charge. The improvement obtained in fuel economy is mainly due to the increase of ratio of specific heats of

working gases and reduction of heat transfer through the combustion chamber walls (Alger et al. 2008). But after an optimum flow rate, if the EGR rate is further increased, the performance of the engine is deeply affected due to misfires deteriorating the fuel economy of the engine.

5.6.3 Brake Thermal Efficiency

The brake thermal efficiency of the engine under LPG operation is observed to be reducing compared to that under gasoline operation. This is because of the increase in ignition delay period owing to higher ignition temperatures of LPG. This increases the combustion duration which in turn increases the rate of fuel consumption there by reducing the overall thermal efficiency [Bayraktar et al. 2005].

The addition of cooled exhaust gas is found to increase the thermal efficiency slightly until the optimum EGR flow rate but any further addition results in a reduction of efficiency as observed from figures 5.169- 5.172. The major reason behind the improvement in brake thermal efficiency is the increase in the ratio of specific heats by the recirculated gases (Caton et al. 2013). As the dilution due to EGR increases, gas temperature decreases, 'ϒ' increases and hence thermal efficiency increases.

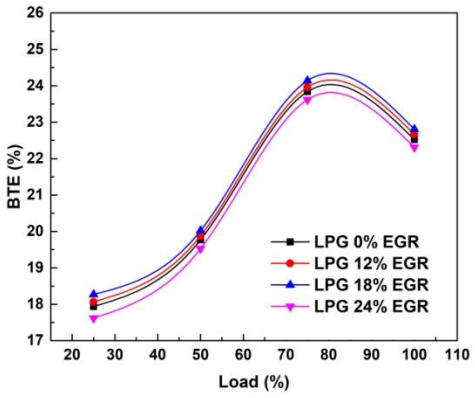

Fig 5.169 Variation in BTE for LPG with part cooled EGR at 2000 rpm

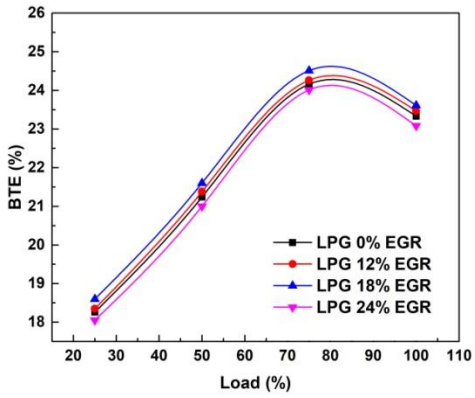

Fig 5.170 Variation in BTE for LPG with part cooled EGR at 2500 rpm

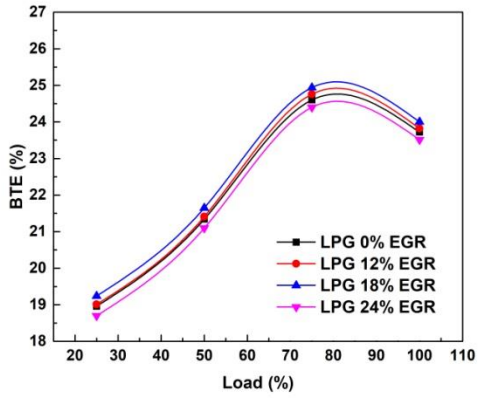

Fig 5.171 Variation in BTE for LPG with part cooled EGR at 3000 rpm

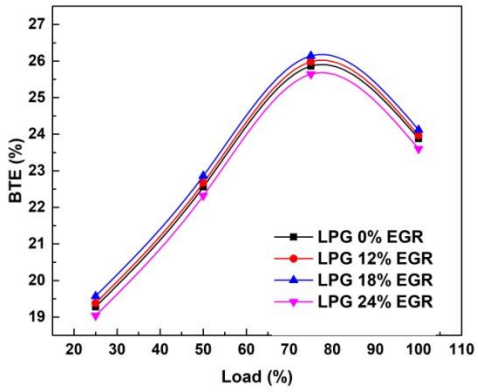

Fig 5.172 Variation in BTE for LPG with part cooled EGR at 3500 rpm

5.6.4 In-cylinder Pressure

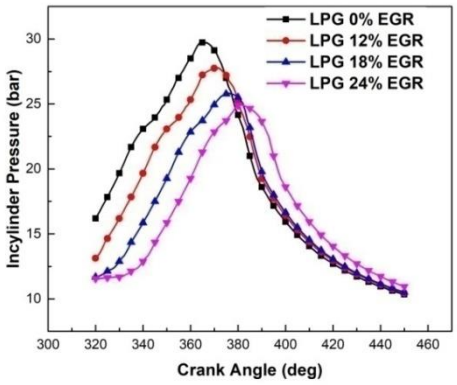

Fig 5.173 Variation in CP with various flow rates of part cooled EGR at 2500 rpm for LPG

The addition of EGR increases the specific heat capacity of gases and decreases the availability of oxygen, thereby reducing the peak values of pressures (Caton et al. 2013). Moreover, the combustion duration is increased with each stage of EGR, shifting the

peak pressure points further away from TDC. The in-cylinder pressure variation with varying rates of part cooled EGR for LPG combustion is represented in figure 5.173.

5.6.5 Net Heat Release rate

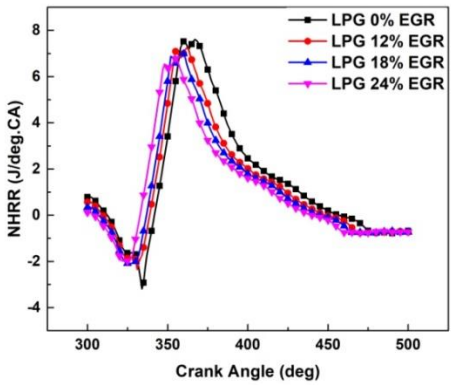

Fig 5.174 Variation in NHRR with various flow rates of part cooled EGR at 2500 rpm for LPG

The laminar burning velocity is substantially reduced due to the ambiguity of burned gases in the unburned cylinder charge. The presence of this burned mass leads to the reduction of heating value per unit mass of the mixture, in turn reducing the adiabatic flame temperatures. As a result of reduced combustion temperatures, the peak heat release rate is also reduced. A shift in the peak HRR is noticed towards BTDC due to a reduction in the combustion rate. The NHRR characteristics of the engine for an engine speed of 2500 rpm are shown in figure 5.174.

5.6.6 Analysis of Stability of Combustion

Figures 5.175 and 5.176 show the coefficient of variations in maximum pressures (P_{max}) and IMEP in 100 consecutive cycles with engine speeds. It is observable from the trends of COV of P_{max} and COV of IMEP that the cyclic variations in combustion increase with EGR flow rates.

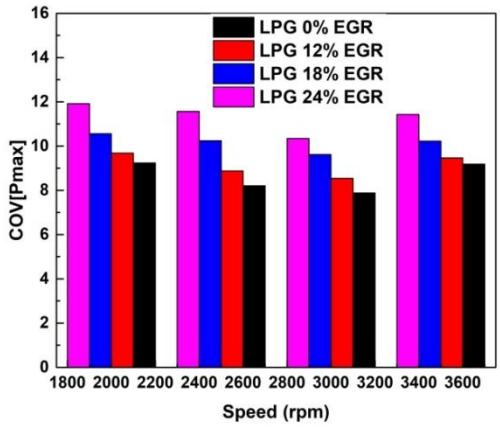

Fig 5.175 Variation of COV of P_{max} of LPG for different flow rates of part cooled EGR

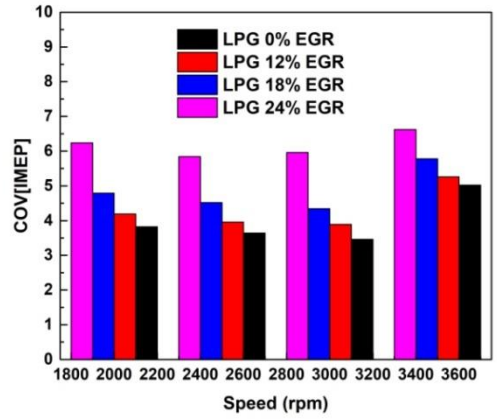

Fig 5.176 Variation of COV of IMEP of LPG for different flow rates of part cooled EGR

This is a direct indication of deterioration in combustion stability with the addition of recirculated gases. At 24% recirculation the COV of IMEP value consistently lie above 5 at all engine speeds, showing the occurrence of misfires. The nonuniform distribution of recirculated gases between the cylinders would also contribute to the increase in cycle-by-cycle variations.

5.6.7 Emission of Carbon monoxide

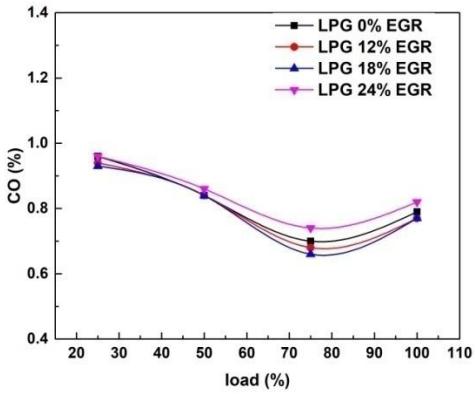

Fig 5.177 Variation in CO emission with different flow rates of EGR for LPG at 2000 rpm

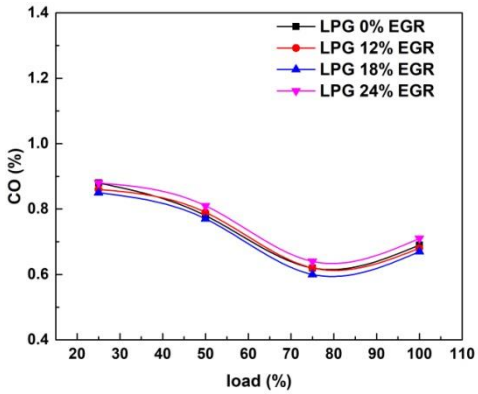

Fig 5.178 Variation in CO emission with different flow rates of EGR for LPG at 2500 rpm

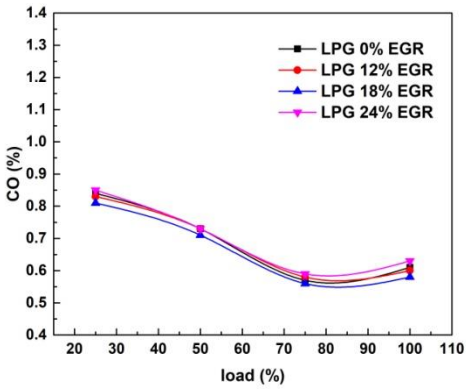

Fig 5.179 Variation in CO emission with different flow rates of EGR for LPG at 3000 rpm

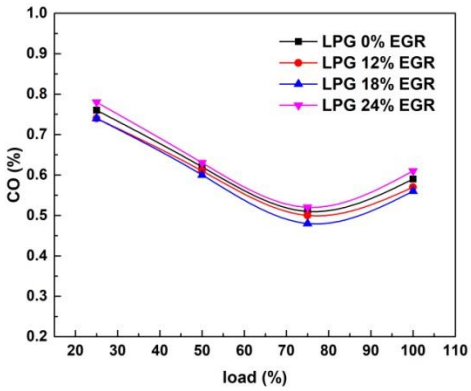

Fig 5.180 Variation in CO emission with different flow rates of EGR for LPG at 3000 rpm

It can be observed that the emission of CO reduces drastically when the engine is fuelled by LPG. This reduction is obtained because of the less carbon content in LPG as well as the enhanced mixing of LPG with air. Not many changes are observed in CO emissions

with the addition of part cooled EGR until the optimum EGR rate. After the optimum flow rate of recirculation, any further addition of exhaust gases cause a rapid increase in the emission of CO. This is due to the onset of misfires caused by the excessive dilution of combustible mixture (Bozic et al. 2017).

5.6.8 Emission of Carbon dioxide

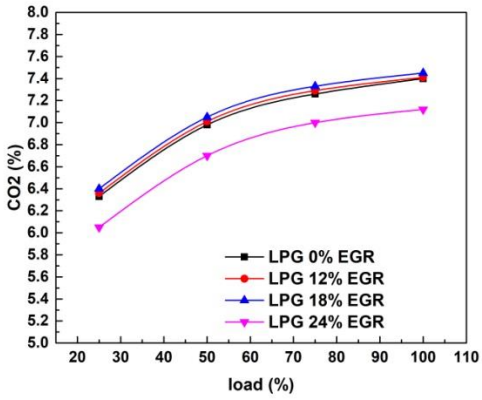

Fig 5.181 Variation in CO_2 emission with different flow rates of EGR for LPG at 2000 rpm

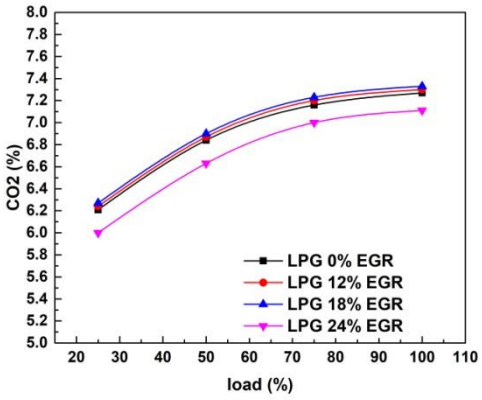

Fig 5.182 Variation in CO_2 emission with different flow rates of EGR for LPG at 2500 rpm

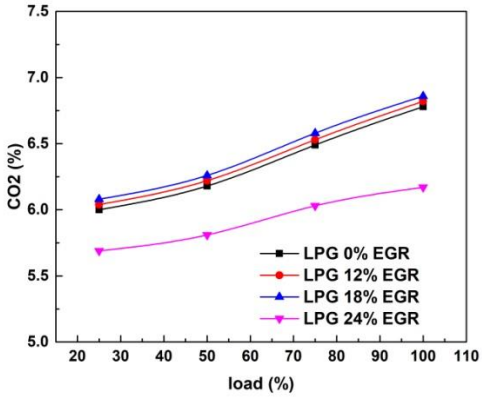

Fig 5.183 Variation in CO_2 emission with different flow rates of EGR for LPG at 3000 rpm

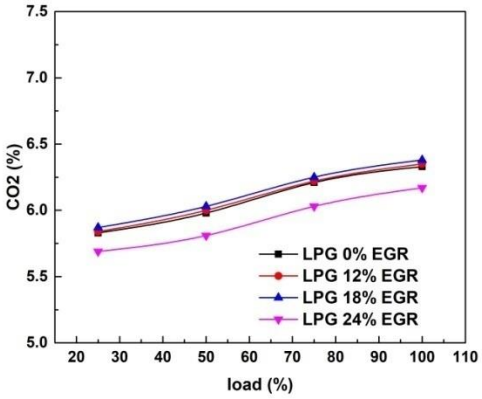

Fig 5.184 Variation in CO_2 emission with different flow rates of EGR for LPG at 3500 rpm

The addition of part cooled EGR is observed to have no significant effect on the emission of carbon dioxide until the optimum flow rate. As the dilution of unburned charge is increased beyond the optimum tolerance limit of the engine, the amount of carbon dioxide in the exhaust decreases.

5.6.9 Emission of Hydrocarbons

When compared to normal gasoline operation, the HC emission reduces up to 48.68% under LPG. As the burn rate decreases and cycle-by-cycle variations increase with increased flow rates of recirculated gases, hydrocarbon emissions also increase proportionally. After the optimum EGR rate is achieved, the HC emissions shoot up drastically because of slow combustion and increased misfires. The inclusion of cooled EGR increases HC content in the exhaust resulting in an increase up to 31.57% with 24% EGR. The emission characteristics of HC are depicted in figures 5.185- 5.188.

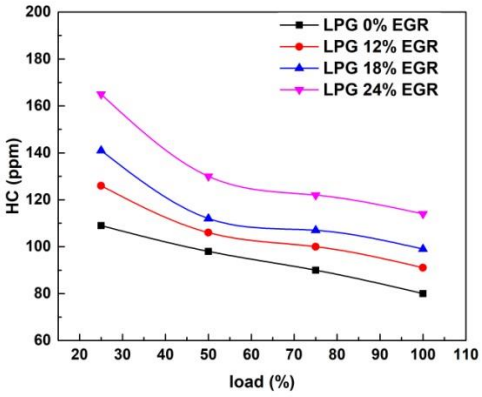

Fig 5.185 Variation in HC emission with different flow rates of EGR for LPG at 2000 rpm

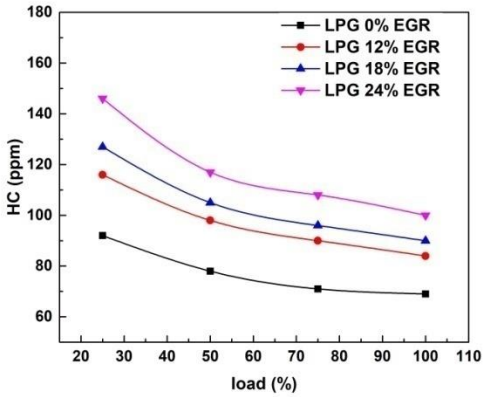

Fig 5.186 Variation in HC emission with different flow rates of EGR for LPG at 2500 rpm

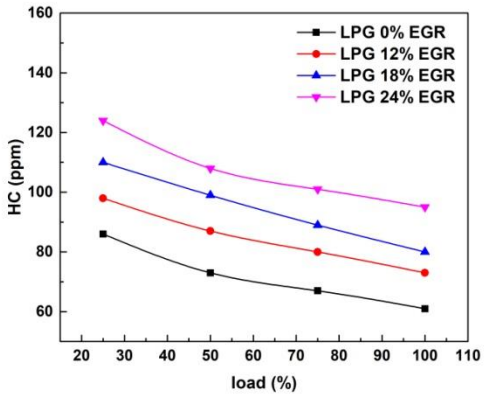

Fig 5.187 Variation in HC emission with different flow rates of EGR for LPG at 3000 rpm

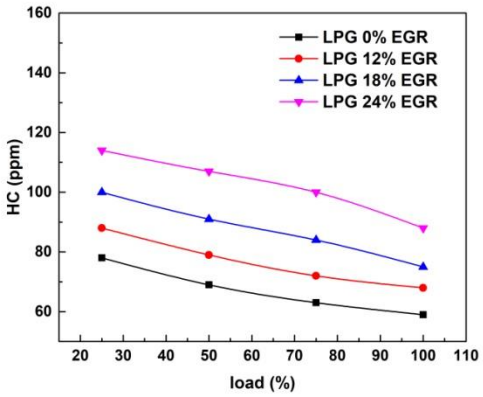

Fig 5.188 Variation in HC emission with different flow rates of EGR for LPG at 3500 rpm

5.6.10 Emission of Oxides of Nitrogen

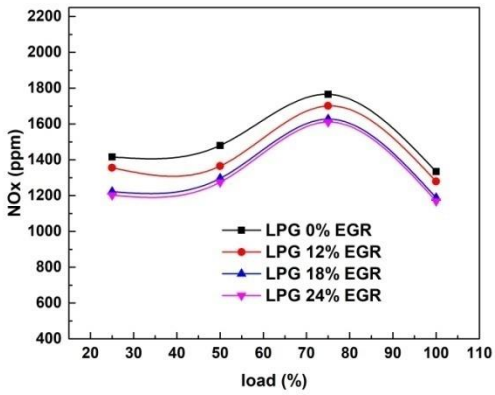

Fig 5.189 Variation in NO_x emission with different flow rates of EGR for LPG at 2000 rpm

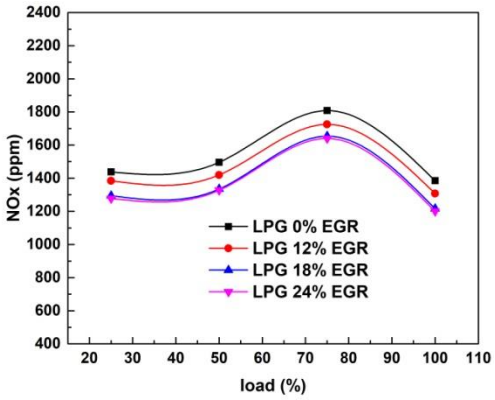

Fig 5.190 Variation in NO_x emission with different flow rates of EGR for LPG at 2500 rpm

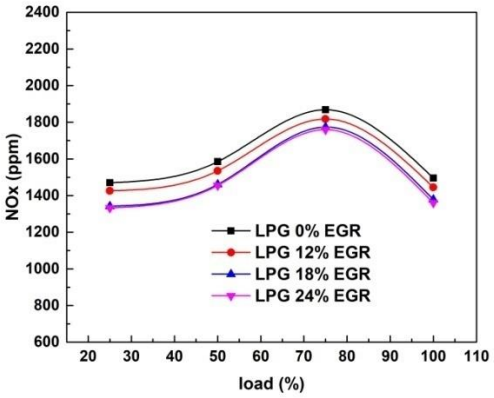

Fig 5.191 Variation in NO_x emission with different flow rates of EGR for LPG at 3000 rpm

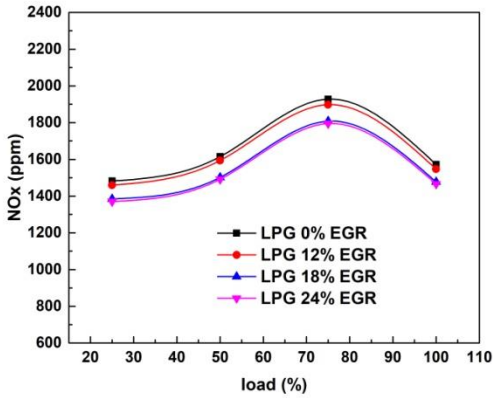

Fig 5.192Variation in NO_x emission with different flow rates of EGR for LPG at 3500 rpm

As a result of increased flame propagation speed of LPG, the cylinder temperatures and pressures will be higher than those obtained in the case of gasoline operation. Thus the emission of NO_x increases drastically under LPG fuelling. The greatest advantage of recirculating cooled exhaust gases lies in the reduction that it offers to the NO_x generation. As the recirculated cooled gases dilute the unburned mixture, the absolute temperature reached after combustion varies inversely with the burnt gas mass fraction [Heywood 1998]. It can be observed from figures 5.189- 5.192 that the generation of NO_x decreases significantly with each stage of EGR addition. A maximum reduction of 7.8% is observed in NO_x generation with the application of 24% of cooled EGR.

Summary

- The effect of different rates of part cooled EGR on the combustion of gasoline and LPG was studied. EGR resulted in the deterioration of power output but improved the fuel economy up to an optimum flow rate for both the fuels.
- The analysis of in-cylinder pressures and Net Heat Release Rates showed that combustion is influenced by the EGR flow rates. With increasing flow rates of part cooled EGR, the in-cylinder pressures reduced and the peak pressure points shifted further away from the TDC due to prolonged combustion durations. Heat

Release rates also showed a decrease with a peak shift towards BTDC positions with EGR.

- The statistical analysis of combustion through the computation of Coefficient of Variation showed that the recirculation of part cooled EGR results in a reduction of combustion stability for both the fuels. The variation in COV is increased drastically with 24% recirculation which shows that quality of combustion is significantly reduced.
- The major disadvantage of LPG as a fuel is the generation of high amounts of NO_x. This problem could be effectively tackled by the application of cooled recirculated gases. Considerable reduction is observed in NO_x emissions with each stage of recirculation of cooled exhaust gases.
- In both the experimented fuels, EGR is observed to be beneficial to fuel economy and thermal efficiency without much compromise on CO and HC emissions until a dilution of 18%. Further addition of EGR resulted in deterioration of performance, combustion and emission characteristics (other than NO_x) of the engine. Hence the optimum flow rate of part cooled EGR is chosen as 18% for further stages of experimentation.

5.7 Effect of Distance (Locus) of Magnetisation on Optimised Magnetic Field Assisted Combustion

This phase of experimentation is intended to investigate the effect of locus of magnetisation from the fuel injector in the already optimised magnetic field assisted combustion. For this purpose, the optimal magnetisation pattern (radial) and intensity (6400 Gauss) is chosen to polarise the liquid phase hydrocarbon (gasoline) up on which the polarisation effect was found to be higher.

Sintered NdFeB rings of magnetic intensity 6400 Gauss with standard Ni-Cu-Ni coatings are mounted on the gasoline fuel line at three positions relative to the fuel injector to investigate the effect of distance of magnetisation on the effectiveness of this technique. The position immediately adjacent to the fuel injector is chosen as the

reference position and is termed as locus 1 in the results. Locus 2 and locus 3 are situated at a distance of 10 cm and 20 cm away from the reference point. The performance and emission characteristics of the engine at these specified locations are studied at different loads and a sample speed of 2500 rpm.

5.7.1 Brake Power

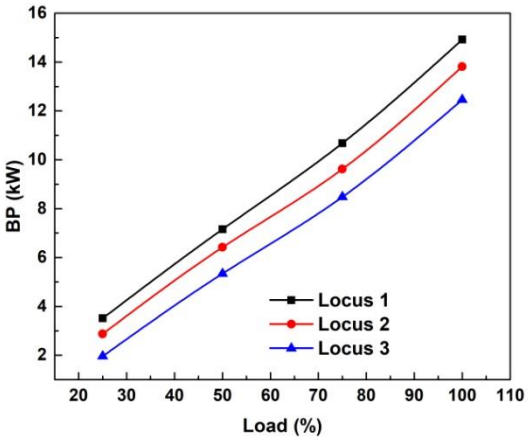

Fig 5.193 Variation in BP with locus of magnetisation at 2500 rpm

The effect produced on the power output of the engine with variation in the locus of magnetisation at a reference speed of 2500 rpm is depicted in figure 5.193. A drop in output power is observed in locus 2 and 3 when the magnetic field is moved further away from the reference point. The reason behind the fall in power is the inverse square law (Spantideas et al. 2015). With reference to locus 1, the power output reduced by 5.43% and 10.29% in locus 2 and locus 3 respectively.

5.7.2 Brake Specific Fuel Consumption

The fuel consumption characteristic of the engine at various locus of magnetisation is represented in figure 5.194. An improvement of fuel economy up to 14.82% was observed in gasoline operation under radial field strength of 6400 Gauss. When the locus of magnetisation is shifted the consumption of fuel is observed to be increasing. When

the locus of magnetisation is shifted away from the injector, the polarised hydrocarbon molecules show a tendency to form pseudo clusters again, thus reducing the impact produced through magnetisation (Sahoo et al. 2019). In locus 2 and locus 3, the BSFC increased by 4.4% and 8.43% with respect to locus 1.

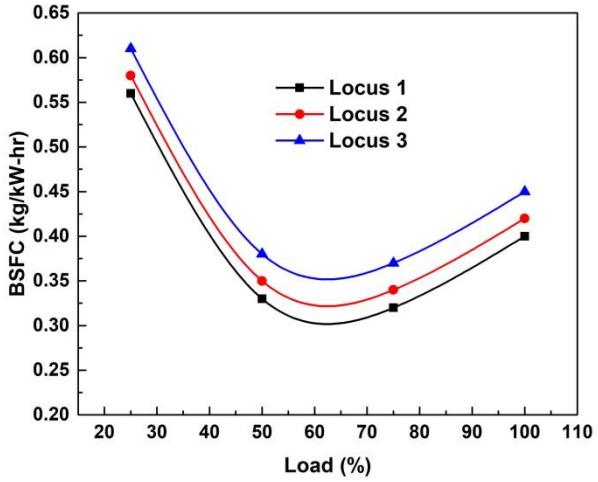

Fig 5.194 Variation in BSFC with locus of magnetisation at 2500 rpm

5.7.3 Brake Thermal Efficiency

The impact produced in the brake thermal efficiency of the engine through a shift in the locus of magnetisation is depicted in figure 5.195. Magnetic field assisted combustion aids in the better conversion of chemical energy of the fuel into thermal energy (Sahoo et al. 2019). When the distance of magnetisation from the reference point is increased, the positive impact resulted from polarisation is found to decrease due to the reversibility of this effect (Govindasamy et al. 2007). At locus 2 and 3, the brake thermal efficiency of the engine remained higher than the non-magnetised fuel, but a considerable reduction is observed when compared with the magnitudes at locus 1. A reduction up to 1.3% and 1.96% are observed at locus 2 and 3 with respect to the efficiency values at locus 1.

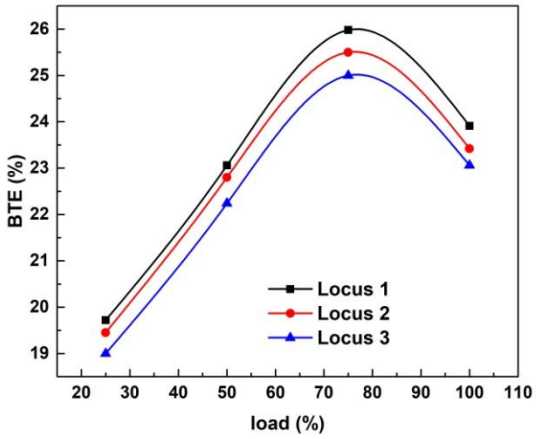

Fig 5.195 Variation in BTE with locus of magnetisation at 2500 rpm

5.7.4 Emission of Carbon monoxide

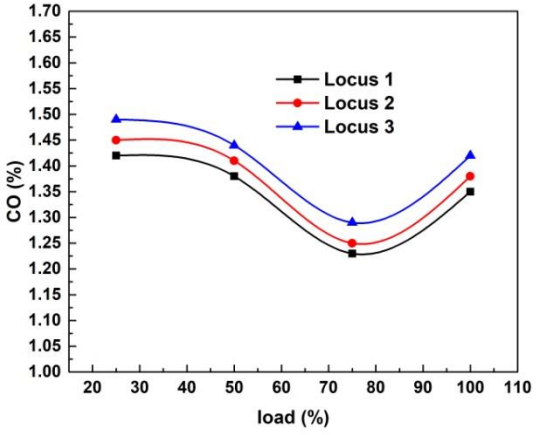

Fig 5.196 Variation in CO emissions with locus of magnetisation at 2500 rpm

As discussed in the previous sections, the emission levels of carbon monoxide is a good indicator of combustion efficiency. Generally, the concentration of carbon monoxide in the engine exhaust decreases as a result of magnetic field assisted combustion. When the locus of magnetisation is shifted away from the injector, the impact produced by the magnetic field on combustion is reduced (Sahoo et al. 2019). As a result the emission

levels of CO slightly increases in locus 2 and locus 3 when compared to locus 1 but remains lower than the combustion of non magnetised fuel. An increase in CO of 2.14% and 4.67% are noted in locus 2 and 3 with respect to the emission levels at locus 1.

5.7.5 Emission of Carbon dioxide

Magnetic field assisted combustion is found to increase the emission percentage of carbon dioxide in the exhaust as observed from the previous results because of the enhanced combustion efficiency. When the location of magnetisation is shifted further away, the percentage content of carbon dioxide in the exhaust reduces, indicating the lowering of combustion efficiency. In comparison with the reference position, the levels of CO_2 reduced by 5.47% and 9.93% respectively in the other two locations experimented. The emission trend of CO_2 with various locus of magnetisation is shown in figure 5.197.

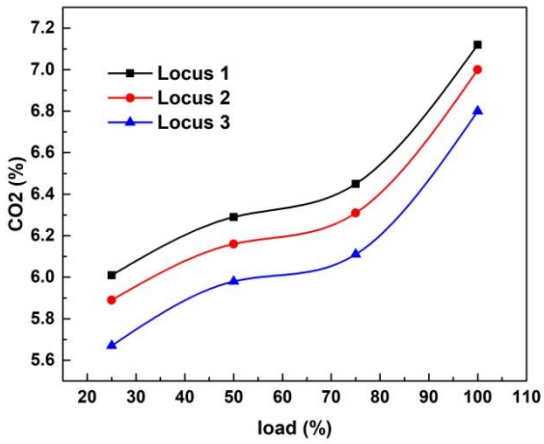

Fig 5.197 Variation in CO_2 emissions with locus of magnetisation at 2500 rpm

5.7.6 Emission of Hydrocarbons

When the distance of magnetisation is shifted further away from the reference position, due to the recombination effect, the influence of magnetic field on combustion is reduced. As the distance increases, the effect of magnetisation reduces proportionally

based on inverse square law (Sahoo et al. 2019). When the polarised hydrocarbon molecules recombine, the extend of association of these molecules with oxygen molecules reduces hence resulting in reduced combustion efficiency. As a result of this, in locus 2 and locus 3, an increase in hydrocarbon emissions up to 7.69% and 14.61% is observed with respect to the emission levels at locus 1. The emission trend of HC with various locus of magnetisation is shown in figure 5.198.

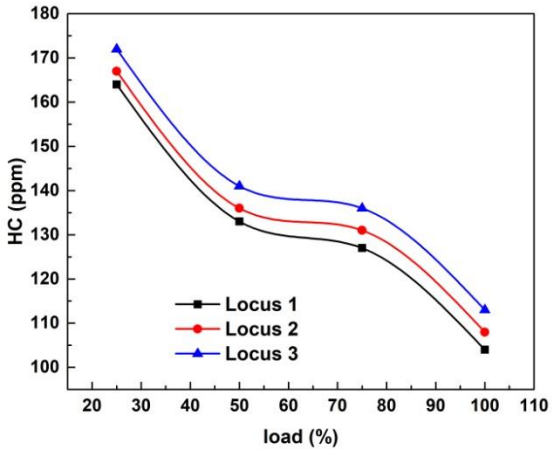

Fig 5.198 Variation in HC emissions with locus of magnetisation at 2500 rpm

5.7.7 Emission of Oxides of Nitrogen

The variation in the concentration of oxides of nitrogen in the engine exhaust with different locus of magnetisation is depicted in figure 5.199. Similar to the other emissions of the engine, the concentration of oxides of nitrogen in parts per million is found to increase very slightly in locus 2 and locus 3. The increase in magnitude is not very significant in the case of NO_x emissions as the impact of magnetic field assisted combustion on NO_x emissions is as such not considerable in magnitude.

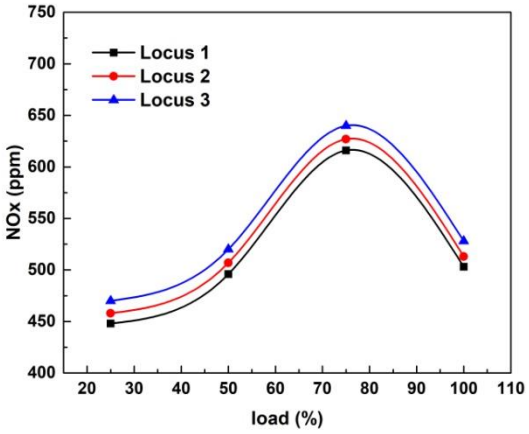

Fig 5.199 Variation in HC emissions with locus of magnetisation at 2500 rpm

Summary

- The optimised conditions like magnetisation pattern, magnetic intensity and the fuel phase in magnetic field assisted combustion are combined to investigate the significance of locus of magnetisation with respect to the injector position.
- Locus 1 which is located adjacent to the injector gave the best results in performance and emissions of the engine. The performance and emissions of the engine deteriorated as the locus is shifted further away from reference point because of loss of magnetisation effect based on recombination and inverse square law. Hence locus 1 is chosen as the position of magnetisation in the remaining phases of experimentation for both the fuels.

5.8 Synergetic Effect of Optimised conditions in Magnetic Field Assisted Combustion and Part Cooled EGR rate in the Combustion of liquid phase hydrocarbons (Gasoline)

In the final stage of experimentation, The synergetic effect of optimised conditions in magnetic field assisted combustion like magnetisation pattern, magnetic intensity and locus of magnetisation on optimised flow rate of part cooled exhaust gas recirculation is investigated at various load and speed conditions of the test engine fuelled by both liquid

phase and gas phase hydrocarbons. Sintered NdFeB rings of magnetic intensity 6400 Gauss with standard Ni-Cu-Ni coatings are mounted on the gasoline fuel line at locus 1 position and EGR valve is positioned to provide a recirculation rate of 18% to investigate the synergetic effect produced on combustion. Initially the engine is fuelled by gasoline and the optimum operating conditions are loaded and the performance, combustion and emission parameters are studied. The synergetic effect is referred to as optimised gasoline in the characteristic curves.

5.8.1 Brake Power

During the earlier phases of experimentation, the individual effect of magnetic field assisted combustion was observed to increase the power output of the engine whereas the sole effect of exhaust gas recirculation was a reduction in output. When all the optimal conditions are combined, the brake power of the engine is found to be higher than that in the normal baseline operation of the engine, but inferior to that under the sole effect of radial magnetic fields. This is due to the compromising effect produced by the dilution of charge by the recirculated gases.

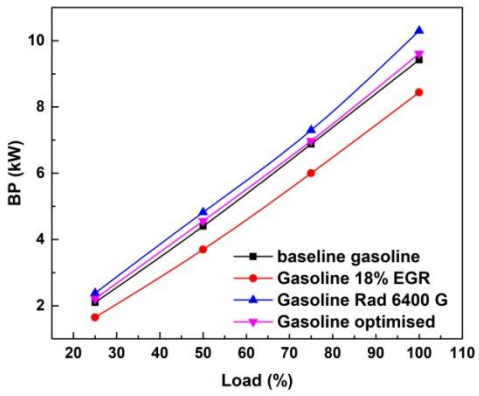

Fig 5.200 Variation in BP with synergetic effect in gasoline at 2000 rpm

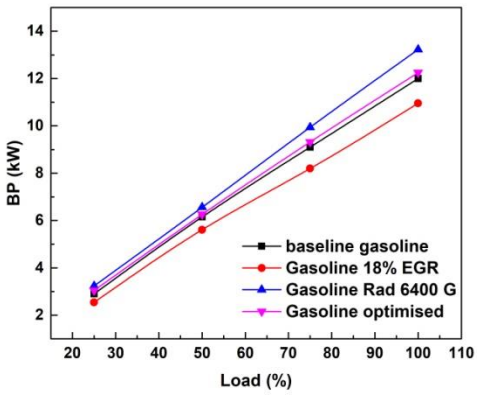

Fig 5.201 Variation in BP with synergetic effect in gasoline at 2500 rpm

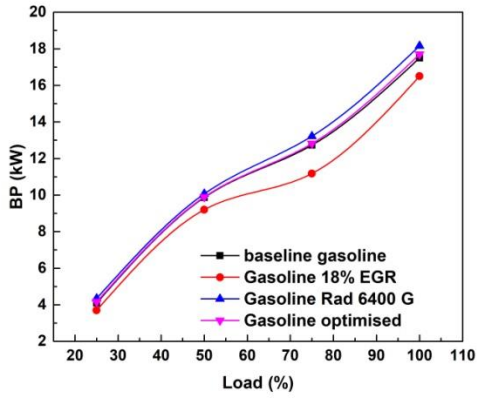

Fig 5.202 Variation in BP with synergetic effect in gasoline at 3000 rpm

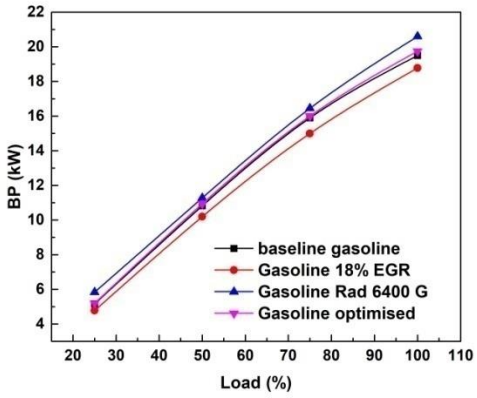

Fig 5.203 Variation in BP with synergetic effect in gasoline at 3500 rpm

The resultant output is observed to be better than under optimal recirculation of cooled exhaust gases which shows that the synergetic effect of magnetic field assisted combustion is beneficial to the engines employing EGR technique. The synergetic effect produced on output power is depicted in figures 5.200- 5.203.

5.8.2 Brake Specific Fuel Consumption

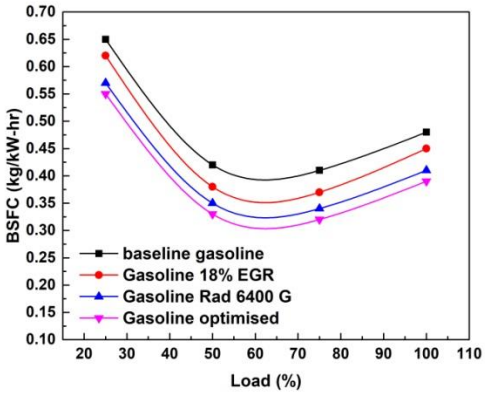

Fig 5.204 Variation in BSFC with synergetic effect in gasoline at 2000 rpm

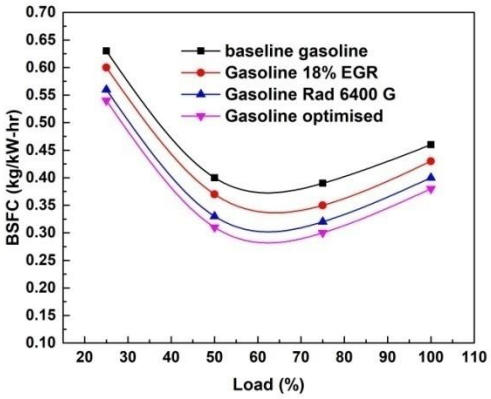

Fig 5.205 Variation in BSFC with synergetic effect in gasoline at 2500 rpm

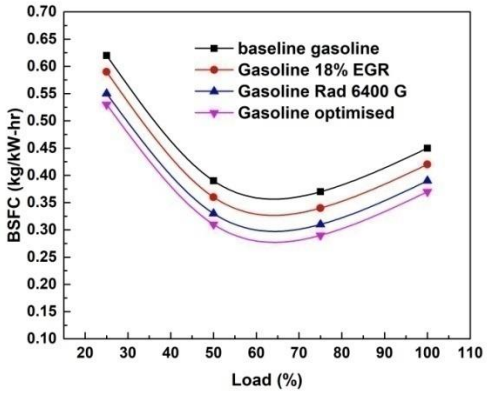

Fig 5.206 Variation in BSFC with synergetic effect in gasoline at 3000 rpm

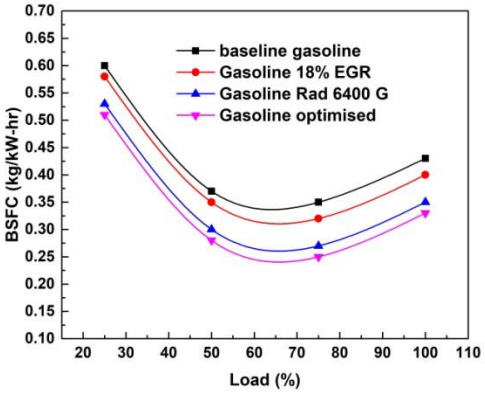

Fig 5.207 Variation in BSFC with synergetic effect in gasoline at 3500 rpm

The fuel consumption characteristics of the engine under the synergetic effect of MFAC and part cooled EGR is shown in figures 5.204- 5.207. As the fuel economy was enhanced under the individual effects of both MFAC and optimal EGR, the combination of these techniques is observed to provide added benefit to the engine's fuel economy. It can be seen from the plots that the consumption of fuel is minimum at the optimised synergy for all the loads and speeds experimented.

5.8.3 Brake Thermal Efficiency

The significant advantage yielded in the fuel economy is reflected in the thermal efficiency characteristics of the engine which are plotted in figures 5.208- 5.210. The thermal efficiency of the engine under the synergetic effect of EGR and MFAC is observed to be higher than the individual effects generated by these techniques. The combined effect of increase in ratio of specific heats through the recirculation and declustering of hydrocarbons result in this enhanced efficiencies.

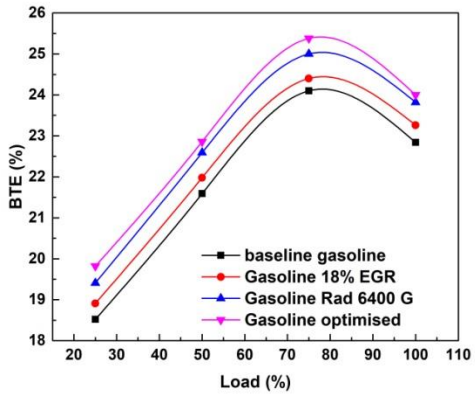

Fig 5.208 Variation in BTE with synergetic effect in gasoline at 2000 rpm

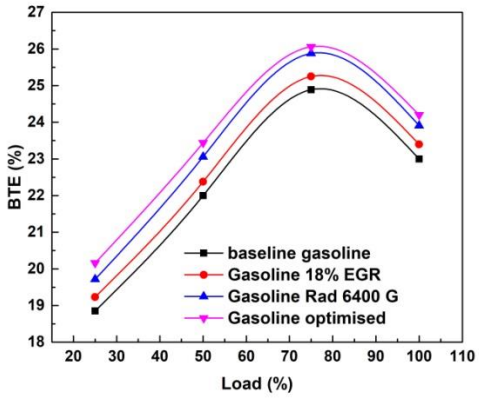

Fig 5.209 Variation in BTE with synergetic effect in gasoline at 2500 rpm

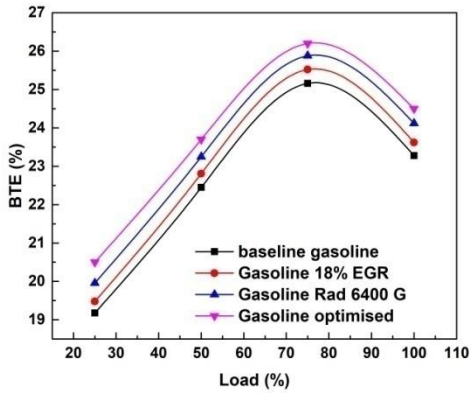

Fig 5.210 Variation in BTE with synergetic effect in gasoline at 3000 rpm

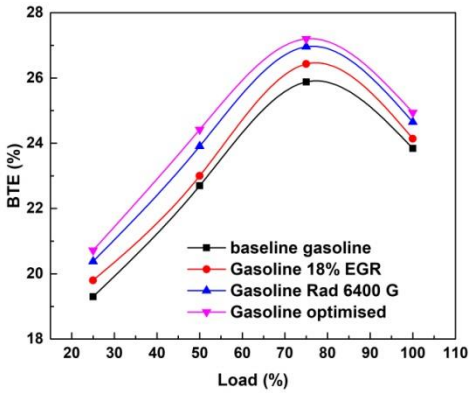

Fig 5.211 Variation in BTE with synergetic effect in gasoline at 3500 rpm

5.8.4 In-cylinder Pressure

The in-cylinder combustion pressure suffers a setback in magnitude when part cooled exhaust gases are recirculated into the cylinder with the peak pressures occurring further away from TDC position whereas magnetic field assisted combustion proved itself to boost the combustion pressures with the peak pressures occurring at the same crank angle

locations. The variation in cylinder pressure with the optimised synergy for gasoline combustion at a sample engine speed of 2500 rpm is shown in figure 5.212.

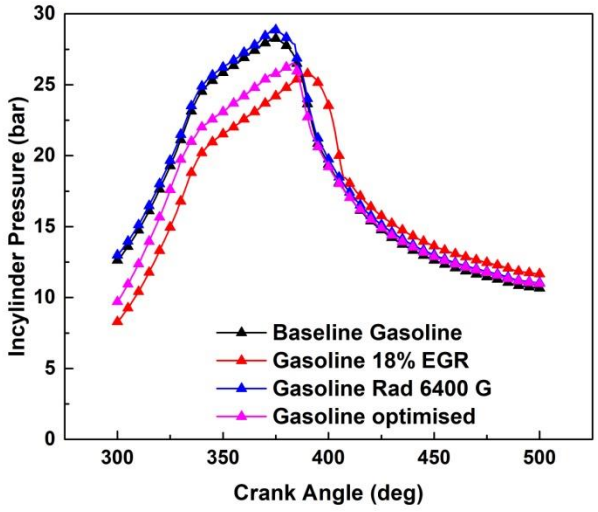

Fig 5.212 Variation in CP with synergetic effect in gasoline at 2500 rpm

It can be observed that the combustion pressures diminished under the synergetic effect with a slight shift in the location of peak pressure further away from TDC with comparison to that of baseline gasoline combustion. The increase in combustion duration with the addition of EGR results in the peak shift and the reduced magnitudes of pressure.

5.8.5 Net Heat Release Rate

The laminar burning velocity is substantially reduced due to the ambiguity of burned gases in the unburned cylinder charge. The presence of this burned mass leads to the reduction of heating value per unit mass of the mixture, resulting in the reduction of peak values of heat release. At the same time, the optimized magnetic field tends to improve the heat release characteristics of the engine by enhancing the combustion process. As a result, the heat release pattern of optimized synergy in gasoline combustion lies in between of the optimized MFAC condition and optimized EGR as shown in figure 5.213.

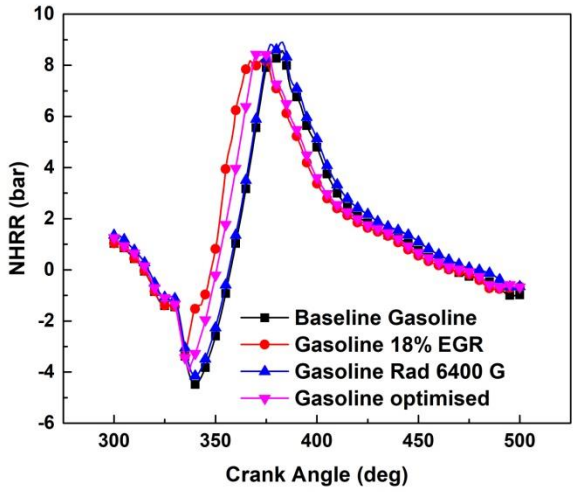

Fig 5.213 Variation in NHRR with synergetic effect in gasoline at 2500 rpm

5.8.6 Analysis of Combustion Stability

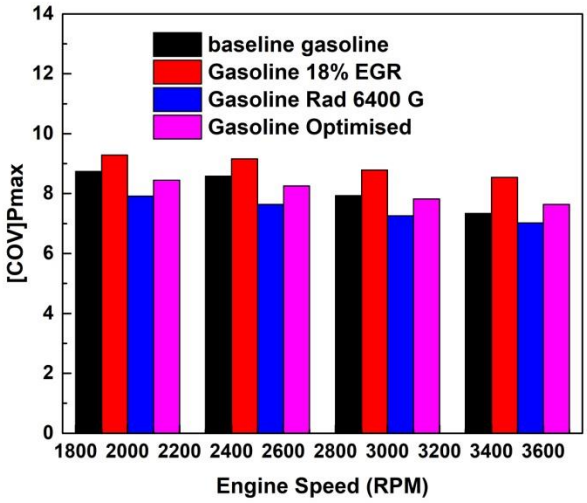

Fig 5.214 Variation in COV of P_{max} with synergetic effect in gasoline combustion

It was observed from the previous experiments that magnetic field assisted combustion and recirculation of cooled exhaust gases have contradicting effects on combustion

stability. Inorder to analyze the stability of combustion, the Coefficient of variation of P_{max} and IMEP are calculated for all engine speeds under experimentation. The variation in COV values for optimised synergy at various speeds is shown in figure 5.214 and 5.215.

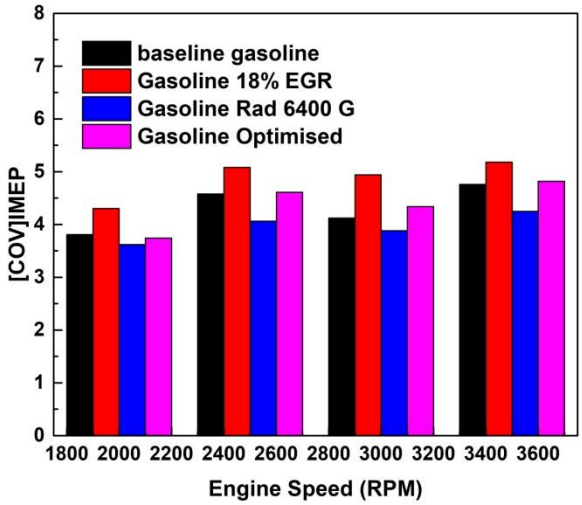

Fig 5.215 Variation in COV of IMEP with synergetic effect in gasoline combustion

It can be observed from the analysis of COV that combustion stability is affected through the inclusion of part cooled EGR, but maintained similar to the combustion in the unmodified (baseline) condition through the incremental effect of magnetic field. The values of COV of IMEP at the optimised synergy dwell within 5 which indicate that combustion is stable at all speeds.

5.8.7 Emission of Carbon monoxide

Optimised magnetic field assisted combustion is capable of reducing the percentage content of carbon monoxide in the exhaust as demonstrated in the previous sections of experimentation. The inclusion of optimal dilution using part cooled exhaust gases also reduces CO emissions marginally. Under optimised synergy in gasoline combustion, the emission of carbon monoxide is minimum when compared to the other experimental

conditions. The emission characteristics of CO for various experimental conditions are presented in figures 5.216- 5.219 in comparison with the optimised synergy.

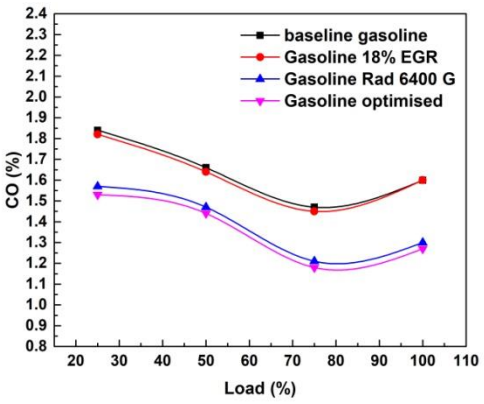

Fig 5.216 Variation in CO emission with synergetic effect in gasoline at 2000 rpm

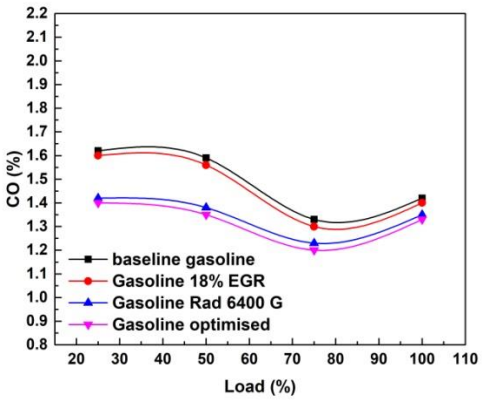

Fig 5.217 Variation in CO emission with synergetic effect in gasoline at 2500 rpm

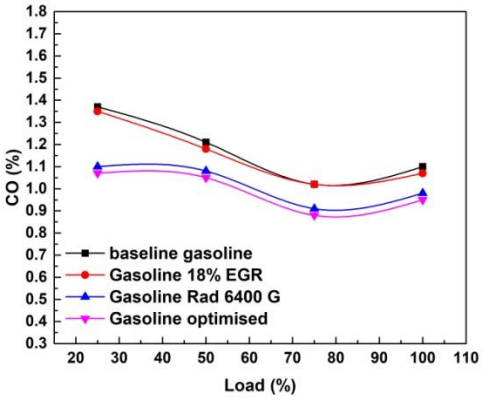

Fig 5.218 Variation in CO emission with synergetic effect in gasoline at 3000 rpm

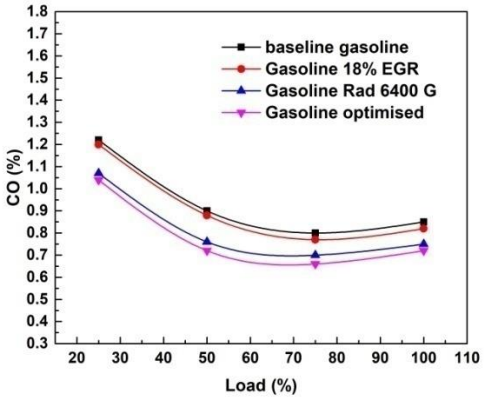

Fig 5.219 Variation in CO emission with synergetic effect in gasoline at 3500 rpm

5.8.8 Emission of Carbon dioxide

The emission of carbon dioxide is found to increase under the effect of MFAC and part cooled EGR. When optimised conditions of both these technologies are combined, the percentage content of carbon dioxide increases even further indicating the enhancement

of combustion efficiency under optimised synergy. The emission characteristics of carbon dioxide in optimised synergy with comparison to other optimised experimental conditions at different load and speed conditions are shown in figures 5.220- 5.223. It can be observed from the plots that the emission level of CO2 is maximum at optimised condition at all speeds.

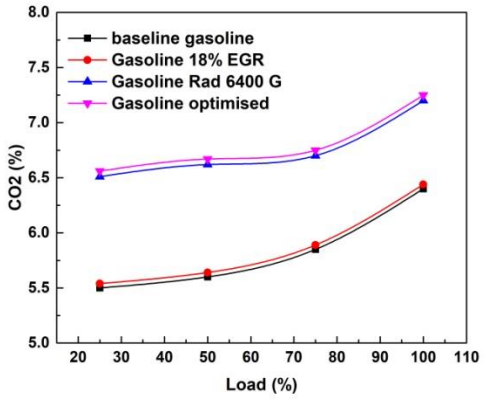

Fig 5.220 Variation in CO_2 emission with synergetic effect in gasoline at 2000 rpm

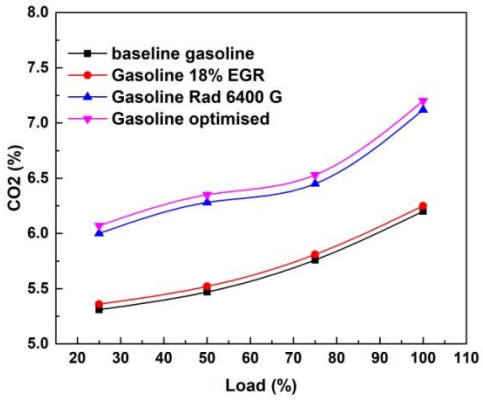

Fig 5.221 Variation in CO_2 emission with synergetic effect in gasoline at 2500 rpm

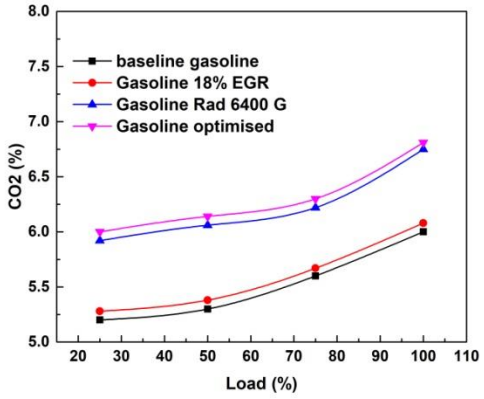

Fig 5.222 Variation in CO_2 emission with synergetic effect in gasoline at 3000 rpm

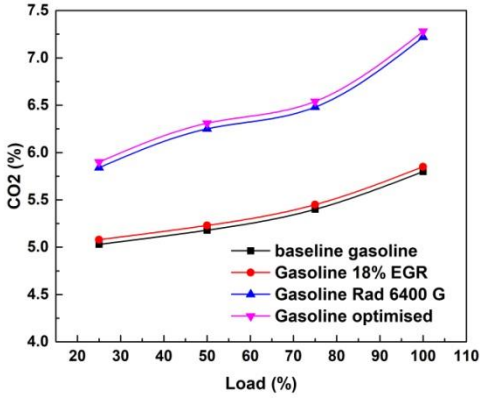

Fig 5.223 Variation in CO_2 emission with synergetic effect in gasoline at 3500 rpm

5.8.9 Emission of Hydrocarbons

Magnetic field assisted combustion and recirculation of part cooled exhaust gases have contradicting impact on the generation of organic emissions as acquired from the previous experimental results.

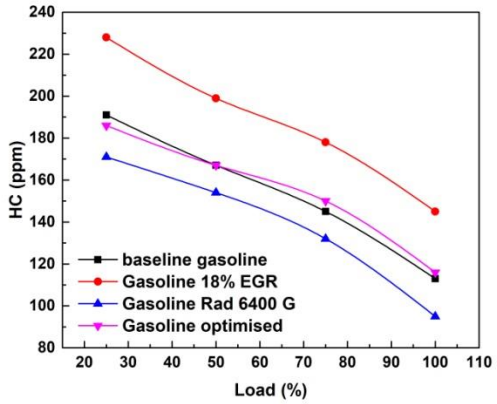

Fig 5.224 Variation in HC emission with synergetic effect in gasoline at 2000 rpm

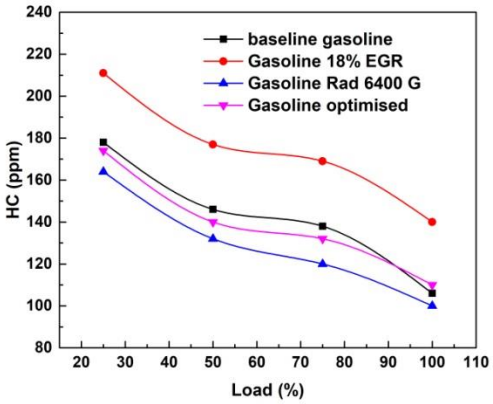

Fig 5.225 Variation in HC emission with synergetic effect in gasoline at 2500 rpm

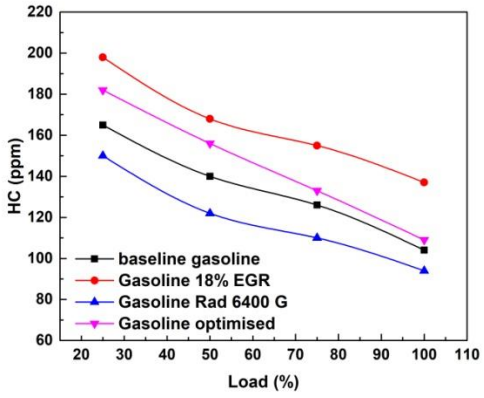

Fig 5.226 Variation in HC emission with synergetic effect in gasoline at 3000 rpm

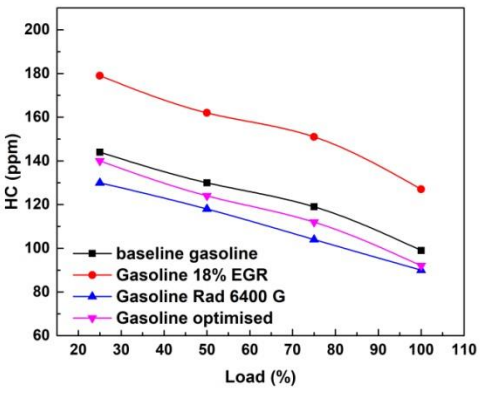

Fig 5.227 Variation in HC emission with synergetic effect in gasoline at 3500 rpm

When the optimised conditions of both these technologies are collaborated simultaneously, the concentration of hydrocarbons in the exhaust is reduced with respect to its magnitude under the sole effect of EGR, but slightly higher than that in the case of

radial magnetic fields. The trends of organic emissions in optimised synergy at different speeds are represented in figures 5.224- 5.227.

5.8.10 Emission of Oxides of Nitrogen

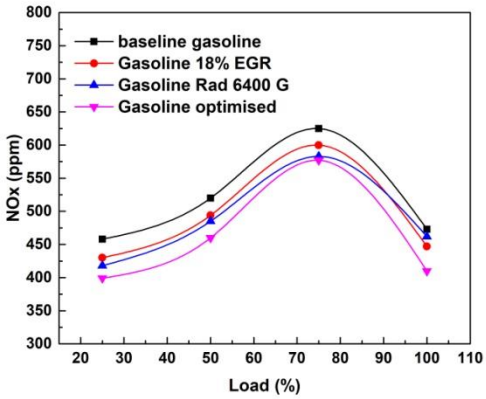

Fig 5.228 Variation in NO_x emission with synergetic effect in gasoline at 2000 rpm

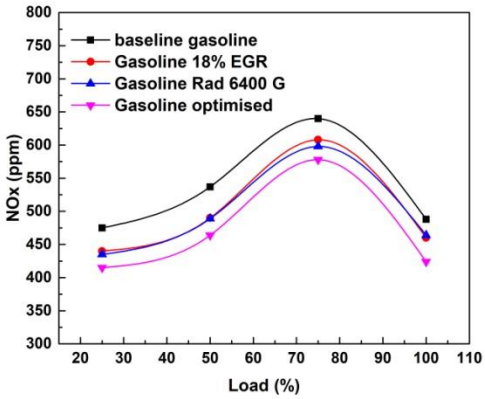

Fig 5.229 Variation in NO_x emission with synergetic effect in gasoline at 2500 rpm

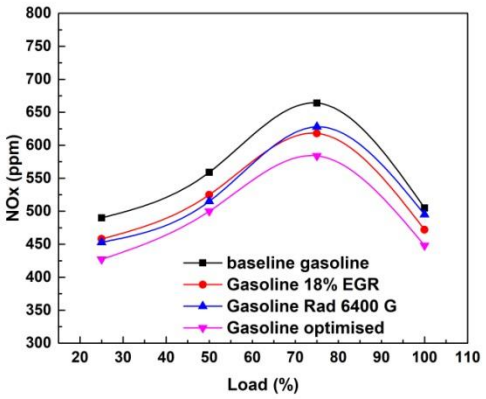

Fig 5.230 Variation in NO_x emission with synergetic effect in gasoline at 3000 rpm

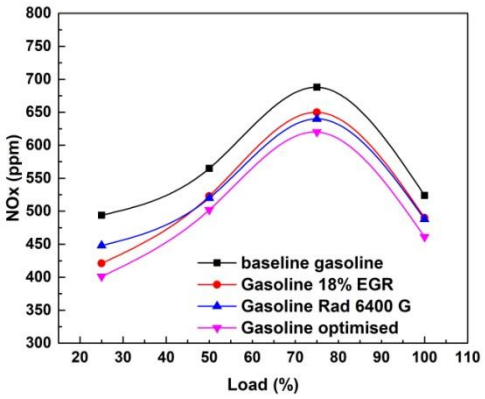

Fig 5.231 Variation in NO_x emission with synergetic effect in gasoline at 3500 rpm

The greatest advantage of recirculating cooled exhaust gases is the reduction it yields in the generation of oxides of nitrogen. As discussed in the earlier sections, magnetic field assisted combustion also has a marginal positive impact on the emission of NO_x. The synergetic effect of optimised conditions of both these technologies results in the further

reduction of NO_x at all engine speeds. The trend of NO_x emission under the synergetic effect is shown in figures 5.228- 5.231.

5.9 Synergetic Effect of Optimised conditions in Magnetic Field Assisted Combustion and Part Cooled EGR rate in the Combustion of gaseous phase hydrocarbons (LPG)

Similar to the discussion made in the previous section, the optimised parameters of magnetic field assisted combustion and part cooled exhaust gas recirculation flow rate are conjoined to study the synergetic effect produced on the combustion of LPG which is a gas phase hydrocarbon. The experimental conditions and the operating parameters are maintained the same as in the case of gasoline combustion and the impact created on the performance, combustion and emissions of the engine are analyzed.

5.9.1 Brake Power

When the engine is fuelled by neat LPG, the power output obtained is comparatively higher than gasoline fuelled operation. This is especially noticeable at higher engine speeds where the flame propagation velocity of LPG is higher compared to gasoline (Nayak et al. 2016).

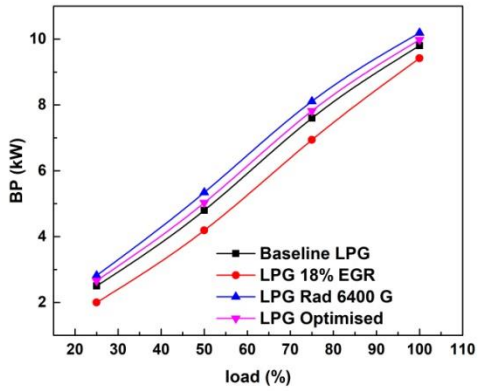

Fig 5.232 Variation in BP with synergetic effect on LPG at 2000 rpm

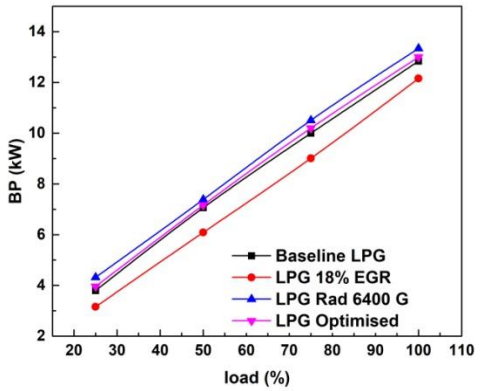

Fig 5.233 Variation in BP with synergetic effect on LPG at 2500 rpm

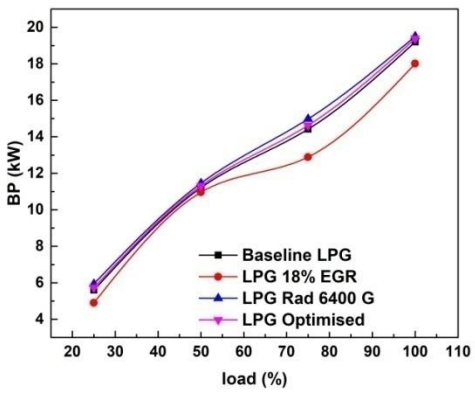

Fig 5.234 Variation in BP with synergetic effect on LPG at 3000 rpm

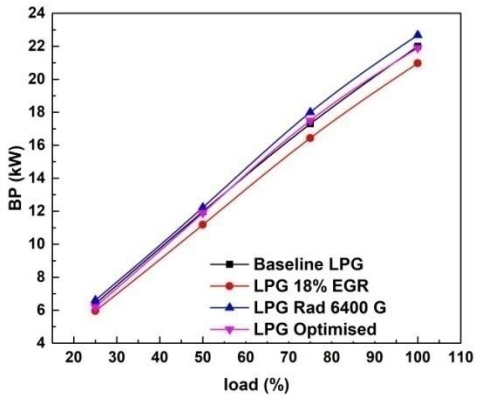

Fig 5.235 Variation in BP with synergetic effect on LPG at 3500 rpm

As the recirculation of cooled gases and magnetic field assisted combustion have conflicting impact on the output power, under the synergetic effect of optimal parameters of both, the brake power of the engine is observed to be in a balance between the power developed by these two optimal conditions. The brake power generated under synergetic effect of MFAC and EGR are shown in figures 5.232- 5.235.

5.9.2 Brake Specific Fuel Consumption

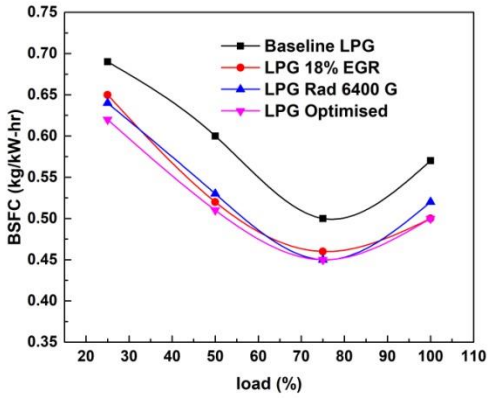

Fig 5.236 Variation in BSFC with synergetic effect on LPG at 2000 rpm

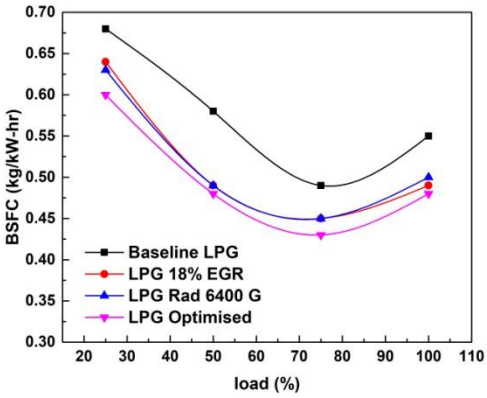

Fig 5.237 Variation in BSFC with synergetic effect on LPG at 2500 rpm

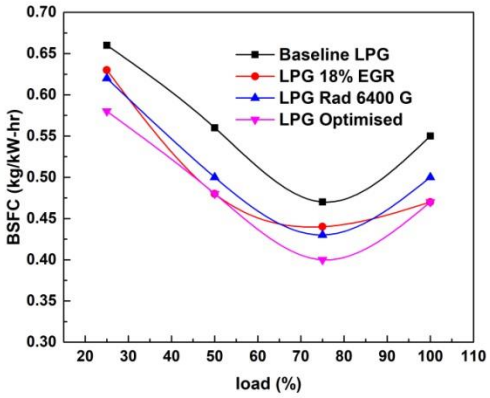

Fig 5.238 Variation in BSFC with synergetic effect on LPG at 3000 rpm

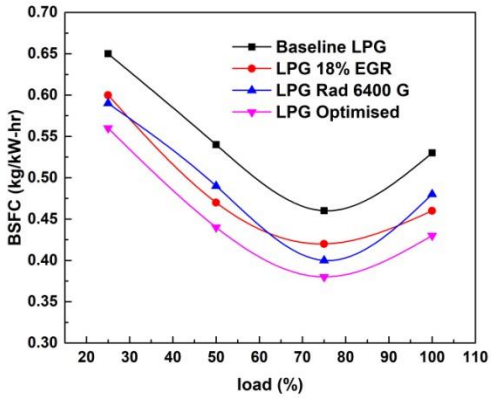

Fig 5.239 Variation in BSFC with synergetic effect on LPG at 3000 rpm

The fuel economy of the test engine fuelled by LPG was observed to improve under the optimal conditions of both magnetic field assisted combustion and part cooled EGR. Under the synergetic effect of these optimal parameters, the fuel economy shows further improvement. Figures 5.236- 5.239 show the variation in specific fuel consumption of the engine under optimised synergy with comparison to other optimal operating conditions. It can be clearly surmised that fuel consumption rate is the minimum at the synergetic condition.

5.9.3 Brake Thermal Efficiency

As discussed in a previous section, the thermal efficiency of the engine operated under neat LPG is lower when compared to the normal gasoline operation. The higher ignition temperature of LPG results in a longer ignition delay and hence higher combustion duration. The resultant reduction in average burning rate causes an increased consumption of fuel which leads to reduction in efficiency (Ceviz et al. 2005). As the optimal parameters in magnetic field assisted combustion and part cooled EGR promote the factors responsible for thermal efficiency, it can be observed that the synergetic effect of both results in maximum thermal efficiency. The thermal efficiencies of the engine under optimal operating conditions are compared in figures 5.244- 5.247.

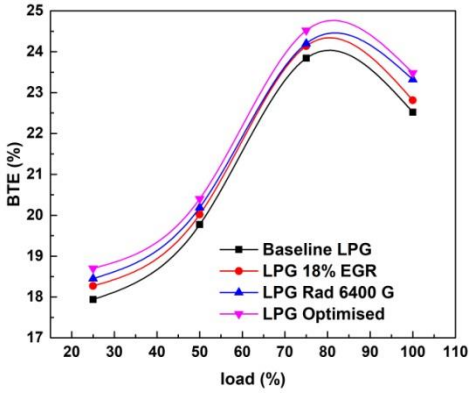

Fig 5.240 Variation in BTE with synergetic effect on LPG at 2000 rpm

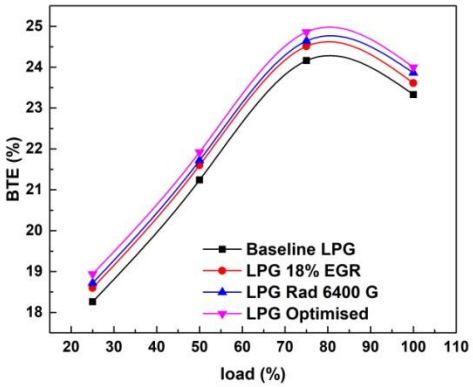

Fig 5.241 Variation in BTE with synergetic effect on LPG at 2500 rpm

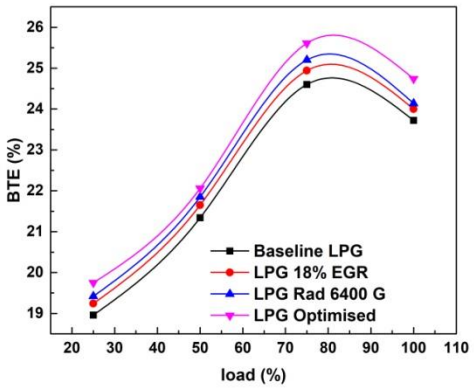

Fig 5.242 Variation in BTE with synergetic effect on LPG at 3000 rpm

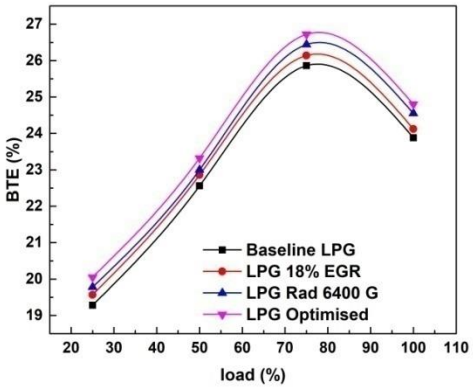

Fig 5.243 Variation in BTE with synergetic effect on LPG at 3500 rpm

5.9.4 In-cylinder Pressure

A slight improvement was noted in the magnitudes of combustion pressures under the influence of radial magnetic fields. This improvement is explained on the basis of higher diffusion of fuel molecules from the free stream to the sub layers under the influence of strong magnetic fields which tends to negate the thickening of boundary layer near TDC due to the effect of high Reynolds number (Govindasamy et al. 2007).

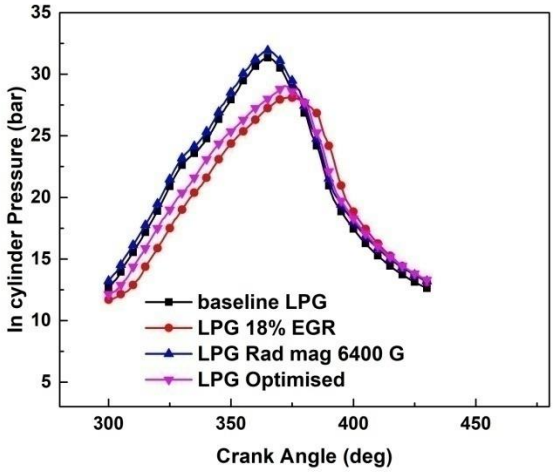

Fig 5.244 Variation in CP with synergetic effect on LPG at 2500 rpm

As a result, reaction rate is enhanced which in turn enhances the combustion and leads to higher pressures in the combustion chamber. At the same time, the recirculation of partially cooled exhaust results in the diminishment of pressure values along with a peak shift further away from TDC. Under the synergetic effect the combustion pressures lie in between the optimal conditions of MFAC and EGR with a slight shift in peak as depicted in figure 5.244.

5.9.5 Net Heat Release rate

The higher availability of oxygen to the hydrocarbon molecules during the magnetic field assisted combustion aids in the higher release of heat in the combustion cycles where as the recirculation of part cooled EGR results in the reduction of heating value per unit mass of the mixture, in turn reducing the adiabatic flame temperatures. As a result of reduced combustion temperatures, the peak heat release rate is also reduced. Because of the contradicting effects of the two experimental conditions, the synergy of optimal conditions of both results in a balance with the values of NHRR lying in between that in the two optimal operating conditions. The variation in NHRR with optimized synergy for LPG combustion is depicted in figure 5.245.

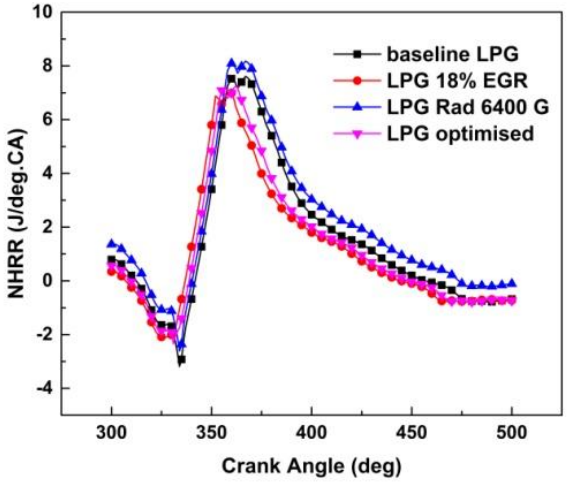

Fig 5.245 Variation in NHRR with synergetic effect on LPG at 2500 rpm

5.9.6 Analysis of Stability of Combustion

Magnetic field assisted combustion results in increased stability of combustion whereas the recirculation of cooled gases result in the deterioration of combustion stability and even causes partial or complete misfires in engine operation. The conflicting impacts of optimal parameters of both these technologies influence the combustion of LPG. Hence the analysis of stability through the statistical calculation of coefficient of variation becomes significant when the synergetic effect is studied. The COV of P_{max} and IMEP are calculated for the engine operating at optimized synergy for all the tested speeds and are shown in figures 5.246 and 5.247 respectively.

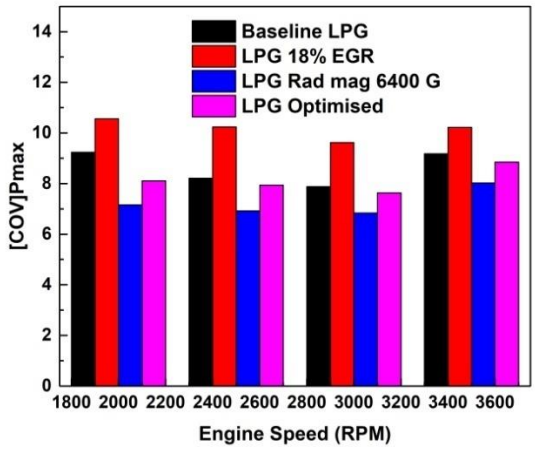

Fig 5.246 Variation in COV of P_{max} with synergetic effect in LPG combustion

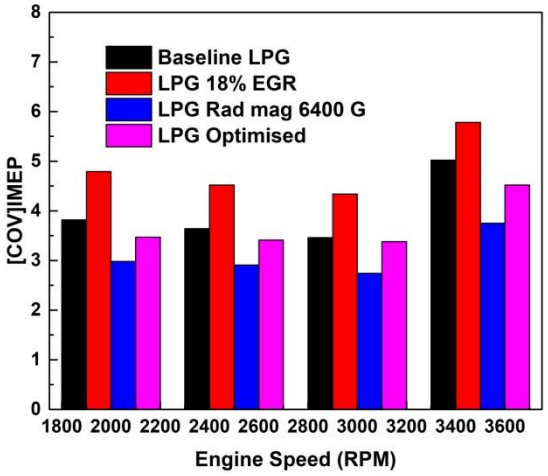

Fig 5.247 Variation in COV of IMEP with synergetic effect in LPG combustion

It can be indisputably conceived that the inclusion of cooled inert exhaust hampers the stability of combustion, but the complimentary effect of magnetic field prevents too much deterioration in stability. The COV values under synergetic effect lie in between that of the two optimal experimental conditions. The COV of IMEP values under optimized synergy fall well within 5, indicating that the combustion is stable.

5.9.7 Emission of Carbon monoxide

As discussed in the case of combustion of liquid phase fuel the synergetic effect of optimal part cooled EGR and optimal MFAC, the emission of carbon monoxide can be reduced further than the individual effect of these parameters. The emission trends of CO under optimized synergy for LPG are shown in figures 5.248- 5.251.

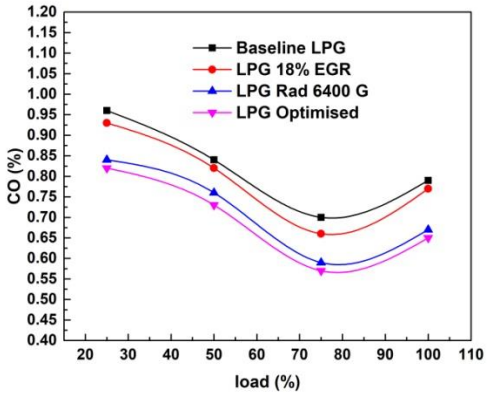

Fig 5.248 Variation in CO emission with synergetic effect on LPG at 2000 rpm

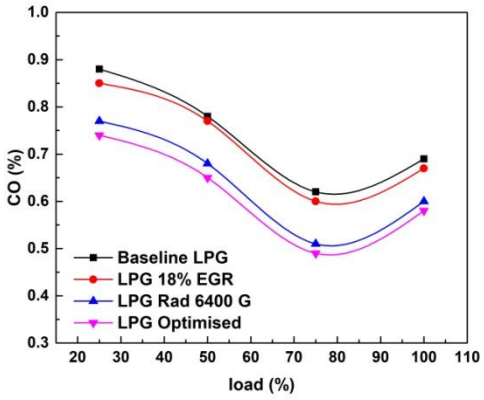

Fig 5.249 Variation in CO emission with synergetic effect on LPG at 2500 rpm

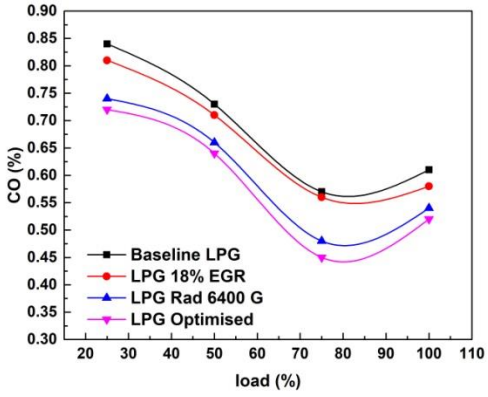

Fig 5.250 Variation in CO emission with synergetic effect on LPG at 3000 rpm

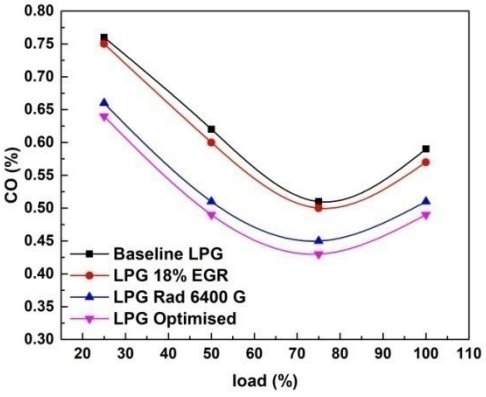

Fig 5.251 Variation in CO emission with synergetic effect on LPG at 3500 rpm

5.9.8 Emission of Carbon dioxide

As discussed in the previous sections, magnetic field assisted combustion and optimal flow rate of part cooled EGR both promote enhanced combustion and hence generates higher percentage of carbon dioxide in the engine exhaust. The emission trends of carbon dioxide for optimized synergy in LPG combustion for different engine speeds are represented in figures 5.252- 5.255. It can be conceived from the plots that the percentage of CO_2 in the exhaust increases under the synergetic effect of these techniques.

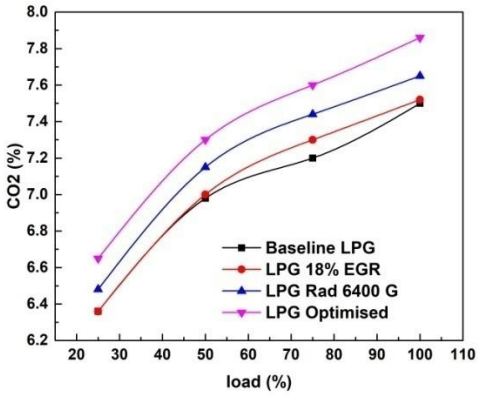

Fig 5.252 Variation in CO_2 emission with synergetic effect on LPG at 2000 rpm

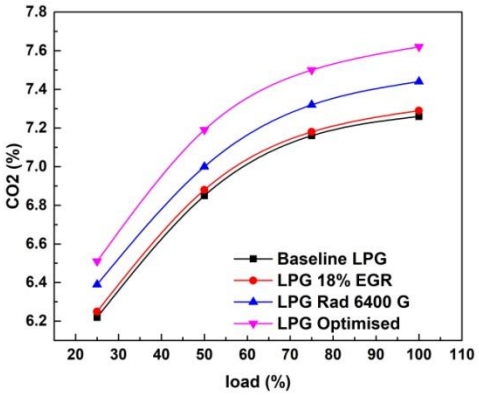

Fig 5.253 Variation in CO_2 emission with synergetic effect on LPG at 2500 rpm

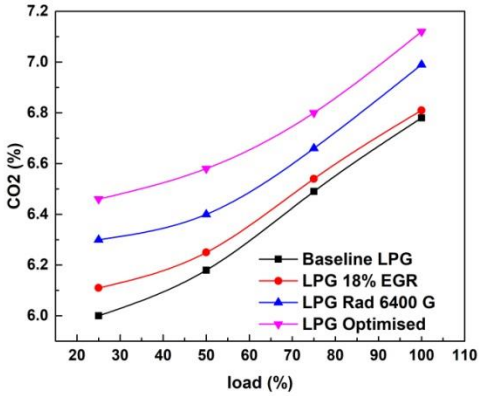

Fig 5.254 Variation in CO_2 emission with synergetic effect on LPG at 3000 rpm

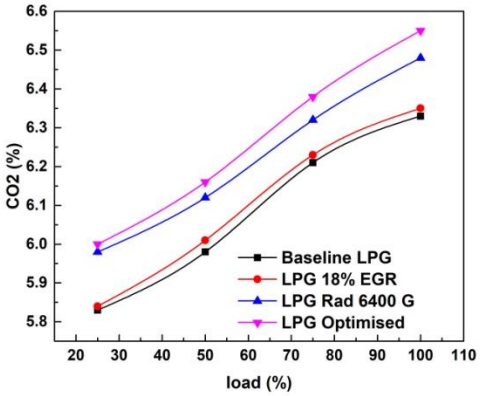

Fig 5.255 Variation in CO_2 emission with synergetic effect on LPG at 3500 rpm

5.9.9 Emission of Hydrocarbons

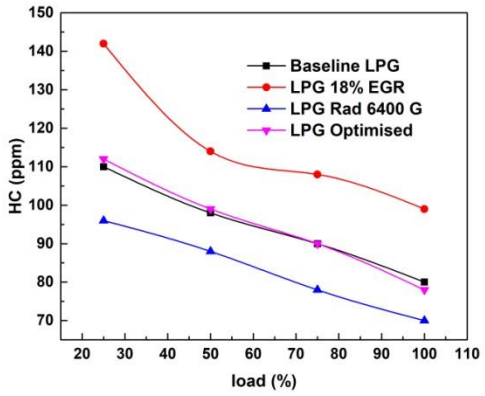

Fig 5.256 Variation in HC emission with synergetic effect on LPG at 2000 rpm

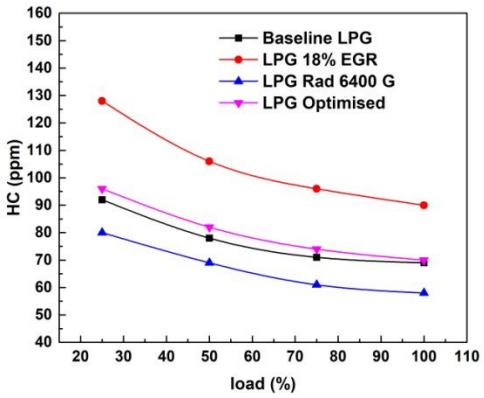

Fig 5.257 Variation in HC emission with synergetic effect on LPG at 2500 rpm

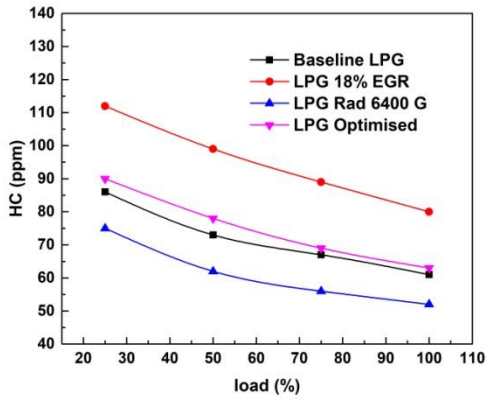

Fig 5.258 Variation in HC emission with synergetic effect on LPG at 3000 rpm

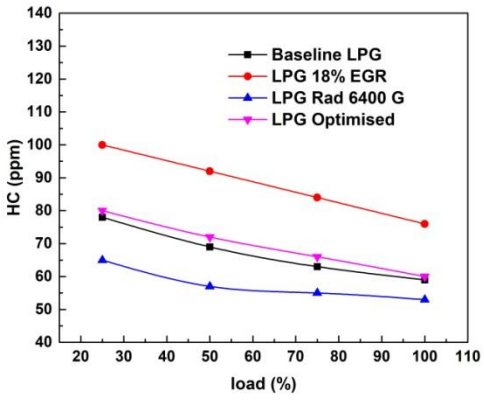

Fig 5.259 Variation in HC emission with synergetic effect on LPG at 3500 rpm

The concentration of organic emissions in the engine exhaust is reduced through the application of optimal magnetic fields since the polarization process results in the disintegration of molecular clusters which hinder the extend of oxidation of fuel molecules (Govindasamy et al. 2007). At the same time, when the partially cooled exhaust gases are recirculated into the combustion chamber, the concentration of

hydrocarbons in the exhaust increases at all tested speeds. When the optimal conditions of both these techniques are collaborated, the concentration of organic emissions is maintained comparable to that in the baseline combustion of LPG. The emission characteristics of hydrocarbons under optimal synergy in LPG combustion are displayed in figures 5.256- 5.259.

5.9.10 Emission of Oxides of Nitrogen

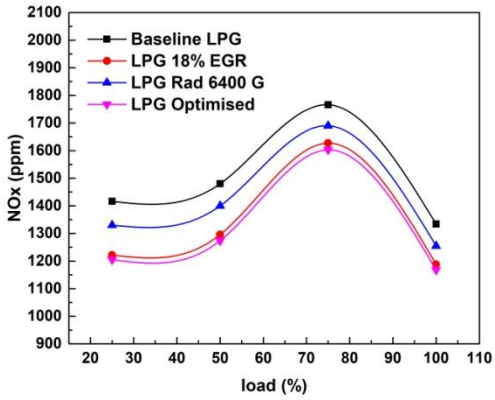

Fig 5.260 Variation in NO_x emission with synergetic effect on LPG at 2000 rpm

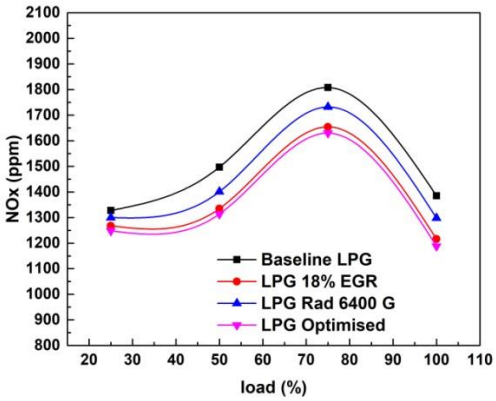

Fig 5.261 Variation in NO_x emission with synergetic effect on LPG at 2500 rpm

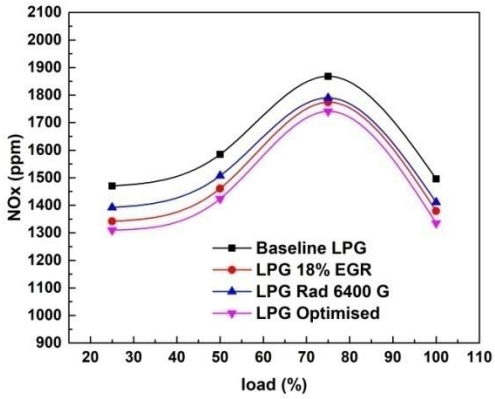

Fig 5.262 Variation in NO_x emission with synergetic effect on LPG at 3000 rpm

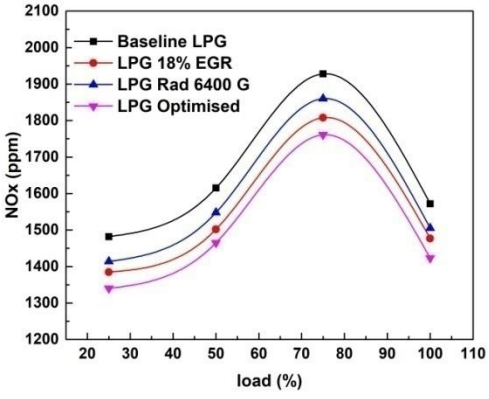

Fig 5.263 Variation in NO_x emission with synergetic effect on LPG at 3500 rpm

The emission trends of NO_x under optimized synergy with comparison to other optimal experimental conditions are displayed in figures 2.260- 2.263. Similar to the case of combustion in liquid phase hydrocarbons, the synergetic effect of MFAC and cooled exhaust gas flow rate results in further reduction of NO_x concentration in the exhaust than in the case of individual effect of these techniques. The emission of NO_x is minimum at optimal synergy condition at all the tested speeds.

CHAPTER 6

CONCLUSION AND SCOPE FOR FUTURE WORK

The present experimental work was focused on the investigation of optimized parameters of magnetic field assisted combustion along with optimal flow rate of part cooled exhaust gas recirculation on multicylinder, multipoint port fuel injection SI engine operating at different load and speed conditions. The investigation was conducted on a Maruthi Zen, 4 cylinder engine with variables like fuel phase, magnetisation pattern, magnetic field intensity, locus of magnetisation and EGR flow rate. The impact of these operating variables is analyzed based on the performance, combustion and emission characteristics of the engine. Each of these experimental parameters is optimized and the synergetic effect was studied for both the fuel phases. The major conclusions that can be summarized based on the experimental research are as follows.

- The performance parameters of the engine like brake power, BSFC and thermal efficiency are found to improve under all stages of axial and radial magnetic fields for both liquid phase and gaseous phase hydrocarbons.
- The combustion parameters like in-cylinder pressure and net heat release rate are positively influenced by magnetic field assisted combustion.
- The stability of combustion which is analyzed statistically through the coefficient of variation of combustion pressures show that Magnetic field assisted combustion is effective in reducing the cyclic fluctuations in combustion which in turn enhances the performance and emission characteristics of the test engine.
- Under both patterns of magnetic fields experimented on both phases of hydrocarbons, the emission of carbon monoxide and hydrocarbons reduce comprehensively. NO_x emissions reduce very slightly with increase in magnetic intensities and the emission of CO_2 is found to increase with all stages of magnetisation.
- Of all the tested magnetic intensities, maximum improvement in combustion and emission attributes are obtained for 6400 gauss field for both the magnetisation

patterns in both phases of hydrocarbons, making it the preferred magnetic intensity for further stages of experimentation.

- The radial magnetic fields generated by sintered NdFeB rings are observed to influence the combustion parameters to an extend higher than axial fields of same intensity because of enhanced interaction with the hydrocarbon molecules.
- Magnetic Field Assisted Combustion is observed to be more effective with the combustion of liquid phase hydrocarbons owing to the contiguous arrangement of molecules.
- The effect of different rates of part cooled EGR on the combustion of gasoline and LPG was studied. Part cooled EGR resulted in the deterioration of power output but improved the fuel economy and thermal efficiency up to an optimum flow rate for both the fuel phases because of the incremental effect on the ratio of specific heats.
- The analysis of in-cylinder pressures and Net Heat Release Rates showed that combustion is influenced by the EGR flow rates. With increasing flow rates of part cooled EGR, the in-cylinder pressures reduced and the peak pressure points shifted further away from the TDC due to prolonged combustion durations. Heat Release rates also showed a decrease with a peak shift towards BTDC positions with EGR.
- The statistical analysis of combustion through the computation of Coefficient of Variation showed that the recirculation of part cooled EGR results in a reduction of combustion stability for both the fuels. The variation in COV is increased drastically with 24% recirculation which shows that quality of combustion is significantly reduced.
- The major disadvantage of LPG as a fuel is the generation of high amounts of NO_x. This problem could be effectively tackled by the application of cooled recirculated gases. Considerable reduction is observed in NO_x emissions with each stage of recirculation of cooled exhaust gases.

- In both the experimented fuels, EGR is observed to be beneficial to the fuel economy and thermal efficiency without much compromise on CO and HC emissions until a dilution rate of 18%.
- The addition of EGR after the optimal flow rate resulted in deterioration of performance, combustion and emission characteristics (other than NO_x) of the engine. Hence the optimum flow rate of part cooled EGR is chosen as 18%.
- The optimised conditions like magnetisation pattern, magnetic intensity and the fuel phase in magnetic field assisted combustion are combined to investigate the significance of locus of magnetisation with respect to the injector position.
- Magnetisation in locus 1 which is located adjacent to the injector gave the best results in performance and emissions of the engine. The performance and emissions of the engine deteriorated as the locus is shifted further away from reference point because of loss of magnetisation effect based on recombination of polarised pseudo clusters and inverse square law. Hence locus 1 is chosen as the optimised position of application of magnetic field for both the fuel phases.
- When all the optimal parameters of magnetic field assisted combustion are collaborated with optimized flow rate of part cooled EGR, the synergetic effect was observed to be positively influencing combustion process.
- Under optimal synergy for both fuel phases, the characteristics like brake specific fuel consumption, brake thermal efficiency, carbon monoxide emission, and emission of oxides of nitrogen got further enhanced due to the complimentary effect of MFAC and EGR in these characteristics.
- In the engine characteristics like power output, in cylinder pressure, net heat release rate, combustion stability and emission of hydrocarbons where the collaborated techniques have contradicting effects, the results of optimal synergy lie in between the individual values of two optimal experimental conditions that are collaborated.

- Both the collaborated experimental techniques results in the enhancement of combustion individually. Hence the emission of carbon dioxide was observed to increase at optimal synergy for both the fuel phases.
- The drawback of this work is the limitation imposed on the intensity of magnetic field that can be implemented on real time automotive engines due to the interference that it creates on the electronic components and advanced control units that are the integral part of modern auto engines.

It can be concluded that magnetic field assisted combustion is an economic and effective technique in the combustion of liquid phase and gaseous phase hydrocarbon based fuels. The incorporation of partially cooled EGR adds to the benefits in combustion and the collaboration of these technologies can effectively cut down the fuel consumption and exhaust emissions which provide higher efficiencies and environmental impact, thus imparting socio-economic significance to this work.

6.1 Scope for future work

- As this research is primarily based on molecular restructuring of hydrocarbons, it can be extended to any existing/developed hydrocarbon based fuels.
- Magnetic field assisted combustion is proven to alter the para state of hydrogen into more active ortho configuration. The impact of such an alteration in molecular configuration can be investigated in hydrogen fuelled combustion engines.
- Liquid LPG injection can be done instead of using the vaporizer and the effect of magnetic fields can be investigated and compared with gaseous LPG.
- With the installation of a programmable ECU, the pulse width of LPG injection can be modified and the synergetic effect produced on MFAC can be investigated.
- Combustion studies with more than 500 combustion cycles can be done to improve the accuracy of results obtained.

- Other NO_x reduction techniques like SCR, fuel additives etc can be experimented along with the optimal magnetic fields to study their impact on magnetic field assisted combustion.
- Research can be done on coatings that can be provided to the rare earth magnets which will enable better resistance to thermal corrosion.
- A suitable covering material can be developed to house the magnet assembly which can reduce the interference on surrounding electronic components without hampering the magnetic focus on the fuel line.

REFERENCES

Abd-Allah, G. H., (2001). "Using exhaust gas recirculation in internal combustion engines: a review." *Energy Conversion and Management,* 43, 1027–1042.

Agarwal, A. K., (2004). "Effect of EGR on the exhaust gas temperature and exhaust opacity in compression ignition engines". Vol. 29.

Agarwal, D., Singh, S. K. and Agarwal, A. K., (2011). "Effect of Exhaust Gas Recirculation (EGR) on performance, emissions, deposits and durability of a constant speed compression ignition engine." *Applied Energy,* 88, 2900–2907.

Agarwal, A. K., Gupta, T., Shukla, P. C. and Dhar, A., (2015). "Particulate emissions from biodiesel fuelled CI engines". *Energy Conversion and Management,* 94, 311-330.

Akramkhodzhayev, A. M. and Amirkhanov, S. K., (1986). "The Mechanism of Petroleum Formation". *International Geology Review,* 28(8), 985-990.

Al-Rawaf, M. A., (2015). "Magnetic Field Effects on Spark Ignition Engine Performance and its Emissions at High Engine Speeds". *Journal of Engineering and Sustainable Development,* 19(4), 37-48.

Attar, A. R., Tipole, P., Bhojwani, V., and Deshmukh, S., (2013). "Effect of magnetic field strength on hydrocarbon fuel viscosity and engine performance". *International Journal of Mechanical Engineering and Computer Applications,* 1(7), 94-98.

Azem, A., Riahi-Zanjani, B., and Balali-Mood, M., (2016). "Effects of air pollution on human health and practical measures for prevention in Iran". *J Res Med Sci*. 21: 65.

Baker, J., and Varagani, R., (2003). "Models and experiments on Laminar Diffusion Flames in non-uniform magnetic fields". *Seventh International workshop on microgravity combustion and chemically reacting systems,* 317-320.

Barmina, I., and Zake, M., (2017). "Magnetic Field Control of Combustion Dynamics", *Latvian Journal of Physics and Technical Sciences,* 53(4), 36-46.

Bayraktar, H., and Durgun, O., (2005). “Investigating the effects of LPG on spark ignition engine combustion and performance”. *Energy conversion and management*, 46(13-14), 2317-2333.

Božić, M., Vučetić, A., Kozarac, D., and Lulić, Z., (2017). “Experimental investigation on influence of EGR on combustion performance in SI Engine”. *Stroke*, 2000, 85.

Brown, D., Ma, B. M., and Chen, Z., (2002). “Developments in the processing and properties of NdFeb-type permanent magnets”. *Journal of magnetism and magnetic materials*, 248(3), 432-440.

Cairns, A., Blaxill, H., and Irlam, G., (2006). “Exhaust Gas Recirculation for Improved Part and Full Load Fuel Economy in a Turbocharged Gasoline Engine.” *SAE Technical Paper series*, 2006-01-0047.

Ceviz, M. and Yuksel, F., (2006). “Cyclic variations on LPG and gasoline fuelled lean burn SI engine.” *Journal of Renewable Energy* 31, 1950-1960.

Ceviz, M. A., and Yüksel, F., (2005). “Effects of ethanol–unleaded gasoline blends on cyclic variability and emissions in an SI engine”. *Applied Thermal Engineering*, 25(5-6), 917-925.

Ceviz, M. A., Kaleli, A., and Güner, E., (2015). “Controlling LPG temperature for SI engine applications”. *Applied Thermal Engineering*, 82, 298-305.

Chaichan, M. T., (2016). “Spark ignition engine performance fueled with hydrogen enriched liquefied petroleum gas (LPG)”. *Scholars Bulletin Journal*, 2(9), 537-546.

Changming Gong, Huang, K., Deng, B., and Liu, X., (2011). “Catalyst light-off behavior of a spark-ignition LPG (liquefied petroleum gas) engine during cold start”. *Energy*, 36(1), 53-59.

Chen, S. K., and Chen, S., (1993). “Engine diagnostics by dynamic shaft measurement: a progress report”. *SAE Transactions*, 1964-1979.

Chen, C, lee, W, Mwangi, J, Wang, L, and Lu, J., (2017). “Impact of magnetic tube on pollutant emissions from the diesel engine”. *Aerosol and Air quality research*, 17, 1097-1104.

Çinar, C., Şahin, F., Can, Ö., and Uyumaz, A., (2016). "A comparison of performance and exhaust emissions with different valve lift profiles between gasoline and LPG fuels in a SI engine". *Applied Thermal Engineering*, 107, 1261-1268.

Dadvand, P., Rivas, I., Basagaña, X., Alvarez-Pedrerol, M., Su, J., Pascual, M. D. C., and Nieuwenhuijsen, M. J., (2015). "The association between greenness and traffic-related air pollution at schools". *Science of the Total Environment*, 523, 59-63.

Durgun, O., (2005). "Investigating the effects of LPG on spark ignition engine combustion and performance". *Energy conversion and management*, 46(13-14), 2317-2333.

Einewall, P., and Johansson, B., (2000). "Cylinder to cylinder and cycle to cycle variations in a six cylinder lean burn natural gas engine". *SAE transactions*, 1810-1822.

Elamin, A. A., Ezeldin, M., Masaad, A. M., and Suleman, N. M., (2015). "Effect of Magnetic Field on Some Physical Characteristics and Cetane Number of Diesel Fuel". *American Journal of Applied Chemistry*, 3(6), 212-216.

Elnajjar, E., Hamdan, M. O., and Selim, M. Y., (2013). "Experimental investigation of dual engine performance using variable LPG composition fuel". *Renewable Energy*, 56, 110-116.

Erkuş, B., Sürmen, A., and Karamangil, M. I., (2013). "A comparative study of carburation and injection fuel supply methods in an LPG-fuelled SI engine". *Fuel*, 107, 511-517.

Evdokimov, I. N., & Kornishin, K. A., (2009). "Apparent disaggregation of colloids in a magnetically treated crude oil". *Energy & fuels*, 23(8), 4016-4020.

Faris, A. S., Al-Naseri, S. K., Jamal, N., Isse, R., Abed, M., Fouad, Z., ... and Jasim, H., (2012). "Effects of magnetic field on fuel consumption and exhaust emissions in two-stroke engine". *Energy Procedia*, 18, 327-338.

Fatih, F., and Saber, G., (2010). "Effect of fuel Magnetism on Engine Performance and Emissions", *Australian Journal of Basic and Applied Sciences*, 4, 6354-6358.

Folinsbee, L.J., (1992). “Human Health Effects of Air Pollution”. *Environ Health Perspect*, 100, 45–56.

Fontana, G., and Galloni, E., (2010). “Experimental analysis of a spark-ignition engine using exhaust gas recycle at WOT operation”. *Applied Energy*, 87(7), 2187-2193.

Gad, M. S., (2016). “Assessment of biodiesel derived from waste cooking oil as an alternative fuel for diesel engines”. *International J. of Chem. Tech. Research*, 9(3), 140-146.

Garg, R., and Agarwal, A., (2013). “Fuel Energizer: The Magnetizer (A Concept of Liquid Engineering)”, *International Journal of Innovative Research & Development*, 2, 617-627.

Gillon, P., Khaldi, F., and Noudem, J., (2005). “On the Similarity between gravity and magneto gravity convection within a non-electro conducting fluid in a differentially heated rectangular cavity”. *International Journal of Heat and Mass Transfer*, 48, 1350-1360.

Gabiña, G., Basurko, O. C., Notti, E., Sala, A., Aldekoa, S., Clemente, M., and Uriondo, Z., (2016). “Energy efficiency in fishing: Are magnetic devices useful for use in fishing vessels?”. *Applied Thermal Engineering*, 94, 670-678.

Govindasamy, P., and Dhandapani, S., (2007). “Experimental investigation of cyclic variation of combustion parameters in catalytically activated and magnetically energized two-stroke SI engine”. *Journal of energy & environment*, 6, 45-59.

Govindasamy, P., and Dhandapani, S., (2007). “Performance and emissions achievements by magnetic energizer with a single cylinder two stroke catalytic coated spark ignition engine”.

Govindasamy, P., and Dhandapani, S., (2007). “Experimental investigation on the effect of magneticflux to reduce emissions and improve combustion performance in a two-stroke, catalytic-coated,spark-ignition engine”. *International journal of automotive technology*, 8(5), 533-542.

Govindasamy, P., and Dhandapani, S., (2007, December). “Reduction of NOx Emission in Bio Diesel Engine with Exhaust Gas Recirculation and Magnetic Fuel Conditioning”. In *GMSARN International Conference on Sustainable Development: Challenges and Opportunities for GMS* (Vol. 14).

Greenstone M., Harish S., Pande R., and Sudarshan A., (2017). “The solvable challenge of air pollution in India”. *India Policy Forum*, 11-12 July 2017.

Gumus, M., (2010). “A comprehensive experimental investigation of combustion and heat release characteristics of a biodiesel (hazelnut kernel oil methyl ester) fueled direct injection compression ignition engine”. *Fuel*, 89(10), 2802-2814.

Guo, H., Chen, Y., and Yao, R., (1986). "A Study of Magnetic effects on the Physicochemical Properties of Individual Hydrocarbons". *IEEE Transactions on Magnetics.*

Haavisto, Touminen, Santa-Nokki, Kankaanpa, Paju, M., Ruuskanen, (2014). “Magnetic behavior of Sintered NdFeB magnets on long term time scale”, *Advances in Materials Science and Engineering* 760584 1-7.

Habbo, A. R. A., A Khalil, R., and S Hammoodi, H., (2011). “Effect of Magnetizing the Fuel on the Performance of an SI Engine”. *AL-Rafdain Engineering Journal (AREJ)*, 19(6), 84-90.

Heywood, J. B. Internal Combustion Engine Fundamentals, Chap. 9: *Combustion in spark-ignition engines*. 1986.

Ishli, K., Sasaki, T., Urata, Y., and Ohno, T., (1997). “Investigation of cyclic variation of IMEP under lean burn operation in spark-ignition engine.” SAE Paper 972830.

Iwata, N., Tsubuki, S., Takaki, Y., Watanabe, K., Sekiguchi, M., Hosoki, E., ... and Saido, T. C., (2000). “Identification of the major Aβ 1–42-degrading catabolic pathway in brain parenchyma: suppression leads to biochemical and pathological deposition”. *Nature medicine*, 6(2), 143-150.

Jain, S., and Deshmukh, S., (2012). “Experimental Investigation of Magnetic Fuel Conditioner in IC Engine”. *IOSR Journal of Engineering*, 2, 27-31.

Jalali, M., Ahmadi, M., Yadaei, F., Azimi, M., and Hoseini, H., (2013). "Enhancement of Benzine Combustion Behaviour inExposure to the Magnetic Field". *Journal of Clean Energy Technologies,* 1, 224-227.

Johnson, E., (2003). "LPG: a secure, cleaner transport fuel? A policy recommendation for Europe". *Energy Policy*, 31(15), 1573-1577.

Jothi, M., Nagarajan, G., Ranganarayanan, S., (2008). "LPG fuelled diesel engine using diethyl ether with Exhaust Gas Recirculation". *International Journal of Thermal Sciences* 47, 450-457.

Jung, S. J., Mehta, J. S., and Tong, L., (2018). "Effects of environment pollution on the ocular surface". *The ocular surface*, 16(2), 198-205.

Kacem, S. A., Ferdaouss, L., Abrerrahim, L., and Mohammed, B., (2016). "Evaluation De L'impact De La Pollution Agricole Sur La Qualite Des Eaux Souterraines De La Nappe Du Gharb". *European Scientific Journal*, 12(11).

Kampa, M., and Castanas, E., (2008). "Human health effects of air pollution". *Environmental pollution*, 151(2), 362-367.

Khatri, C. G., (2009). "An introduction to multivariate statistics".

Khedvan, A., Gaikwad, V., (2015). "Review on Effect of Magnetic Field on Hydrocarbon Refrigerant in Vapour Compression Cycle", *International Journal of Scientific Engineering and Technology Research*, 4, 1374-1378.

Kline, S. J., and McClintock, F. A,. (1953). "Analysis of uncertainty in single-sample experiments". *Mechanical Engineering*, 75, 3-9.

Kristiantoro, T., Idayanti, N., Sudrajat, N., and Septiani, A., (2016, November). "Application of bonded NdFeB magnet for C-Band circulator component". In *Journal of Physics: Conference Series* (Vol. 776, No. 1, p. 012030). IOP Publishing.

Kumar, M., Agarwal, S., Kumar, V., Khan, G., Shakher, C., (2015). "Experimental investigation on butane diffusion flame under the influence of magnetic field by using digital speckle pattern interferometry," *Applied Optics*, 54(9), 2450-2460.

Kunzli, McConnell, R., Islam, T., Shankardass, K., Jerrett, M., Lurmann, F., Gilliland, F., ... & Peters, J. (2010). "Childhood incident asthma and traffic-related air

pollution at home and school". *Environmental health perspectives,* 118(7), 1021-1026.

Kurji, H. J., and Imran, M. S., (2018). "Magnetic field effect on compression ignition engine performance". *ARPN Journal of Engineering and Applied Sciences*, 13(12), 3943-3949.

Kurniawan, Purba, Setiadi, Simbolon, Warman, Sebayang, (2017). "Effect of Fe-Mn addition on microstructure and magnetic properties of NdFeB magnetic powders". *Journal of Physics-Conference Series* 985 012044.

Lahane, S., and Patil, N. G., (2016). "Analysis of performance and emission characteristics of a homogeneous charge compression ignition (HCCI) engine". *Procedia Technology*, 25, 854-861.

Lee, K. H., and Kim, K., (2001). "Influence of initial combustion in SI engine on following combustion stage and cycle-by-cycle variations in combustion process". *International Journal of Automotive Technology*, 2(1), 25-31.

Lee, S., Oh, S., and Choi, Y., (2009). "Performance and Emission characteristics of an SI engine operated with DME blended with LPG fuel". *Fuel*, 88, 1009-1015.

Lee, K., and Ryu, Jeaduk, (2004). "An experimental study of the flame propagation and Combustion characteristics of LPG fuel". Fuel, 84, 1116-1127.

Legros, G., Gomez, T., Fessard, M., Guibert, P., and Torero, J., (2010). "Magnetically induced Flame Flickering", *Proceedings of the Combustion Institute,* 33, 1095-1103

Li, Y., Hou, S., Zheng, N., Tang, L., Ji, X., and Hua, X., (2019). "Pollution characteristics, sources, and health risk assessment of human exposure to Cu, Zn, Cd and Pb pollution in urban street dust across China between 2009 and 2018". *Environment international*, 128, 430-437.

Litak, G., Kamiński, T., Czarnigowski, J., Sen, A. K., and Wendeker, M., (2009). "Combustion process in a spark ignition engine: analysis of cyclic peak pressure and peak pressure angle oscillations". *Meccanica,* 44(1), 1-11.

Litak, G., Kamiński, T., Czarnigowski, J., Żukowski, D., and Wendeker, M., (2007). "Cycle-to-cycle oscillations of heat release in a spark ignition engine". *Meccanica*, 42(5), 423-433.

Loganathan, B. G., Ramesh, A., Archibong, A. E., Hood, D. B., and Guo, Z., (2011). "Global environmental distribution and human health effects of polycyclic aromatic hydrocarbons". *Global contamination trends of persistent organic chemicals*, 95-124.

Loskutova, O., Walker, T. R., Crittenden, P. D., Dauvalter, V. A., Jones, V., Kuhry, P., and Pystina, T., (2009). "Multiple indicators of human impacts on the environment in the Pechora Basin, north-eastern European Russia". *Ecological indicators*, 9(4), 765-779.

Ma, F., Li, S., He, Y., Wang, M., Jiang, L., and Zhao, S., (2011). "Experimental study on combustion and emission characteristics of a hydrogen-enriched compressed natural gas engine under idling condition". *International journal of hydrogen energy*, 36(20), 13150-13157.

Masi, M., (2012). "Experimental analysis on a spark ignition petrol engine fuelled with LPG (liquefied petroleum gas)". *Energy*, 41(1), 252-260.

Masum, B.M., Kalam, M.A.,Palash, S.M., and Abedin, M.J., (2013). "Effect of ethanol gasoline blend on NOx emission in SI engine". Renewable and Sustainable Energy Reviews, 24, 209-222.

Mathur, M. L., & Sharma, R. P. (2010). IC engine.

Mingzhang, P., Pan, M., Shu, G., Wei, H., Zhu, T., Liang, Y., and Liu, C., (2014). "Effects of EGR, compression ratio and boost pressure on cyclic variation of PFI gasoline engine at WOT operation". *Applied Thermal Engineering*, 64(1-2), 491-498.

Morcos, A. C., Brown, D. N., and Campbell, P., (2002, April). "Nd-Fe-B magnets for electric power steering (EPS) applications". In *2002 IEEE International Magnetics Conference (INTERMAG)* (p. FT3). IEEE.

Morganti, K. J., Foong, T. M., Brear, M. J., da Silva, G., Yang, Y., and Dryer, F. L., (2013). "The research and motor octane numbers of liquefied petroleum gas (LPG)". *Fuel*, 108, 797-811.

Morozov, Y. G., and Kuznetsov, M. V., (1999). "Effect of magnetic fields on combustion electromotive force". *Combustion, Explosion and Shock Waves*, 35(1), 18-22.

Muljadi, Ramlan, Sardjono P., Setiyabudidaya D., Gulo, F., (2019). "Mechanical, Magnetic Properties and Corrosion resistance of hybrid bonded magnet NdFeB-$BaFe_{12}O_{19}$". *IOP Conf. Series:Journal of Physics:Conf.Series* 1191:012048. doi:10.1088/1742-6596/1191/1/012048

Nayak, V., Chitragar, P. R., Shivaprasad, K. V., Bedar, P., and Kumar, G. N., (2016). "An experimental study on combustion and emission analysis of four cylinder 4-stroke gasoline engine using pure hydrogen and LPG at idle condition". *Energy Procedia*, 90, 525-534.

Niaki, S. O. D., Khatamnejad, H., Khalilarya, S., Jafarmadar, S., Mirsalim, M., and Gharehghani, A., (2019). "Experimental investigation on the effect of natural gas premixed ratio on combustion and emissions in an IDI engine". *Journal of Thermal Analysis and Calorimetry*, 138(6), 3977-3986.

Nemoianu, L., Pana, C., Negurescu, N., Cernat, A., Fuiorescu, D., and Nutu, C., (2017). "Study of the cycle variability at an automotive diesel engine fuelled with LPG". In *MATEC Web of Conferences* (Vol. 112, p. 10006). EDP Sciences.

Olmo, N.R., Hila, I.P., Santos, U.D.P., Alberto, L., Pereira, A., (2011). "A review of low-level air pollution and adverse effects on human health : implications for epidemiological studies and public policy". *Clinics* 66, 681–90. doi:10.1590/S1807-59322011000400025.

Ozcan, H., and Yamin, J. A., (2008). "Performance and emission characteristics of LPG powered four stroke SI engine under variable stroke length and compression ratio". *Energy Conversion and Management*, 49(5), 1193-1201.

Ozdor, N., Dulger, M., and Sher, E., (1994). "Cyclic variability in spark ignition engines a literature survey". *SAE transactions*, 1514-1552.

Patel, P. M., Rathod, G. P., and Patel, T. M., (2014). "Effect of magnetic field on performance and emission of single cylinder four stroke diesel engine". *IOSR Journal of Engineering*, 4(5), 28-34.

Ponnusamy, M. P., Haridas, D., Jain, M., Ganti, A. K., and Batra, S. K., (2012). "Targeting the EGFR signaling pathway in cancer therapy". *Expert opinion on therapeutic targets*, 16(1), 15-31.

Pourkhesalian, A. M., Shamekhi, A. H., and Salimi, F., (2010). "Alternative fuel and gasoline in an SI engine: A comparative study of performance and emissions characteristics". *Fuel*, 89(5), 1056-1063.

Pundir, B. P., Zvonow, V. A., and Gupta, C. P., (1981). "Effect of charge non-homogeneity on cycle-by-cycle variations in combustion in SI engines". *SAE Transactions*, 2354-2366.

Rakopoulos, C. D., Rakopoulos, D. C., Mavropoulos, G. C., and Kosmadakis, G. M., (2018). "Investigating the EGR rate and temperature impact on diesel engine combustion and emissions under various injection timings and loads by comprehensive two-zone modeling". *Energy*, 157, 990-1014.

Ravi, K., Bhasker, J. P., and Porpatham, E., (2017). "Effect of compression ratio and hydrogen addition on part throttle performance of a LPG fuelled lean burn spark ignition engine". *Fuel*, 205, 71-79.

Sahoo, R. R., and Jain, A., (2019). "Experimental analysis of nanofuel additives with magnetic fuel conditioning for diesel engine performance and emissions". *Fuel*, 236, 365-372.

Saksono, N., (2005). "Magnetising Kerosene for Increasing Combustion Efficiency", *Jurnal teknologi*, 2, 155-162.

Sala, A., Notti, E., (2014). "Preliminary Tests of New Magnetic Device for Fuel Saving and Emission Reduction in Fisheries", *Third International Symposium on Fishing Vessel Energy Efficiency,* 1-5.

Saraf, R.R., Thipse, S.S. and Saxena, P.K., (2009). “Comparative emission analysis of gasoline/LPG automotive bifuel engine”, *International Journal of Environmental Science and Engineering*, 1(4), 198-201.

Shankar, K.S., and Mohanan, P., (2010). “The effect of LPG injection on combustion, performance and emission characteristics of a MPFI engine.” *Journal of Middle European construction and Design of Cars,* 8, 40-48.

Shoenung, M., (2001). “Hydrogen vehicle fueling alternatives: an analysis developed for the international agency”. *SAE World Congress*, 2001-01-2528.

Shojaeefard, M. H., Tahani, M., Etghani, M. M., Akbari, M., (2013). “Cooled EGR for a Turbo Charged SI Engine to Reduce Knocking and Fuel Consumption.” *International Journal of Automotive Engineering,* 3.

Singh, A., (2015). “Measurement of fuel flow behaviour of Propane Diffusion Flame by Dimensionless Numbers under Magnetic Field Application”, *International Journal of Combined Research and Development,* 4, 585-586.

Siregar, H., Nainggolan, R., (2012). “Electromagnetic Fuel saver for Enhancing the Performance of the Diesel Engine”, *Global Journal of Researches in Engineering, Mechanical and Mechanics Engineering,* 12.

Song, D., Jia, N., Guo, X., and Ma, X., (2014). "Low Pressure Cooled EGR for Improved Fuel Economy on a Turbocharged PFI Gasoline Engine," *SAE Technical Paper* 2014-01-1240, doi:10.4271/2014-01-1240.

Sulaiman, M., Ayob, M., and Meran, I., (2013). “Performance of a single cylinder Spark Ignition engine fuelled by LPG”, *Procedia Engineering*, 53, 579-585.

Tao, R., (2004). “Investigate Effects of Magnetic Fields on Fuels”, Department of Physics, Temple University, Philadelphia.

Tao, R., and Xu, X., (2006). “Reducing the Viscosity of Crude Oil by Pulsed Electric or MagneticField”, *Energy & Fuels,* 20, 2046-2051.

Tian, G., and Richards, P., (2010). “Laminar burning velocities of 2, 5-dimethyl furan compared with ethanol and gasoline”, *Energy and Fuels,* 24(7), 3898-3905.

Tung, H., Cédric, D., Anne, V., Agnès, J., & Gilles, L., (2010). "A global tool for environmental assessment of roads–Application to transport for road building". In *European Conference of Transport Research Institutes.* The Hague.

Tutak, W., and Jamrozik, A., (2011). "A study of performance and emissions of SI engine with a two-stage combustion system". *Chemical and Process Engineering*, 453-471.

Ueno, S., and Harada, K., (1985). "Effect of Magnetic fields on Flames and Gas flow", *IEEE Transactions on Magnetics,* Vol. Mag-21, No.5.

Ueno, S., and Harada, K., (1987). "Combustion Process under strong DC Magnetic Fields", *IEEE Transactions on Magnetics,* Vol. Mag-23, No.5, 2752-2754.

Ugare, V., Dhoble, A., Lutade, S., and Mudafale, K., (2014). "Performance of internal combustion (CI) engine under the influence of stong permanent magnetic field". *Journal of Mechanical and Civil Engineering*, 3, 11-17.

Vianna, J. D. S., Reis, A. D. V., Oliveira, A. D. S., Fraga, A. G., and de Sousa, M. T., (2005). "Reduction of pollutants emissions on SI engines: accomplishments with efficiency increase". *Journal of the Brazilian Society of Mechanical Sciences and Engineering*, 27(3), 217-222.

Vijayakumar, P., Patro, S., and Pudi, V., (2014). "Experimental Study of a Novel Magnetic Fuel Ionization Method in Four Stroke Diesel Engines", *International Journal of Mechanical Engineering and Robotics Research,* 3, 151- 159.

Villarroel, M., (2004). "*The effects of cycle-to-cycle variations on nitric oxide (NO) emissions for a spark-ignition engine: Numerical results* (Doctoral dissertation, Texas A&M University).

Wakayama, N., (1992). "Effect of a Gradient Magnetic Field on the Combustion ofMethane in Air", *Chemical Physics Letters,* 188, 279-281.

Walker, A. P., and Blakeman, P. G., (2008). "*Emission control options to achieve Euro IV and Euro V on heavy duty diesel engines",* SAE Technical Paper (No. 2008-28-0021).

Wang, Z., and Wang, J., (2010). "*Knocking suppression using stratified stoichiometric mixture in a DISI engine",* SAE Technical Paper (No. 2010-01-0597).

Whitelaw, J. H., and Xu, H. M., (1995). "Cyclic variations in a lean-burn spark ignition engine without and with swirl". *SAE transactions*, 1202-1220.

Wu, C., Puzinauskas, P. V., and Tsai, J. S., (2003). "Performance analysis and optimization of a supercharged Miller cycle Otto engine". *Applied Thermal Engineering*, 23(5), 511-521.

Wu, W., Qu, J., Zhang, K. and Chen, W., (2016). "Experimental Studies of Magnetic Effect on Methane Laminar Combustion Characteristics", *Combustion Science and Technology*, 1563-521X.

Xing, Y. F., Xu, Y. H., Shi, M. H., and Lian, Y. X., (2016). "The impact of PM2. 5 on the human respiratory system". *Journal of thoracic disease*, 8(1), E69.

Xiang Chi, Ying Li, De-quan Er, Xu-hao Han, Xiu-li Duan, Ji-bing Sun, and Chun-xiang Cui, (2018). "Study of Structure and Magnetic Properties of SmCo10 Alloy Prepared by Different Methods". Advances in Materials Science and Engineering 2018: 1-10.

Xu, J., Geng, W., and Geng, X., (2020). "Study on the association between ambient air pollution and daily cardiovascular death in Hefei, China". *Environ Sci Pollut Res* 27: 547–561. https://doi.org/10.1007/s11356-019-06867-4.

Yamamoto, H. and Misumi, M., (1987). "Analysis of Cyclic Combustion Variation ina lean operating SI engine." SAE Paper 870547.

Zervas, E., Politis, D., and Bampatsou, C., (2017). "Air pollution and birth-related characteristics".

Zhuang, Y., and Hong, G., (2013). "Primary investigation to leveraging effect of using ethanol fuel on reducing gasoline fuel consumption." *Fuel* 105, 425-431.

APPENDIX I

Specifications of the Experimental Set up

Engine	Make: Maruti, Model: Zen MPFI, Type: 4 Cylinder, 4S, Petrol, CR 9.4:1, SOHC
Dynamometer	Make: Saj Test Plant Pvt Ltd., Model: AG80, Type: Eddy current, water cooled.
Dynamometer loading unit	Make: Cuadra, Model: AX-153, Type: variable speed,Supply: 230 V AC.
Propeller Shaft	Make: Hindustan Hardy Spicer, Model:1260, Type:A with universal joints
Air Box	M S fabricated with orifice meter and manometer
Fuel tank	Capacity 15 lit with glass fuel metering column
Manometer	Make: Apex, Model: MX-104, Range 100-0-100 mm, Type :U Tube.
Piezo Sensor	Make: PCB Piezotronics, Model: HSM111A22, Range 5000 psi, diaphragm stainless steel type and hermetic sealed.
Crank angle sensor	Make: Kubler, Germany, Model: 8.3700.1321.0360, dia:37 mm, shaft size: (6*12.5) mm, Supply: 5-30 V DC.
Engine Indicator	Make: Cuadra, Model: AX -104, Type: dual channel
Engine interface	Make: Cuadra, Model: AX -408, No of channels: 8.
Load Sensor	Make: Sensotronics Sanmar Ltd., Model: 60001, Type S beam, Universal, Capacity 0-50 kg, Load cell type: strain guage

Fuel flow transmitter	Make: Yokogawa, Model: EJA 110-EMS-5A- 92NN, Calibration range: 0-500 mm H_2O, Output Linear DP transmitter.
Fuel measuring unit	Make: Apex, Glass, Model: FF0.090
Rotameter	Make: Eureka, Engine cooling 100-1000 LPH; Calorimeter 25-250 LPH.
Pump	Type: Monoblock
Calorimeter	Type: Pipe in pipe
Add on Card	Make: Dynalog, Model: PCI1050, Resolution-12 bit, 8/16 input, Mounting PCI slot
Software	IC Engine soft V 15.0
Overall dimensions	W 2000 x D 2750 x H 1750 mm

APPENDIX II

Specifications of Gas ECU

Model: Sequential gas injection controller of IV generation OSCAR- N OBD CAN of Europe gas

Parameters	**Specifications**
Processor	16 bit /50 MHz
Voltage supply	12 V DC
Input Signals	Gas Temperature
	Gas Pressure
	Petrol Injection time
	O_2 sensor
Output Signals	Gas injectors

LIST OF PUBLICATIONS BASED ON PhD RESEARCH WORK

International Journals:

1. **Libin P Oommen** and Kumar G N; "Experimental Studies on the impact of part-cooled high pressure loop EGR on the combustion and emission characteristics of Liquefied Petroleum Gas", *Journal of Thermal Analysis and Calorimetry*, (2020), DOI: https://doi.org/10.1007/s10973-020-09762-0.
2. **Libin P Oommen** and Kumar G N; "Assimilative Capacity approach for Air Pollution Control in Automotive Engines through Magnetic field assisted combustion of Hydrocarbons", *Environmental Science and Pollution Research*, (2020), DOI: https://doi.org/10.1007/s11356-020-11923-5.
3. **Libin P Oommen** and Kumar G N; "Experimental Studies on the influence of axial and radial fields of sintered neo-delta magnets in reforming the combustion and emission properties of a hydrocarbon fuel", *Energy Sources Part- A, Recovery, Utilization and Environmental Effects*, (2020), DOI: https://doi.org/10.1080/15567036.2020.1767729.
4. **Libin P Oommen** and Kumar G N; "Experimental Analysis of Synergetic effect of Part Cooled EGR on Magnetic field assisted Combustion of Liquefied Petroleum Gas", *Arabian Journal for Science and Engineering*, (2020), DOI: https://doi.org/10.1007/s13369-020-04696-z
5. **Libin P Oommen** and Kumar G N; " A Study on the Effect of Magnetic Field on the Properties and Combustion of Hydrocarbon fuels", *International Journal of Mechanical and Production Engineering Research and Development*, (2019),Vol. 9, Issue 3, pp 89-98.
6. **Libin P Oommen** and Kumar G N; "Influence of Magneto Combustion on Regulated Emissions of an Automotive Engine under Variable Speed Operation", *International Journal of Vehicle Structures and Systems*, Vol. 12, Issue 8, DOI: http://dx.doi.org/10.4273/ijvss.12.1.25

International Conferences:

1. **Libin P Oommen** and Kumar G N; "Influence of Magneto Combustion on Regulated Emissions of an Automotive Engine under Variable Speed Operation",

Proceedings of 2nd International Conference on Recent Developments in Mechanical Engineering, March 2019, Chennai

2. **Libin P Oommen** and Kumar G N; "Analysis of Cyclic variations in combustion of a gasoline fueled MPFI Engine under uniform Magnetic Fields", *Proceedings of 11th Exergy, Energy and Environment Symposium*, July 2019, SRM University, Chennai.
3. **Libin P Oommen** and Kumar G N; "Experimental Studies on the impact of part-cooled high pressure loop EGR on the combustion and emission characteristics of Liquefied Petroleum Gas", *Proceedings of 2nd International Mechanical Engineering Congress*, November 2019, NIT Trichy.
4. **Libin P Oommen** and Kumar G N; "Assimilative Capacity approach for Air Pollution Control in Automotive Engines through Magnetic field assisted combustion of Hydrocarbons", *Proceedings of 5th International Conference on Recent Advancements in Chemical Energy and Environmental Engineering*, February 2020, SSN University, Chennai.

National Conference:

1. **Libin P Oommen** and Kumar G N; "Experimental Studies on the effect of varying rates of part cooled EGR in high pressure loop on an MPFI Engine under Variable Speed Operation", *Proceedings of 26th National Conference on IC Engines and Combustion*, November 2019, NIT Kurukshetra, Haryana.

Book Chapter:

1. **Libin P Oommen** and Kumar G N; "Experimental Studies on the effect of varying rates of part cooled EGR in high pressure loop on an MPFI Engine under Variable Speed Operation", *Chapter 37, Advances in IC Engine and Combustion Technology, Lecture Notes in Mechanical Engineering* (Springer) https://doi.org/10.1007/978-981-15-5996-9_37

Under Process Journals

1. **Libin P Oommen** and Kumar G N; "Analysis of Cyclic variations in combustion of a gasoline fueled MPFI Engine under uniform Magnetic Fields", *Thermal Science and Engineering Progress*. (Under Review)
2. **Libin P Oommen** and Kumar G N; "Experimental Diagnostics of Conjoint effect of semi cooled exhaust recirculation on Magnetic field assisted combustion of liquid phase hydrocarbons", *Combustion Science and Technology*. (Under Review)
3. **Libin P Oommen** and Kumar G N; "Experimental Analysis of the impact of Magnetic Field Assisted Processing of Hydrocarbon Fuels on the attributes and stability of Combustion in Automotive Engines", *International Journal of Oil Gas and Coal Technology.* (under review)

BIO-DATA

Libin P Oommen

Department of Mechanical Engineering, NITK Surathkal

Home town: Alappuzha, Kerala.

- Post Graduation (2012) M. Tech in IC Engines and Turbo-machinery from Government Engineering College, Thrissur.
- Graduation in Mechanical Engineering (2010) from Sun College of Engineering and Technology, Kanyakumari.

International Journal Publications

- Libin P Oommen & Ramesh A; Energy and Exergy Analysis of a 1400 TPD Kiln System of a Cement Industry, International Journal of Earth Sciences and Engineering 01(SPL Jan 2012):541-546.
- Libin P Oommen & Kumar G N; " A Study on the Effect of Magnetic Field on the Properties and Combustion of Hydrocarbon fuels", International Journal of Mechanical and Production Engineering Research and Development, Vol. 9, Issue 3, pp 89-98.
- Libin P Oommen & Kumar G N; "Influence of Magneto Combustion on Regulated Emissions of an Automotive Engine under Variable Speed Operation", International Journal of Vehicle Structures and Systems, DOI: http://dx.doi.org/10.4273/ijvss.12.1.25
- Libin P Oommen & Kumar G N; "Experimental Studies on the impact of part-cooled high pressure loop EGR on the combustion and emission characteristics of Liquefied Petroleum Gas", Journal of Thermal Analysis and Calorimetry, DOI: https://doi.org/10.1007/s10973-020-09762-0.
- **Libin P Oommen** and Kumar G N; "Assimilative Capacity approach for Air Pollution Control in Automotive Engines through Magnetic field assisted

combustion of Hydrocarbons", Environmental Science and Pollution Research, (2020), DOI: https://doi.org/10.1007/s11356-020-11923-5.

- Libin P Oommen & Kumar G N; "Experimental Analysis of Synergetic effect of Part Cooled EGR on Magnetic field assisted Combustion of Liquefied Petroleum Gas", Arabian Journal of Science and Engineering, DOI: https://doi.org/10.1007/s13369-020-04696-z
- Libin P Oommen & Kumar G N; "Experimental Studies on the influence of axial and radial fields of sintered neo-delta magnets in reforming the combustion and emission properties of a hydrocarbon fuel", Energy Sources Part- A Recovery, Utilization and Environmental Effects. DOI: https://doi.org/10.1080/15567036.2020.1767729
- Libin P Oommen & Kumar G N; "Experimental Analysis of the impact of Magnetic Field Assisted Processing of Hydrocarbon Fuels on the attributes and stability of Combustion in Automotive Engines", International Journal of Oil Gas and Coal Technology (under review)
- Libin P Oommen & Kumar G N; "Experimental diagnosis of conjoint effect of semi-cooled Exhaust Recirculation on Magnetic field assisted Combustion of liquid phase hydrocarbons", Combustion Science and Technology (under review)
- Libin P Oommen & Kumar G N; "Analysis of Cyclic Variations and Combustion Behavior of liquefied petroleum gas under Uniform Axial and Radial Magnetic Fields", Thermal Science and Engineering Progress (communicated)

International/ National Conferences

- Libin P Oommen & Kumar G N, "Assimilative Capacity approach for Air Pollution Control in Automotive Engines through Magnetic Field assisted Combustion of Hydrocarbons", International Conference on Recent Advancements in Chemical, Energy and Environmental Engineering, SSN College of Engineering, Chennai, February 2020.

- Libin P Oommen & Kumar G N, “Experimental studies on the effect of part cooled high pressure loop EGR on the performance and emissions of a multicylinder engine”, National Conference on IC Engines and Combustion, NIT Kurukshetra, November 2019.
- Libin P Oommen & Kumar G N, “Experimental Studies on the effect of part cooled EGR on high pressure loop in the combustion of liquefied petroleum gas”, International Mechanical Engineering Congress, National Institute of Technology Trichy, November 2019.
- Libin P Oommen & Kumar G N; “ Analysis of Cyclic variations in combustion of a gasoline fueled MPFI Engine under uniform Magnetic Fields”, International Exergy, Energy and Environment Symposium, SRM University, Chennai, July 2019.
- Libin P Oommen & Kumar G N; “Influence of Magneto Combustion on Regulated Emissions of an Automotive Engine under Variable Speed Operation”, International Conference on Recent Developments in Mechanical Engineering, S.A. Engineering College, Chennai; March 2019.
- Libin P Oommen & Geo Sebastian; “An experimental approach towards blending multiple nanoparticles in diesel fuel for cleaner emissions and enhanced performance of CI engines”, International Conference on Advances in Energy Research, IIT Bombay, December 2015.
- Libin P Oommen & Sajnulal Franc; “A comparison of emissions of SI and CI engines in a low-nitrogen oxycombustion environment”, International Conference on Emerging Trends in Science and Cutting Edge Technology, New Delhi, August 2014.
- Libin P Oommen & Ramesh A; Energy and Exergy analysis of a 1400 TPD kiln system in a cement plant, International Conference on recent advances and challenges in energy, Manipal Institute of Technology, 2012.
- Libin P Oommen & Ramesh A; A study on Smart Ceramic Materials for Homogenous Combustion in Internal Combustion Engines, International

Conference on Materials for Future, Government Engineering College Thrissur, 2011.

Awards and recognitions

- Best Paper Award, fifth International Conference on Recent Advancements in Chemical, Energy and Environmental Engineering; SSN College of Engineering, Chennai.
- Best Paper Award, 11th International Exergy, Energy and Environment Symposium, SRM University, Chennai.
- Best Paper Award, International Conference on Recent Developments in Mechanical Engineering, S.A. Engineering College, Chennai.
- Best Paper Award, Mechanical Engineers' National Symposium, Sun College of Engineering and Technology, Kanyakumari.